Volume 8, Number 1
January–February 2000

ISSN: 0869-5938

STRATIGRAPHY AND GEOLOGICAL CORRELATION

English Translation of *Stratigrafiya, Geologicheskaya Korrelyatsiya*

Editor-in-Chief
Boris S. Sokolov

http://www.maik.rssi.ru

Journal of the Fundamental and Applied Aspects of Stratigraphy and the Correlation of Geologic Events and Processes in Time and Space

МАИК "НАУКА/INTERPERIODICA" PUBLISHING

Stratigraphy and Geological Correlation

(Stratigrafiya, Geologicheskaya Korrelyatsiya)

ISSN: 0869-5938

Editor-in-Chief
Boris S. Sokolov
Member of the Russian Academy of Sciences,
Counsellor of the Presidium of the Russian Academy of Sciences (RAS)

Address for correspondence: Staromonetnyi per. 22, Moscow, 109180 Russia
Phones: 7 (095) 951-2164; Fax: 7 (095) 233-5590.

Deputy Editor-in-Chief
Mikhail A. Semikhatov
Member of the Russian Academy of Sciences
Head of Laboratory, Geological Institute, RAS
E-mail: semikhatov@ginran.msk.su

Assistant Editor
Aleksei B. Herman
Senior Scientist,
Geological Institute, RAS
E-mail: herman@ginran.msk.su

EDITORIAL BOARD

Mikhail A. Akhmet'ev
Dr. Sci. (Geol.–Min.),
Head of Laboratory, Geological Institute, RAS
akhmetev@ginran.msk.su

Aleksandr S. Alekseev
Professor, Department of Paleontology,
Moscow State University
aaleks@geol.msu.ru

Mikhail N. Alekseev
Dr. Sci. (Geol.–Min.),
Chief Scientist, Geological Institute, RAS
alekseev@ginran.msk.su

Ivan A. Basov
Dr. Sci. (Geol.–Min.), Deputy Director,
Institute of the Lithosphere, RAS
basov@ilsan.msk.ru

Michael G. Basset
Professor, National Museum of Wales,
Cardiff, UK

William A. Berggren
Professor, Department of Geology and
Geophysics, Woods Hole Oceanographic
Institute, USA

Elena V. Bibikova
Dr. Sci. (Geol.–Min.), Chief Scientist,
Vernadskii Institute of Geochemistry and
Analytical Chemistry, RAS
sergei@bibikov.genebee.msu.su

Nikita A. Bogdanov
Corresponding Member of
the Russian Academy of Sciences,
Director, Institute of the Lithosphere, RAS
bogdanov@ilsan.msk.ru

Kiyotaka Chinzei
Professor, Institute of Geology,
University of Tokyo,
Tokyo, Japan

Nikolai M. Chumakov
Dr. Sci. (Geol.–Min.),
Chief Scientist, Geological Institute, RAS
chumakov@ginran.msk.su

Yurii B. Gladenkov
Dr. Sci. (Geol.–Min.),
Head of Laboratory, Geological Institute, RAS
gladenkov@ginran.msk.su

Dmitrii L. Kaljo
Professor, Institute of Geology, Tallinn, Estonia

Victor E. Khain
Member of the Russian Academy of Sciences,
Chief Scientist, Institute of the Lithosphere, RAS

Lidiya A. Nevesskaya
Dr. Sci. (Biol.), Laboratory Chief,
Institute of Paleontology, RAS
lenin33@paleo.ru

Aleksandr G. Ponomarenko
Dr. Sci. (Biol.), Chief Scientist,
Institute of Paleontology, RAS
vtopor@paleo.ru

Jurgen Remane
Professor, Institute de Géologie,
Université de Neuchâtel, Switzerland

Aleksei Yu. Rozanov
Dr. Sci. (Geol.–Min.),
Director, Institute of Paleontology, RAS
aroza@paleo.ru

Boris A. Sokolov
Dr. Sci. (Geol.–Min.), Professor, Dean, Faculty
of Geology, Moscow State University
mfedon@paleo.ru

Otto Walliser
Professor, Göttingen University, Göttingen,
Germany

Sun Weigo
Professor, Nanjing Institute of Geology
and Paleontology, Academia Sinica, China

Victor A. Zakharov
Dr. Sci. (Geol.–Min.), Head of Laboratory,
Institute of Geology, Geophysics, and
Mineralogy, Siberian Branch, RAS, Novosibirsk

Aleksandr I. Zhamoida
Corresponding Member of the Russian Academy of
Sciences, Russian Geological Institute, St. Petersburg

Staff Editor Tamara V. Trishkina

Editor of the English Translation Anatolii Ya. Sharas'kin, Dr. Sci. (Geol.–Min.)

SCOPE

Stratigraphy and Geological Correlation (Stratigrafiya. Geologicheskaya Korrelyatsiya) is the only journal in the world designed to provide comprehensive coverage of the fundamental and applied aspects of stratigraphy and the correlation of geological events and processes in time and space. Articles are based on the results of multidisciplinary research and are directed toward researchers, university professors, students, and geologists interested in understanding stratigraphy and the chronological features of the world's geological record.

Stratigraphy and Geological Correlation is abstracted and/or indexed in *Petroleum Abstracts*, *Research Alert*, *SciSearch*, *Current Contents* (*Physical, Chemical*, and *Earth Sciences*) and *World Translations Index*.

SUBSCRIPTION OFFICE
INTERPERIODICA
P.O. BOX 1831, BIRMINGHAM, AL 35201-1831 USA
PHONE: (800) 633-4931; (205) 995-1567 (outside US and Canada)
FAX: (205) 995-1588

PUBLISHER
INTERNATIONAL ACADEMIC PUBLISHING
COMPANY "NAUKA/INTERPERIODICA"
PROFSOYUZNAYA UL. 90, MOSCOW, 117864 RUSSIA
PHONE: 7 (095) 336-1600; FAX: 7 (095) 336-0666
E-mail: compmg@maik.rssi.ru
Web Site: http://www.maik.rssi.

SUBSCRIPTION PRICES (2000, Volume 8, 6 issues)
US $980.00 (North America), $1125.00 (elsewhere). A 5% discount is given on 2-year orders. Subscriptions may be entered at any time. Orders may be placed at agencies or directly. There is a 5% discount to all subscription agencies. Cancellations not allowed except for duplicate payment. Prepayment required. Advance payment required in US$/US bank. MasterCard/Visa accepted. Make checks payable to *Stratigraphy and Geological Correlation* or Interperiodica.

Stratigraphy and Geological Correlation (ISSN: 0869-5938) is published bimonthly for US $980.00 (North America), outside North America for $1125.00 per year by MAIK "Nauka/Interperiodica", 5724 Hwy. 280 East, Birmingham, Alabama 35242-5724 USA. Periodical postage paid at Birmingham, Alabama, and additional mailing offices. POSTMASTER: Send address changes to *Stratigraphy and Geological Correlation*, P.O. Box 1831, Birmingham, Alabama 35201 USA.

The journal was founded in 1993.

Original Russian Edition Copyright © 2000 by the Russian Academy of Sciences
and Division of Geology, Geophysics, Geochemistry, and Mining Sciences.
English Translation Copyright © 2000 by MAIK "Nauka/Interperiodica" (Russia).

Contents

Vol. 8, No. 1, 2000

Simultaneous English language translation of the journal is available from MAIK "Nauka/Interperiodica" (Russia).
Stratigraphy and Geological Correlation ISSN 0869-5938.

Geochronology, Distribution, and Ice Volume on the Earth during the Last Glacial Maximum: Inferences from New Data
A. A. Velichko, Yu. M. Kononov, and M. A. Faustova 1

Middle Riphean Sedimentary Basin in the Junction Area between the Russian Platform and South Urals: Lithology, Facies, Paleogeography, and Evolutionary Trend
A. V. Maslov 13

Bivalve Zonation in Permian Deposits of Northeastern Asia
A. S. Byakov 30

The Lower Boundary of the Triassic and Its Correlation in Marine Sediments: Article 2. Boreal Sections of the Basal Triassic and Their Correlation with the Permian–Triassic Boundary Deposits of the Tethys
A. A. Shevyrev 49

The Pliocene of the Pontic–Caspian Region and Its Correlation
V. A. Zubakov 60

Biometric Dating of Elephants of the *Archidiskodon–Mammuthus* Lineage
E. A. Vangengeim and M. A. Pevzner 77

The Tsagan-Agui Cave (Mongolia): Pleistocene Stratigraphy, Archeology, and Paleoecology
A. P. Derevyanko, E. V. Devyatkin, A. N. Simakova, J. Olsen, O. A. Kulikov, and Z. N. Gnibedenko 84

Short Communications

Early Paleogene Mollusks of Kamchatka: Assemblages and Paleogeographic Environment
Yu. B. Gladenkov 99

Stratigraphy and Geological Correlation, Vol. 8, No. 1, 2000, pp. 1–12. Translated from Stratigrafiya. Geologicheskaya Korrelyatsiya, Vol. 8, No. 1, 2000, pp. 3–16.
Original Russian Text Copyright © 2000 by Velichko, Kononov, Faustova.
English Translation Copyright © 2000 by MAIK "Nauka/Interperiodica" (Russia).

Geochronology, Distribution, and Ice Volume on the Earth during the Last Glacial Maximum: Inferences from New Data

A. A. Velichko, Yu. M. Kononov, and M. A. Faustova

Institute of Geography, Russian Academy of Sciences, Straromonetnyi per. 29, Moscow, 109017 Russia

Received February 24, 1998

Abstract—The evaluated area and volume of ice sheets on the Earth during the Last Glacial Maximum (18–20 thousand years ago, oxygen isotope stage 2) are adjusted to the most recent data and our subglobal to global paleoglaciological reconstructions published between 1986 and 1997. In the West Eurasian Arctic sector (Svalbard and Franz Josef Land), the compensation uplift rate, calculated on the basis of radiocarbon dating of risen marine terraces, is considerably lower than that estimated using the model of an ice sheet stretched over the whole Barents Sea shelf. From the viewpoint of isostasy and new radiocarbon dates, according to which sediments left by the ice sheet of the Kara Sea are older than 40 ka, the idea suggesting a solid ice mass that existed in this region appears to be invalid. Glaciation in the Novaya Zemlya and Polar Urals was also autonomous. Glaciers in mountain valleys were typical of Taimyr and northeastern Siberia. Data on the western hemisphere again suggest a limited extent of glaciation in high latitudes, e.g., in the Canadian Arctic Archipelago. At the same time, ice sheets were most extensive in North America as compared to all others in the northern hemisphere. Outside the Antarctic continent, glaciation in the southern hemisphere was not intense; and limited ice sheets were mainly characteristic of southern South America and New Zealand. The total area of ice sheets during the Last Glacial Maximum was 36 million km^2 and progressively decreased to 9600 thousand km^2 about 13 ka ago and to 4700 thousand km^2 about 10 ka years ago.

Key words: *Pleistocene, Last Glacial Maximum, ice sheets, moraines, fluvioglacial, deglaciation.*

During the last million years, the Earth's biosphere developed in a distinct pulsative regime dependent on alternation of glacial and interglacial epochs, which considerably affected the climate and landscape. In order to understand interactions in the ocean–atmosphere–land system during the glacial periods, it is necessary to have quantitative data on the size and time–space dynamics of glacial systems and respective ice volumes. Most reliable data of this kind can be obtained for the Last Glacial Maximum (Valdai, Vistula, Wisconsin, or Sartana Glacial) that happened 18–20 ka ago. The suggested reconstructions for this epoch are based on research data of the International Geological Correlation Program (project no. 24 "Quaternary Glaciations in the Northern Hemisphere"), the international project PAGES, and the national program of the State Committee on Science and Engineering no. 18 "Global Environmental and Climatic Changes" (project "Most Recent Climatic Changes"). These projects yielded new results of investigations in marine and terrestrial regions of polar and middle latitudes, including data obtained by comprehensive geological study of natural exposures, research drilling, and seismic profiling. The results are used as a basis for reconstruction of regional, subglobal, and global charts presented in a series of publications (*Chetvertichnye...*, 1987; Velichko and Faustova, 1989; *Quaternary Stratigraphy...*, 1992; and some other works). In order to perform quantitative calculations, we used cartographic charts characterizing areas of greatest Laurentide (North America) and Scandinavian (Europe) ice sheets and also the distribution of glaciers in particular mountain systems, those of Asia included.

The plotted maps and schemes showed that the well-known idea of the circumpolar Panarctic Ice Sheet (Denton and Hughes, 1981; Grosval'd, 1983) is inconsistent with new data. Being of particular interest for glaciology and paleogeography, this discordance must also be taken into account in climatic models and in analysis of sea level fluctuations, as the latter have been disregarded in some works (Peltier, 1994).

Considering the problem in the light of new data, we found additional arguments in favor of our concept suggesting a limited development of ice sheets in the high Arctic latitudes.

In the eastern hemisphere, the glacial systems were quite evolved only in the west of the Arctic basin, but even in the British Isles (the extreme peri-Atlantic part of the basin), the land was locally free of ice and ice sheets of this region and Scandinavia were disconnected (Boulton *et al.*, 1991). Data on glaciation in the Barents Sea and glacio-isostasy in Svalbard (Spitsbergen) and Franz Josef Land are known from several recent works (Bishof *et al.*, 1996; Forman *et al.*, 1996, 1997; Landvik *et al.*, 1992; Zale and Brydsten, 1993).

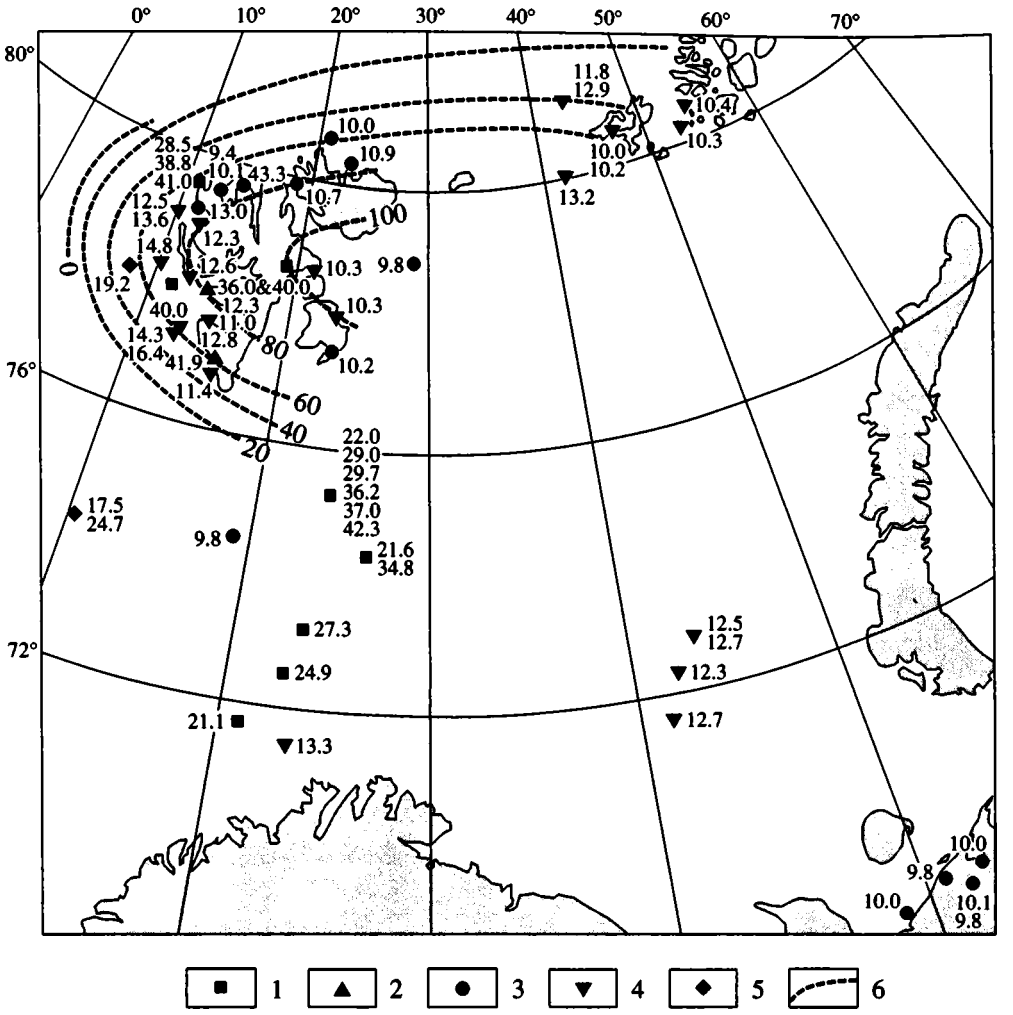

Fig. 1. Radiocarbon dates for various rock types (1–5) of the Valdai Glaciation and isobases (6) of postglacial uplift in the Barents Sea: (1) moraine; (2) deposits underlying moraine; (3) coastal-marine organogenic deposits; (4) deposits overlying moraine; (5) isobase.

According to isobase maps (Bishof *et al.*, 1996), the postglacial uplift is distinct in both archipelagoes. Additional detailed investigations of sea terrace levels in Franz Josef Land and radiocarbon dates for many shells, plant detritus, and whale bones suggest that, prior to the Holocene, this archipelago was comparable in size to its present area, or even smaller. The calculated rate of postglacial compensatory uplift turned out to be 50–80% lower than that estimated in accordance with the model of thick ice sheets covering the Barents and Kara sea shelves (Peltier, 1994; 1996). Analyzing the uplift magnitudes in Svalbard and Franz Josef Land, Forman and his colleagues (1997) assumed that the ice sheets of the two archipelagoes could be integrated into one system, whose center was located near Kongsoya Island at the eastern periphery of the archipelago. However, they also noted a considerable difference between the two archipelagoes in uplift magnitude, which is twice as low in Franz Josef Land as in Svalbard (Fig. 1). Consequently, it is possible as well that the system consisted of two individual ice sheets, the thicker of which was that of Svalbard, and its center migrated eastward in the course of the ice cupola's growth. The separate position of the ice sheets under consideration seems to correspond better to the lack of glaciomarine deposits in Franz-Victoria Strait between the archipelagoes (Lubinsky *et al.*, 1996). In addition, pelagic sediments replace glaciomarine deposits pinching out in the southern part of the Barents Sea shelf. Musatov, Rybalko, and Spiridonov, who studied all aspects of sedimentology in the whole area of the sea, also concluded that the ice sheet occupied only the northwestern zone adjacent to Svalbard and Franz Josef Land (Musatov, 1998). According to Forman *et al.* (1997), the idea of the development of a solid ice mass in central and southern parts of the Barents Sea contradicts not only sedimentological criteria, but also data

on the northern Scandinavian shelf, where glacio-isostatic uplifts have not been established.

Nevertheless, Landvik *et al.* (1998) published radiocarbon dates for sedimentary samples from the meridional zone between Scandinavia and Svalbard, which, as they believe, favor the idea of an ice sheet spread over the whole Barents Sea. We would like to mention here that eight of ten widely ranging dates are within the interval of 24–42 ka (Fig. 1), which corresponds to the Kap Ekholm Interstadial, as stated in the cited work. In the stratigraphic scheme for Svalbard (Mangerud *et al.*, 1998), this interglacial stage is an equivalent of the Alesund Interstadial of Scandinavia, when, according to Mangerud (1981), the very thick Scandinavian ice sheet completely degraded. Consequently, the wide range of quoted dates appears to be a result of glacial dispersal of erratic material, when the ice thawed at the early phase of the late Pleistocene glacial epoch. It is also remarkable that Landvik *et al.* (1998) consider the suggested overall glaciation in the Barents Sea to be synchronous to the so-called Kara Ice Sheet, but the data presented below discard the idea that this event was possible during the Last Glacial Maximum 18–20 ka ago.

In general, Forman *et al.* (1997), who analyzed all glacio-isostatic data known from the Franz Josef Land, Svalbard, and Novaya Zemlya archipelagoes for the time period of 9–5 ka, concluded that the extent of glaciation in the Barents Sea was 50–80% lower compared to that estimated by Peltier (1994, 1996).

Another attempt to consider coalescence of the Scandinavian and Novaya Zemlya Ice Sheets as responsible for glaciation in the entire Barents Sea (Polyak, 1996) also fails in view of the facts. Geological and geomorphological features, like moraine ramparts or dislocations, which may point to collisions between these sheets, are so far unknown. At the same time, there is a distinct terminal moraine located 150 km westward off Novaya Zemlya, marking the farthest advance of the last ice sheet over the eastern shelf margin (Pavlidis, 1992). It is not inconceivable, however, that an ice sheet of this size was older than the Last Glacial Maximum (18–20 ka), when the glaciation area was less, according to recent data, than the land area of the archipelago. Additional data of interest have been obtained by palynological study and radiocarbon dating of peat bogs in Novaya Zemlya, Sverdrup Island situated 110 km eastward, and the coastal zone of Baidaratskaya Bay (Serebryanny *et al.*, 1998; Malyasova and Serebryanny, 1993). These data suggest a greater size of glaciation in the archipelago compared to that modeled by Pavlidis (1992); but a significant part of the land was still free of ice here, because in two places it was populated 15–16 ka ago by tundra plant communities with *Betula nana*. As suggested in the cited works, the Kara shelf and southern coastal areas of Novaya Zemlya represented zones of intense permafrost and erosion. The above conclusion finds additional support from data on the low significance of glacio-isostatic events in the Novaya Zemlya archipelago (Forman *et al.*, 1997).

The problem of a local glaciation center in the Paj Hoj–Urals area is still unsolved. Glaciation here was likely of the mountain-valley type. This is evident from terminal glacial formations left by alpine-type glaciers, although their age is so far problematic (Matushkov and Astakhov, 1996). Morainal deposits are known only in the northwest of the Yamal Peninsula, and this is also an argument in favor of insignificant glaciation extent in the region under consideration.

In addition to data discussed in our previous works, there are important new results concerning the Kara Ice Sheet. Recent chronostratigraphic studies showed that deposits, which are presumably related in origin to this glaciation center, are overlain by sediments yielding the radiocarbon dates >40 ka (Gataulin and Forman, 1997), Results of this work not only discredit the idea that the Kara shelf was covered with an ice sheet during the glacial maximum, but also support our earlier conclusion that the glaciation did not advance at that time into northern West Siberia from the side of the Kara Sea shelf. The possibility of such a far glaciation advance southward in Siberia was based, as we should keep in mind, on the residual ice mass located in the Yenisei River valley to the south off Igarka (the Ledyanaya Gora locality). However, the radiocarbon dates for deposits overlying this ice mass turned out to be unexpectedly old, older than 40 ka (Astakhov and Isaeva, 1985). The isotopic dating of planktonic foraminifers (Knies *et al.*, 1996) also suggests that the Kara Ice Sheet could have existed during oxygen isotope stage 4 but not at the time of the Last Glacial Maximum (stage 2). According to observations of the Russian–Canadian expedition in Taimyr, there were only local glaciers advancing to this region from the Byrranga Mountains and Noril'sk Plateau (Velichko *et al.*, 1997).

All considerations concerning the Kara Ice Sheet are closely related to the problem of the origin and age of glacial deposits in north-northeastern areas of the East European plain. Beginning from our first publication (Velichko and Faustova, 1989), we have always stressed that the radiocarbon dates for deposits underlying moraines of the Scandinavian Ice Sheet in its southern and southeastern marginal zones are considerably younger than age values measured in deposits below moraines of the Pechora basin located farther to the east. In the last region, the measured dates are within the range of 45–33 ka or older and have been interpreted as indications of heterochronous phases of ice sheet growth, when glaciation advanced to the northeast of the East European plain prior to the glacial maximum 18–20 ka ago. This interpretation contradicts the idea suggested by Astakhov (1979), who assumed that glaciers advanced from the Kara glaciation center to the northeast of the East European plain and northern West Siberia to cover the area from the Pechora basin

to the lower courses of the Yenisei River, surroundings of the Obskaya Guba included. Astakhov argued for the Great Kara Ice Sheet of the Late Valdai Glacial for a long time, but new facts have now forced even him to reject his former viewpoint and to develop the concept, which has no principal disagreements with our schemes, demonstrating a limited extent of glaciation in northern Eurasia during the Last Glacial Maximum (Velichko and Faustova, 1989; Velichko *et al.*, 1994). Until recently, Astakhov and his colleagues (Astakhov, 1998; Mangerud *et al.*, 1996) tried to show that the last glaciation was able to advance 30–15 ka ago from the western sector of the Kara Sea and the Novaya Zemlya archipelago in the northeast of the East Siberian plain. They placed the glaciation boundary in the Pechora basin to the north off the Arctic circle (67°N); this is inconsistent with radiocarbon dates measured in this region and also with the limited extent of the late Valdai glaciation in the Novaya Zemlya (see above). In their latest publication (Svendsen *et al.*, 1999), they finally displaced this boundary from the right-hand side of the Onega River to the north toward the White Sea, from where it extends into the Barents Sea shelf leaving southward the southern island of the Novaya Zemlya Archipelago and curving round Franz Josef Land and Spitsbergen. Consequently, the cited authors considerably changed their opinion about the glacial relief age in the northeast of European Russia, considering the respective topographic features to be older than those of the Valdai or Vistula time. Arkhipov (1980, 1993) also cherished a hope that the last glaciation advanced far to the south beyond the Obskaya Guba. He believes that the glacial relief forms are sufficiently young here and substantiates the idea by age data on deposits underlying moraines in the lower courses of the Ob' River. In addition, there are terraces above the floodplain in the middle and upper courses of the river that are related, in his opinion, to the ice-dammed lakes of the late Zyrjanka time. We should note, however, that the age data accepted by Arkhipov for the Salekhard area disagree with a series of radiocarbon dates recently measured in peat-bog deposits of the Yamal and Gydanskii peninsulas. These dates again discard the existence of a Great Kara Ice Sheet that advanced at the Last Glacial Maximum from the shelf side. Moreover, the genesis and age of terrace deposits are inadequately studied and cannot be used for the forgoing correlation. Thus, all the data under consideration suggest that extreme glaciation in the northeast of European Russia and northern East Siberia is admissible only for the early Valdai epoch.

Another invalid idea assumes the development of large pre-Boreal ice surges from the Kara glacial center. It is based on data that formerly suggested the pre-Boreal age of moraine in the Markhida locality. New radiocarbon dates and results of geological and geomorphological observations in this locality of the Pechora basin (Mangerud *et al.*, 1996) showed that deposits below the moraine appear to be older than the Last Glacial Maximum. The pre-Boreal age here characterizes only nonglacial, for instance solifluction, sediments overlying the main morainal body. Consequently, one should admit that Tveranger *et al.* (1995), who consider one or two upper moraines of the Pechora basin to be related in origin to the Kara Ice Sheet movements during the late Valdai time, must present a more solid argument for their idea. Our interpretation of available data on glaciation in northern Eurasia and inferred boundaries of ice sheets is illustrated in Fig. 2.

According to results of recent studies, it is impossible as well that a large continuous ice sheet was spread over the Laptev Sea shelf and adjacent lowlands of northeastern Siberia. This is evident from the general geological–geomorphological situation and especially from the presence of glacial loess cover extending from land to the shelf (Siegert and Romanovsky, 1996). In addition, seismic investigation of the Laptev Sea (Niessen *et al.*, 1996) revealed the undersea continuation of large Siberian river beds developed when the shelf represented the past land area and sea level in the Arctic Ocean was considerably lower than at present. In the Vil'kitskii Strait between the southern island of Novaya Zemlya and the northern coast of the Taimyr Peninsula, the investigation also detected a 100-m-thick sequence of glaciomarine deposits typical of proximal glaciation zones. The deposits' distribution suggests that an ice sheet did not cover the islands of the Siberian Arctic shelf, which were decorated with isolated ice caps only.

Thus, the most recent data support our conclusion that the vast lowlands of western, central, and eastern Siberia represented periglacial landscapes during the Last Glacial Maximum, when considerable areas of the Arctic Ocean were free of ice sheets.

Chronological data based on analysis of cosmogenic ^{36}Cl point to a limited extent of glaciation in the mountains of the Chukchi Peninsula, where significant areas (e.g., the Anadyr Lowland) were free of ice during the entire late Pleistocene (Chaltieri *et al.*, 1997). Any model of extensive glaciation has no support in this region, as is stated in above work. Glaciation of the mountain-valley type was widespread within the mountain systems of northeastern Asia, being quasi-sheet type only in the Verkhoyansk area (*Chetvertichnye ...*, 1987).

In the mountain ridges of southern and southeastern Eurasia (Caucasus, Pamir, Tien Shan, Altai, Sayan, Tibet, Himalayas, the Baikal region, and southern areas of the Far East), glaciers were of the mountain-valley type almost everywhere. Existence of an ice sheet was suspected only for elevated areas of the Tibetan Plateau, but this idea was discredited in the course of recent Chinese, Russian, and Chinese–German expeditions to this region. Ice caps here covered the isolated mountain systems, and a more extensive glaciation left its marks only in the northern margin of the plateau (Binyan and Tijun, 1991; Lehmkuhl, 1993).

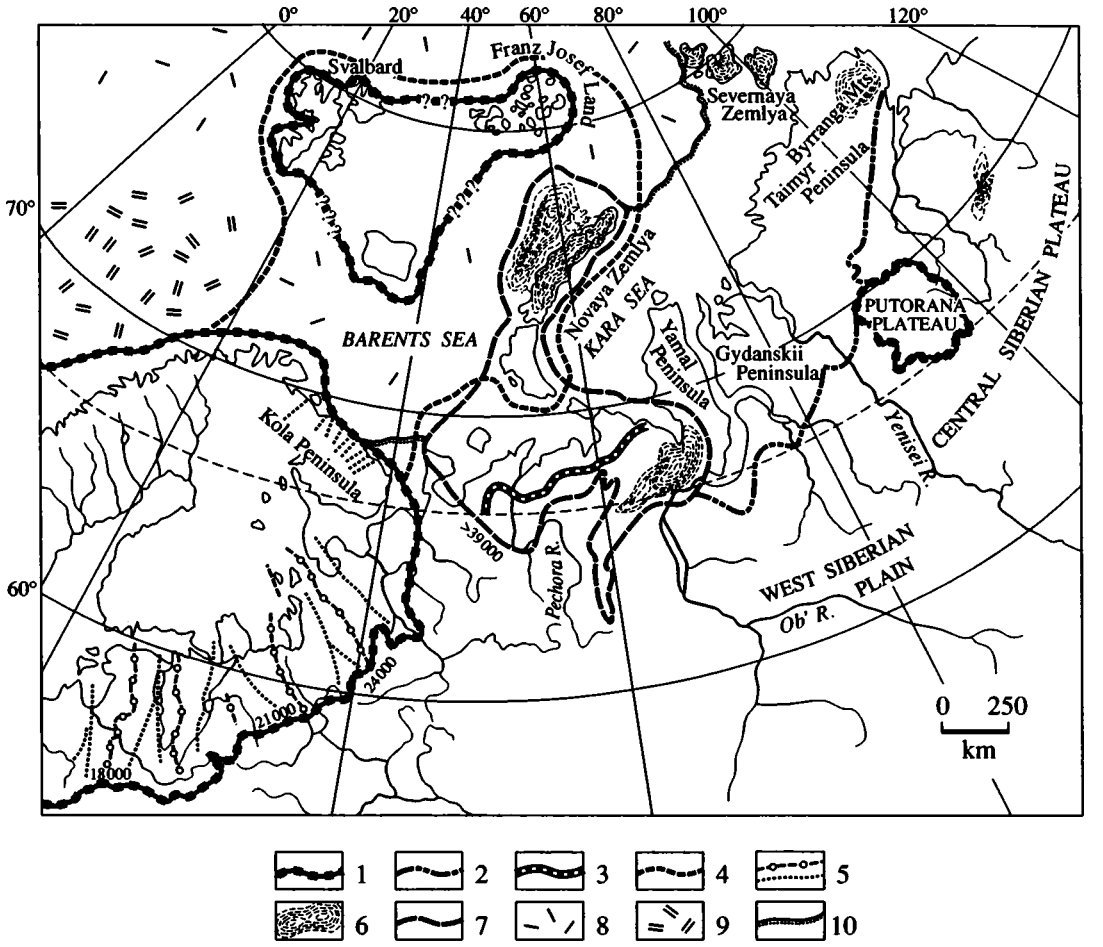

Fig. 2. Glaciation areas in northern Eurasia during the Last Glacial Maximum: (1) ice sheet boundaries according to our data; (2) distribution limits of the Kara Ice Sheet after Astakhov (1979); (3) distribution limits of the Novaya Zemlya Ice Sheet after Astakhov (1998); (4) distribution limits of the Barents Ice Sheet after Svendsen *et al.* (1999); (5) lines dividing ice flows and separating the lobes of Scandinavian Ice Sheet; (6) distribution limits of quasi-sheet and mountain glaciation during the Last Glacial Maximum; (7) distribution limits of the Novaya Zemlya Ice Sheet about 40 ka ago; (8) distribution limits of all-year ice floes; (9) distribution limits of seasonal ice floes; (10) coastal line at the Last Glacial Maximum.

The decreasing extent of glaciation in Eurasia from the west toward the east is understandable in terms of an asymmetric cryosphere that was responsible for a specific climatic situation, gave rise to the growth of the Scandinavian Ice Sheet at the maximum of cooling, and reduced the degree of glaciation in mountain systems of northeastern Russia and Siberia (Velichko, 1987).

The essence of the suggested concept consists in variable influence of the atmospheric centers controlling heat and humidity transport in northern Eurasia during consequent phases of the glacial epoch. As is known, the Atlantic Ocean is the main moisture source for this region; meteoric water penetrates inside the continent with western cyclonic circulation. In the first half of the glacial epoch, when cooling was still below the maximum, a considerable part of the North Atlantic Ocean remained free of ice and moisture saturated the air masses, which advanced far to the east because of insufficient development of high-pressure atmospheric zone above Siberia. These environments were favorable for the active development of glacial systems in northeastern Eurasia (this agrees well with factual data), whereas the rather high heat supply to western areas of the continent limited accumulation of snowfall and reduced ice sheets here.

In the next period of maximum cooling during the glacial epoch, ice floes covered the Atlantic Ocean for the greater part of the year and blocked the main moisture source. In addition, moisture penetration inside the continent was limited by the active anticyclone system that appeared above Siberia under conditions of intense global cooling. Environments favorable to accumulation of snowfall were characteristic only of western regions of the continent. Thick ice sheets developed exactly here, whereas they were of limited extent in Siberia despite the cooling peak of the last glacial epoch.

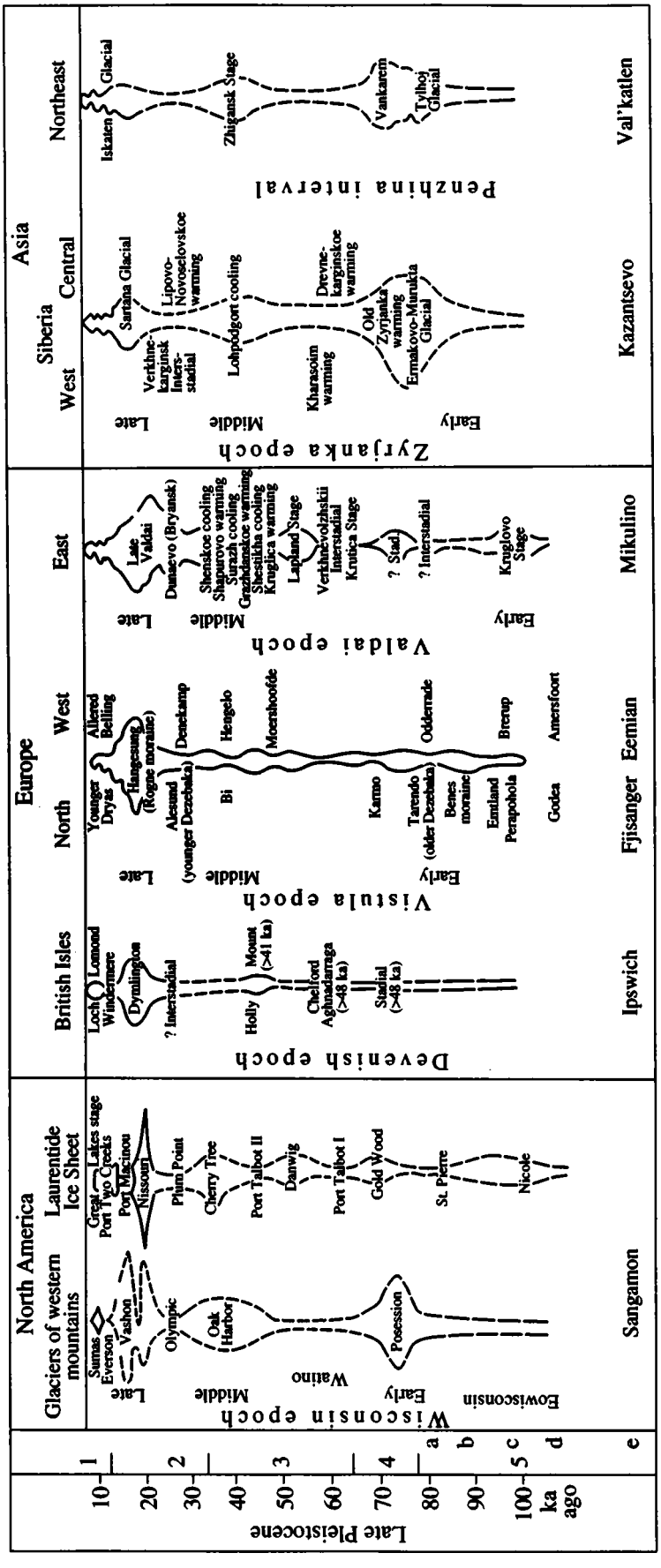

Fig. 3. Principal stages of the late Pleistocene glaciation in the northern hemisphere.

The above considerations are illustrated in Fig. 3 plotted on the basis of data for high latitudes of the western hemisphere, where certain islands of the Canadian Arctic Archipelago were completely free of ice and some, for instance, Banks Island, were crowned with local ice caps (*Quaternary Stratigraphy...*, 1984; Dyke *et al.*, 1982; and personal observations of Velichko).

The Laurentide Ice Sheet was the largest in the western hemisphere and covered a considerable part of Canada and the United States; in the west, it made contact with the mountain glaciers of the Cordilleras. Debates concerning the width of the zone, which was free of ice during the Last Glacial Maximum, are now close to an end. It was apparently narrower than the width estimated on the basis of age data (results of ^{36}Cl dating) for erratic quartzite boulders collected inside the presumed 130-km-wide zone (Jackson *et al.*, 1997) zone.

The principal ice sheet of the southern hemisphere is that of Antarctica. As estimated (Kotlyakov, 1984; Heusser, 1989), during the Last Glacial Maximum it was no smaller in size than now; and according to results of the ANTOSTRAT project, the ice thickness in the peripheral zones, for instance, in the Ross Ice Shelf, was even greater (Cooper *et al.*, 1995). Geochronology of the glaciation stages in this hemisphere is elucidated to a lesser extent than in the northern one. According to data published in the volume *Quaternary Glaciations in the Southern Hemisphere* (1990), glaciers were most widespread in the mountain systems of Tasmania, Australia, and Africa prior to the Last Glacial Maximum. A significant advance of glaciers in the period of 24–18 ka is recorded only in Patagonia and New Zealand. In South America, glaciation maximums were asynchronous in different regions. In the northern and central Andes, glaciers were most abundant between 34 and 27 ka. In the equatorial Andean province, terminal zones of glaciers were situated 1000 m below their present position, and the snow line lowered by 800 m and more (Clapperton, 1993). Later, in the period 25–12 ka, the climate here was cold and arid and this activated diluvial and eolian processes. In the southern Andes accessible to oceanic moisture, glaciation was most intense during the Last Glacial Maximum; its peak was thus concurrent with glaciations in the northern hemisphere and western Antarctica (Fig. 4). Quite reliable dates are known for glaciation maximums in the mountain systems of Chile (20–19 ka ago) and Tasmania (21–19 ka ago). Recent observations in a central part of the Argentine–Chilean Andes showed that the glacier of the Rio Mendoza valley advanced 22 km southward and 1000 m downward from its present terminus in the period 24.2–2 ka (Espizua, 1993). In Bolivia and Peru, similar events took place later, soon after the Last Glacial Maximum.

In general, the inferable ice sheets of the Last Glacial Maximum had separate cupolas, whose dynamics was autonomous, especially during the deglaciation stages.

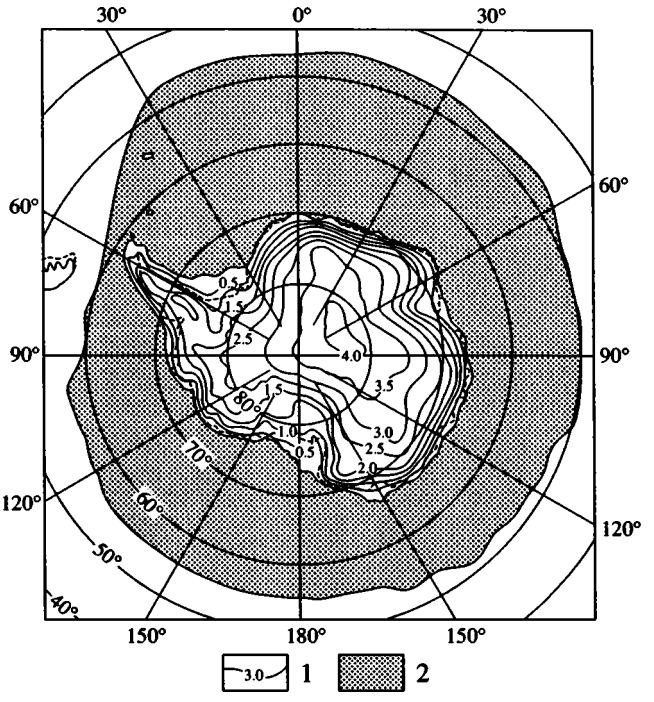

Fig. 4. Antarctic Ice Sheet during the Last Glacial Maximum (17–21 ka ago): (1) ice thickness, km; (2) distribution area of shelf ice sheets and ice floes.

New paleoglaciology data were used to plot the chart of the main glaciation regions (Fig. 5) and to calculate areas and volumes of the glaciers at the time of the Last Glacial Maximum (20–18 ka ago) in order to compare them with available parameters based on different paleoglaciological models. Volumes of Scandinavian and Laurentide Ice Sheets, whose surface morphology is known, are calculated using the equation suggested by Suetova (1982):

$$V = 2/35H - SH_{av}, \quad (1)$$

where S is the ice sheet area, H is its maximum height above sea level, and H_{av} is the average height of relief below the ice sheet.

If only the distribution area of the glaciers was known, we used an empirical formula relating this parameter to the volume:

$$\log V = 1.23(\log S - 1). \quad (2)$$

Precision of the calculations based on both formulas is estimated to be about 20%. Comparison of our results with published data shows that the total land area covered with glaciers was 8000 km^2 less than that accepted in alternative models (see Table 1).

Comparing our appraisals on ice volumes, which take into account all recent results of paleoglaciology, with data based on the model of the Panarctic Ice Sheet, we can naturally see the greatest discordance in the case of Eurasia. The difference in ice volumes for this continent approaches 60%, if the Novaya Zemlya

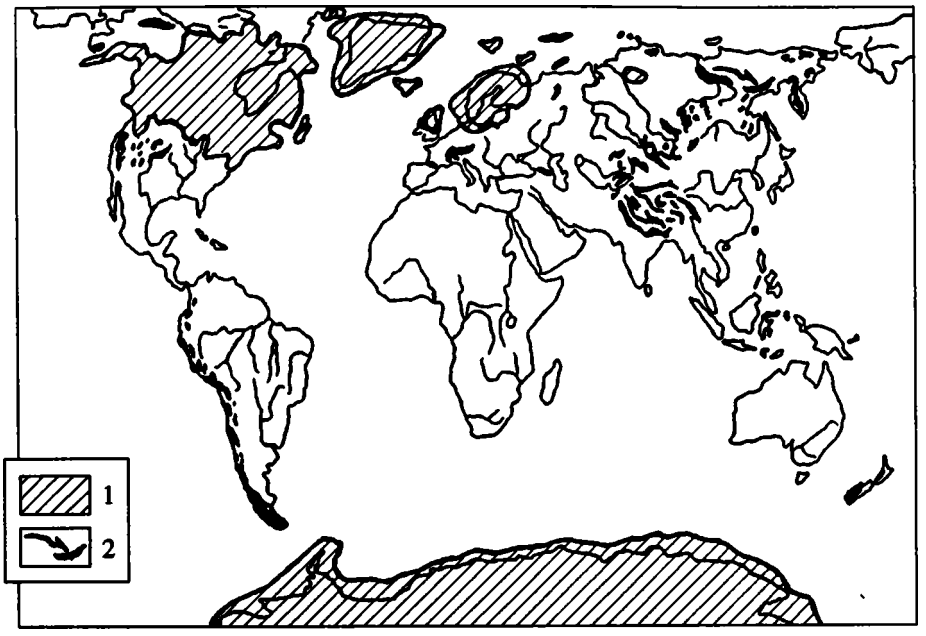

Fig. 5. Glaciation regions of the Earth during the Last Glacial Maximum (18–20 ka ago): (1) ice sheets; (2) mountain glaciers.

Ice Sheet (volume 0.69 million km^3 and area 562.8 thousand km^2) is not excluded from consideration (Velichko *et al.*, 1997). According to our calculation results, the total ice volume in the northern hemisphere was 10 million km^3 less than in the alternative model; but when we compare the global data, the discordance almost disappears. This reflects the fact that the volume of the Antarctic Ice Sheet accepted in the model of "extreme glaciation" is 11 million km^3 less than that calculated on the basis of new glaciological data. If we add this volume to the global value characterizing the extreme model, the result will be close to 89 million km^3, which is inconsistent with the water volume extracted from the global ocean according to the maximum sea-regression marks at the level of –130 m.

Degradation of last glacial systems in the northern hemisphere is divisible into stages (Fig. 6) characterizing different types of deglaciation (Faustova, 1994). At the first stage, lobes of the Scandinavian Ice Sheet retreated progressively and almost synchronously until 15 ka ago and the regressive type of deglaciation prevailed here. The Laurentide Ice Sheet was more mobile than that of Scandinavia, as it is evident from the extent of lobes' regression and also from their oscillatory movements within the time interval of 20–15.5 ka.

Significant changes in the balance of large glaciers took place after the time mark of 15 ka (second stage), when shearing of the ice-sheet margin was very intense in the western sector of the Laurentide Ice Sheet southern slope. Between 15 and 14 ka ago, the edges of this sheet always pulsated and its individual lobes advanced 150–600 km outside the frontal line forming the very diverse relief that consists of a mosaic of characteristic glacial forms. For instance, N. Rutter and T. Little demonstrated to one of us a perfect drumlin belt and channels of ice water discharge during a field excursion of 1997 in the Red Deer River valley (Alberta, western Canada).

At nearly the same time (about 15.5 ka ago), the Scandinavian Ice Sheet advanced forward in its western and central sectors with numerous oscillating tongues, which left a series of terminal moraines and related ice-water surface levels.

From the terminal substage of the second deglaciation stage (Older Dryas about 13 ka ago), the oscillatory dynamics of the marginal ice-sheet zones were complicated further, because ice shearing in individual glaciers and their lobes developed under conditions of climatic fluctuations. Development regimes of cupolas in the Laurentide Ice Sheet were surprisingly diverse. Between 13 and 12.5 ka ago, glaciers of the sheet actively advanced at least twice. In the Atlantic sector (St. Lawrence Lowland, Atlantic coastal areas, and surroundings of Lake Michigan), there are also traces of ice progradation. Two aggradation phases are recorded along the western periphery of the Laurentide shield in the contact zone with glaciers that descended from the Rocky Mountains in the south of Alberta. In other areas (e.g., southwestern Dakota), regressive deglaciation sequentially developed. These opposite trends of glaciation dynamics reflect the different reaction of glaciers to climatic fluctuations in humid perioceanic and relatively arid continental regions. In the last case, records of glacial rhythms are somewhat veiled; a good example is the Scandinavian Ice Sheet. A minor ice-shearing phase of the sheet about 13 ka ago is well recorded in

Table 1. Areas and volumes of ice accumulated in terrestrial regions during the Last Glacial Maximum 18–20 ka ago

Glaciation regions	This work		Suetova (1982)	
	Area, thousand km^2	Volume, million km^3	Area, thousand km^2	Volume, million km^3
EURASIA				
Scandinavian Ice Sheet	2748	4.8	3343	6.1
British Ice Sheet	399	0.45	582	0.8
Barents Ice Sheet	42.8	0.69	2135	4.0
Kara Ice Sheet	–	–	1614	2.4
Uralian ice sheet	–	–	196	0.1
Putorana Ice Sheet	101.6	0.08	500	0.6
Spitsbergen Ice sheet	115	0.1	–	–
Franz Josef Land Ice sheet	80	0.06	–	–
Mountain Glaciers of northeastern Russia, Siberia, the Far East, Central Asia, Europe, and the Himalayas	1178.9	0.59	707 (only for Siberia, northeastern Russia, and the Far East)	0.7
Mountain Glaciers of southern Eurasia	–	–	1470	1.4
In total	4665.3	6.1	11084	16.5
NORTH AMERICA				
Laurentide Ice Sheet	10991.6	26.95	12462	27.5
Ice sheet of Cordilleras	1512	1.5	2060	2.0
Greenland Ice Sheet	2296.8	3.9	2977	3.7
Innuithish Ice Sheet	–	–	822	1.0
Newfoundland Ice sheet	96.4	0.07	–	–
Glaciation in the Canadian Arctic Archipelago	265.5	0.2	–	–
Mountain glaciers of the following regions:				
Alaska	630	0.6	–	–
Western United States	100	0.1	–	–
In total	15892.3	33.3	18321	34.2
NORTHERN HEMISPHERE IN TOTAL	20557.6	39.4	29405	50.7
SOUTH AMERICA	634.8	0.4	830	0.83
New Zealand, Australia, Tasmania, and Africa	38.5	0.04	0.471	0.001
ANTARCTICA	14500	37.7	13200	25.95
SOUTHERN HEMISPHERE IN TOTAL	15174.3	38.14	14030	26.78
LAND REGIONS IN TOTAL	35730.9	77.5	43435	77.5

the south and southwest of Sweden (Low Baltic phase), northwestern (phase D) and southern (Lista phase) Norway, and also in the British Isles. The regime of predominant regressive deglaciation of the Scandinavian Ice Sheet began about 12.7 ka ago and included more or less extended periods of stagnation of the retreating sheet's edges.

The period from 12.9–12.7 to 10.8–10.3 ka (late Glacial or Younger Dryas) corresponds to the time of quick contraction of large ice sheets in the northern hemisphere. At that time the impulsive Laurentide Ice Sheet became almost two times smaller in area. The general trend of its contraction was irregular and included quick phases of ice movement (surges) in some lobes (*Late Quaternary...*, 1983). For instance, the Ontario and Erie lobes showed a progradation phase between 12.7 and 12.6 ka ago, whereas the Huron, Michigan, and Green Bay lobes pulsated two or three times between 12.9 and 11.6 ka ago. The Scandinavian Ice Sheet contracted steadily and retreated from the Baltic Sea area into the mountain regions of Scandinavia (*Paleogeografiya...*, 1982; Raukas, 1992).

In mountains of North America between British Columbia and Alberta (north of latitude 47°N), the size fluctuations of glaciers were insignificant between 12 and 11 ka ago; their edges approached or retreated from

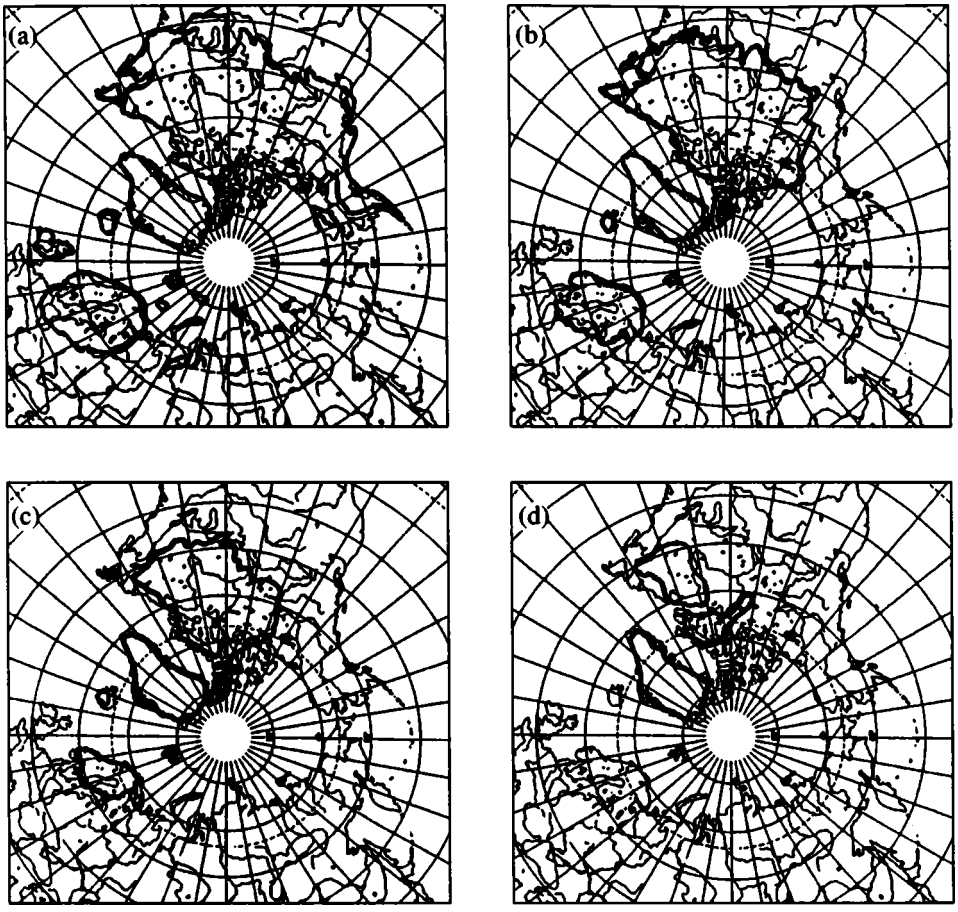

Fig. 6. Dynamics of deglaciation in the northern hemisphere: (a) 18–20 ka ago; (b) 13 ka ago; (c) 10 ka ago; (d) 7 ka ago.

their present position within a distance of few dozen kilometers. These fluctuations were at a minimum in the period of 11–10 ka, when the total glaciation area was less here than now. In the Sierra Nevada of California, the ice movement phase, well known as the "Recess Peak" and formerly attributed to the Holocene, actually happened, according to new tephrochronological and radiocarbon dates, between 13.1 and 11.2 ka ago. As a point of interest, it followed the phase of complete deglaciation. Two glacier progradation events are recorded for the Younger Dryas in this region (Osborn *et al.*, 1995).

During the general contraction of glaciation areas in the southern hemisphere between 18 and 13.5 ka ago, some local glaciers pulsated in size, sometimes to a considerable extent. For instance, in the Alpine system of New Zealand and also in the Peruvian and Chilean Andes, an important readvance of glaciers between 15 and 14 ka ago is recorded (Clapperton, 1993). The event was most significant in southeastern Peru.

In order to understand the contraction degree of glaciation areas in the northern hemisphere from 13 ka to the Younger Dryas, we used the glaciation charts of Canadian and American researchers (*Quaternary Stratigraphy of Canada...*, 1984; *Quaternary Glaciations...*, 1986), which illustrate how the edge of the Laurentide Ice Sheet retreated after each millennium. In addition, we analyzed the model of the last deglaciation period suggested by Faustova on the basis of orig-

Table 2. Changes in ice sheet size during deglaciation

Ice sheet	12 ka ago		10 ka ago	
	area, thousand km^2	volume, million km^3	area, thousand km^2	volume, million km^3
Laurentide	7750	13183	3690	7079
Scandinavian	1850	3020	1002	1412

inal and published data. Results of our calculations are presented in Table 2.

ACKNOWLEDGMENTS

The work was supported by the Ministry of Science and Technology of the Russian Federation, theme 08.01.04, project 4.5.2, and by the Russian Foundation for Basic Research, project nos. 97-05-64490 and 96-05-65487.

Reviewers S.A. Arkhipov and M.N. Alekseev

REFERENCES

Arkhipov, S.A., The Late Zyryanka (Sartana) Glaciation: Stratigraphy and Ice Sheet Distribution, in *Paleogeografiya Zapadno-Sibirskoi ravniny v maksimum pozdnezyryanskogo oledeneniya* (Paleogeography of West Siberia at the Peak of Late Zyryanka Glaciation), Novosibirsk: Nauka, 1980, pp. 7–12.

Arkhipov, S.A., Late Pleistocene Stratigraphy and Paleogeography of the Northern Part of the West Siberian Plain, *Razvitie landshaftov i klimata Severnoi Evrazii* (Development of Landscapes and Climate in Northern Eurasia), Velichko, A.A., Ed., Moscow: Nauka, 1993, pp. 28–32.

Astakhov, V.I., New Data on the Latest Activity of Kara Shelf Glaciers in West Siberia, *IGCP Project 73/1/24. Quaternary Glaciations in the Northern Hemisphere*, Prague, 1979, pp. 22–31.

Astakhov, V.I., The Last Ice Sheet of the Kara Sea: Terrestrial Constraints on Its Age, *Quat. Int.*, 1998, vol. 45/46, pp. 19–28.

Astakhov, V.I. and Isaeva, L.L., Radiocarbon Age of the Last Glaciation in the Lower Courses of the Yenisei River, *Dokl. Akad. Nauk SSSR*, 1985, vol. 283, no. 2, pp. 438–440.

Bischof, J., Lund, G., and Ecke, H., Palynomorphs of Ice-Rafted Clastic Sedimentary Rocks in Late Quaternary Glacial Marine Sediments of the Norwegian Sea as Provenance Indicators, *Palaeogeogr. Palaeoclimatol. Palaeoecol.*, 1996, vol. 129, nos. 3–4, pp. 329–360.

Boulton, G.S., Peacock, J.D., and Sutherand, D.G., Quaternary of Scotland, *Geology of Scotland*, Craid, G.Y., Ed., London: Geol. Soc. London, 1991, pp. 117–124.

Chaltieri, L., Brigham-Grette, G., Mostoller, D., *et al.*, Abstracts of Papers, *27th Arctic Workshop*, Lewkowicz, A. and Kokelj, S., Eds., Ottawa: Univ. of Ottawa, 1997, pp. 95–96.

Chetvertichnye oledeneniya na territorii SSSR (Quaternary Glaciations in the USSR Territory), Moscow: Nauka, 1987.

Clapperton, M.C., Nature of Environmental Changes in South America at the Last Glacial Maximum, *Palaeogeogr. Palaeoclimatol. Palaeoecol.*, 1993, vol. 101, pp. 189–208.

Cooper, A., Webb, P., and Brancolini, G., Studies Made in Understanding Antarctic Stratigraphy and Cenozoic Glacial History, *EOS*, 1995, vol. 76, no. 10, pp. 97–110.

Denton, Y.H. and Hughes, T.V., *The Last Great Ice Sheets*, New York, 1981.

Dyke, A.S., Dredge, L.A., and Vincent, J.S., Configuration and Dynamics of Laurentide Ice Sheet during the Late Wisconsin Maximum, *Geogr., Phys., Quat.*, 1982, vol. 36, nos. 1–2, pp. 5–14.

Espizua, L.E., Quaternary Glaciations in the Rio Mendoza Valley, Argentine Andes, *Quaternary Res.*, 1993, vol. 40, no. 2, pp. 150–162.

Faustova, M.A., Deglaciation and Glacial Relief Types in the European Part of Russia, *Paleogeograficheskaya osnova sovremennykh landshaftov (rezul'taty russko-pol'skikh issledovanii)* (Paleogeographic Base of Recent Landscapes: The Results of Russian–Polish Investigations), Velichko, A.A. and Starkel, L.M., Eds., St. Petersburg: Nauka, 1994a, pp. 30–40.

Faustova, M.A., Deglaciation Rhythms at the Pleistocene–Holocene Boundary, in *Korotkoperiodnyye i rezkie landshaftno-klimaticheskie izmeneniya za poslednie 15000 let* (Short-Term and Contrast Landscape–Climatic Changes during the Last 15000 Years), Moscow: Inst. Geogr. Ross. Akad. Nauk, 1994b, pp. 94–103.

Forman, S.L., Lubinski, D., Miller, G.H., *et al.*, Postglacial Emergence of Western Franz Josef Land, Russia, and Retreat of the Barents Sea Ice Sheet, *Quat. Sci. Rev.*, 1996, pp. 44–61.

Forman, S.L., Weihe, R., Lubinsky, D., *et al.*, Holocene Relative Sea-Level History of Franz Josef Land, Russia, *Bull. Geol. Soc. Am.*, 1997, vol. 109, no. 9, pp. 1116–1133.

Gataulin, V. and Forman, S., Abstracts of Papers, *27th Arctic Workshop*, Lewkowicz, A. and Kokelj, S., Eds., Ottawa: Univ. Ottawa, 1997, p. 78.

Grosval'd, M.G., *Pokrovnye ledniki kontinental'nykh shel'fov* (Ice Sheets of Continental Shelves), Moscow: Nauka, 1983.

Heusser, C., Polar Perspective of Late-Quaternary Climates in the Southern Hemisphere, *Quat. Res.*, 1989, vol. 32, no. 1, pp. 60–71.

Jackson, L.E., Phillips, F.M., Shimamura, K., and Little, E.C., Cosmogenic ^{36}Cl Dating of the Foothills Erratic Train, Alberta, Canada, *Geology*, 1997, vol. 25, no. 3, pp. 195–198.

Knies, J., Weiel, D., Niessen, F., and Stein, R., Abstracts of Papers, *First Annual Workshop of the EST Scientific Program "Quaternary Environment of the Eurasian North (QUEEN),"* Strasburg, Geomar, 1996, pp. 63–64.

Kotlyakov, V.M., Recent Antarctic Glaciations, in *Glyatsiologicheskii slovar'* (Glossary of Glaciology), Moscow: Gidrometeoizdat, 1984.

Landvik, J.V., Bondevik, S., Elverhoi, A., *et al.*, The Glacial Maximum on Svalbard and the Barents Sea Area: Ice Sheet Extent and Configuration, *Quat. Sci. Rev.*, 1998, vol. 17, pp. 43–75.

Landvik, J.Y., Hansen, A., Kelly, M., *et al.*, The Last Deglaciation and Glaciomarine–Marine Sedimentation on Barentsoya and Edgeoya, Eastern Svalbard, *LUNDQUA Rep.*, 1992, vol. 35, pp. 61–84.

Late Quaternary Environments of the United States, 2 vols., Wright, H.E. and Porter, S.L., Eds., Minneapolis: Univ. of Minnesota Press, 1983. Translated under the title *Prirodnye usloviya SShA v pozdnechetvertichnoe vremya*, Moscow: Gidrometeoizdat, 1986.

Lehmkuhl, F., Abstracts of Papers, *Meeting on IGCP Project 253 "Termination of the Pleistocene," June 26–28, 1993*, Winnipeg, 1993, p. 30.

Lubinski, D.J., Forman, S.L., and Miller, G.H., Holocene Glacier and Climate Fluctuations of Franz Josef Land, Arctic Russia, *Quat. Sci. Rev.*, 1998, vol. 14, no. 80, pp. 1–22.

Malyasova, E.S. and Serebryannyi, L.R., Natural History of the Novaya Zemlya, *Novaya Zemlya* (The Novaya Zemlya),

Boyarskikh, V.V., Ed., Moscow: Inst. Kul't. Prir. Naslediya, 1993, vol. 2, pp. 10–22.

Mangerud, J., The Early and Middle Weichselian in Norway: A Review, *Boreas*, 1981, vol. 10, pp. 381–383.

Mangerud, J., Dokken, T., Hebbeln, D., *et al.*, Fluctuations of the Svalbard–Barents Sea Ice Sheet during the Last 150000 Years, *Quat. Sci. Rev.*, 1998, vol. 17, nos. 1–3, pp. 11–42.

Mangerud, J., Svendsen, J.-I., Astakhov, V.I., and Tveranger, J., Abstracts of Papers, *First Annual Workshop of the EST Scientific Program "Quaternary Environment of the Eurasian North (QUEEN),"* Strasburg, Geomar, 1996, pp. 81–82.

Matiouchkov, A. and Astakhov, V., Abstracts of Papers, *First Annual Workshop of the EST Scientific Program "Quaternary Environment of the Eurasian North (QUEEN),"* Strasburg, Geomar, 1996, pp. 84–85.

Musatov, E.E., Abstracts of Papers, *Vserossiiskoe soveshchaniye "Glavneishie itogi v izuchenii chetvertichnogo perioda i osnovnye napravleniya issledovanii v XXI veke"*, (All–Russia Conf. "Principal Advances in Quaternary Research and Main Lines of Investigation in XXI Century"), St. Petersburg: Vseross. Geol. Inst., 1998, p. 202.

Nissen, F., Weiel, D., Ebel, T., *et al.*, Abstracts of Papers, *First Annual Workshop of the EST Scientific Program "Quaternary Environment of the Eurasian North (QUEEN),"* Strasburg, Geomar, 1996, pp. 90–91.

Osborn, G., Clapperton., M.C., Davis,. P.T., *et al.*, Potential Glacial Evidence for the Younger Dryas Event in the Cordillera of North and South America, *Quat. Sci. Rev.*, 1995, pp. 823–832.

Palaeogeographic Atlas of the Shelf Regions of Eurasia for the Mesozoic and Cenozoic, Alekseev, M.N., Ed., Llandudno: Robertson Group, 1996.

Paleoclimates and Paleoenvironment of the Northern Hemisphere (Late Pleistocene–Holocene), Stuttgart: Gustav Fisher, 1992.

Paleogeografiya Evropy za poslednie sto tysyach let (Atlas-monografiya) (European Paleogeography during the Last 100000 Years: Atlas and Monograph), Moscow: Nauka, 1982.

Pavlidis, Yu.A., *Shel'f mirovogo okeana v pozdnechetvertichnoe vremya* (The World Ocean Shelf in the Late Quaternary Time), Moscow: Nauka, 1992.

Peltier, W.R., Ice Age Paleotopography, *Science*, 1994, vol. 265, pp. 195–201.

Peltier, W.R., Mantle Viscosity and Ice-Age Ice Sheet Topography, *Science*, 1996, vol. 273, pp. 1359–1364.

Polyak, L., Abstracts of Papers, *First Annual Workshop of the EST Scientific Programme "Quaternary Environment of the Eurasian North (QUEEN),"* Strasburg: Geomar, 1996, pp. 101–103.

Quaternary Glacial Distribution Map of the Qinghai–Xizang Plateaux Tibet, Binynan, L. and Tijun, L., Eds., Beijing: Science., 1991.

Quaternary Glaciations in the Northern Hemisphere, Sibrava, V., Bowen, D.Q., and Richmond, G.M., Eds., Oxford: Pergamon, 1986.

Quaternary Glaciations in the Southern Hemisphere, Clapperton, C. M., Ed., *Quat. Sci. Rev*, 1990, vol. 9, nos. 2–3.

Quaternary Stratigraphy, Glacial Morphology, and Environmental Changes, Robertson, A.V., Ed., Uppsala, 1992.

Quaternary Stratigraphy of Canada: Canadian Contribution to IGCP Project 24, Fulton, R.J., Ed., Ottawa: Geol. Surv. Can., 1984.

Raukas, A., Ice Marginal Formations of the Palivere Zone in the Eastern Baltic, *Sver. Geol. Unders.*, 1992, vol. 81, pp. 277–284.

Rutter, N., Pleistocene History of the Western Canadian Ice-Free Corridor, in *Quaternary Stratigraphy of Canada: Canadian Contribution to IGCP Project 24*, Fulton, R.J., Ed., Ottawa: Geol. Surv. Can., 1984, pp. 49–56.

Serebryanny, L., Andreev, A., Malyasova, E., *et al.*, Late Glacial and Early-Holocene Environments of Novaya Zemlya and the Kara Sea Region of the Russian Arctic, in *Holocene Research Papers*, 1998, pp. 323–329.

Siegert, Ch. and Romanovksy, N.N., Abstracts of Papers, *First Annual Workshop of the EST Scientific Program "Quaternary Environment of the Eurasian North (QUEEN)"*, Strasburg, Geomar, 1996, pp. 122–123.

Suetova, I.A., Areas and Volumes of the Quaternary Ice Sheets of the Earth, in *Geograficheskie issledovaniya chetvertichnogo perioda* (Study on Quaternary Geography), Moscow: Mosk. Gos. Univ., 1982, pp. 22–33.

Svendsen, J.I., Astakhov, V.I., Bolshiyanov, D.Yu., *et al.*, Maximum Extent of the Eurasian Ice Sheets in the Barents and Kara Sea Region during the Weichselian, *Boreas*, 1999, vol. 28, no. 1, pp. 234–242.

Tveranger, J., Astakhov, V., and Mangerud, J., The Margin of the Last Barents–Kara Ice Sheet at Markhida, Northern Russia, *Quat. Res.*, 1995, vol. 44, no. 3, pp. 328–340.

Velichko, A.A., Tendency of Glaciation Development in Northern Eurasia and Methods of Investigation, in *Chetvertichnye oledeneniya na territorii SSSR* (Quaternary Glaciations in the USSR Territory), Moscow: Nauka, 1987, pp. 8–13.

Velichko, A.A., Borisova, O.K., and Kremenetskii, K.V., Migrations of the Tundra–Forest Boundary according to Climatic Changes, *Priroda*, 1997, no. 2, pp. 34–40.

Velichko, A., Kononov, Yu., and Faustova, M., The Last Glaciation of Earth: Size and Volume of Ice-Sheets, *Quat. Int.*, 1997, vols. 41–42, pp. 43–51.

Velichko, A.A., Kononov, Yu.M., and Faustova, M.A., The Last Glaciation of the Late Pleistocene in the Earth, *Priroda*, 1994, no. 7, pp. 63–67.

Velichko, A.A. and Faustova, M.A., Model Schemes of Last Glaciation in the Northern Hemisphere during the Late Pleistocene (18000–20000 Years Ago), *Dokl. Akad. Nauk SSSR*, 1989, vol. 309, no. 6, pp. 1465–1468.

Yubbrten., H.-W., Melles, M., Siegert, C., and Bolshiyanov, D.Yu., Abstracts of Papers, *First Annual Workshop of the EST Scientific Program "Quaternary Environment of the Eurasian North (QUEEN)"*, Strasburg, Geomar, 1996, p. 17.

Zale, R. and Brydsten, L., The Pre-Holocene Marine Limit on Hopen, Svalbard, *Boreas*, 1993, vol. 22, pp. 159–164.

Zheng Benhing, Controversy Regarding the Existence of Large Ice Sheet on the Qinghai–Xizang (Tibet) Plateau during the Quaternary Period, *Quat. Res.*, 1989, vol. 32, no. 1, pp. 121–123.

Stratigraphy and Geological Correlation, Vol. 8, No. 1, 2000, pp. 13–29. Translated from Stratigrafiya. Geologicheskaya Korrelyatsiya, Vol. 8, No. 1, 2000, pp. 17–34.
Original Russian Text Copyright © 2000 by Maslov.
English Translation Copyright © 2000 by MAIK "Nauka/Interperiodica" (Russia).

Middle Riphean Sedimentary Basin in the Junction Area between the Russian Platform and South Urals: Lithology, Facies, Paleogeography, and Evolutionary Trend

A. V. Maslov

Institute of Geology and Geochemistry, Uralian Division, Russian Academy of Sciences, Pochtovyi per. 7, Yekaterinburg, 620151 Russia

Received January 27, 1998; in final form, May 14, 1998

Abstract—The paper considers the structure, lithology, and facies characteristics of the Yurmatin and Serafimovka groups of the Bashkir meganticlinorium and Volga–Urals region. The analyzed distribution schemes of facies associations and complexes are plotted, based on these data, for the accumulation periods of the Zigal'ga, Tukaevo, Zigazino–Komarovo formations, Akberdino Horizon, and Avzyan and Ol'khovka formations. Accumulation of thick volcanogenic and siliciclastic, mainly peritidal deposits in the easternmost areas was characteristic of the initial stages of the basin's evolution (approximately 1.34–1.35 Ma ago). The westerly areas represented at that time an elevated and differentiated land, whose eastern boundaries are marked by large lenses and beds of pebble–boulder conglomerates. In the mid-Middle Riphean time, sediments accumulated mainly in shallow-water, often well-aerated settings. In the paleogeographic aspect, the basin of this period probably represented a sea with flat bottom surrounded by islands. By the end of the Middle Riphean, the expanding transgression resulted in accumulation of several carbonate successions, mostly consisting of subtidal and moderately deep-water sediments in the eastern areas, which graded westward into siliciclastic associations of shallow and very shallow settings.

Key words: *Middle Riphean, sedimentary basin, Volga–Urals region, western slope of the southern Urals.*

INTRODUCTION

The growing interest of Russian researchers in the Late Precambrian evolutionary patterns of sedimentary basins and peculiar accumulation history of thick sedimentary successions of this time period (Veis and Semikhatov, 1989; Petrov, 1993; Maslov, 1994, 1995, 1997a, 1997b; Veis and Petrov, 1994, Khabarov, 1994; Petrov and Veis, 1995; Surkov *et al.*, 1996; Olovyanishnikov, 1997; Petrov and Semikhatov, 1997; Sovetov, 1997; and others) demonstrates the progress in joint application of stratigraphic, sedimentological, lithological–geochemical, and geophysical, particularly seismic profiling, data. These data together with the isotopic–geochronological database for the Upper Precambrian lithostratigraphic units, which might be obtained in the future, may be used as a substantial basis for comprehensive basin analysis. Another important aspect of the problem was clearly outlined by Surkov *et al.* (1993): "The occurrence of oil and gas deposits in the Riphean basins of passive margins of the Siberian craton is a serious guide for geological prospecting aimed at the study of Riphean geology and oil and gas potential of the East European platform." A significant success is evident now in the understanding of the Riphean sequences of Siberia and the Riphean stratotype on the western slope of the South Urals.

The comprehensive geophysical investigation in the Volga–Urals region carried out several years ago (Lozin and Khasanov, 1991; Lozin 1994; and others), deep-drilling data (Isherskaya and Romanov, 1993; Romanov and Isherskaya, 1994a, 1994b, 1997, 1998; Kozlov *et al.*, 1995), and lithological–paleogeographic studies showed that the sedimentary succession of the Riphean stratotype is replaced in the westerly (platform) regions by thick rock sequences accumulated in the same sedimentary basin. The peculiar structure and evolution of the Early Riphean sedimentary basin were considered earlier (Maslov, 1994, 1995). In this paper, the structural–textural features, facies associations and their lateral and vertical distribution in the Middle Riphean sequences of the Volga–Urals region and Bashkir meganticlinorium are considered.

MIDDLE RIPHEAN LITHOSTRATIGRAPHY OF THE JUNCTION AREA BETWEEN THE RUSSIAN PLATFORM AND SOUTH URALS

Bashkir Meganticlinorium

The Yurmatin Group of the Bashkir meganticlinorium, which represents the Middle Riphean type, comprises four lithostratigraphic units (from the base upward): Mashak, Zigal'ga, Zigazino–Komarovo, and Avzyan formations. *The Mashak Formation* is exposed

only in the eastern limb of the Bashkir meganticlinorium. Its sections are mostly composed of fine- and medium-grained sandstones, greenish or lilac-gray, massive, and/or displaying the small- to medium-scale unidirectional cross-bedding. Sometimes, the rocks show molds of desiccation cracks and ripple marks. At some levels, massive (or vaguely banded) sandstones alternate with rock varieties characterized by cross, rectilinear, or flattened lamination. Locally, the rocks reveal trough- or wedgelike cross bedding, as well as reactivation structures. Sections of the formation include abundant conglomerate beds. The latter usually lack any bedding, although the thickest members of these rocks enclose some layers with large-scale cross-bedding and imbricate pebble arrangement or lentils of coarse-grained sandstones with unidirectional cross-bedding. The fragment size in the conglomerates ranges from 3 to 40 cm across; the extent of pebble concentration is very high. Pebbles and boulders are mainly represented by quartzite sandstones similar in their appearance to rocks of the Lower Riphean Yusha Formation (Anfimov *et al.*, 1978; Rotaru, 1983), whereas the diabase, siltstone, and carbonaceous–clayey shale fragments do not exceed 3–5% of their total coarse clastic fraction. The fragments are trihedral to polyhedral with well-rounded angles and also egg-shaped, spherical, and other in form. Siltstone, carbonaceous–clayey shale, and their alternating beds play a subordinate role in the sections of the Mashak Formation. Siltstone beds are either massive or show thin horizontal banding and sometimes thin lenticular to lenticular-sinuous lamination and lenticular cross-bedding. Bedding surfaces of siltstone layers sometimes bear small ripple and current marks. In some packets of alternating beds, there are desiccation cracks, although their most characteristic features are the gentle sinuous alternation of different lithological layers and sinuous, irregularly sinuous, and microconvolute lamination inside the layers. The thickness of the Mashak Formation varies from 1500 to more than 3000 m.

The Rb–Sr isochron age of acid volcanics from the Mashak Formation is 1341 ± 41 Ma, their U–Pb zircon age is 1348 ± 30 Ma (Krasnobaev *et al.*, 1985; Kozlov *et al.*, 1989).

The main rock types of *the Zigal'ga Formation* (550–700 m thick) are massive gray and light gray medium- to fine-grained sandstones. Less common are rocks displaying horizontal and multidirectional lamination of small and medium scale, ripple and current marks, primary current linearity, desiccation cracks, and intervals enriched in foliated shaly breccia. In the area of the Bakal siderite mines, the basal part of the formation encloses lenses of boulder–pebbly conglomerate. In the northeastern part of the Bashkir meganticlinorium, the formation rests with angular unconformity on the erosion surface of different members of the Lower Riphean Bakal Formation (Mochalova, 1957; Yanitskii and Sergeev, 1962; Garan', 1963). In the western limb of the Yamantau anticlinorium (central areas of the meganticlinorium), the Zigal'ga Formation transgressively overlies rocks of the Lower Riphean Yusha Formation, whereas in the eastern limb, it is conformably underlain by volcanogenic–terrigenous successions of the Mashak Formation.

The Zigazino–Komarovo Formation (1000–1200 m thick) is largely composed of silty–clayey rocks intercalated with sandstone, limestone, and dolomite interbeds. By lithology and rock coloration, it is subdivided into the Seregin, Ambarka, and Tukan subformations. The dark-colored rocks of the first and third subformation are enriched in finely dispersed carbonaceous material; in contrast, deposits of the Ambar Subformation are characterized by bluish or bluish gray shadowing. This level of the Riphean stratotype is marked by abundant packets and members of alternating layers (5–10 cm thick) of clayey and carbonaceous–clayey shale, sandstone, and siltstone. Thin horizontal to gentle sinuous bedding and fine or sinuous cross-lamination are characteristic of these layers (Maslov, 1991a). Some interbeds represent a combination of small lenses with symmetric and asymmetric ripple marks; multidirectional lamination is often visible in neighboring layers. The base of many thin (1–3 cm) sandstone and siltstone interbeds is marked by desiccation cracks. Some bed packets of this kind are represent the peculiar "worm rhythmites" (term of Maslov, 1991a), which show thin irregular alternation of siltstone and carbonaceous–clayey shale layers, where the primary bedding is strongly disturbed. Bed packets of another type lack structural features indicative of intermittent or frequent sediment desiccation and usually show fine (with intervals of 1–5 cm) gentle wavelike, or coarse (with intervals of 5–15 cm) alternation of layers with different lithology. Subordinate rock types of the Zigazino–Komarovo Formation are fine-grained siltstone and clayey or carbonaceous–clayey shales either massive or characterized by thin horizontal banding. In addition, there are interbeds of massive to fine-banded dolomite and limestone having an admixture of clayey–silty material and intercalated with thin packets and individual layers of clayey shale.

The Avzyan Formation (800–2000 m thick) is the terminal one in the section of the Yurmatin Group. It is divided into six subformations (*Stratotip rifeya...*, 1983; *Stratigraficheskie...*, 1993). O.P. Goryainova, E.A Fal'kova, A.I. Olli, Z.M. Starostina, M.I. Garan', and other researchers characterized siliciclastic and carbonate rocks of the formation in detail. At the stratigraphic level under consideration, there are abundant alternating packets of the following rocks: (1) sandstone, siltstone, and shale; (2) siltstone and shale; (3) low-carbonaceous fine-grained siltstone, limestone, and synsedimentary carbonate breccia with flat rock clasts. They all have variable structures and show thin horizontal bedding or fine, lenticular, and sinuous cross-lamination; ripple marks; and other features suggesting sedimentation in very shallow and shallow settings (Maslov, 1990, 1997b). Some sections of the for-

mation include abundant interbeds of fine-grained siltstone and shale, massive or with obscure fine lamination. Most carbonate rocks of the Avzyan Formation are represented by dolomites displaying a massive structure or obscure horizontal banding and enclosing stromatolitic beds and lenses; there are also intervals with troughlike, gentle wavelike, and cross lamination.

The K–Ar whole-rock age of gabbro–diabase dikes from the Middle Riphean sedimentary successions of the Bashkir meganticlinorium varies from 1000 ± 20 to 1080 ± 30 Ma (*Stratotip rifeya...*, 1983). The K–Ar age of authigenic glauconite from the Avzyan Formation, which had been determined at the beginning of the 1960s, is about 1220–1230 Ma (Garris *et al.*, 1964). However, the oldest age that was recently measured on glauconite from the Middle and Upper Riphean deposits of the stratotype section not exceed 800 Ma because of significant epigenetic recrystallization of this mineral (Gorozhanin, 1997) and, consequently, the quoted dates should be verified.

Junction area between the Volga–Urals region and Bashkir meganticlinorium

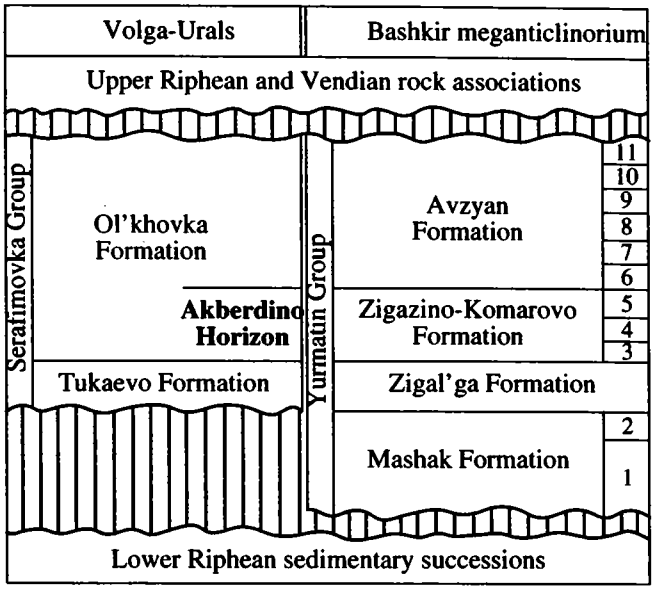

The Volga–Urals Region

In the Volga–Urals region, the Yurmatin Formation is correlative with sedimentary rocks of the Serafimovka Group drilled in the northern, eastern, and (partly) southern areas of Bashkortostan and in eastern Tatarstan (*Rabochaya skhema...*, 1981; Andreev *et al.*, 1981; Isherskaya and Romanov, 1993; Romanov and Isherskaya, 1998; and others). The basal layers of the Serafimovka Group rest transgressively upon different strata of the Lower Riphean Nadezhdino and Kaltasy formations and on rock of the crystalline basement (Isherskaya and Romanov, 1993). They are in turn overlain above the erosion surface by basal strata of the Upper Riphean Abdulino Group (Usa Formation) and sometimes by Upper Devonian sedimentary successions (table). The Middle Riphean in the Volga–Urals region corresponds to the Serafimovka Formation in terms of K.R. Temergazin, who subdivided it into two units: the lower sandy and upper carbonate–terrigenous sequences, which were subsequently ranked as the Tukaevo and Ol'khovka formations. Later, the Serafimovka Formation was ranked as a group, whereas its constituent units became regarded as autonomous formations. Based on lithological properties, Ozhiganova (1974) included the Usa Formation in the Serafimovka Group. Further study of cores from deep boreholes (North Kushkul' 1, Kushkul' 100, and others) showed that rocks of the Usa Formation are closely connected with rocks of the overlying Upper Riphean Leonidovka Formation and together form one formational complex (unpublished report by Morozov, 1972; Isherskaya and Romanov, 1993; Romanov and Isherskaya, 1997). This is evident from the similarity of the rock varieties, their position in the section, relationships with underlying and overlying sequences, and CDP records depicting these deposits as a single seismostratigraphic complex; and it is also confirmed by correlation with the Riphean stratotype deposits. Recently, these formations were renamed (*Novokipchak* and *Demino*, respectively) and characterized by new stratotypes (Romanov and Isherskaya, 1997, 1998), which, however, have been adopted to a limited extent at present. Therefore, the old formation names are used in this work.

The Tukaevo Formation in the platform part of Bashkortostan is largely represented by fine- to medium-grained feldspar–quartz arkose and quartz sandstones enclosing subordinate siltstone and shale interbeds. Sandstones are cherry-brown or light yellowish to pinkish gray and often contain lenses and pockets of gravel–pebble material with sporadic admixture of quartz grains 1.5 mm in size. Locally, they are intercalated with rocks displaying medium-scale cross or thin wavelike and cross-wavy bedding. Some sandstone layers enclose interbeds and lenses of coarse-grained quartz material displaying the troughlike or irregular wavy bedding. Pinkish gray inequigranular sandstones with angular, differently oriented dolomite fragments (from 3–5 mm to 2–3 cm) represent another variety of this lithotype. Siltstones are chocolate brown, cherry-gray, light gray or pinkish in color. They show obscure thin lamination and bear dispersed quartz grains from 0.5 to 1.5 mm in size. These rocks enclose gentle sinuous interbeds of silt and thin bands of gravel material, the intervals between which are equal to 5–6 cm. Some bedding planes of rocks are marked by pseudomorphs after halite. Pinkish to light gray massive siltstones enclose rare shale lentils and show an obscure banding. Another variety of cherry-gray siltstone exhibits abundant thin (fractions of a millimeter) laminae of crimson shales occurring at intervals of 2–5 mm and emphasizing fine gentle cross-lamination flattening toward the

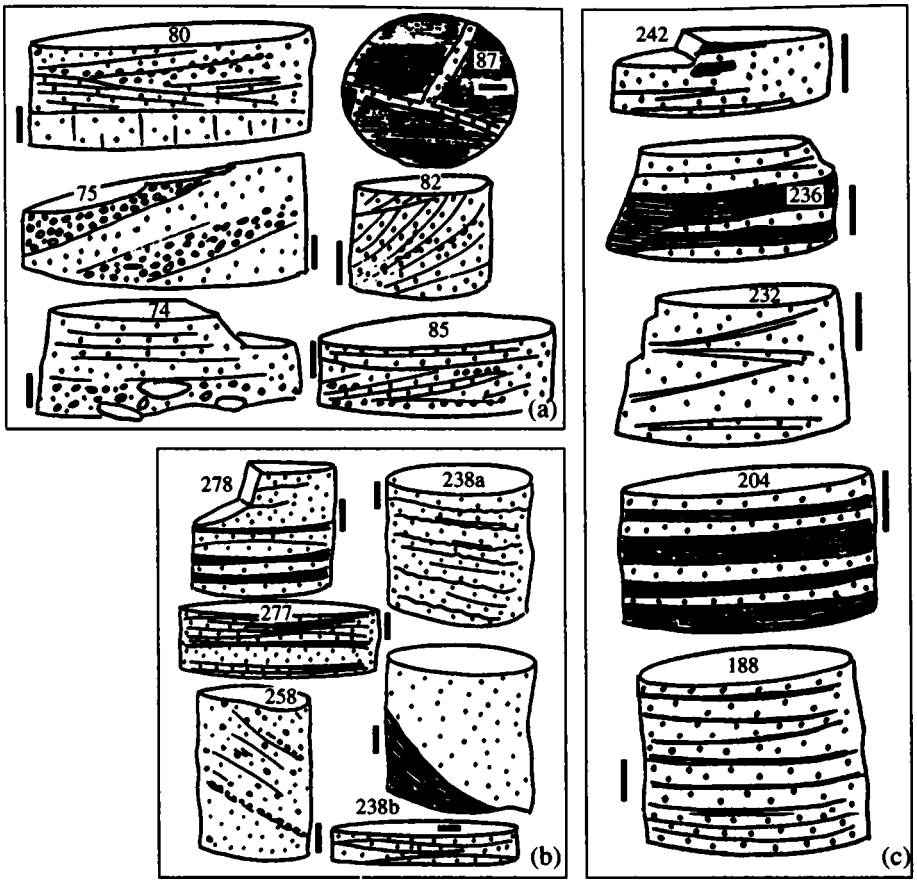

Fig. 1. Some structural features of rocks from the Tukaevo Formation of the Serafimovka Group, samples of borehole sections Asly-Kul' 4 (a), Kipchak 1 (b), and Kabakovo 62 (c). Hereinafter, sample numbers correspond to those collected by M.V. Isherskaya (Institute of Geology, Ufa Scientific Center, Russian Academy of Sciences); for sample positions in formation sections see Fig. 2. The scale bar is 1 cm.

base of the laminae. There are also dark greenish gray (rarely crimson) massive and thin-platy, obscurely banded siltstones. Their occasional light gray varieties with lilac shadowing show cuneate, multidirectional, and fine cross lamination; they enclose argillite plates. Silty shales are represented in the formation by dark gray or almost black massive low-carbonaceous varieties with obscure bands (2–3 mm thick), and also by greenish gray layers with thin irregular lentils of the silty material. In the last case, bedding planes are sometimes marked by pseudomorphs after halite. In many sections characteristic of the formation there are packets and members composed of the alternating lithotypes mentioned above and different in structure. Fig. 1 demonstrates some structural features of rocks from the Tukaevo Formation. Their distribution, lateral granulometric variations, and facies associations of the formation are shown in Fig. 2.

The Tukaevo Formation thickness is 465 m in the Asly-Kul' 4 borehole and grows to 630 m in the Kabakovo 62 borehole (Romanov and Isherskaya, 1997).

The K–Ar age of glauconite from sandstones of the lower part of the Tukaevo Formation is 1252–1297 Ma in the Serafimovka 119 borehole and 1286 Ma in the Leonidovka 352 borehole (Polevaya and Kazakov, 1961; Kazakov, 1963; Garris *et al.*, 1964; *Stratotip rifeya...*, 1983). Glauconites from sandstones of another locality (Kipchak 1 borehole) yielded the K–Ar age of 1253 ± 20 and 1274 ± 12 Ma (Romanov and Isherskaya, 1997).

The Ol'khovka Formation is connected with the Tukaevo Formation by a gradual transition. In most boreholes, the basal part of the formation corresponds to the so-called *Akberdino Horizon* (Andreev *et al.*, 1981; *Stratotip rifeya...*, 1983; Romanov and Isherskaya, 1998) represented by dark gray and almost black silty shales and argillites with rare siltstone interbeds. The thickness of the horizon varies from 40 to 70–80 m. Middle and upper parts of the formation are composed of argillites, marls, and dolomites with rare siltstone, sandstone, and gravelstone interbeds; these rocks are crimson, rose, or green in color.

Gravelstones are characterized by red and pinkish yellow to pinkish gray coloration and reveal gentle cross bedding with signs of rhythmic sorting of detrital material in laminae and the presence of rare small

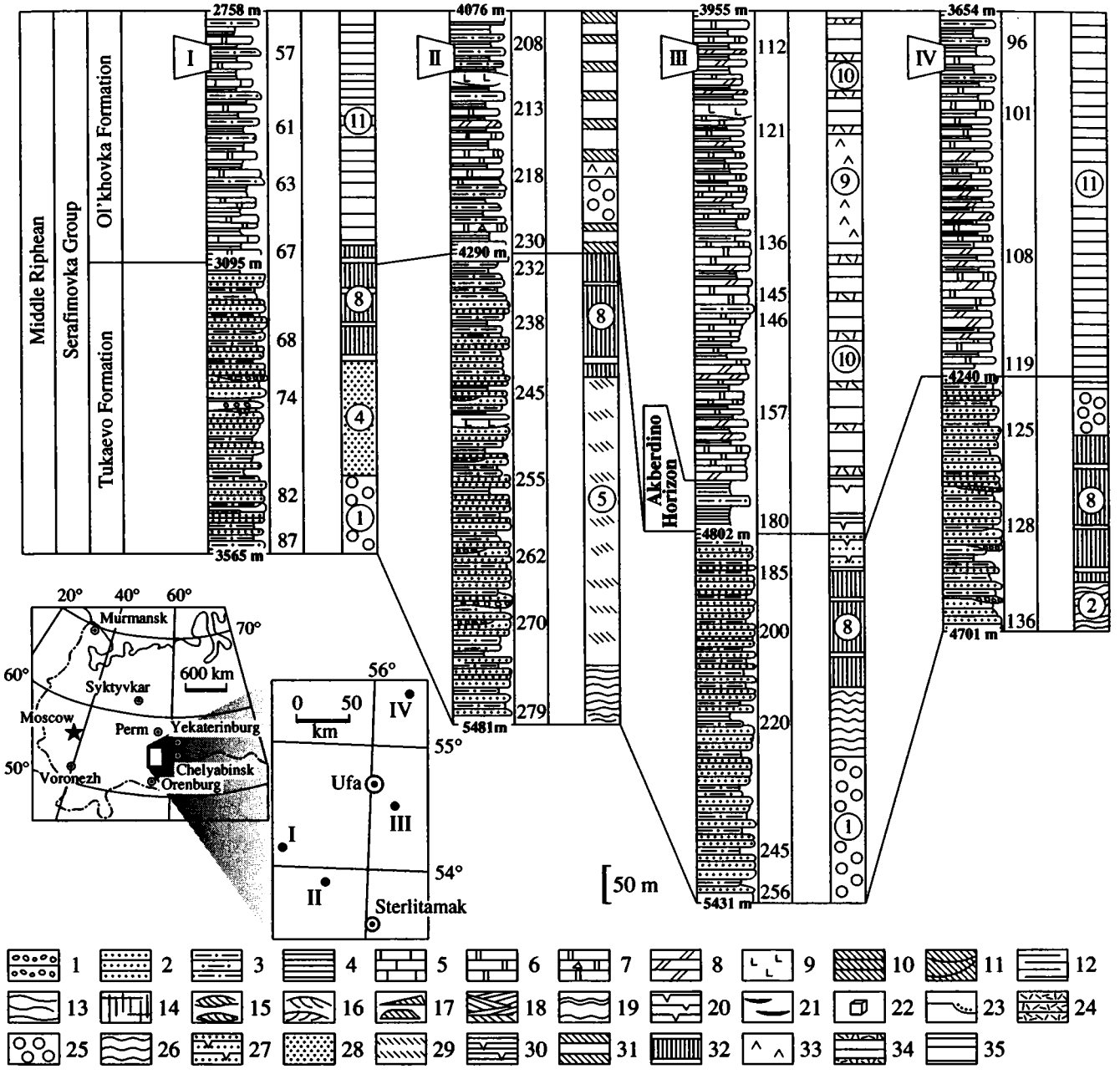

Fig. 2. Sections of the Serafimovka Group recovered from boreholes Asly-Kul' 4 (I), Kipchak 1 (II), Kabakovo 62 (III), and Kush-Kul' 100 (IV); structural features characterizing rocks from the Tukaevo and Ol'khovka formations and facies associations: (1) gravelstone, (2) sandstone, (3) siltstone, (4) argillite, (5) limestone, (6) dolomite, (7) synsedimentary dolomite breccia with flattened clasts, (8) dolomitic marl, (9) gabbro–diabase dikes, (10) unidirectional cross lamination of medium and small scale, (11) unidirectional troughlike cross lamination, (12) horizontal lamination and banding, (13) gentle and irregular wavy lamination, (14) intervals of massive structures, (15) fine wavy and troughlike cross lamination, (16) multidirectional wavy cross lamination, (17) sharp-crest and sinusoidal ripple marks (mainly small-scale and isolated), (18) fine symmetrical cuneate and multidirectional cross lamination, (19) sinusoidal asymmetric lamination, (20) desiccation cracks, (21) interbeds with indications of silting, (22) pseudomorphs after halite, (23) small scours (channels) and washout structures, (24) intervals of carbonate and shale breccia with platy clastics. Facies associations: (25) first, (26) second, (27) third, (28) fourth, (29) fifth, (30) sixth, (31) seventh, (32) eighth, (33) ninth, (34) tenth, (35) eleventh.

quartz pebbles. Sometimes, they show thin laminae of clayey material or plates of green shale. Their particular beds with obscure banding (the latter is mainly emphasized by variable granulometric characteristics of neighboring laminae, some of which consist of green shale dissected by desiccation cracks and occur at intervals of 1–3 cm) associate with coarse-grained sandstones displaying gentle cross bedding and bearing

small irregularly dispersed quartz pebbles. Laminae in these rocks are also variable in granulometric composition of their material. Fine-grained sandstones are chocolate brown or pinkish gray, mostly massive, and characterized by obscure gentle wavelike to striate bedding and cross lamination. Greenish to pinkish gray siltstones enclose interbeds with quartz grains (0.5–1 mm in size). The lithotype also includes chocolate and crimson massive siltstones with obscure banding and occasional argillite plates at the bedding surfaces. Chocolate brown silty shales often contain abundant small quartz pebbles. Additional rock types are foliated irregularly colored shales and greenish gray, somewhat irregularly colored argillites with slight bluish shadowing and chipping fracture. Structural features resembling those of desiccation cracks sometimes mark their bedding planes. Dark gray, almost black carbonaceous shales also occur in the formation.

Sections of the Ol'khovka Formation quite often consist of bed packets and members consisting of alternating lithotypes mentioned above and spanning intervals of several dozen meters. Most characteristic is thin ($n \times 1$ mm) gentle sinuous alternation of dark greenish gray or chocolate brown shale and pinkish or light gray siltstone. Relatively thick siltstone intercalations reveal gentle cross bedding; thinner interbeds show series of beaded lentils with distinct ripple marks. Pseudomorphs after halite may also be present in the latter and also occur in packets of irregularly alternating pinkish gray or cream-colored dolomite and fine-grained siltstone (cubes with facets from 1.5 to 2–3 mm across). Another type of thin alternation involves dark greenish and pinkish gray interbeds of silty shale and clayey(?) carbonate, which are separated by distinct even boundaries.

Carbonate rocks, mostly concentrated in the middle part of the Ol'khovka Formation, are clustered in several lithotypes. These are massive pelitomorphic or microcrystalline dolomites colored dark gray, gray, and cream-gray with slight greenish shadowing. Another lithotype includes greenish and crimson rocks, massive or with the thin diffuse banding; some dolomite varieties are clayey, intercalated with thin interbeds of crimson silty shale. The associated rocks are crimson clayey dolomites with thin, subhorizontal or irregular wavelike bedding, which is emphasized by shale interbeds or marly bands 1–3 mm thick. Some rock varieties have thin horizontal and gentle troughlike cross bedding. Subordinate carbonate deposits of the Ol'khovka Formation are lilac-gray, with a pale tint, microcrystalline limestones and irregularly colored (greenish gray, crimson, brown, and others) pelitomorphic microcrystalline dolomitic marls with obscure banding, sometimes sprinkled with clayey material at bedding planes. Some primary structures of sedimentary rocks from the Ol'khovka Formation are shown in Fig. 3.

The recovered thickness of the formation ranges from 340 m in the Asly-Kul' 4 borehole to 840 m in the Kabakovo 62 borehole. Toward the Urals, the thickness substantially increases; and, according to Romanov, who analyzed seismic profiling records, the formation is almost 2000–2200 m thick at the latitude of Sterlitamak.

Gabbro–diabases, which intruded the Ol'khovka Formation (Serafimovka 119 and Staro-Petrovo 5 boreholes), yielded the K–Ar age (whole-rock samples) of 1000–1050 to 1250 ± 50 Ma (Garris *et al.*, 1967; *Rabochaya skhema...*, 1981; *Stratotip rifeya...*, 1983; Romanov and Isherskaya, 1998).

The Tukaevo Formation of the Serafimovka Group in the Volga–Urals region is correlative with the Zigal'ga Formation of the stratotype section; the Akberdino Horizon of the Ol'khovka Formation corresponds to the Zigazino–Komarovo interval, whereas the middle and upper parts of the formation are equivalents of the Avzyan Formation (*Rabochaya skhema...*, 1981; Andreev *et al.*, 1981; Isherskaya and Romanov, 1993; Romanov and Isherskaya, 1994a, 1994b, 1997). This is substantiated by the following fact: (1) the deposits occur between two major stratigraphic unconformities in both regions; (2) the Tukaevo and Ol'khovka formations are similar in lithology to the Yurmatin Group;[1] (3) geochronological data are consistent with the suggested correlation; (4) the easternmost Riphean sections in the platform part of Bashkortostan are well correlated on the basis of deep-drilling data from Kabakovo 62, Shikhan 5, and Akhmerovo 6 boreholes, with the westernmost Middle Riphean section of the Bashkir meganticlinorium penetrated by the Kulgunino 1 borehole (Romanov and Isherskaya, 1994b); and (5) interpretation of CDP records shows that sedimentary successions of the Yurmatin Group known on the western slope of South Urals directly grade into deposits of the Serafimovka Group in the Volga–Urals region (Fig. 4).

AVAILABLE CONCEPTS OF ACCUMULATION ENVIRONMENTS OF MIDDLE RIPHEAN SEDIMENTARY ASSOCIATIONS

Different viewpoints on the accumulation conditions of Middle Riphean deposits of the Bashkir meganticlinorium were analyzed in detail in a special publication (Maslov, 1997b); this is why only a brief

[1] According to Andreev *et al.*, (1981), the Tukaevo and Ol'khovka formations represent "...a distinct sedimentary cycle, whose lower part is composed of sandstone and quartzite, the middle part is represented by black shales, and the upper one consists of variegated shales and dolomites." On the basis of drilling and seismic profiling data, Romanov and Isherskaya (1994b) also note that uniform successions represented by sandstones and siltstones in the lower part and by argillites, marls, and dolomites in the upper part are widespread in the platform area of Bashkortostan. According to the above authors, "the variegated silt–argillite–carbonate sequence of the Ol'khovka Formation becomes colored gray in general and is characterized by a higher content of carbonate rocks... In the Kulgunino 1 borehole, this stratigraphic level corresponds to the Avzyan Formation."

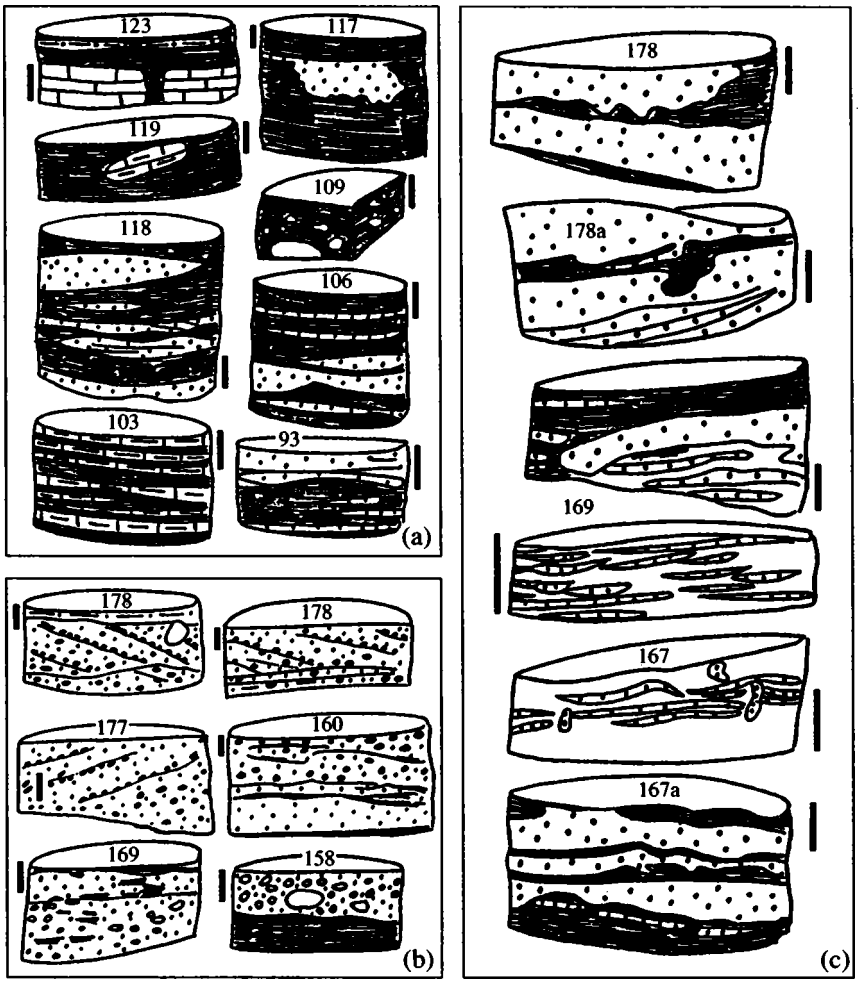

Fig. 3. Structural features of rocks from the Ol'khovka Formation in borehole sections Sergeevka 800 (a) and Kabakovo 62 (b) and (c). Sample positions in the formation sections are shown in Fig. 2; the scale bar is 1 cm.

review is presented below.[2] Goryainova, Fal'kova, Garan' and Olli, considered the Middle Riphean sedimentary associations mainly as products of sedimentation in a shallow basin. Feoktistov *et al.*, (unpublished report, 1977) classed deposits of the Mashak Formation with the coastal-deltaic sediments. In opinion of Shvetsov (1974), single lenses of the Mashak Formation represent continental deposits that fringed an insular land. According to Parnachev *et al.* (1986), the lower intervals of the Mashak Formation are mainly composed of alluvial–proluvial deposits, whereas marine sediments occupy its higher intervals. The majority of researchers consider the Zigal'ga Formation as spanning the range of coastal and shallow-water marine deposits. It is also thought that this stratigraphic level of the Yurmatin Group is characterized in the south of the Bashkir meganticlinorium by deltaic rock associations. Some specialists believe that the Zigazino–Komarovo Formation exemplifies siliciclastic deposits of a vast shallow basin, whereas others think that it includes sediments of the so-called "paralic shoals" or evaporite basins. A model similar in some features to the playa model was also proposed for these deposits. The Avzyan Formation, as is assumed in many publications, was accumulated in coastal, shallow, and moderately deep settings, the lagoonal included, of a paleobasin with normal or slightly elevated salinity. Distribution patterns of rare elements in the Middle Riphean deposits of the western slope of South Urals presumably imply a semiarid climate with humid episodes in the drainage system areas at the time of their accumulation (Gareev and Veretennikova, 1987; Gareev, 1989; Podkovyrov and Gareev, 1995).

Problems of facies typification and sedimentation environments of the Serafimovka Group were considered to a different extent in many publications. For instance, Timergazin interpreted deposits of the Tukaevo and Ol'khovka formations as representing shallow-water sediments. Ivanova *et al.* (1969) and Aliev *et al.*, (1977) share a similar viewpoint. The

[2] Maslov and Isherskaya (1998) considered the same problem with respect to the Riphean deposits of the Volga–Urals region.

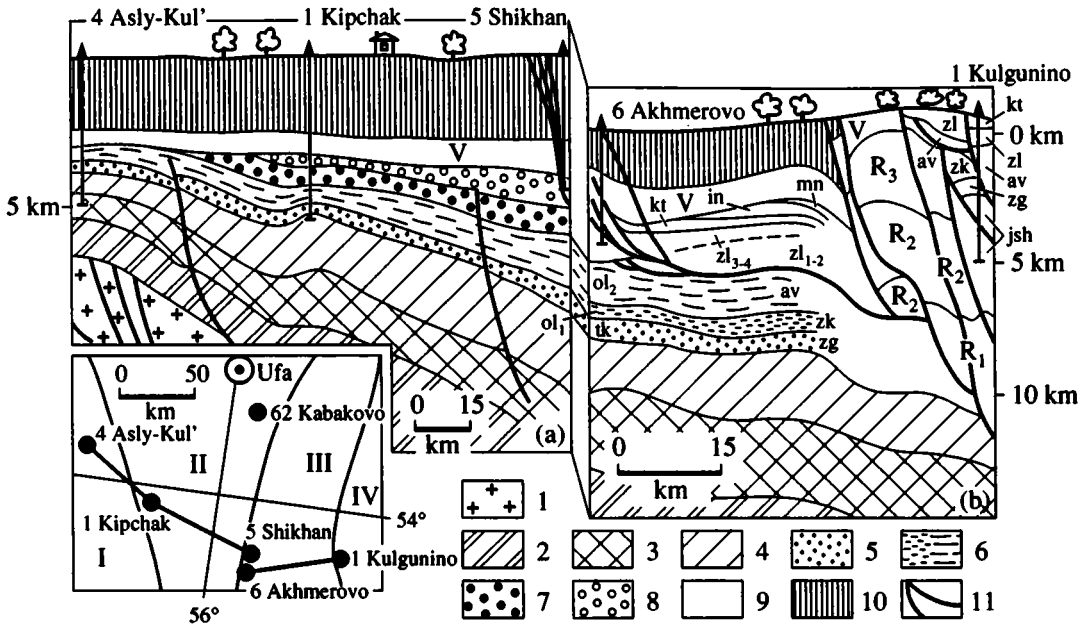

Fig. 4. Schematic structural–geological profiles for Asly-Kul'–Shikhan (a) and Akhmerovo–Kulgunino (b); compilation on the basis of seismic CDP data by Isherskaya and Romanov (1993), Romanov and Isherskaya (1994b): (1) Archean–Lower Proterozoic crystalline basement, (2) Kama, (3) Kaltasy, (4) Nadezhdino, (5) Tukaevo, (6) Ol'khovka, (7) Usa–Leonidovka, and (8) Priyutovka formations, (9) Vendian, (10) Paleozoic, (11) faults. Indices: (R_1) Lower Riphean; (R_2) Middle Riphean; (R_3) Upper Riphean; formations: (jsh) Yusha, (zg) Zigal'ga, (tk) Tukaevo, (zk) Zigazino–Komarovo, (ol_1) Akberdino Horizon of the Ol'khovka Formation, (ol_2) middle and upper parts of the Ol'khovka Formation, (av) Avzyan, (us+in) Usa and Leonidovka undivided, (zl) Zil'merdak, (zl_{1-2}) Bir'yan and Nugush subformations of the Zil'merdak Formation, (zl_{3-4}) Lemezino and Bederysh subformations of the Zil'merdak Formation, (kt) Katav, (in) Inzer, (mn) Min'yar. Tectonic elements: (I) Sernovodsk–Abdulino trough; (II) Kama–Bel'sk trough; (III) West Uralian pericratonic zone; (IV) western slope of the South Urals (Bashkir meganticlinorium).

occurrence of a "primary" dolomite matrix together with barite, anhydrite, and gypsum crystals in terrigenous rocks suggests, as some authors believe, that the basin was characterized by elevated salinity and was probably isolated to a certain extent. Taking into consideration the distribution patterns of rare elements in Riphean deposits of western Bashkortostan, Ivanova and Edrenkina (1971) suggested that their source rocks were formed under hot and humid climatic conditions. Other researchers (Balashova and Morozov, 1973; Nizamutdinov *et al.*, 1990) are of a similar opinion. Almost all Middle Riphean terrigenous deposits in the northern flank of the Sernovodsk–Abdulino trough were referred, according to some geochemical parameters, to sediments of brackish-water shallow basins. Based on the occurrence of desiccation cracks and some other sedimentary structures in deposits of the Tukaevo (Shtandy) and Ol'khovka (Gozhan) formations, Lagutenkova and Chepikova (1982) regarded them as indications of extreme shoaling in the basin and intermittent regression episodes in its particular zones. According to Lozin (1994), the Middle Riphean was marked in the considered region by the formation of a spacious shelf zone, where shallow siliciclastic sequences accumulated under stable paleogeographic conditions.

Some researchers from Moscow State University (Milanovskii *et al.*, 1994; Nikishin *et al.*, 1997) express another opinion. They suggest that the multidirectional horizontal compression of the East European craton at the end of the Early Riphean eliminated the intracontinental rift-type basin that existed before and caused *a long-term break in sedimentation* (italicization is mine).

FACIES ASSOCIATIONS AND COMPLEXES

At present, facies and their associations (lithological–facies complexes) of the Middle Riphean stratotype section in the South Urals are relatively well characterized (Maslov, 1991b, 1997a, and others). Sections of the *Mashak Formation* are established to consist of two principal rock complexes. One complex of volcanogenic–terrigenous deposits of coastal–marine genesis corresponds to the Kuz'elga–Karan lithostratigraphic level (six lower subformations in the Mashak Formation scheme by Rotaru, 1983). The overlying shallow-water terrigenous deposits represent the next Shakitar–Yamantau level. Despite their lithological differences, the Zigal'ga and Zigazino–Komarovo formations mainly consist of marine siliciclastic sediments accumulated in shallow and very shallow settings, which are constituents of two sedimentary complexes known in

the region. The Zigal'ga Formation includes the following types of facies: sandstones accumulated in open-sea shoals with active hydrodynamic environments; sandy sediments of coastal shoals also influenced by active hydrodynamics; sandy–silty–clayey deposits of sea shoals with rather stable hydrodynamic conditions; silty–sandy sediments of sea shoals affected by moderately intense hydrodynamics; and some other facies. Fine-grained terrigenous sediments devoid of debris-flow structures and accumulated in moderately deep settings (below the storm-wave base) appear only in the Zigazino–Komarovo Formation, where these facies are subordinate and most characteristic of eastern areas of the Bashkir meganticlinorium (Maslov, 1991a, 1997b). Associations of marine deposits of shallow and very shallow settings are almost equally abundant in all three subformations of the section interval under consideration. A characteristic feature of the formation as a whole is also the absence of pericontinental and riparian rock complexes; this allows me to use the general term "very shallow-water deposits" instead of the term "intertidal deposits," which is more appropriate from the viewpoint of primary sedimentary structures. As is known, sedimentation areas of the latter correspond to a zone (lateral or vertical) that is transitional to settings of the continental deposits proper; but sedimentary beds of this kind are unknown in both the Zigal'ga and Zigazino–Komarovo formations of the stratotype section. In paleogeographic aspect, the western slope of the South Urals represented in the Zigazino–Komarovo time is most likely a mosaic combination of intermittently and frequently drained zones and areas with slightly more stable, though to a different extent ephemeral, underwater sedimentation.

The Avzyan level of the stratotype is represented by alternating terrigenous and carbonate sedimentary successions accumulated in very shallow, shallow, and moderately deep marine settings (Maslov, 1997b).

Turning now to the Middle Riphean facies associations of the Volga–Urals region, I should note that discrimination of characteristic rock complexes of different composition and genesis in the Riphean stratotype section is based on materials of lengthy and detailed lithological–facies analysis, in which genetic types of sediments, facies, and their different-scale associations, as they are defined by P.P. Timofeev, have been considered. Rock complexes of the Serafimovka Group discussed below undoubtedly correspond to the large-scale facies associations if we take into account that long intervals of sections drilled in this region have not been sampled. Eleven associations of this kind may be distinguished within the Serafimovka Group.

The first facies association is represented by red and variegated sandstones associated with subordinate coarse-grained psammitic varieties and siltstones; small-pebble conglomerate, gravelstone, and shale interbeds are also constituent rocks of the association. Desiccation cracks, pseudomorphs after halite, breccia interbeds with flat shale fragments, and ripple and current marks are the main structural features controlling the general appearance of rocks in the association. Among the less common characteristics, I should mention the following: medium- and small-scale unidirectional lamination plain-parallel or flattening toward the base of the rock series (sometimes with signs of rhythmic sorting of clastic material in the cross-bedded layers); wavy and ripple drift cross lamination; erosional pockets and structures of small scours; and indications of silting in particular beds. Judging from these characteristics, it may be concluded that the considered facies association represents continental or riparian deposits accumulated under oxidizing environments of wandering riverbeds and ephemeral lakes of the coastal plain. The association is characteristic of some intervals of the Ol'khovka (North Kush-Kul' 1, Sergeevka 800, and Kipchak 1 boreholes) and Tukaevo (Kabakovo 62 and Kush-Kul' 100 boreholes) formations.

The second association is largely composed of siltstones and fine- to medium-grained sandstones intercalated with subordinate shales and coarse-grained arenites. These rocks exhibit the medium to fine wavy and ripple drift cross lamination. The presence of platy shale breccia horizons indirectly suggests desiccation events in some areas of the basin. The associated beds of fine-grained sandstones with small-scale multidirectional lamination and symmetrical ripple marks are usually massive but some of them show wavy lamination. This allows me to assume that the association accumulated in open-sea shoals with fairly intense hydrodynamics, i.e., on the inner shelf above the fair weather wave base. The association is typical of the lower (Kipchak 1 and Kush-Kul' 100 boreholes) and middle (Kabakovo 62 borehole) parts of the Tukaevo Formation.

Fine- to medium-grained sandstones with subordinate coarser grained varieties and siltstones are referred to *the third facies association.* Its rocks are usually massive or, less commonly, show horizontal lamination and intervals with desiccation cracks. In this case, genetic interpretation of sedimentation environments is rather difficult. Desiccation cracks represent the only indication that the deposits were accumulated in intermittently or frequently drained parts of the basin. The association is typical of the Tukaevo Formation (Kabakovo 62 borehole).

The fourth facies association (the Tukaevo Formation interval in the Asly-Kul' 4 borehole section) includes fine- to medium-grained sandstones (dominant), siltstones, and shales intercalated with single interbeds of coarse- and variably grained arenites. These rocks are massive as a rule; less common are beds displaying horizontal and wavy bedding, or fine unidirectional, wavy, and ripple drift cross lamination. Accumulation of sediments probably took place near deltaic areas of the basin at their junction with the continental edge, where sedimentation was still under the

influence of unidirectional currents (the so-called mobile deltaic shoals).

The fifth facies association is mainly represented by red and variegated fine- to medium-grained sandstones, siltstones, and shales irregularly alternating or forming more or less uniform packets and thin members. Typical of these rocks are horizontal or wavy and ripple drift cross lamination and also massive structures of beds. The association appears to be a result of sedimentation in small shallow bays and lagoons above the fair weather wave base. The absence of rocks with desiccation cracks suggests that sedimentation could have taken place below the low-tide boundary. The association is typical of lower and middle intervals of the Tukaevo (Kipchak 1 borehole) and Ol'khovka (Sergeevka 800 borehole and others) formations.

The sixth facies association almost entirely consists of shales sometimes intercalated with thin siltstone interbeds. The latter are marked by horizontal bedding or by sinuous and ripple drift cross lamination; at some levels, they reveal wavy lamination and desiccation cracks. This allows the assumption that sedimentation developed in quiet coastal (lagoonal) areas of sea shoals, which were, to a large extent, isolated from wave influence and intermittently or fairly often experienced draining. The association is characteristic of the Akberdino Horizon of the Ol'khovka Formation (borehole Kabakovo 62).

The seventh facies association (the upper part of the Ol'khovka Formation in the Kipchak 1 and North Kush-Kul' 1 borehole sections) includes fine- and, sometimes, medium-grained sandstones, siltstones, and shales alternating gently in a wavelike manner. Characteristic inner structural features of the rocks are horizontal and wavy (locally gentle) lamination and also ripple and current marks of low amplitude. The association is probably a typical example of deposits accumulated in quiet shelf areas relatively distant from the coast. The influence of wind-induced waves was insignificant compared with that in sedimentation settings characteristic, for instance, of the fifth association. The alternation of different lithotypes is most likely a response to irregular, spasmodic (?) influxes of sandy and silty material, which disturbed the quiet background accumulation of fine-grained siliciclastic sediments.

The eighth facies association is represented by fine- to medium-grained sandstones (dominant), siltstones, shales, and, occasional gravelstones. Rocks are predominantly massive, but some of them show horizontal (often obscure and poorly expressed) lamination. In particular thin bed packets and members, there is seen gentle sinuous alternation of the lithotypes listed above. Pseudomorphs after evaporite minerals, desiccation cracks, and structures indicating sedimentation within the zone of wave influence are missing; and this suggests that the deposits in question most likely accumulated below the fair weather wave base, i.e., in the inner shelf areas. Rocks of this association are characteristic of the middle (Kush-Kul' 100 borehole) and upper (Kipchak 1, Kabakovo 62, and Asly-Kul' 4 boreholes) parts of the Tukaevo Formation.

The ninth facies association (the Ol'khovka Formation interval in the Kabakovo 62 borehole section) mostly consists of carbonate rocks: dolomites (preponderant), limestones, and their varieties with variable terrigenous admixture; shale interbeds are subordinate. Rocks display wavy to horizontal bedding, and sinuous or ripple drift cross lamination. This appears to be characteristic of sedimentation in the coastal zone of a basin with active hydrodynamic conditions.

The tenth facies association recorded in the section of the Ol'khovka Formation (Kabakovo 62 borehole) includes mainly dolomites and subordinate limestones and stromatolitic (?) carbonate rocks; shales occur here as thin interbeds. Carbonate rocks are usually massive, locally intercalated with synsedimentary breccia consisting of flattened clastics; less common are their intervals where carbonate rocks and shales alternate in a gentle wavelike manner, and also intervals of dolomites with obscure horizontal banding. Structures similar to those of stromatolites and intervals of distinct and gentle wavy lamination suggest certain hydrodynamic activity in sedimentation settings. Nonetheless, the preponderance of massive rock varieties and the insignificant role of terrigenous rocks may indicate the development of sedimentation mainly below the fair weather wave base.

The eleventh facies associations (the lower part of the Ol'khovka Formation in the Kush-Kul' 100 borehole section) is largely represented by carbonate rocks dominated by dolomites. Subordinate in abundance are stromatolitic (?) varieties, rocks with terrigenous admixture, and rare shale interbeds. Dolomites sometimes reveal horizontal banding (lamination?). There are also intervals of gentle sinuous alternation of dolomites or limestones with shales. The association most likely accumulated in the outer shelf zone, where hydrodynamics was not active.

The position of considered associations in the model profiles of the past sedimentary basin is shown in Fig. 5.

LATERAL VARIABILITY OF MIDDLE RIPHEAN DEPOSITS IN THE JUNCTION AREA BETWEEN THE RUSSIAN PLATFORM AND SOUTH URALS

The analysis of distribution patterns of characteristic sedimentary rock complexes and facies associations in the sections of the Yurmatin and Serafimovka groups elucidates schemes of their relationships (Figs. 6, 7). Taking into consideration the fragmentary character of the data available at present, the schemes represent a substantial addition to the previously published paleogeographic and lithological–facies maps of different

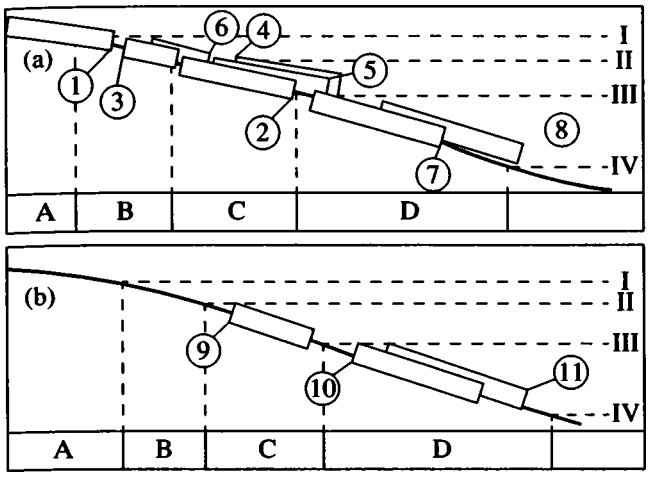

Fig. 5. Model distribution of facies associations along the profile of the sedimentary basin: (a) terrigenous shelf; (b) shelf accumulating terrigenous-carbonate and carbonate sediments: (I) highest tide boundary; (II) low-tide boundary; (III) boundary of the fair weather wave base; (IV) boundary of storm wave base; (A) coastal plain; (B) littoral or very shallow sedimentation setting; (C) inner shelf and subtidal zone; (D) outer shelf zone. Encircled numbers correspond to facies associations described in the text.

Middle Riphean stratigraphic levels in the junction area between the Russian platform and South Urals.

The highly diverse deposits of the Middle Riphean sections of the Bashkir meganticlinorium, whose variable facies accumulated in different paleogeographic settings, are grouped, with due regard for sediment genesis, into several sedimentary (lithological–facies) complexes representing associations of allied facies and macrofacies of individual settings and corresponding to particular stages of basin evolution (Maslov, 1991b, 1997a). The majority of facies associations distinguished in the Riphean sections of the Volga–Urals region can also be considered, as shown above, as the constituent elements of these complexes. For instance, the first association may represent a part of the complex of terrigenous, mainly alluvial and alluvial–deltaic, deposits. The third and sixth associations are very similar to deposits of the terrigenous complex of very shallow settings, whereas the second, fourth, fifth, and ninth associations are correlative in lithology and sedimentation parameters with complexes of terrigenous and carbonate rocks of the shallow-sea genesis (Maslov, 1997a).

Figure 6 demonstrates the principal distribution patterns of facies associations in the Middle Riphean sections of the Volga–Urals region and their probable relationships with sedimentary complexes of the stratotype region. For technical reasons, only dominant facies associations are shown in some profiles. Schemes of the lateral distribution of facies associations and sedimentary complexes (Fig. 7) depict probable distribution of different sedimentation settings.

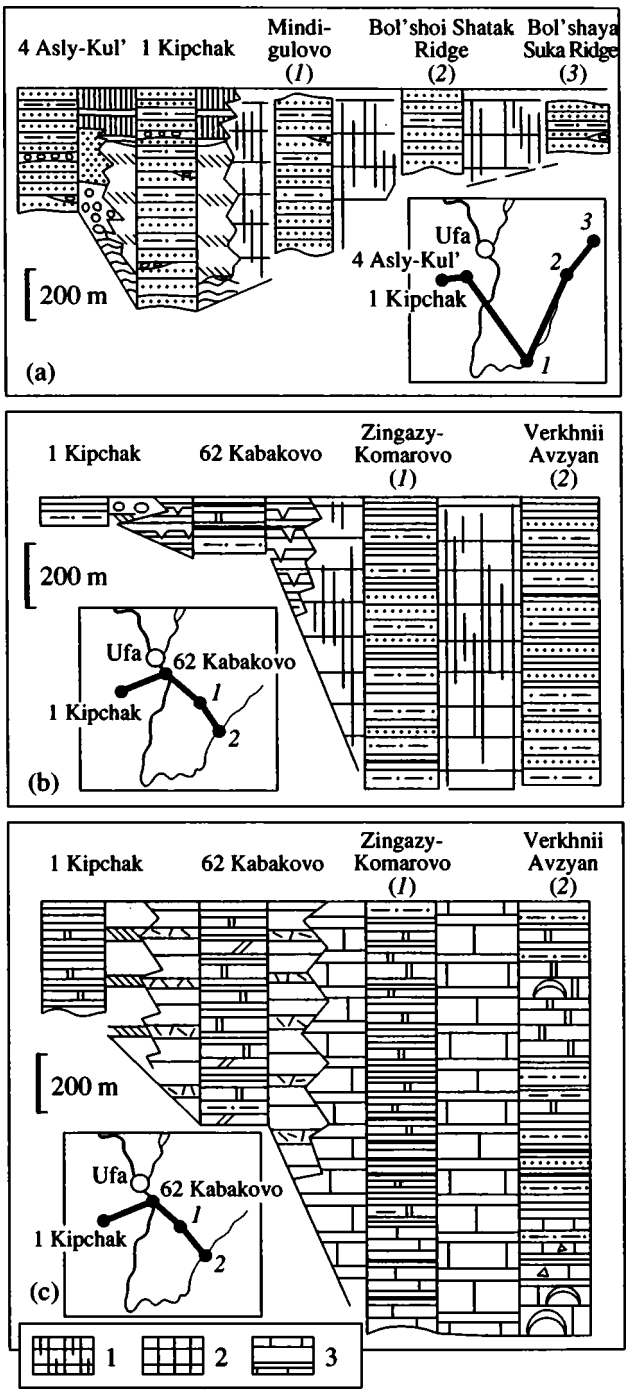

Fig. 6. Relationships between facies associations and sedimentary complexes along some sublatitudinal profiles: the Zigal'ga–Tukaevo (a), Zigazino–Komarovo–Akberdino (b), and Avzyan–Ol'khovka (c) intervals of the Middle Riphean; (1) terrigenous deposits accumulated in shallow marine sedimentation zones with intermittent or frequent very shallow settings; (2) terrigenous sediments of the shallow shelf; (3) complex of alternating siliciclastic and carbonate shallow-water sediments (other symbols as in Fig. 2).

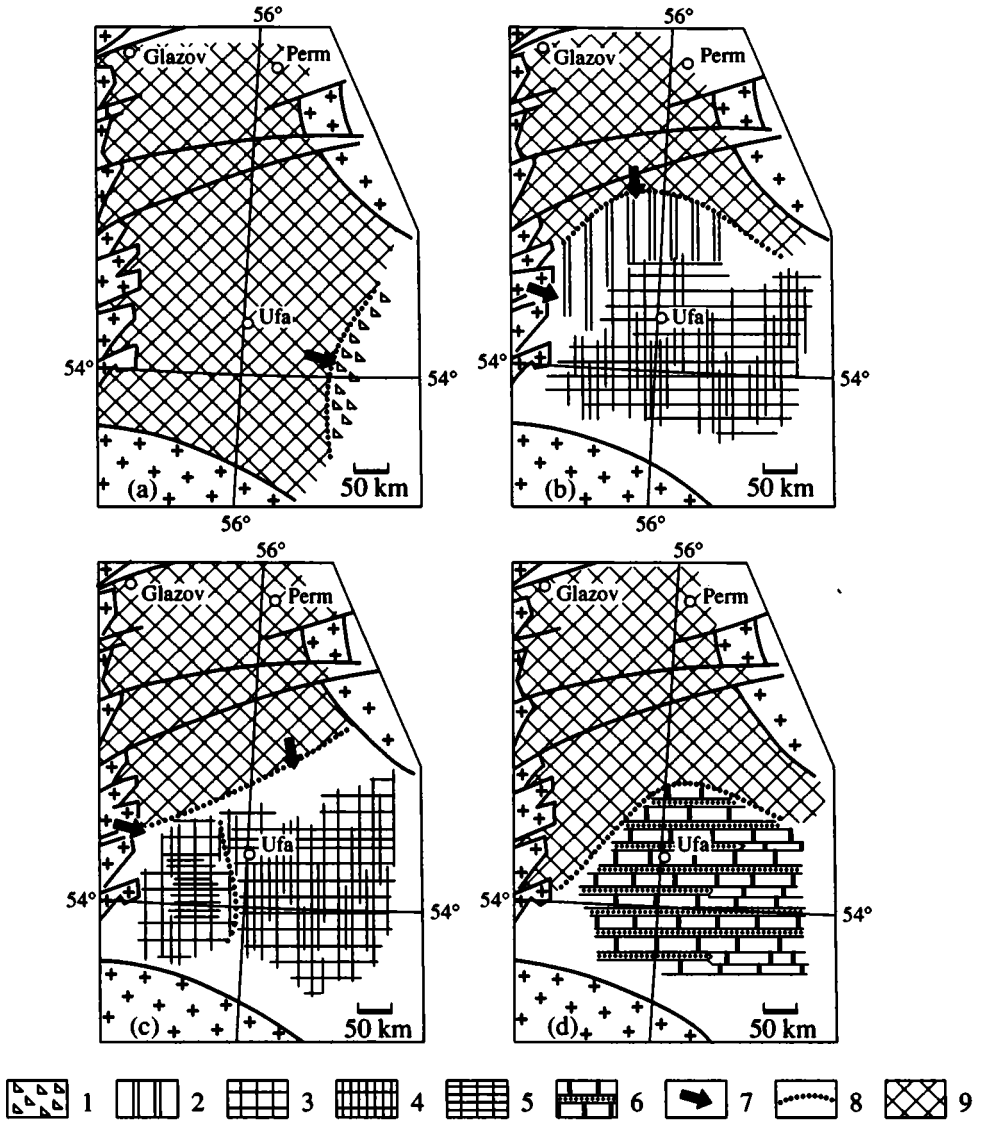

Fig. 7. Schematic distribution of sedimentary associations of variable composition and genesis in the Volga–Urals region and Bashkir meganticlinorium during the Mashak (a), Zigal'ga–Tukaevo (b), Zigazino–Komarovo (c), and Avzyan–Ol'khovka (d) time: (1) volcanogenic–terrigenous mostly coastal-marine deposits; (2) terrigenous alluvial and alluvial–deltaic deposits; (3) shallow-water marine siliciclastic deposits; (4) the same sediments in association with those of very shallow sedimentation settings; (5) association of shallow-water, fine-grained siliciclastic (accumulated below the fair weather wave base), terrigenous, and carbonate deposits; (8) boundaries of lithological–facies zones; (9) areas barren of deposits (other symbols as in Fig. 2).

Deposits coeval with volcanogenic–sedimentary rocks of the *Mashak Formation* of the stratotype region are most likely missing from the central and western areas of Bashkortostan (Isherskaya and Romanov, 1993; Romanov and Isherskaya, 1998). It can be assumed that, during the Mashak time, nearly the whole region represented a variably differentiated land with exposed sedimentary and sedimentary–metamorphic rocks and only a small (?) central area of the present Bashkir meganticlinorium accumulated thick sequences of coastal-marine terrigenous and volcanogenic deposits (Fig. 7a). The analysis of the isopach map reveals a deep asymmetric trough, where the maximum total thickness values of deposits (up to 2400–2600 m) and of boulder conglomerate beds and lenses (3–5 to 30–40 m) is characteristic of its flank zones; eastward, the thickness of volcanogenic–terrigenous deposits decreases and sandy–silty sequences become prevalent in the formation sections (Rotaru, 1983; *Stratotip rifeya...*, 1983; Parnachev *et al.*, 1986) (Fig. 8a).

At *the Zigal'ga–Tukaevo level*, the distribution of rock complexes and facies associations of different genesis can be modeled only for some areas of the Volga–Urals region, because deposits of the Tukaevo Formation are unknown north of the latitude of Elabuga (Romanov and Isherskaya, 1994a, 1998). Sediments of

the Tukaevo Formation accumulated almost everywhere within their distribution area in the shallow-water setting of the inner shelf, where hydrodynamic activity was low and sedimentation developed under persistent influence of waves and bottom currents redistributing the detrital material. In my opinion, deposits accumulated in continental-type settings are present only in the lower part of the formation interval of the Asly-Kul' 4 borehole section and probably in the northernmost distribution areas of this formation (Figs. 6a, 7b). Similar sedimentation environments were also characteristic of the greater part of the Bashkir meganticlinorium, where sediments are mainly represented by sandstones and subordinate siltstones displaying wavy to horizontal bedding and simple or wavy cross lamination, ripple and current marks, and occasional desiccation cracks. Deposits of the Zigal'ga–Tukaevo level are rather uniform in thickness; they are thickest within the zone located not far away to the south–southeast of Ufa and stretching approximately in the meridional direction (Fig. 8b).

The Zigazino–Komarovo–Akberdino interval recorded changes in the paleogeographic situation within central and western Bashkortostan. Distribution of rock complexes and facies associations of different composition and genesis was interpreted for this period of basin evolution as being apparently irregular. This fact may suggest significantly larger dimensions for the sedimentary basin as compared with those observed nowadays. A similar assumption was expressed earlier (Ozhiganova and Isherskaya, 1977, unpublished report). Sections of the Akberdino Horizon are composed of different facies associations (Figs. 6b, 7c). Amid its rocks there are fine-grained siliciclastic deposits rich in dispersed organic matter and exemplifying the basinal type of sedimentation proper, terrigenous and carbonate–terrigenous deposits of a coastal zone that experienced wave disturbance, and terrigenous–carbonate deposits of extreme shoal sedimentation settings. Some sediments of the Zigazino-Komarovo Formation accumulated in the basin areas, where subaerial and underwater conditions of sedimentation frequently alternated. In different regions of the Bashkir meganticlinorium, rocks of the formation reveal desiccation cracks; ripple marks of different kinds; simple; wavy; and lenticular cross lamination; and flaser structure (Maslov, 1991a). The isopach maps outline a distinct depocenter in southern and central areas of the Bashkir meganticlinorium (Fig. 8c).

The transgressive trend in development of the Middle Riphean basin of the Bashkir meganticlinorium is marked by the appearance of a peculiar complex composed of alternating terrigenous–carbonate sequences of basinal and shallow-water deposits at the *Avzyan–Ol'khovka level.* In the westerly direction, the monotonous carbonate sequences gradually become intercalated with the shallow-water terrigenous and terrigenous–carbonate members (Figs. 6c, 7d) accumulated above the base of permanent wave activity. Finally, they wedge out completely. This is well exemplified in sections of the Revet' Subformation (Klyuchikhin, unpublished report, 1985). In western areas of the study

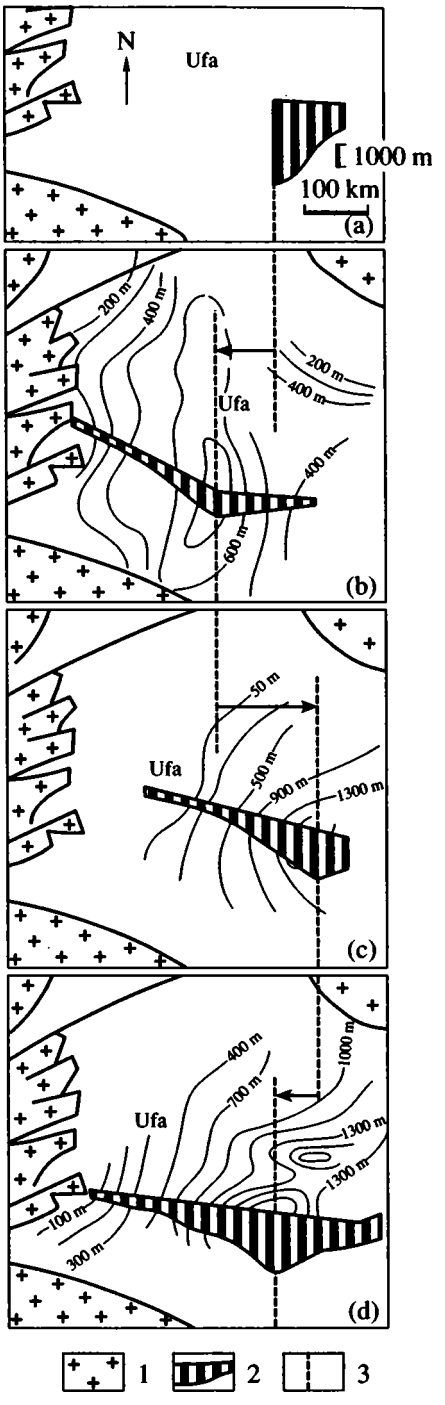

Fig. 8. Schematic isopach maps of the Volga–Urals region and Bashkir meganticlinorium for the Mashak (a), Zigal'ga–Tukaevo (b), Zigazino–Komarovo–Akberdino (c), and Avzyan–Ol'khovka (d) levels (arrows show direction of successive depocenter migration): (1) surface of the crystalline basement overlain by Devonian deposits; (2) schematic structural profile; (3) depocenter position.

region, the Ol'khovka Formation is almost entirely composed of marine siliciclastic deposits of shallow settings. The thickness of the Avzyan–Ol'khovka deposits decreases westward from the east by more than one order of magnitude. The deposits are of maximum thickness in central and southwestern areas of the Bashkir meganticlinorium, where isopachs of 2000 and 1500 m outline several structural depressions. At the longitude of Elabuga–Sarapul, the thickness of the Ol'khovka Formation does not exceed 100 m (Fig. 8d).

CONCLUSION

The studied structural–textural properties of rocks from the Serafimovka Group of the Volga–Urals region revealed that its sections include several facies associations similar to characteristic sedimentary complexes of the Yurmatin stratotype section. This furnishes an opportunity to reveal peculiarities of the lateral relationships between different zones of sedimentation in the considered region during the Middle Riphean and to elucidate their lateral migration with time. Simultaneously, the main features of the Middle Riphean sedimentary basin can be outlined based on these data.

Initial stages of the basin development (approximately 1.34–1.35 Ma ago) are characterized by accumulation of a specific substantially thick rock complex composed of volcanogenic and siliciclastic, mainly coastal deposits in the extreme eastern areas of the region. Westerly areas were occupied by an elevated and differentiated land; its eastern boundaries are most likely marked by large lenses of boulder–pebble conglomerates exposed in sections of the Mashak Formation. In the mid-Middle Riphean time, almost the entire region represented areas of sedimentation mainly in subaerial or shallow-water settings, where these conditions changed from one to another. In the paleogeographic respect, the basin of that time probably represented a sea with a flat bottom surrounded by islands. Peripheral parts of the sea were occupied by spacious lowlands or by riparian and coastal-marine plains somewhat similar to modern playa landscapes. The expanding transgression in the terminal Middle Riphean resulted in the accumulation of several carbonate and terrigenous rock successions in the territory of the present Bashkir meganticlinorium, which mainly represent subtidal deposits. Westward, they graded into siliciclastic associations of shallow and very shallow(?) sedimentation settings.

Comparing the available data, we can see that the main evolutionary features of sedimentary basins that existed in the junction area between the Russian platform and South Urals in the Early and Middle Riphean, were obviously similar. For instance, the initial stage of the Early Riphean basin in the northeast of the Bashkir meganticlinorium was marked by accumulation of volcanogenic–terrigenous deposits (the lower part of the Ai Formation of the Burzyan Group; Maslov, 1994, 1995), whereas coeval siliciclastic alluvial, riparian, and coastal-marine associations in the Volga-Urals region (the Kama Formation of the Kyrpino Group) occupied significantly larger areas having a comparable thickness (about 1200–1500 m). The middle evolutionary stages of the Middle Riphean basin corresponded to a period of weak transgression and prolonged existence of peculiar, very shallow sedimentation settings, which accumulated almost exclusively siliciclastic sediments, whereas the middle Early Riphean was marked in the region under consideration by deposition of thick (to 3000–3500 m) carbonate successions (the Satka and Kaltasy formations). The isopach maps show that the Lower Riphean sedimentary successions of the region are characterized by a centripetal tendency in the thickness distribution (Maslov, 1997a); the successions are thickest in areas located somewhat to the southeast of Ufa. To the west and east from this depocenter, their thickness significantly decreases. Deposits of the Serafimovka and Yurmatin groups do not reveal such distinct distribution patterns of the thickness. At the very beginning of the Yurmatin time, sedimentation was in progress only in some areas of the western slope of the South Urals. At the Zigal'ga–Tukaevo level, there are no distinct maxima and minima in thickness distribution, which suggests stabilization of both tectonic and paleogeographic environments in the sedimentation area. The Zigazino–Komarovo–Akberdino level shows an eastward displacement of maximum thickness values. Finally, the depocenter of the Avzyan–Ol'khovka time was located approximately in the junction zone between the southwestern areas of the Bashkir meganticlinorium and the Volga–Urals region. Thus, the discussed materials indicate that initiation and development of the Middle Riphean sedimentary basin progressed under conditions different from those of the Early Riphean time (Maslov, 1994, 1995). The data obtained emphasize a specific evolution of Riphean sedimentation in the junction area between the Russian platform and South Urals.

ACKNOWLEDGMENTS

I am grateful to M.V. Isherskaya (Institute of Geology, Ufa Scientific Center, Russian Academy of Sciences) for the opportunity to study the deep-drilling cores and for her advice and consultations. Critical comments by M.A. Semikhatov and P.Yu. Petrov significantly improved the manuscript. The work was supported by the Russian Foundation for Basic Research (project 97-05-65107).

Reviewers P.Yu. Petrov and M.A. Semikhatov

REFERENCES

Aliev, M.M., Morozov, S.G., Postnikova, I.E., *et al.*, *Geologiya i neftegazonosnost' rifeiskikh i vendskikh otlozhenii Volgo-Ural'skoi provintsii* (Geology and Oil and Gas

Potential of Riphean and Vendian Deposits in the Volga–Ural Province), Moscow: Nedra, 1977.

Andreev, Yu.V., Ivanova, T.V., Keller, B.M., *et al.*, Upper Proterozoic Stratigraphy of the Eastern Margin of Russian Plate and of the Western Slope of South Urals, *Izv. Akad. Nauk SSSR, Ser. Geol.*, 1981, no. 10, pp. 57–68.

Anfimov, L.V., Kozlov, V.I., and Eremeeva, A.V., Density of Quartz Grains from the Upper Precambrian Clastic Deposits of the Bashkir Meganticlinorium, in *Dokembriiskie tolshchi Bashkirskogo megantiklinoriya na Urale i ikh metallogeniya* (Precambrian Deposits of the Bashkir Meganticlinorium of the Urals and Their Metallogeny), Sverdlovsk: Ural Nauchn. Tsentr Akad. Nauk SSSR, 1978, pp. 33–43.

Balashova, M.M. and Morozov, S.G., Geological Structure and Oil and Gas Potential of the Riphean and Vendian Deposits of the Eastern Russian Platform, in *Geologiya i neftegazonosnost' severa Uralo-Povolzh'ya. Perm'* (Geology and Oil and Gas Potential of the Northern Volga–Urals Region), Perm: Perm Knizh. Izd., 1973, pp. 141–150.

Garan', M.I., The Western Slope and Central Area of the South Urals, in *Stratigrafiya SSSR, T. 2. Verkhnii dokembrii* (Stratigraphy of the USSR, vol. 2: The Upper Precambrian), Moscow: Gosgeoltekhizdat, 1963, pp. 114–161.

Gareev, E.Z., Geochemistry of Sedimentary Deposits from the Riphean Stratotype, *Abstract of Cand. Sci. (Geol.–Mineral.) Dissertation*, Moscow: Vernadsky Inst. of Geochemistry and Analytical Chemistry, 1989.

Gareev, E.Z. and Veretennikova, T.Yu., Petrochemistry and Geochemistry of Clay–Carbonate Deposits in the Avzyan Formation Stratotype of the South Urals, in *Mikroelementy v magmaticheskikh, metamorficheskikh i rudnykh formatsiyakh Urala* (Microelements in Magmatic, Metamorphic, and Ore Formations of the Urals), Ufa: Bashkir Fil. Akad. Nauk SSSR, 1987, pp. 61–68.

Garris, M.A., Kazakov, G.A., Keller, B.M., *et al.*, The Geochronological Scale of the Upper Proterozoic (Riphean and Vendian), in *Absolyutnyi vozrast geologicheskikh formatsii* (Absolute Ages of Geological Formations), Moscow: Nauka, 1964, pp. 431–455.

Garris, M.A., Postnikov, D.V., Popov, Yu.P., *et al.*, Age of Gabbroic Rocks in the Volga–Urals Area, in *Voprosy datirovki drevneishikh (katarkheiskikh) geologicheskikh obrazovanii i osnovnykh porod* (Problems of Dating the Oldest (Katarchean) Geological Formations and Basic Rocks), Moscow: Nauka, 1967, pp. 36–44.

Gorozhanin, V.M., Geochronology of the Upper Precambrian Lithogenesis in the South Urals, in: *Magmatizm, metamorfizm i glubinnoe stroenie Urala* (Magmatism, Metamorphism, and Deep Structure of the Urals), Yekaterinburg: Inst. Geol. Geokhim., Ural Otd. Ross. Akad. Nauk, 1997, part 1, pp. 230–231.

Isherskaya, M.V. and Romanov, V.A., *K stratigrafii rifeiskikh otlozhenii Zapadnoi Bashkirii* (The Riphean Stratigraphy of Western Bashkortostan), Ufa: Inst. Geol., Ufa Nauchn. Center, Ross. Akad. Nauk, 1993.

Ivanova, T.V. and Edrenkina, O.K., Geochemical Data as Indicators of Paleogeographic Features of the Riphean–Vendian (Bavla) Epoch in Western Bashkiria, in *Geologicheskoe stroeniya i perspektivy neftenosnosti Bashkirii* (Geological Structure and Oil and Gas Potential of Bashkiria), Ufa: Ufim. Nauchno–Issled. Inst., 1971, pp. 118–127.

Ivanova, Z.P., Veselovskaya, M.M., Klevtsova, A.A., *et al.*, *Doordovikskie otlozheniya tsentral'nykh i vostochnykh oblastei Russkoi platformy, T. 1.Neftegazonosnye i perspektivnye kompleksy tsentral'nykh i vostochnykh oblastei Russkoi platformy* (Pre-Ordovician Deposits in Central and Eastern Areas of the Russian Platform, vol. 1: Prospective Oil and Gas–Bearing Complexes of Central and Eastern Areas of the Russian Platform), Leningrad: Nedra, 1969.

Kazakov, G.A., Possibility of Using Glauconite for the Absolute Dating of Sedimentary Deposits, *Abstract of Cand. Sci. (Geol.–Mineral.) Dissertation*, Moscow: Vernadsky Inst. of Geochemistry and Analytical Chemistry, 1963.

Khabarov, E.M., Riphean Formations and Evolution of Sedimentation in the Eastern Zones of the Enisei Ridge, *Geol. Geofiz.*, 1994, no. 10, pp. 44–54.

Kozlov, V.I., Krasnobaev, A.A., Larionov, N.N., *et al.*, *Nizhnii rifei Yuzhnogo Urala* (The Lower Riphean of the South Urals), Moscow: Nauka, 1989.

Kozlov, V.I., Muslimov, R.Kh., Gatiyatullin, N.S., *et al.*, *Verkhnii dokembrii vostochnykh raionov Tatarstana i perspektivy ego neftegazonosnosti* (The Upper Precambrian and Oil and Gas Potential of Eastern Tatarstan), Ufa: Ufim. Nauchn. Tsenter Ross. Akad. Nauk, 1995.

Krasnobaev, A.A., Bibikova, E.V., Stepanov, A.I., *et al.*, Age of Volcanics from the Mashak Formation and Radiometric Dating of the Lower–Middle Riphean Boundary, in *Problemy izotopnogo datirovaniya protsessov vulkanizma i osadkoobrazovaniya* (Problems of Isotopic Dating of Volcanic and Sedimentary Processes), Moscow: Nauka, 1985, pp. 162–175.

Lagutenkova, N.S. and Chepikova, I.K., *Verkhnedokembriiskie otlozheniya Volgo-Ural'skoi oblasti i perspektivy ikh neftegazonosnosti* (Upper Precambrian Deposits of the Volga–Urals Region and Their Oil and Gas Potential), Moscow: Nauka, 1982.

Lozin, E.V. and Khasanov, V.Kh., Seismic–Geological Data on the Deep Structure of the Platform Margin and South Urals, in *Geologiya, geofizika i poleznye iskopaemye Yuzhnogo Urala i Priural'ya* (Geology, Geophysics, and Mineral Deposits of the South Urals and Adjacent Region), Ufa: Bashkir. Nauchn. Tsentr, Ural. Otd. Akad. Nauk SSSR, 1991, pp. 48–58.

Lozin, E.V., *Tektonika i neftenosnost' platformennogo Bashkortostana* (Tectonics and Oil Potential of the Platform Area in Bashkortostan), Moscow: Vseross. Nauchno–Issled. Inst. Obshch. Ekon. Neft. Geol., 1994, pt. 1.

Maslov, A.V., Textural–Structural Features of the Zigazino–Komarovo and Avzyan Formations Near the Verkhnii Avzyan, in *Geologiya dokembriya Yuzhnogo Urala i vostoka Russkoi plity* (The Precambrian Geology of the South Urals and Eastern Russian Platform), Ufa: Bashkir Fil. Akad. Nauk SSSR, 1990, pp. 73–82.

Maslov, A.V., Reference Sections and Sedimentation Environments of the Middle Riphean Zigazino–Komarovo Formation, the South Urals, *Izv. Akad. Nauk SSSR, Ser. Geol.*, 1991a, no. 9, pp. 97–110.

Maslov, A.V., Sedimentary Complexes in the Riphean Sections of the South Urals, *Litol. Polezn. Iskop.*, 1991b, no. 4, pp. 66–82.

Maslov, A.V., The Early Riphean Sedimentary Basin of the Volga–Urals Region, *Litol. Polezn. Iskop.*, 1994, no. 5, pp. 99–118.

Maslov, A.V., The Early Riphean Sedimentary Basin in the Eastern Part of the East European Platform and South Urals, *Otech. Geol.*, 1995, no. 4, pp. 45–52.

Maslov, A.V., Riphean Sedimentary Basins in the Western Slope of the South Urals: Facies, Lithological–Facies Complexes, Paleogeography, Evolutionary Trends, *Doctoral (Geol.–Mineral.) Dissertation*, Yekaterinburg: Inst. Geol. Geochem., Ural Division Russ. Acad. Sci., 1997a.

Maslov, A.V., *Osadochnye assotsiatsii rifeya stratotipicheskoi mestnosti (evolyutsiya vzglyadov na usloviya formirovaniya, litofatsial'naya zonal'nost')* (Sedimentary Associations of the Riphean Stratotype Area: Evolution of Views on Their Formation and Lithofacial Zones),. Yekaterinburg: Inst. Geol. Geokhim., Ural Otd. Ross. Akad. Nauk, 1997b.

Maslov, A.V. and Isherskkaya, M.V., *Osadochnye assotsiatsii rifeya Volgo-Ural'skoi oblasti (usloviya formirovaniya i litofatsial'naya zonal'nost')* (Riphean Sedimentary Associations of the Volga–Urals Region: Formation History and Lithological—Facies Zones), Yekaterinburg: Ural. Otd. Ross. Akad. Nauk, 1998.

Milanovskii, E.E., Nikishin, A.M., and Furne, A.V., The Riphean Evolution of the East European Craton, *Dokl. Ross. Akad. Nauk*, 1994, vol. 339, no. 4, pp. 513–517.

Mochalova, L.M., Ancient Washout of the Bakal Formation, in *Voprosy razvitiya Bakal'skoi rudnoi bazy* (Problems of Evolution of the Bakal Ore Zone), Sverdlovsk: Ural. Fil. Akad. Nauk SSSR, 1957, pp. 85–92.

Nikishin, A.M., Furne, A.V., and Tsigler, P., The Riphean–Vendian Geological History and Geodynamics of the East European Craton, *Vestn. Mosk. Univ., Ser. 4. Geol.*, 1997, no. 4, pp. 12–22.

Nizamutdinov, A.T., Baranov, V.V., and Didenko, A.N., Geochemical Investigations of the Upper Proterozoic Deposits in the Izmailovo Area of Eastern Tatarstan, in *Dokembrii vostoka Russkoi plity* (The Precambrian of the Eastern Russian Platform), Kazan: Kazan Univ., 1990, pp. 78–117.

Olovyanishnikov, V.G., Terrain Model of Late Precambrian Evolution of the Eastern Part of the European Platform, in *Rifei Severnoi Evrazii. Geologiya. Obshchie problemy stratigrafii* (The Riphean of Northern Eurasia: Geology and General Problems of Stratigraphy), Yekaterinburg: Inst. Geol. Geokhim., Ural Otd. Ross. Akad. Nauk, 1997, pp. 217–223.

Ozhiganova, L.D., New Data on Stratigraphy of the Upper Proterozoic Bavla Deposits in Bashkiria, in *Geologicheskoe stroenie i perspektivy neftegazonosnosti Zapadnoi Bashkirii* (Geological Structure and Oil and Gas Potential of Western Bashkiria), Ufa: Bashkir Fil. Akad. Nauk SSSR, 1974, pp. 22–36.

Parnachev, V.P., Rotar', A.F., and Rotar', Z.M., *Srednerifeiskaya vulkanogenno-osadochnaya assotsiatsiya Bashkirskogo megantiklinoriya (Yuzhnyi Ural)* (The Middle Riphean Volcanogenic–Sedimentary Association of the Bashkir Meganticlinorium, South Urals), Sverdlovsk: Ural. Otd. Akad. Nauk SSSR, 1986.

Petrov, P.Yu., Structure and Sedimentation Environments of the Riphean Bezymyannyi Formation in the Turukhansk Uplift, Siberia, *Stratig. Geol. Korrelyatsiya*, 1993, vol. 1, no. 5, pp. 20–32.

Petrov, P.Yu. and Semikhatov, M.A., Structure and Formation of the Upper Riphean Transgressive Complex: The Miroedikha Formation of the Turukhansk Uplift, Siberia, *Litol. Polezn. Iskop.*, 1997, no. 1, pp. 14–35.

Petrov, P.Yu. and Veis, A.F., Facial–Ecological Structure of the Derevnya Formation Microbiota: Upper Riphean, Turukhansk Uplift, Siberia, *Stratigr. Geol. Korrelyatsiya*, 1995, vol. 3, no. 5, pp. 13–41.

Podkovyrov, V.N. and Gareev, E.Z., Compositional Evolution of Terrigenous Deposits of the Riphean Yurmatin Group of the South Urals, in *Geologicheskoe izuchenie i ispol'zovanie nedr* (Geological Investigations and Development of Mineral Resources), Moscow: Geoinformmark, 1995, issue 1, pp. 25–36.

Polevaya, N.N. and Kazakov, G.A., Age Calibration and Correlation of Ancient "Barren" Deposits on the Ar^{40}/K^{40} Ratio in Glauconite, *Tr. Lab. Geol. Dokembriya, Akad. Nauk SSSR*, 1961, no. 12, pp. 103–122.

Rabochaya skhema stratigrafii i korrelyatsii razrezov verkhnego proterozoya Zapadnoi Bashkirii (metodicheskie rekomendatsii) (The Working Scheme of Upper Proterozoic Stratigraphy and Correlation for Western Bashkiria), Ufa: Bashkir Fil. Akad. Nauk SSSR, 1981.

Romanov, V.A. and Isherskaya, M.V., *K izucheniyu rifeiskikh otlozhenii Zapadnoi Bashkirii* (Studies on the Riphean Deposits in Western Bashkortostan), Ufa: Inst. Geol., Ufim. Nauchn. Tsenter Ross. Akad. Nauk, 1994a.

Romanov, V.A. and Isherskaya, M.V., *Rifei Kulguninskoi skvazhiny i korrelyatsiya ego s odnovozrastnymi otlozheniyami smezhnykh raionov Bashkirii* (The Riphean Sequence of the Kulgunino Well and Its Correlation with Coeval Deposits in Adjacent Areas of Bashkortostan), Ufa: Inst. Geol., Ufim. Nauchn. Tsenter Ross. Akad. Nauk, 1994b.

Romanov, V.A. and Isherskaya, M.V., *Srednii rifei platformennogo Bashkortostana* (The Middle Riphean of Platform Areas in Bashkortostan), Ufa: Akad. Nauk Respubl. Bashkirtostan, 1997.

Romanov, V.A. and Isherskaya, M.V., *Stratigrafiya rifeya platformennogo Bashkortostana* (The Riphean Stratigraphy of the Platform Areas of Bashkortostan), Ufa: Akad. Nauk Republic Bashkirtostan, 1998.

Rotaru, A.F., The Riphean Mashak Formation of the South Urals: Stratigraphy, Composition, and Tectonics, *Abstract of Cand. Sci. (Geol.–Mineral.) Dissertation*, Sverdlovsk: Inst. Geol. Geochem., Ural. Sci. Center, Acad. Sci. USSR, 1983.

Shvetsov, P.N., The Lower and Middle Riphean Deposits of the Western Urals, Bashkiria: Principles of Structural–Formational Analysis, *Abstract of Cand. Sci. (Geol.–Mineral.) Dissertation*, Kazan: Kazan Univ., 1974.

Sovetov, Yu.K., Late Riphean Rifting and Baikalian Cycle of Geodynamic Development of the Siberian Platform, in *Rifei Severnoi Evrazii. Geologiya. Obshchie problemy stratigrafii* (The Riphean of Northern Eurasia: Geology and General Problems of Stratigraphy), Yekaterinburg: Inst. Geol. Geokhim., Ural Otd. Ross. Akad. Nauk, 1997, pp. 223–230.

Stratigraficheskie skhemy Urala (dokembrii, paleozoi) (Stratigraphic Schemes for the Urals: Precambrian and Paleozoic), Yekaterinburg: Roskomnedra, 1993.

Stratotip rifeya. Stratigrafiya. Geokhronologiya (The Riphean Stratotype: Stratigraphy and Geochronology), Keller, B.M. and Chumakov, N.M., Eds., Moscow: Nauka, 1983.

Surkov, V.S., Korobeinikov, V.P., and Grishin, M.P., Siberian Basins Bearing Oil and Gas: Development during the Neogean, *Otech. Geol.*, 1993, no. 6, pp. 39–45.

Surkov, V.S., Korobeinikov, V.P., Krylov, S.V., *et al.*, Geodynamic and Sedimentation Environments of the Riphean Complexes Bearing Oil and Gas in the Western Margin of the Siberian Paleocontinent, *Geol. Geofiz.*, 1996, vol. 37, no. 8, pp. 154–165.

Veis, A.F. and Petrov, P.Yu., The Main Peculiarities of the Environmental Distribution of Microfossils in the Riphean Basins of Siberia, *Stratigr. Geol. Korrelyatsiya*, 1994, vol. 2, no. 5, pp. 97–129.

Veis, A.F. and Semikhatov, M.A., The Lower Riphean Omakhta Assemblage of Microfossils from Eastern Siberia: Composition and Formation Settings, *Izv. Akad. Nauk SSSR, Ser. Geol.*, 1989, no. 5, pp. 36–54.

Yanitskii, A.L. and Sergeev, O.P., *Bakal'skie zhelezorudnye mestorozhdeniya i ikh genezis* (The Bakal Iron Ore Deposits and Their Genesis), Moscow: Akad. Nauk SSSR, 1962.

Stratigraphy and Geological Correlation, Vol. 8, No. 1, 2000, pp. 30–48. Translated from Stratigrafiya. Geologicheskaya Korrelyatsiya, Vol. 8, No. 1, 2000, pp. 35–54.
Original Russian Text Copyright © 2000 by Byakov.
English Translation Copyright © 2000 by MAIK "Nauka/Interperiodica" (Russia).

Bivalve Zonation in Permian Deposits of Northeastern Asia

A. S. Byakov

Rostov State University, ul. Zorge 40, Rostov-on-Don, 344090 Russia

Received September 8, 1997

Abstract—Detailed stratigraphical and paleontological investigations of many sections in the Kolyma and Omolon river basins and the Okhotsk area resulted in the elaboration of biostratigraphic bivalve zonation of Permian deposits in northeastern Asia (excluding the Koryak Upland). The zonal scheme consists of 11 zones. In addition, two auxiliary units (beds with fauna) were recognized in the Gizhiga Horizon of the Upper Permian. All zones are characterized by zonal bivalve assemblages, and are by nature biostratigraphic zones. The zonation is based on stages in the phylogenetic evolution of inoceram-like bivalves, which are least dependent on facies factors and usually occur in abundance. Possible correlations of the established zonation with those in the Verkhoyansk and Baikal regions, Novaya Zemlya, Taimyr, northern Russian platform, North America, Australia, New Zealand, and other regions are demonstrated.

Key words: *Permian, bivalves, zones, correlation, Northeastern Asia.*

INTRODUCTION

In northeastern Asia, Permian deposits are widespread in the Yana–Kolyma fold system and within the Okhotsk and Omolon median massives together with their surrounding structures. Almost everywhere, Permian deposits are characterized by great thickness (up to 7 km), noticeable facies variability, monotonous structure, and scarcity of faunal and floral remains. They contain no orthostratigraphic groups, such as fusulinids and conodonts. Rare ammonoids are recorded in the Lower and basal Upper Permian deposits. The fossils found are predominantly brachiopods, bivalves, and smaller foraminifers; the thick monotonous sandy–clayey sequences bear mainly bivalves and gastropods.

Traditionally, the biostratigraphic subdivision and correlation of the sections are based mainly on brachiopods (Zabodovskii, 1970; Ganelin, 1973, 1984) and, to a lesser extent, on smaller foraminifers (Karavaeva, 1990) and ammonoids (Andrianov, 1985). Up to the present, no other groups of fossils have been used for stratigraphic purposes.

The Permian deposits of northeastern Russia are subdivided into regional horizons (*Resheniya...*, 1978) in accordance with stages of biota development. Later, within the horizons, Ganelin (1984) distinguished regional assemblage zones as units substantiated in geohistorical aspect. These units were mainly recognized on the basis of brachiopods because of inadequate data on other fossils.

This gap was filled up after foraminiferal investigation by Karavaeva (1990) and my study on bivalves (Byakov, 1990). These materials were taken into account for the comprehensive substantiation of the regional assemblage zones (Ganelin *et al.*, 1990).

Up to the present, bivalves have been little used to solve stratigraphic problems. The pioneering studies were those by B.K. Likharev, D.F. Maslennikov, Yu.N. Popov, E.M. Lyutkevich, O.V. Lobanova, and V.A. Muromtseva. The first attempt to use bivalves for subdivision and correlation of the Verkhoyansk regional sequences was made by Kuznetsov (1972). In the 1980s, Permian bivalves (mainly from the Verkhoyansk region) were investigated by Muromtseva, K.A. Astaf'eva-Urbaitis, and M.M. Astaf'eva, who did not use these fossils to establish the low-rank biostratigraphic units. This problem is considered in detail in a series of my publications (Byakov, 1988, 1990, 1991a, 1991b, 1991c, 1991d, 1995; Biakov, 1996) and in the present article. The recent publication of Kurushin *et al.* (1996) showed the bivalve zonation to be valid for the West Verkhoyansk region.

The collection used was predominantly made by me between 1982 and 1992 while working in the Central Joint Expedition of the PGO Sevvostgeologiya (Magadan). During this term, I studied in detail nearly 20 Permian key sections in the Kolyma River basin and Okhotsk region (the northeastern rim of the Okhotsk massif, Ayan-Yuryakh anticlinorium, Balygychan Upland, Omolon massif, and southeastern surrounding structures). In addition, I used Karavaeva's descriptions of some sections and bivalve collection from the southeastern Omolon massif, and Taigonos Peninsula, as well as some paleontological collections of many other geologists mostly from the Omolon massif, Balygychan Upland, and Ayan-Yuryakh anticlinorium. Between 1982 and 1994, I also identified fossils from different areas to the north and south of Verkhoyansk

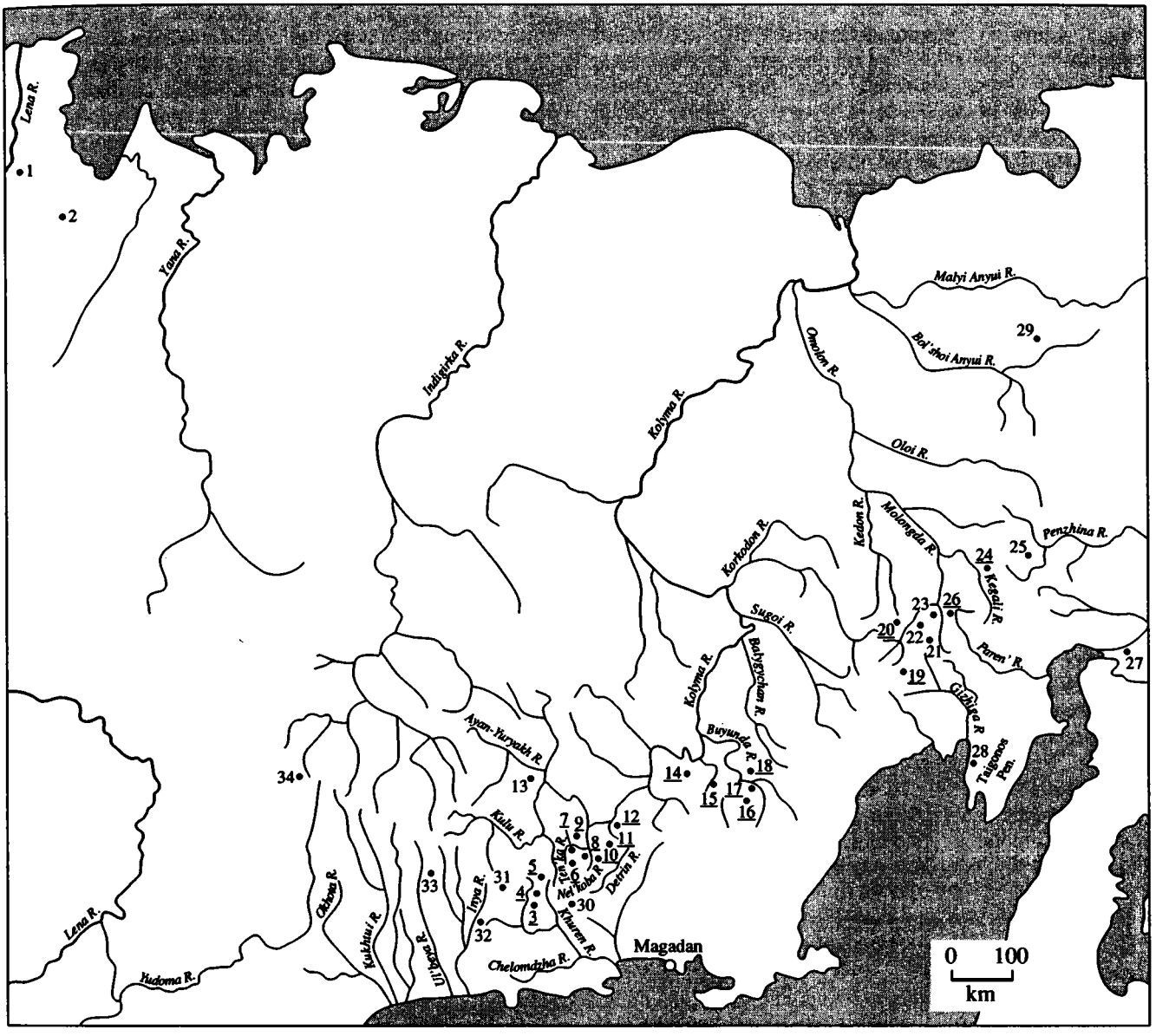

Fig. 1. Main sections studied and bivalve localities.

(1–2) northern Verkhoyansk region: (1) Chekurovka River, (2) Kharaulakh Ridge; (3–5) and (30–31) northeastern surrounding structures of the Okhotsk massif, (3–4, 30) the Khuren River upper course: (3) Sineva Creek, (4) Beglyi Creek, (30) Plastovyi Creek, (5) upper reaches of the Khuren River, Titan Creek, (31) Burgagylkan River upper course, Druzhba River; (6–13) Ayan-Yuryakh anticlinorium: (6) upper reaches of the Tenke River, Gorbatyi Creek, (7) Krasivyi Creek, (8) Rodionovskii Creek, (9) Broshennyi Creek, (10) upper reaches of the Nel'koba River, Tikhonya Creek, (11) Vakkhanka Creek, (12) Detrin River mouth, (13) Arga-Yuryakh River; (14–18) Balygychan Uplift, (14) upper reaches of the Pautovaya River, (15) upper reaches of the Pravyi Srednekan River, (16–18) Bol'shaya Kupka River, (16) Poiskovik Creek, (17) Smorodinnyi Creek, (18) Bol'shaya Kupka; (19–24) Omolon massif: (19) Vodopadnyi Creek, (22–23) interfluve of the Bol'shaya and Malaya Aulandzhi rivers, (24) Avlandya lower course, (25–26) eastern and southeastern surrounding structures of the Omolon massif; (25) upper reaches of the Penzhina River, (26) upper reaches of the Paren' River, Fedorovskii Creek; (27) Pontoneiskie Mountains; (28) Taigonos Peninsula; (29) upper courses of the Bol'shoi Anyui River; (32–33) Okhotsk region: (32) Inya River middle courses, (33) Ul'bei–Nadbaki interfluve; (34) southern Verkhoyansk region, Suntar River basin. Underlined numbers are those of the sections studied by me.

and from the Sea of Okhotsk, Taimyr, Baikal regions, and North Kamchatka. Over 10000 of bivalve specimens were studied. The main sections studied and fossil occurrences are shown in Fig. 1. For comparative purposes, I also examined Permian bivalves stored at the Chernyshev Central Research Geological Prospecting Museum of St. Petersburg.

The bivalve zonation is elaborated through investigations of the most complete, continuous and well studied sections of the Omolon massif (predominantly at

Vodopadnyi Creek and the Russkaya-Omolonskaya River), where bivalves are associated with brachiopods, foraminifers, and other faunal remains. In the Lower and basal Upper Permian beds they were found together with ammonoids (*Opornyi...*, 1990). These sections are characterized by relatively thin conformable bedding favorable for reliable calibration and correlation. This fact is especially important, because many significant stratigraphic errors stem from the complicated dislocated structure of most Verkhoyansk sections. Most of the established zones were recognized within thick deep-water sandy–clayey facies of folded structures surrounding the median massives (Fig. 2).

The Permian zonation (except for the basal Lower Permian) is based on stages in the development of inoceram-like bivalves of the family Colymiidae. The stages are recognized on the basis of morphogenetic analysis of Colymiidae throughout the section and phylogenetic reconstructions (Fig. 3), which guarantees the absence of any significant gaps in the scheme. Zonation for basal Lower Permian beds lacking Colymiidae is based on other bivalve groups.

The established biostratigraphic zones are bodies of strata that were formed during certain developmental stages of all bivalve groups of the region and are by nature assemblage zones (*Stratigraphic...*, 1992). The lower boundary of each biostratigraphic zone is, as a rule, drawn at the first occurrence level of the index species. The stratigraphic scope of the bivalve zones corresponds to that of the regional assemblage zones. In some areas, the Gizhiga Horizon corresponding to one bivalve zone is subdivided into beds with fauna. This makes the zonation more detailed. Stratigraphic ranges of bivalves are shown in Fig. 4.

The Permian reference sections are described in the following publications: Ganelin and Karavaeva, 1977; Ganelin, 1984; *Opornyi...*, 1990; Byakov and Vedernikov, 1990.

ZONAL SCHEME

Lower Permian

Munugudzhak Horizon. The Munugudzhak Horizon spans two bivalve zones (*Palaeoneilo parenica* and *Lithophaga gigantea*) corresponding to its lower and upper parts.

Palaeoneilo parenica Zone

Index species: *Palaeoneilo parenica* Biakov (Byakov, 1998; Figs. 3a–3c)

Type area: southeastern surrounding structures of the Omolon massif, Rinkhopora Creek, the tributary of the Fedorovskii Creek, upper courses of the Paren' River; the middle and upper parts of the Magiveem Formation, Exposure 17, members 2–6 (Ganelin, 1984).

Stratigraphic scope. The lower zonal boundary is drawn at the first occurrence level of the index species. This boundary may not be coincident with the lower boundary of the regional *Jakutoproductus mirandus* Zone; this question needs to be additionally studied. In the type area, the zonal assemblage is confined to the lower half of the zone generally correspondent to the regional *J. expositus* Zone. No bivalves were found in the upper half of the zone of the area. In other sections (in the Bol'shaya and Malaya Aulandzhi interfluve), the upper half of the zone is characterized by rare *Myophossa* cf. *subarbitrata* (Dick.).

Paleontological characteristics. The zonal assemblage consists of *Palaeoneilo parenica* Biakov, *Polidevcia* cf. *kolyvanica* Murom., *Aviculopecten mirus* Lob., *Astartella omolonica* Murom., *Myophossa subarbitrata* Dick., *Cypricardinia borealica* Murom., and *Lithophaga* sp. The important forms are also *Palaeolima laticostata* Tschern., *Permophorus* cf. *oblongus* (M. et H.), and *Astartella permocarbonica* Tschern. unknown from the underlying beds and passing into the succeeding zone. *Streblopteria* sp., *Praeundulomya urbajtisae* Murom. and *Grammysiopsis omolonicus* Murom. are inherited at this level from the Upper Carboniferous deposits and disappear in this zone. Transitional species are *Aviculopecten mutabilis* Lich. and *Streblopteria* cf. *englehardti* (Eth. et Dun). Rare *Wilkingia?* sp. indet., *Permophorus?* sp. indet., *Astartella?* sp. indet., *Nuculopsis* sp. indet., and *Schizodus?* sp. indet. were also found.

Age substantiation and correlation. The lower boundary of the zone is arbitrarily taken as coincident with that of the Asselian Stage, and the upper one is placed at the base of the Artinskian Stage because of the occurrence of goniatite *Neoshumardites triceps* Ruzh. in the middle part of the *rugosus* Zone (Ganelin, 1984). The zonal assemblage differs from the Late Carboniferous bivalve assemblages, since it shows the following: the absence of representatives of genus *Leiopteria*; appearance of genera *Astartella, Myophossa*, and *Stutchburia*; sharply decreased abundance of the gen-

Fig. 2. Bivalve-based correlations of the main Permian sections in northeastern Asia.

The section numbers above the columns correspond to those in Fig. 1; figures to the right of the columns denote thickness, m:

(1) conglomerate; (2) sandstone; (3) siltstone; (4) mudstone; (5) sandy siltstone; (6) diamictite; (7) admixed scattered gravel-size grains; (8) basic lava; (9) intermediate tuff; (10) acidic tuff; (11) tuff; (12) tuffite; (13) limestone; (14) clayey limestone; (15) sandy limestone; (16) siliceous deposits; (17) location of index species of the bivalve zones or elements of zonal assemblages; (18) unexposed interval. Species:

(*K.o.*) *Kolymaella ogonerensis*; (*M.r.*) *Mongolosia russiensis*; (*O.s.*) *Omolonia snjatkovi*; (*T.b.*) *Terrakea borealis*; (*T.k.*) *Terrakea korkodonensis*; (*M.b.*) *Magadania bajkurica*; (*A.d.*) *Aphanaia dilatata*; (*K.i.*) *Kolymia inoceramiformis*; (*K.p.*) *Kolymia plicata*; (*K.m.*) *Kolymia multiformis*; (*M.p.*) *Merismopteria permiana*; (*G.b.*) *Glyptoleda borealica* (the same for Fig. 5).

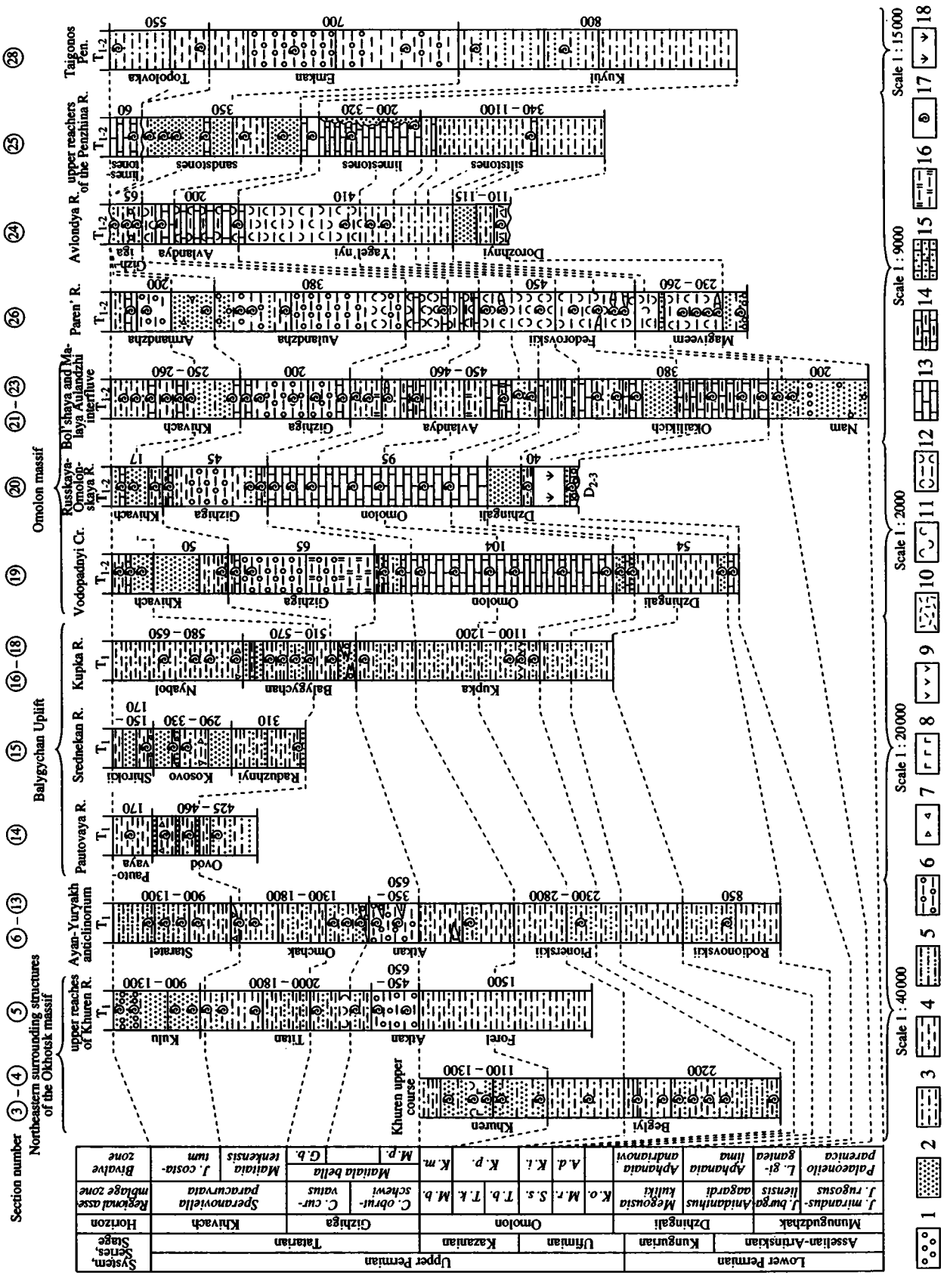
Section number
Northeastern surrounding structures of the Okhotsk massif
Balygychan Uplift
Omolon massif
Scale 1 : 40000
Scale 1 : 20000
Scale 1 : 2000
Scale 1 : 9000
Scale 1 : 15000
Lower Permian
Upper Permian
Asselian-Artinskian
Kungurian
Dzhingali
Munugudzhak
Ufimian
Kazanian
Tatarian
Omolon
Gizhiga
Khivach
Taigonos Pen.
upper reaches of the Penzhina R.
Avlondya R.
Paren' R.
Bol'shaya and Malaya Anlandzhi interfluve
Russkaya-Omolonskaya R.
Vodopadnyi Cr.
Kupka R.
Srednekan R.
Pautovaya R.
Ayan-Yuryakh anticlinorium
upper reaches of Khuren R.
Khuren upper course
Kuyul
Topolovka
Emkan
sandstones
limestones
siltstones
Dorozhnyi
Yagel'nyi
Avlondya
Gizhiga
Armandzha
Aulandzha
Fedorovskii
Magiveem
Nam
Okaliilich
Khivach
Gizhiga
Avlandya
Aulandzha
Armandzha
Dzhingali
Omolon
Gizhiga
Khivach
Dzhingali
Omolon
Gizhiga
Khivach
Kupka
Baygychan
Nyabol
Raduzhnyi
Kosovo
Shirokii
Ovdd
Pautovaya
Rodionovskii
Ponerskii
Atkan
Omchak
Staraiel
Forel'
Atkan
Tiian
Kulu
Begiyi
Khuren
Taigonos Pen.
upper reaches of the Penzhina R.
Avlondya R.
Paren' R.
Bol'shaya and Malaya Anlandzhi interfluve
Russkaya-Omolonskaya R.
Vodopadnyi Cr.
Kupka R.
Srednekan R.
Pautovaya R.
Ayan-Yuryakh anticlinorium
upper reaches of Khuren R.
Khuren upper course
Munugudzhak
Dzhingali
Omolon
Gizhiga
Khivach
Taigonos Pen.
upper reaches of the Penzhina R.
Avlondya R.
Paren' R.
Bol'shaya and Malaya Anlandzhi interfluve
Russkaya-Omolonskaya R.
Vodopadnyi Cr.
Kupka R.
Srednekan R.
Pautovaya R.
Ayan-Yuryakh anticlinorium
upper reaches of Khuren R.
Khuren upper course
Palaeoneilo parenica
L. gi-ganlea
Aphanaia lima
Aphanaia andrianovi
Megousia kuliki
J. birgo-densis
Antiadanthus aagardi
J. mirandus-J. rugosus
K. o.
M. r.
S. s.
T. b.
T. k.
M. b.
A. d.
K. i.
K. p.
K. m.
M. p.
Maitaia bella
G. b.
C. obrui-schewi
C. cur-vatus
Maitaia tenkensis
J. cosia-tum
Bivalve zone
Regional asse mblage zone
Speranovielia paracurvata
Khivach
Gizhiga
Omolon
Ufimian
Kazanian
Tatarian
Upper Permian
Kungurian
Dzhingali
Munugudzhak
Asselian-Artinskian
Lower Permian
System, Series, Stage
Horizon
1
2
3
4
5
6
7
8
9
10
11
12
13
14
15
16
17
18

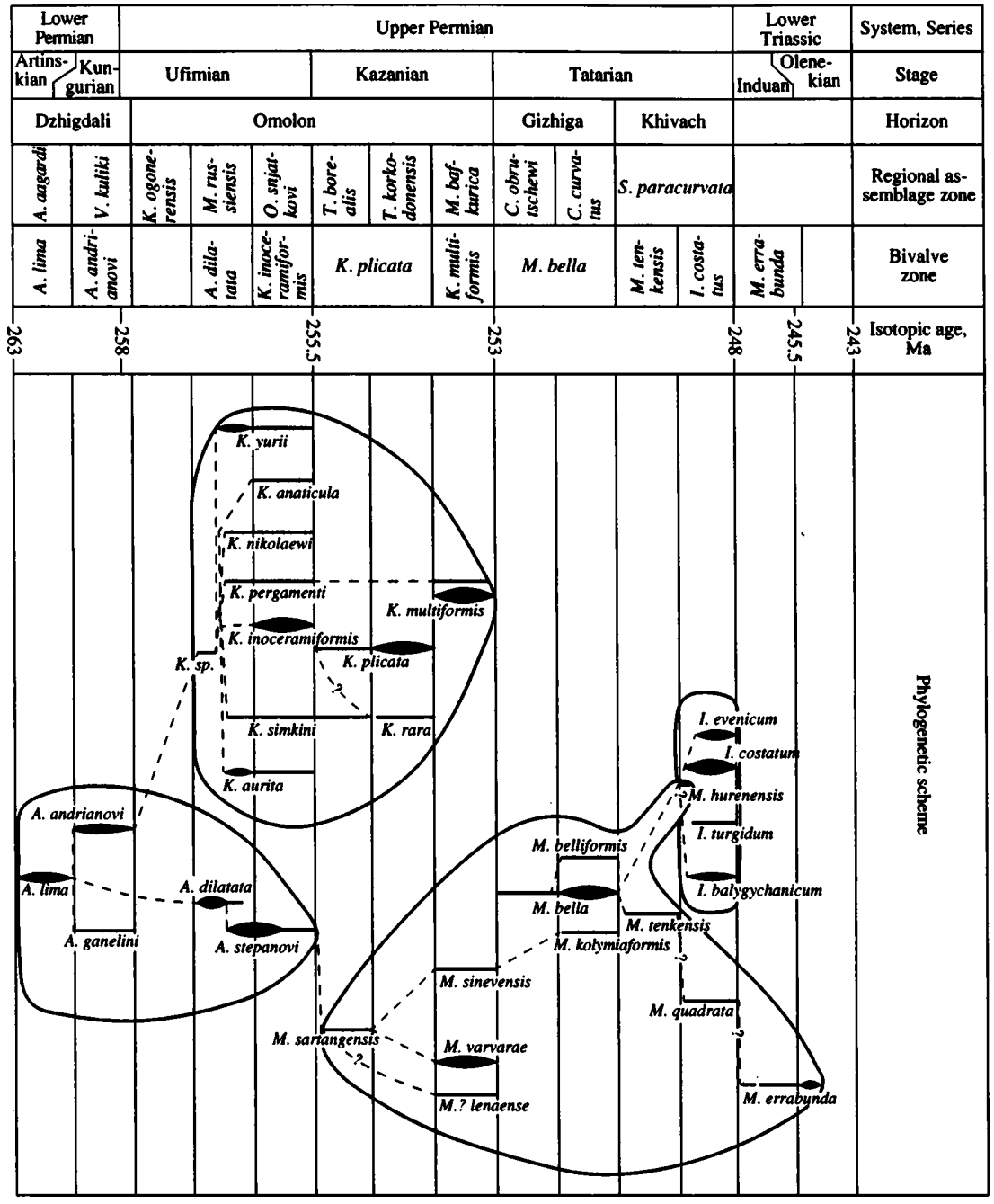

Fig. 3. Phylogeny of the Permian inoceram-like bivalves of northeastern Asia (geochronology according to Harland *et al.*, 1982).

era *Palaeoneilo, Palaeolima, Wilkingia*, and *Lithophaga*; and some changes in species composition of the transitional genera. Some species of the zonal assemblages were recorded in the Lower Permian deposits (the upper Megen, Kygyltas, and Dzhuptaga formations) of the Verkhoyansk region (Muromtseva and Gus'kov, 1984; Astaf'eva and Astaf'eva-Urbaitis, 1988; Kurushin *et al.*, 1996). *C. borealica* Murom. was identified from the Sakmarian deposits of the Pechora basin (Chuvashov *et al.*, 1991). According to my identifications of *Polidevcia kolyvanica* Murom., *Cypricardinia* cf. *borealica* Murom., and *Permophorus* cf. *oblongus* (M. et H.) from the collection of S.M. Sinitsa, zone analogues can be recognized in the Zhipkhoshin Formation of the eastern Baikal region. *M. subarbitrata* (Dick.) is known from the Lower Permian deposits of Australia (Dickins, 1963).

Distribution: eastern and southeastern parts of the Omolon massif and its surrounding structures; the distribution patterns of the index species and some other

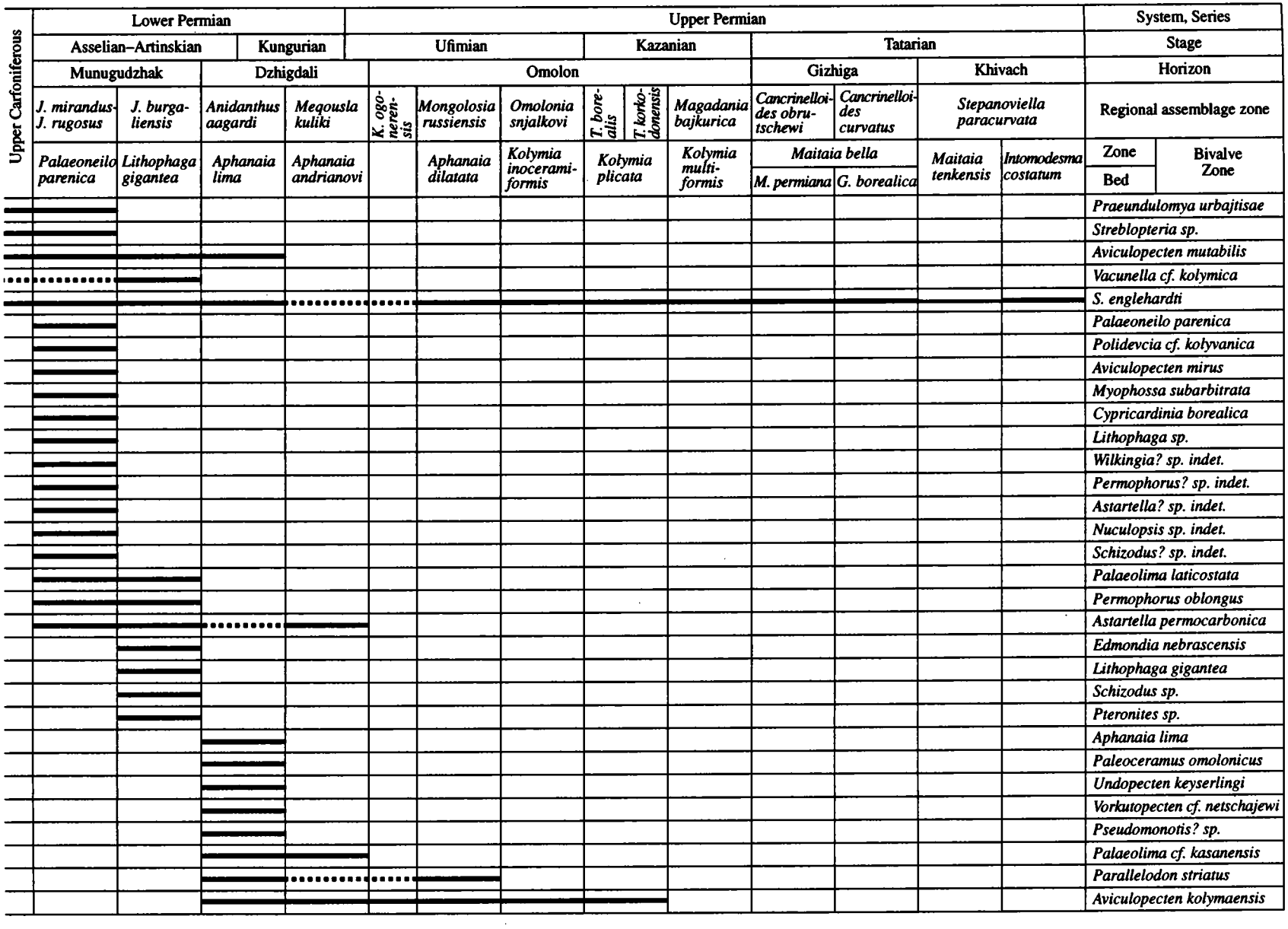

Fig. 4. Stratigraphic ranges of Permian bivalves from northeastern Asia.

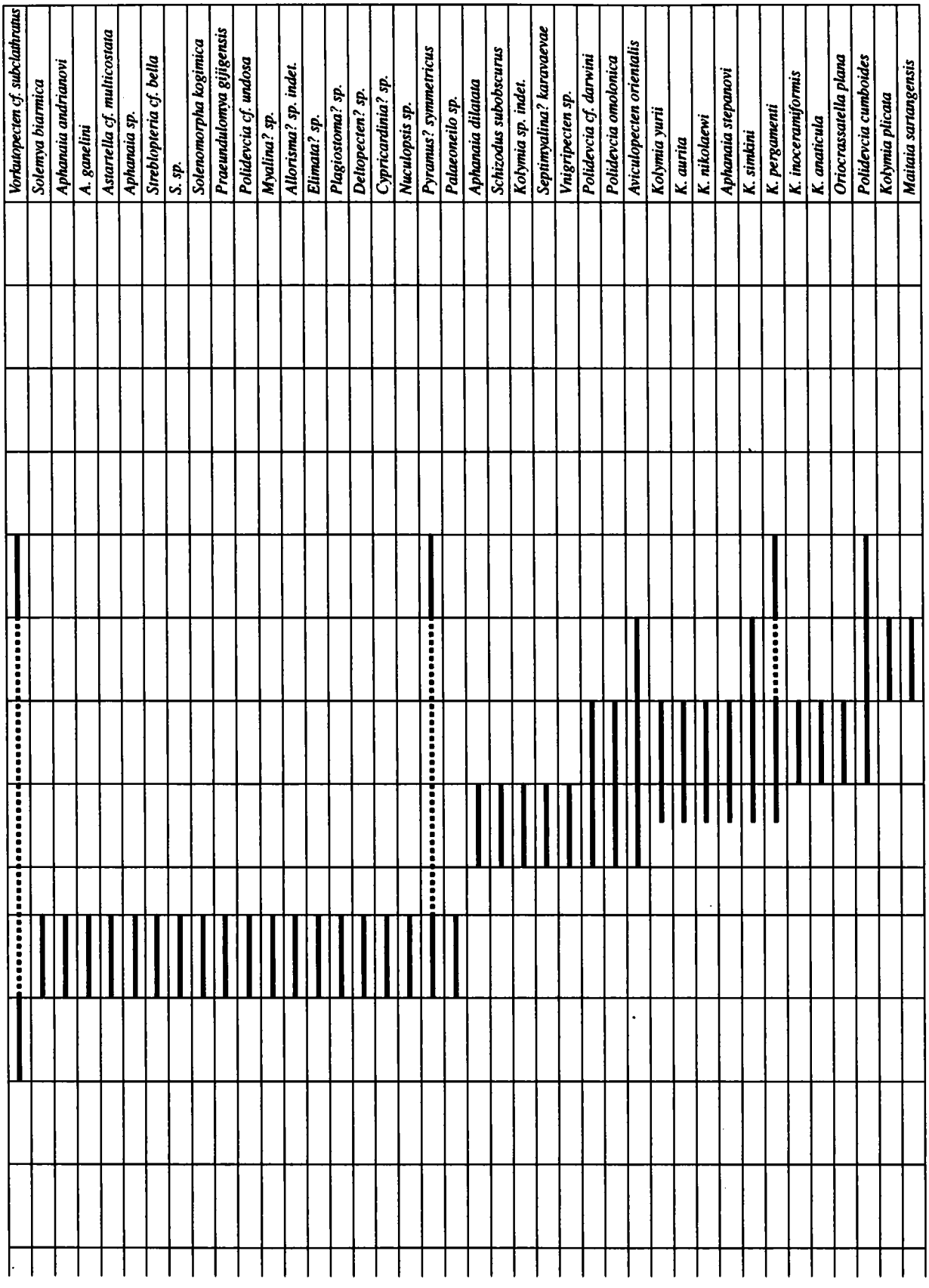
Vorlutopecten cf. subclathratus
Solemya biarmica
Aphanaia andrianovi
A. ganelini
Astartella cf. multicostata
Aphanaia sp.
Streblopteria cf. bella
S. sp.
Solenomorpha kogimica
Praeundulomya gijigensis
Polidevcia cf. undosa
Myalina? sp.
Allorisma? sp. indet.
Elimata? sp.
Plagiostoma? sp.
Deltopecten? sp.
Cypricardinia? sp.
Nuculopsis sp.
Pyramus? symmetricus
Palaeoneilo sp.
Aphanaia dilatata
Schizodus subobscurus
Kolymia sp. indet.
Septimyalina? karavaevae
Vnigripecten sp.
Polidevcia cf. darwini
Polidevcia omolonica
Aviculopecten orientalis
Kolymia yurii
K. aurita
K. nikolaewi
Aphanaia stepanovi
K. simkini
K. pergamenti
K. inoceramiformis
K. anaticula
Oriocrassatella plana
Polidevcia cumboides
Kolymia plicata
Maiaia sartangensis

Fig. 4. (Contd.)

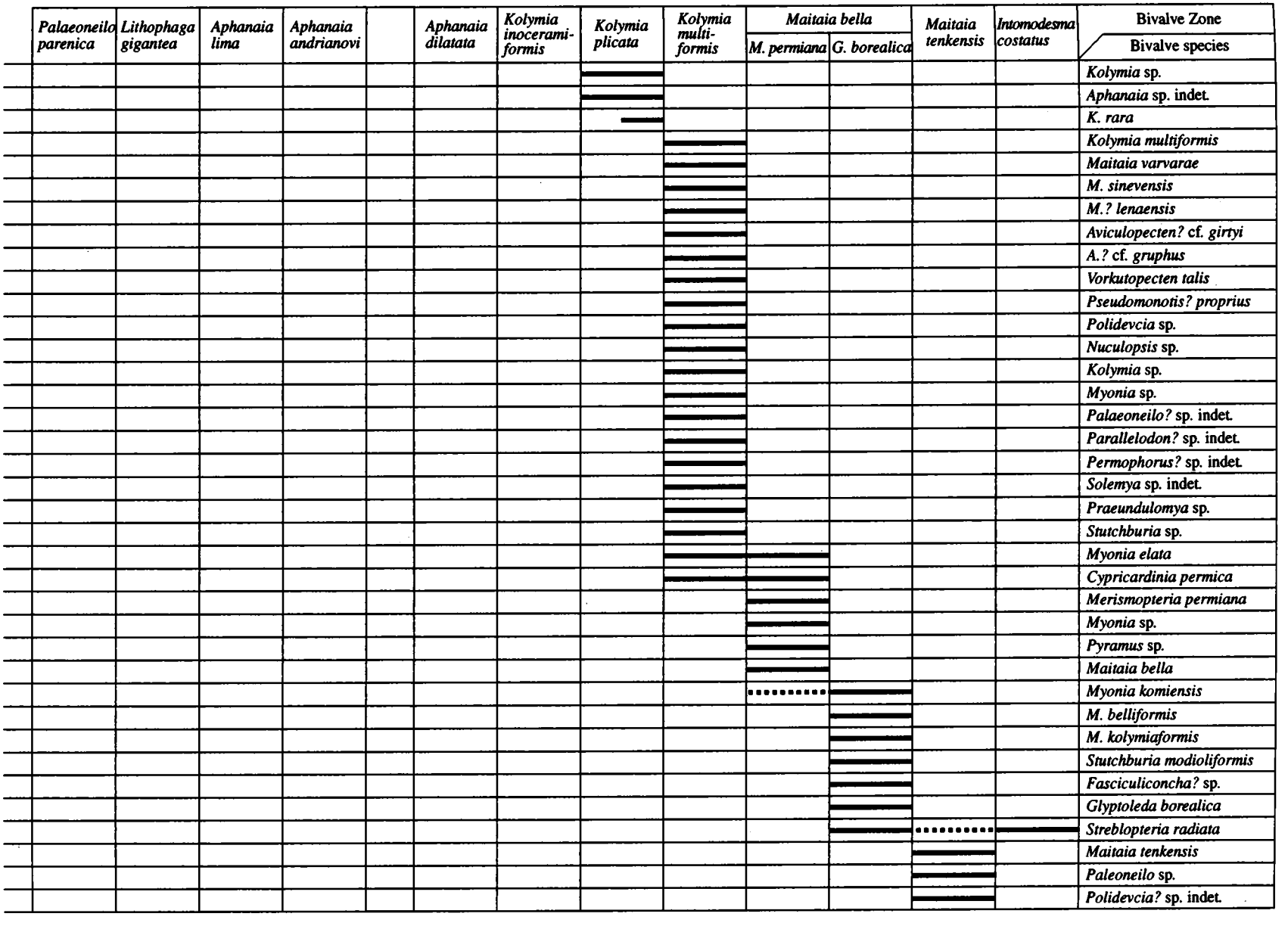
Palaeoneilo parenica
Lithophaga gigantea
Aphanaia lima
Aphanaia andrianovi
Aphanaia dilatata
Kolymia inocerami-formis
Kolymia plicata
Kolymia multi-formis
Maitaia bella
M. permiana
G. borealica
Maitaia tenkensis
Intomodesma costatus
Bivalve Zone
Bivalve species
Kolymia sp.
Aphanaia sp. indet.
K. rara
Kolymia multiformis
Maitaia varvarae
M. sinevensis
M.? lenaensis
Aviculopecten? cf. girtyi
A.? cf. gruphus
Vorkutopecten talis
Pseudomonotis? proprius
Polidevcia sp.
Nuculopsis sp.
Kolymia sp.
Myonia sp.
Palaeoneilo? sp. indet.
Parallelodon? sp. indet.
Permophorus? sp. indet.
Solemya sp. indet.
Praeundulomya sp.
Stutchburia sp.
Myonia elata
Cypricardinia permica
Merismopteria permiana
Myonia sp.
Pyramus sp.
Maitaia bella
Myonia komiensis
M. belliformis
M. kolymiaformis
Stutchburia modioliformis
Fasciculiconcha? sp.
Glyptoleda borealica
Streblopteria radiata
Maitaia tenkensis
Paleoneilo sp.
Polidevcia? sp. indet.

Fig. 4. (Contd.)

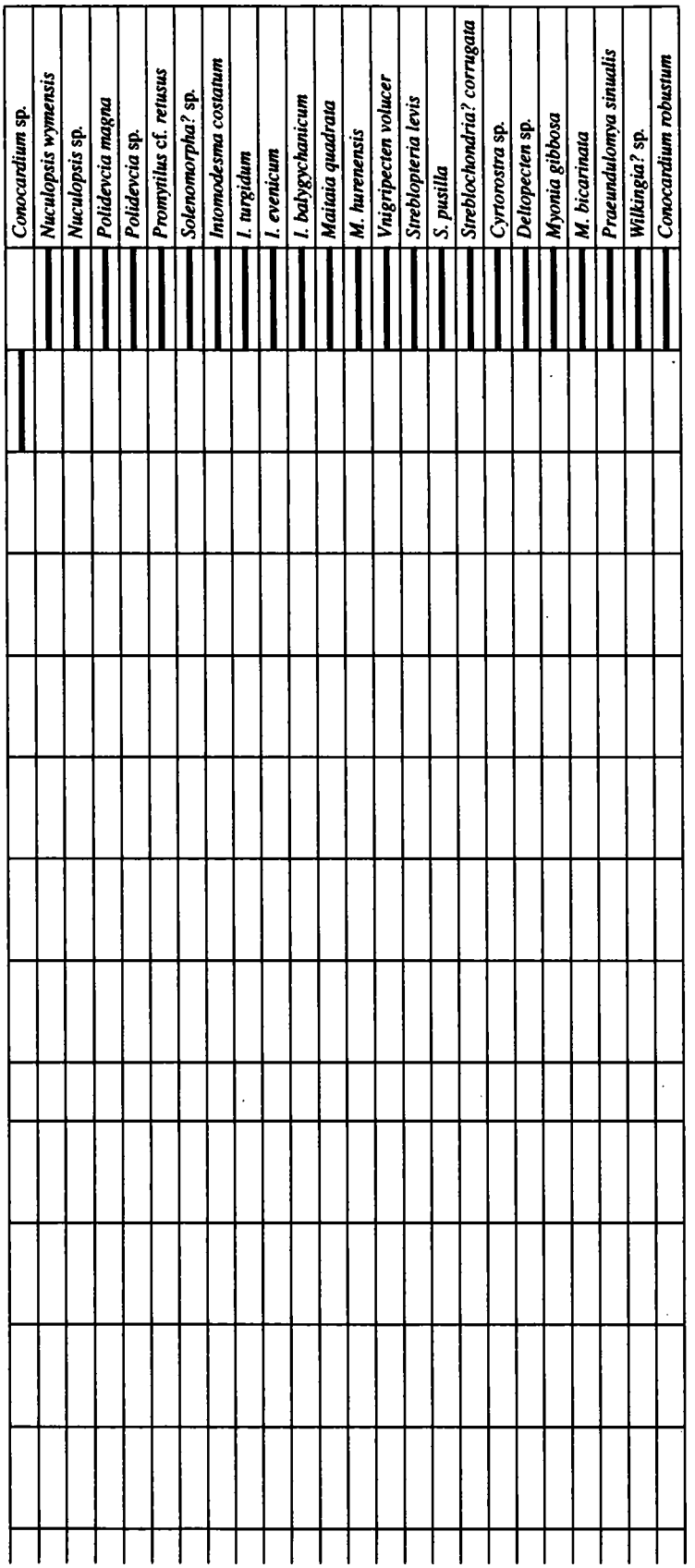
Conocardium sp.
Nuculopsis wymensis
Nuculopsis sp.
Polidevcia magna
Polidevcia sp.
Promytilus cf. retusus
Solenomorpha? sp.
Intomodesma costatum
I. turgidum
I. evenicum
I. babygychanicum
Maiuaia quadrata
M. hurenensis
Vnigripecten volucer
Streblopteria levis
S. pusilla
Streblochondria? corrugata
Cyrtorostra sp.
Deltopecten sp.
Myonia gibbosa
M. bicarinata
Praeundulomya sinuatis
Wilkingia? sp.
Conocardium robustum

Fig. 4. (Contd.)

components of the zonal assemblage suggest the occurrence of the zone in the southern and western Verkhoyansk region (Muromtseva and Gus'kov, 1984; Kurushin, 1996) and in the Baikal region.

Lithophaga gigantea Zone

Index species *Lithophaga gigantea* (Stuckenberg) (=*Modiola gigantea* Stuckenberg; Stuckenberg, 1898, p. 207, Plate 1, Fig. 38).

Type area: the southeastern Omolon massif, the Bol'shaya and Malaya Aulandzhi interfluve; the upper Nam Bed 2. In 1984, L.D. Shkol'nyi described the following section of the upper Munugudzhak Horizon at Aelita Creek, which was taken as the zone stratotype (from the base upward):

(1) siltstone with sandstone and gravelstone interbeds containing brachiopods *Jakutoproductus rugosus* Gan. and *Jakutoproductus* sp. in association with the bivalve *Myophossa* cf. *subarbitrata* (Dick.) of the bivalve *Palaeoneilo parenica* Zone;

(2) light gray fine-grained calcareous sandstone with gray siltstone interbeds containing brachiopods *Jakutoproductus* sp. and bivalves *Edmondia nebrascensis* (Gein.), *Lithophaga gigantea* Stuck., *Astartella* cf. *permocarbonica* Tschern., and *Palaeolima* cf. *laticostata* Tschern. (thickness is 30 m);

(3) clayey limestones of the lower Dzhigdali Horizon (the bivalve *Aphanaia lima* Zone) bearing brachiopods *Anidanthus aagardi* (Toula) and bivalves *Aphanaia* cf. *lima* (Lutk. et Lob.).

Stratigraphic scope. The lower boundary of the zone is drawn at the first occurrence level of the index species and zonal species assemblage. It is not quite clear whether this boundary coincides with the base of the regional *Jakutoproductus burgaliensis* Zone or lies inside the underlying regional *J. rugosus* Zone. This needs to be specially studied.

Paleontological characteristics. The zonal assemblage is not diverse, and its composition should be defined more precisely. It includes *Edmondia nebrascensis*, *Lithophaga gigantea* Stuck., and *Pteronites* sp. There are also *Palaeolima* cf. *laticostata* Tschern.; *Permophorus* cf. *oblongus* (M. et H.); and *Astartella permocarbonica* Tschern., which passed from the underlying zone. *Vacunella* cf. *kolymica* Murom., *Aviculopecten mutabilis* Lich., and *Streblopteria englehardti* (Eth. et Dun) are of Upper Carboniferous origin; and the rare *Schizodus* sp. is an accessory element.

Age substantiation and correlation. The occurrence of the early Artinskian goniatites *Neoshumardites* in the middle part of the regional *rugosus* Zone (Ganelin, 1984) indicates the initial mid-Artinskian age of the zone. According to Astaf'eva and Astaf'eva-Urbaitis (1988), *E. nebrascensis* Gein. and *L. gigantea* Stuck. were found only in the Artinskian bivalve assemblage of the East European subprovince. In contrast to the specific composition, the generic composition of the zonal assemblage is similar to that of the underlying deposits.

Distribution: eastern and southeastern parts of the Omolon massif and its surrounding structures; the distribution of some species of the zonal assemblage (Muromtseva and Gus'kov, 1984) suggests that the zone may also be recognized in the southern and even western Verkhoyansk region (Kurushin *et al.*, 1996).

Dzhigdali Horizon. The horizon consists of two bivalve zones, *Aphanaia lima* and *Aphanaia andrianovi*, whose scopes approximate those of the corresponding regional assemblage zones.

Aphanaia lima Zone

Index species: *Aphanaia lima* (Lutkevich et Lobanova) (=*Kolymia lima* Lutkevich et Lobanova; Lobanova and Lyutkevich, 1970, p. 46, Plate 57, Fig. 2).

Type area: southeastern Omolon massif and the Pravyi Vodopadnyi Creek of the Gizhiga River basin; lower beds of the Dzhigdali Formation, Exposure 1, Beds 1–3 (*Opornyi...*, 1990).

Stratigraphic scope. The lower boundary of the zone is drawn at the first occurrence of the inoceramlike bivalves and representatives of the zonal assemblages.

Paleontological characteristics. The zonal assemblage contains *Aphanaia lima* (Lutk. et Lob.), *Paleoceramus omolonicus* Biakov, gen. et sp. nov. (in manuscript), *Undopecten keyserlingi* (Fred.), and *Vorkutopecten* cf. *netschajewi* (Lich.). Abundant forms are also *Palaeolima* cf. *kasanensis* (Netsch.); *Aviculopecten kolymaensis* Masl., *Parallelodon striatus* (Schloth.); *Vorkutopecten* cf. *subclathratus* (Keys.), which appeared in these deposits and passed into the overlying ones; and *Aviculopecten mutabilis* Lich., which became extinct within the zone. The first occurrence of the genus *Pseudomonotis* is characteristic. Abundant species of the genus *Streblopteria* dominate in the carbonate facies.

Age substantiation and correlation. The late Artinskian–early Kungurian age of the zone is defined by its stratigraphic position between the lower–middle Artinskian and Kungurian deposits with ammonoids (*Opornyi...*, 1990). Species *U. keyserlingi* (Fred.), *V. subclathratus* (Keys.), *V. netschajewi* (Lich.), and *A. kolymaensis* Maslen. are characteristic of the Kungurian bivalve assemblages of the Pechora basin (the Kozhim Formation), Pai-Hoi, and Verkhoyansk region (Gus'kov *et al.*, 1980; Muromtseva and Gus'kov, 1984; Gus'kov, 1988; Chuvashov *et al.*, 1991). Noticeable changes in the faunal assemblages, namely, the appearance of inoceram-like forms of bivalves and the extinction of the characteristic *Jakutoproductus* species, mark a significant biostratigraphic level of biotic development (Ustritskii, 1975; Ganelin, 1984; Leven *et al.*, 1996). At this level, five bivalve genera (*Aphanaia, Paleoceramus, Undopecten, Vorkutopecten*, and *Pseudmonotis*)

are newcomers and five others (*Grammysiopsis, Vacunella, Pteronites, Lithophaga*, and *Edmondia*) become extinct.

Distribution: the Omolon massif, its southeastern surrounding structures, and probably the Verkhoyansk region.

Aphanaia andrianovi Zone

Index species: *Aphanaia andrianovi* (Muromzeva et Kusnezov) (=*Atomodesma andrianovi* Muromzeva et Kusnezov; Muromtseva and Kuznetsov, 1984, p. 48, Plate 20, Fig. 4).

Type area: southeastern Omolon massif, Pravyi Vodopadnyi Creek of the Gizhiga River basin; the lower Dzhigdali Formation, Beds 4 and 5 (*Opornyi...*, 1990).

Stratigraphic scope. The lower boundary of the zone is drawn at the first occurrence of the index species and zonal assemblage. The largest (upper 18 m) part of the stratotype is barren of faunal remains. Therefore, the upper boundary is arbitrarily placed within the barren interval.

Paleontological characteristics. The abundant and diverse zonal assemblage of the stratotype area contains *Polidevcia* cf. *undosa* (Murom.), *Solemya biarmica* Vern., *Aphanaia andrianovi* (Murom. et Kusn.), *A. ganelini* Biak., *Streblopteria* cf. *bella* Gusk., *Solenomorpha kogimica* Murom., *Praeundulomya gijigensis* (Maslen.), *Astartella* cf. *multicostata* Demb., and *Palaeolima* cf. *kasanensis* (Netsch.); the latter two species are also occasionally found in the *Aphanaia lima* Zone. The important elements of the assemblage are transitional species, such as *Aviculopecten kolymaensis* Maslen., *Streblopteria englehardti* (Eth. et Dun), and *Astartella permocarbonica* Tschen.; the latter becomes extinct at this level. *Pyramus? symmetricus* (Lutk. et Lob.) appears here for the first time and exists until the late Omolon time. No less important are forms that are assigned (in some cases conditionally) to the genera *Myalina, Allorisma, Plagiostoma, Deltopecten, Cypricardinia, Nuculopsis*, and *Palaeoneilo* but are unidentifiable at the specific level.

Age substantiation and correlation. Most likely, the lower part of the zone is of the Kungurian age and the upper one corresponds to the lower Ufimian (Ganelin *et al.*, 1990). However, the Ufimian age may be admitted for the lower part of the zone too, because many species characteristic of this interval have recently been found in deposits referred to the Ufimian Stage of the Pechora basin (Chuvashov *et al.*, 1991). The zone yields nine species: first of all, *S. birmica* Vern., *St. bella* Gusk., *Sol. kogimica* Murom., *A. multicostata* Demb., *P.? symmetricus* (Lutk. et Lob.), and *Pr. gijigensis* (Maslen.), all occurring as well in the Pechora basin (the Lek-Borkuta Formation). Some species are known from coeval deposits of the Verkhoyansk region, Taimyr, Pai-Khoi, and Urals (Muromtseva and Gus'kov, 1984; Astaf'eva and Astaf'eva-Urbaitis, 1988; Gus'kov, 1988; Chuvashov *et al.*, 1991). The level is characterized by seven new bivalve genera, *Solemya, Pyramus, Solenomorpha, Myalina, Elimata, Plagiostoma*, and *Deltopecten*; and only two extinct genera, *Undopecten* and *Paleoceramus*, are recorded here.

Distribution: southeastern Omolon massif; the Ayan-Yuryakh anticlinorium; the southern Verkhoyansk region, the Dyba River basin; the western Verkhoyansk region, the Endyba lithological zone (?).

Upper Permian

Omolon Horizon. The horizon is divided into four bivalve zones (*Aphanaia dilatata, Kolymia inoceramiformis, Kolymia plicata*, and *Kolymia multiformis*). The lower part of the horizon, which corresponds to the regional *Kolymaella oronerensis* Zone, contains no characteristic bivalves.

Aphanaia dilatata Zone

Index species: *Aphanaia dilatata* Biakov (Byakov, 1991a, p. 30, Plate 3, Fig. 2).

Type area: southeastern Omolon massif, Vodopadnyi Creek; boundary deposits of the Dzhigdali and Omolon formations, Exposure 2, Beds 2–4 and Exposure 3, Beds 1–16 (*Opornyi...*, 1990).

Stratigraphic scope. The lower boundary is drawn at the first occurrence of the index or other species of the zonal assemblages. The zone corresponds to the lower part of the regional *Mongolosia russiensis* Zone.

Paleontological characteristics. The zonal assemblage includes *Polidevcia omolonica* Biak. (appears at the base of the zone and passes into the following one), *Parallelodon striatus* (Schloth.) (becomes extinct within the zone), *Septimyalina? karavaevae* Biak., *Aphanaia dilatata* Biak., *Schizodus subobscurus* Lich., and *Vnigripecten* sp. Another characteristic species is *Aphanaia stepanovi* (Murom.), which appears in the second fourth of the zone and passes into the succeeding unit. *Kolymia simkini* Popow, *K. aurita* Astaf., *K. yurii* Astaf., *K. nikolaewi* (Vor.), and *K. pergamenti* Murom. appear in the upper beds of the zone. Most abundant transitional species are *Aviculopecten kolymaensis* Maslen. and *Streblopteria englehardti* (Eth. et Dun). Rare characteristic *Kolymia* sp. indet from the lower beds of the zone and the first occurrence of single *Polidevcia* cf. *darwini* (Kon.) and *Aviculopecten* cf. *orientalis* Fred. are worth mentioning.

Age substantiation and correlation. The mid-Ufimian age of the zone is indicated by the occurrence of the ammonoid genus *Sverdrupites* (Ganelin *et al.*, 1990). A significant event in bivalve development was the appearance of the genus *Kolymia*, which dominated throughout the Omolon time. The typical Late Permian form is *S. subobscurus* Lich. (Muromtseva and Gus'kov, 1984; Logan, 1967). The appearance of *Vnigripecten* sp. similar to *V. phosphaticus* (Girty) from

the Roadian (Ufimian) Phosphoria Formation of North America (Girty, 1910; Ciriacks, 1963) is remarkable. *Vnigripecten* representatives, such as *V. volucer* (Lutk. et Lob.), are more characteristic of the Khivach (upper Tatarian) deposits of the Kolyma–Omolon and Verkhoyansk regions and Novaya Zemlya.

Thus, three genera (*Kolymia, Vnigripecten*, and *Septimyalina*) first appeared within the zone and four genera (*Solenomorpha, Myalina, Elimata*, and *Plagiostoma*) of Kungurian origin became extinct. The genus *Astartella*, which was found for the first time in Carboniferous deposits, disappeared too. The zone contains some species known from the Kozhim Formation of the Pechora basin, the Tab-Yu Formation of the Pai-Khoi, and the lower Gerkina Subformation of Novaya Zemlya.

Distribution: southeastern Omolon massif and northeastern surrounding structures of the Okhotsk massif (upper courses of the Khuren River).

Kolymia inoceramiformis Zone

Index species: *Kolymia inoceramifromis* Licharew gen. et sp. indet. (*Aphanaina*?); Likharev, 1934, p. 76, Plate X, Fig. 13).

Type area: southeastern Omolon massif, the Levyi Vodopadnyi Creek, the lower Omolon Subformation, Exposure 3, Beds 17–37 (*Opornyi...*, 1990).

Stratigraphic scope. The lower boundary of the zone is drawn at the first occurrence of the index species and zonal fossil assemblage. The zone corresponds to the regional *Omolonia snjatkovi* Zone.

Paleontological characteristics. The zonal assemblage consists of *Polidevcia omolonica* Biak., *P. darwini* (Kon.), abundant *Aphanaia stepanovi* (Murom.), *Kolymia inoceramiformis* Lich., *K. aurita* Astaf., *K. anaticula* Astaf., *K. pergamenti* Murom., *K. yurii* Astaf., *K. nikolaewi* (Vor.), abundant *K. simkini* Popow, and *Oriocrassatella plana* (Gol.). Rare *Polidevcia cumboides* (Lutk. et Lob.) is a newcomer. Transitional species are numerous *Aviculopecten kolymaensis* Maslen., *A. orientalis* Fred., and *Streblopteria englehardti* (Eth. et Dun).

Age substantiation and correlation. The zone has the late Ufimian age, although the early Kazanian age should not be excluded. The first dating is based on occurrences of the ammonoids *Sverdrupites* sp. and *S. harkeri* (Ruzh.) in the upper beds of the zone in the southeastern surrounding structures of the Okhotsk massif (Byakov and Vedernikov, 1990) and on the bivalves *O. plana* (Gol.) and *A. orientalis* Fred. known from analogues of the Ufimian Stage in the Pechora basin and Kanin Peninsula (Chuvashov *et al.*, 1990; Muromtseva and Gus'kov, 1984). The Kazanian age is suggested by the presence of *K. nikolaewi* (=*Parainoceramus nikolaewi* Vor.), which was first described in association with *Maitaia? lenaensis* (=*Parainoceramus lenaensis* Vor.) from the Upper Permian deposits of the Bulkur anticline (the northern Verkhoyansk region). The assemblage also includes *Maitaia*? *menneri* (Kulikov), which is similar to the latter form and was described from the lower Kazanian deposits of the northern Russian platform (Kulikov, 1978). Thus, the upper part of the zone is presumed to be of the early Kazanian age.

In the taxonomic aspect, the bivalve assemblage demonstrates subregional endemism (it has only four species in common with the West Arctic assemblages). The summary interval of *inoceramiformis* and *dilatata* zones can be correlated with the lower part of the Delenzha Horizon of the Verkhoyansk region.

Distribution. The zone can be recognized virtually everywhere in northeastern Asia. The index species was recorded in the lower Antiya Formation of the Borzya field of the Baikal region (the collection of Sinitsa) and in the lower Belosnezhka Horizon of East Taimyr (Solomina and Preobrazhenskaya, 1993).

Kolymia plicata Zone

Index species: *Kolymia plicata* Biakov (Byakov, 1999, p. 13, Figs. 2a, 2c–2e).

Type area: southeastern Omolon massif, the Levyi Vodopadnyi Creek; the Middle Omolon Subformation, Exposure 3, Beds 38–53 (*Opornyi...*, 1990).

Stratigraphic scope. The lower boundary of the zone is drawn at the first occurrence of the index species. The zone corresponds to the regional *Terrakea borealis* and *Terrakea korkodonensis* zones.

Paleontological characteristics. The poor zonal assemblage includes *Kolymia plicata* Biak., *K. rara* Biak., and *Maitaia sartangensis* (Murom. et Kusn.). Scarce forms are *Kolymia simkini* Popow, *Kolymia* sp., *Aphanaia* sp. indet., and *Polidevcia cumboides* (Lutk. et Lob.). In some sections, the transitional species *Aviculopecten orientalis* Fred., *A. kolymaensis* Maslen. (become extinct), and *Streblopteria englehardti* (Eth. et Dun) are dominant.

Age substantiation and correlation. The zone may be dated as late Kazanian in age. The bivalve assemblage is highly endemic in subregional (three species in common with the West Arctic assemblages) and provincial (four species in common with the Verkhoyansk region assemblages) terms.

Distribution: the Omolon massif and southeastern surrounding structures; the index species, which I initially identified as *K.* cf. *inoceramiformis* Lich., was found in the Soktui Formation (the upper Antiya Horizon) of the Borzya field of the Baikal region (Kotlyar *et al.*, 1990). The latest data (Kurushin *et al.*, 1996) suggests the occurrence of the zone in the western Verkhoyansk region.

Kolymia multiformis Zone

Index species: Kolymia multiformis Biakov (Byakov, 1992, p. 31, Plate III, Figs. 4–7).

Type area: southeastern Omolon massif, the Levyi Vodopadnyi Creek; the Upper Omolon Subformation, Exposure 3, Beds 54–61 (*Opornyi...*, 1990).

Stratigraphic scope. The lower boundary of the zone is drawn at the first occurrence of the index species and zonal species assemblage. The zone corresponds to the regional *Magadania bajkurica* Zone.

Paleontological characteristics. Abundant zonal taxa are *Kolymia multiformis* Biak., *Maitaia varvarae* Biak.; *M. sinevensis* Biak.; *Maitaia? lenaensis* (Vor.); *Vorkutopecten talis* (Lutk. et Lob.); *Aviculopecten?* cf. *girtyi* New.; *A.?* cf. *gryphus* New.; *Pseudomonotis? proprius* Biak; as well as *Myonia elata* (Popow) and *Cypricardinia permica* Lich., both of which pass into the lower part of the succeeding zone. In addition, there are the transitional species *Polidevcia cumboides* (Lutk. et Lob.), *Kolymia* cf. *pergamenti* Murom., *Pyramus? symmetricus* (Lutk. et Lob.) and species that become extinct within the zone, such as *Polidevcia* sp., *Nuculopsis* sp., *Kolymia* sp., *Vorkutopecten* ex gr. *subclathratus* (Keys.), *Streblopteria englegardti* (Eth. et Dun), and *Myonia* sp. Rare *Palaeoneilo?* sp. indet., *Parallelodon?* sp. indet., *Permophorus?* sp. indet., *Solemya* sp. indet., *Praeundulomya* sp., and *Pyramus* sp. were found in the northeastern surrounding structures of the Okhotsk massif. *Stutchburia* sp. appeared for the first time in some sections.

Age substantiation and correlation. The zone is attributed to the Kazanian Stage, although many species, such as *V. talis* (Lutk. et Lob.), *V. subclathratus* (Keys), *C. permica* Lich., *P.? symmetricus* (Lutk. et Lob.), and *P. cumboides* (Lutk. et Lob.), are known from deposits referred to the Ufimian Stage (Muromtseva and Gus'kov, 1984; Astaf'eva and Astaf'eva-Urbaitis, 1988), probably due to miscorrelations. *P.? proprius* Biak. is most similar to *Pseudomonotis* sp. (Maslennikov, 1935) from the Kazanian deposits of the northern Russian platform and to *P. speluncaria* (Schloth.) from East Greenland (Newell, 1955). *Maitaia? lenaense* (Vor.) is very similar (if not identical) to the early Kazanian species *Maitaia? menneri* (Kul.) from the northern Russian platform (Kulikov, 1978) and to *"Atomodesma" permica* (=*Posidonia permica* New.) from the *Posidonia* Shales of East Greenland. The Kazanian age of the zone is supported by occurrences of the brachiopod genera *Olgerdia* and *Magadania*, which are vicarious forms of the East European genera *Licharewia* and *Globiella* (Solomina and Preobrazhenskaya, 1993; Ganelin *et al.*, 1990) and of *Bajtugania* characteristic of the Kazanian Stage in the Urals (Grunt, 1980).

The occurrence of pectenids *Avicuopecten?* cf. *girtyi* New. and *A.?* cf. *gryphus* New. very similar to forms described from the Word Formation of the Glass Mountains of Texas (Newell, 1938) is very significant. They were previously identified by me as *Vorkutopecten* ex gr/ *subclathratus* (Keys).

It is interesting that the characteristic species *M. varvarae* Biak. shows morphological similarity with some specimens of *Maitaia gigantea* (Kon.) described by Waterhouse (1979) from Australia.

In general, the zone is characterized by the disappearance of the genus *Aphanaia* and by high diversification of the genus *Maitaia*. The genus *Kolymia* is usually represented by a single species, which, as a rule, occurs in abundance. The zonal assemblage shows affinity with bivalve faunas from the West Arctic (seven species in common) and Verkhoyansk regions (eight species in common). The zone can be correlated with the upper part of the Delenzha Horizon in the Verkhoyansk region, lower beds of the Tsvetochnaya Horizon in Taimyr, and upper beds of the Gusinaya Zemlya and Gerkina formations in Novaya Zemlya.

Distribution. The zone can be recognized virtually everywhere in the Kolyma and Omolon river basins, within the Okhotsk region, and probably in the south and west of the Verkhoyansk region and Taimyr.

Gizhiga Horizon. The horizon corresponds to one bivalve *Maitaia bella* Zone.

Maitaia bella Zone

Index species: *Maitaia bella* Biak (Byakov, 1992, p. 33, Plate IV, Fig. 5).

Type area: the Omolon massif, the Russkaya-Omolonskaya River; the Gizhiga Formation, Exposure 31, Beds 15–21 (*Opornyi...*, 1990).

Stratigraphic scope. The lower boundary is drawn at the first occurrence of the zonal species assemblage. The index species was predominantly found in the upper half of the zone, but some sections show it at the lower boundary of the zone as well.

Paleontological characteristics. The representative zonal assemblage includes *Maitaia bella* Biak., *Myonia komiensis* (Maslen.), *Merismopteria permiana* (Kul.), *Myonia elata* Popow, *Myonia* sp., *Cypricardinia permica* Lich. (the latter four species are especially abundant in the lower half of the zone), *Maitaia belliformis* Biak., *M. kolymiaformis* Biak., *Stutchburia modioliformis* (King), *Fasciculiconcha?* sp., and *Glyptoleda borealica* Biak. (these species characterize the upper half of the zone). In addition, there are the *Streblopteria* species *S. englegardti* (Eth. et Dun) and *S. radiata* (Lutk. et Lob.). Rare *Pyramus* sp. were found in the lower half of the zone.

Age substantiation and correlation. There is no direct data to reliably date the zone. Most probably, it can be assigned to the first half of the Tatarian Stage. At this level, three genera, *Merismopteria, Fasciculiconcha*, and *Glyptoleda*, appeared (the latter two genera first occur in the second half of the zone) and representatives of six genera, *Parallelodon, Solemya, Kolymia, Aviculopecten, Pseudomonotis*, and *Permophorus*, became extinct. There are also significant changes in the species composition. Therefore, the zonal assemblage may represent the early to earliest late Tatarian

phase in bivalve development. This supposition is supported by the paleomagnetic data (*Opornyi...*, 1990). The coeval deposits of Novaya Zemlya and Kolguev Island yield *M. bella* Biak. (my identification from the collection of Muromtseva at the Chernyshev Central Research Geological Prospecting Museum), *S. modioliformis* (King), and *Glyptoleda* forms (Muromtseva, 1981). Noteworthy is the concurrence of the Austral genera *Merismopteria* and *Glyptoleda* and the Tethyan genus *Fasciculiconcha* in the assemblage. The zonal assemblage has seven species in common with assemblages of the West Arctic (the Pechora basin, Novaya Zemlya) and Taimyr. Almost all forms were also found in the Verkhoyansk region. The collection of Kotlyar contains samples with index species (my identification) from the Borzya Formation of the Baikal region (Kotlyar *et al.*, 1990) and from the middle Osakhta Formation of the Amur basin (Kotlyar, 1997). The zone can be correlated with the lower part of the Dulgalakh Horizon of the Verkhoyansk region and lower beds of the Shadrovskii and Savina formations of Novaya Zemlya. It is worth mentioning that *Maitaia bella* and *M. belliformis* are similar in morphology to the Austral forms described as *Trabeculatia trabeculum* by Waterhouse (1979) from New Zealand.

The Austral species *Atomodesma variabile* Wanner from the northern Verkhoyansk region (Popov, 1957; Muromtseva and Gus'kov, 1984), which was first described from the Basleo Beds of Timor Island, may also be confined to the lower half of the zone.

Distribution. The zone can be traced everywhere in the Kolyma and Omolon river basins and the Okhotsk region. It may be recognized in the Verkhoyansk region, Novaya Zemlya, and Baikal and Amur regions.

To make the biostratigraphic scheme more refined, I distinguished two auxiliary biostratigraphic units (beds with fauna) within some sections of the zone: *Merismopteria permiana* Beds in the lower part of the horizon in the Omolon massif and *Glyptoleda borealica* Beds in the upper part in the Ayan-Yuryakh anticlinorium and the northeastern Omolon massif.

Merismopteria permiana Beds

Index species: *Merismopteria permiana* (Kulikov) (=*Kolymia? permiana* Kulikov; Kulikov, 1967, p. 118, Plate 1, Figs. 14, 15).

Type area: the Omolon massif, the Russkaya-Omolonskaya River; the lower Gizhiga Formation, Exposure 31, Beds 15 and 16 (*Opornyi...*, 1990).

Stratigraphic scope. The beds are established in the lower part of the *M. bella* Zone, and the unit approximately corresponds to the lower half of the brachiopod *Cancrinelloides obrutschewi* Zone. The lower boundary of beds coincides with those of the zone and the Gizhiga Horizon and is drawn at the first occurrence of the index species of the beds. The beds can be recognized in three areas: in the southeastern and eastern Omolon massif (the Russkaya-Omolonskaya River basin), the Avlondya River basin, and the Borzya field (the upper part of the Sosuchei Horizon). They are assumed to occur in the northern Verkhoyansk region, where the index species was first described (Kulikov, 1967).

Paleontological characteristics. The beds yield *Merismopteria permiana* (Kul.), *Maitaia* cf. *bella* Biak., *Myonia elata* (Popow), *M. komiensis* (Maslen.), *Myonia* sp., *Cypricardinia permica* Lich., and *Pyramus* sp.

Glyptoleda borealica Beds

Index species: *Glyptoleda borealica* Biakov (Byakov, 1998, Figs. 3e, 3f).

Type area: the Ayan-Yuryakh anticlinorium in the right bank of upper courses of the Tenke River, the lower Omchak Subformation (excluding the basal 90 m); the Staratel–Gorbatyi Creek watershed (Byakov and Vedernikov, 1990).

Stratigraphic scope. The beds are distinguished in the upper part of the *M. bella* Zone and approximately correspond to the upper half of the brachiopod *Cancrinelloides curvatus* Zone. Their lower boundary is drawn at the first occurrence of the index species within the upper part of the brachiopod *Cancrinelloides curvatus* Zone. Their upper boundary coincident with that of the Gizhiga Horizon is drawn at the last occurrence of the index species of the beds. The beds were recognized in two areas: northeastern structures surrounding the Okhotsk massif (upper reaches of the Khuren River) and the Ayan-Yuryakh anticlinorium. It should not be excluded that part of the Savina Formation in Novaya Zemlya and correlative beds of Kolguev Island, which contain *Gryptoleda colei* (Flet.) (*Permskie...*, 1981) similar to *G. borealica* Biak., have the same stratigraphic position. The beds under consideration may also be distinguished in the middle part of the Imtachan Formation of the southern Verkhoyansk region, where *Glyptoleda* sp. was found (Muromtseva and Gus'kov, 1984).

Paleontological characteristics. The beds yield *Maitaia bella* Biak., *M. belliformis* Biak., and *Glyptoleda borealica* Biak.

Khivach Horizon. The horizon spans two bivalve zones (*Maitaia tenkensis* and *Intomodesma costatum*) approximately corresponding to its lower and upper halves.

Maitaia tenkensis Zone

Index species: *Maitaia tenkensis* Biakov (Byakov, 1999, p. 13, Figs. 2b, 2f).

Type area: the Ayan-Yuryakh anticlinorium in the right bank of upper courses of the Tenke River and the middle and upper (excluding the topmost 120 m) Omchan subformations; the Staratel–Gorbatyi Creek watershed (Byakov and Vedernikov, 1990).

Stratigraphic scope. The lower zonal boundary is drawn at the first occurrence of the index species being

coincident with that between the Gizhiga and Khivach horizons. The zone was established in two areas: the Ayan-Yuryakh anticlinorium and northeastern Okhotsk massif in the upper courses of the Khuren River.

Paleontological characteristics. The zonal assemblage is represented only by the index species. In the Khuren River upper courses, the upper beds of the zone contain rare *Palaeoneilo* sp., *Polidevcia?* sp. indet., and *Conocardium* sp.

Age substantiation and correlation. The dating and interregional correlation of the zone are ambiguous due to the endemism of the index species. The upper Tatarian age is assumed.

Distribution: northeastern surrounding structures of the Okhotsk massif and the Ayan-Yuryakh anticlinorium.

Intomodesma costatum Zone

Index species: *Intomodesma costatum* Popow (Popov, 1957, p. 49, Plate 1, Fig. 5).

Type area: northeastern surrounding structures of the Okhotsk massif; the Khuren River upper courses; upper beds of the Upper Titan Subformation (120 m); and the Kulu Formation, Exposures 2 and 3, Beds 4–19 (Byakov and Vedernikov, 1990).

Stratigraphic scope. The zonal lower boundary is drawn at the first occurrence of the index species and zonal assemblage. In the stratotype area, the occurrence of the index species was recorded only from the second fourth of the zone. Therefore, the lower boundary of the zone is defined there by the appearance of the zonal assemblage. It is possible to divide the zone into three subzones using the phylogenetic succession *Maitaia hurenensis* → *Intomodesma costatum* → *Intomodesma evenicum*. The possibility is supported by some stratigraphic data.

Paleontological characteristics. The abundant and diverse zonal assemblage includes *Nuculopsis wymensis* (Keys.), *Polidevcia magna* (Popow), *Pro-mytilus* cf. *retusus* Chron., *Intomodesma costatum* Popow, *I. turgidum* Popow, *I. evencum* Kusn., *I. balygychanicum* Biak., *Maitaia quadrata* (Lutk. et Lob.), *M. hurenesis* Biak., *Vnigripecten volucer* (Lutk. et Lob.), *Streblopteria levis* (Lutk. et Lob.), *Streblochondia? corrugata* (Lutk. et Lob.), *Euchondria* aff. *paucicostata* Yin, *Cyrtorostra* sp., *Myonia gibbosa* (Maslen.), *M. bicarinata* Ast.-Urb., *Praeundulomya simualis* Biak., *Wilkingia?* sp., and *Conocardium robustum* Flet. Shallow-water carbonate facies contain representatives of the genus *Streblopteria*, such as *S. englehardti* (Eth. et Dun), *S. pusilla* (Schloth.), *S. radiata* (Lutk. et Lob.), and *Deltopecten* sp., whereas the deep-water clayey facies bear *Polidevcia* sp., *Nuculopsis* sp., and *Solenomorpha?* sp.

Age substantiation and correlation. Five genera, *Intomodesma, Cyrtorostra, Streblochondria, Euchondria*, and *Promytilus*, first appear; and six genera *Merismopteria, Cypricardinia, Stutchburia, Fasciculiconcha, Glyptoleda*, and *Pyramus*, become extinct within the zone. The species composition is entirely renewed. These facts indicate a new, late Tatarian phase in bivalve development. *Cyrtorostra, Streblochondria*, and *Vnigripecten* are typical components of the Late Permian Tethyan assemblages (Girty, 1910; Kotlyar *et al.*, 1983). The bivalve assemblage shows close compositional similarity to coeval assemblages of the Verkhoyansk region, where the Tyungnya Formation in the north, the upper beds of the Dulgalakh Formation in the west, and the Imtachan Formation in the south yield 15 species in common (Muromtseva and Gus'kov, 1984), and also to the assemblage from upper beds of the Shadrovskii Formation in Novaya Zemlya, where eight common species are known (Muromtseva, 1981).

Distribution. The zone can be recognized everywhere in northeastern Asia and probably in Novaya Zemlya.

Remarks. Some researchers (Ganelin, 1984; Solomina and Preobrazhenskaya, 1993; Kotlyar, 1997) assumed a considerable hiatus between the Permian and Triassic marine deposits of northeastern Asia. However, it seems that either there was no break in sedimentation at all (at least in the deepest basins of northeastern Asia) or it could be in the elevated tectonic structures (the Omolon massif) and was short within the Permian. This is evident from the gradual transition between the Permian and Triassic deposits in the Detrin River mouth section of the Ayan-Yuryakh anticlinorium (Byakov and Vedernikov, 1990). In addition, the absence of the hiatus is proved by the occurrence of *Euchondria* aff. *paucicostata* Yin in the upper part of the zone in the Omolon massif, which is similar to the form described from Changxingian in southeastern China (Yin, 1982).

CORRELATION

The Permian bivalves have never previously been used for intraregional or interregional correlation, although their potential appeared to be as good as that of many other faunal groups.

As mentioned above (under the subheadings *Age substantiation and correlation*), many of the established zones can be recognized in other Boreal areas (Fig. 5). The index species and elements of zonal assemblages from the Boreal Permian sections were either identified by me from the collections of many geologists at the Chernyshev Central Research Geological Prospecting Museum or described in publications.

However, the main problem of the bivalve-based correlations is that many fossils from the stratotypes of the adjacent regions have not been adequately studied and identified. The stratigraphic position of fossils, which received comprehensive treatment, either has not been established or is doubtful. Therefore, most of the correlations described herein are conventional.

Almost all established zones can be recognized in the Verkhoyansk region, many of them in Novaya Zem-

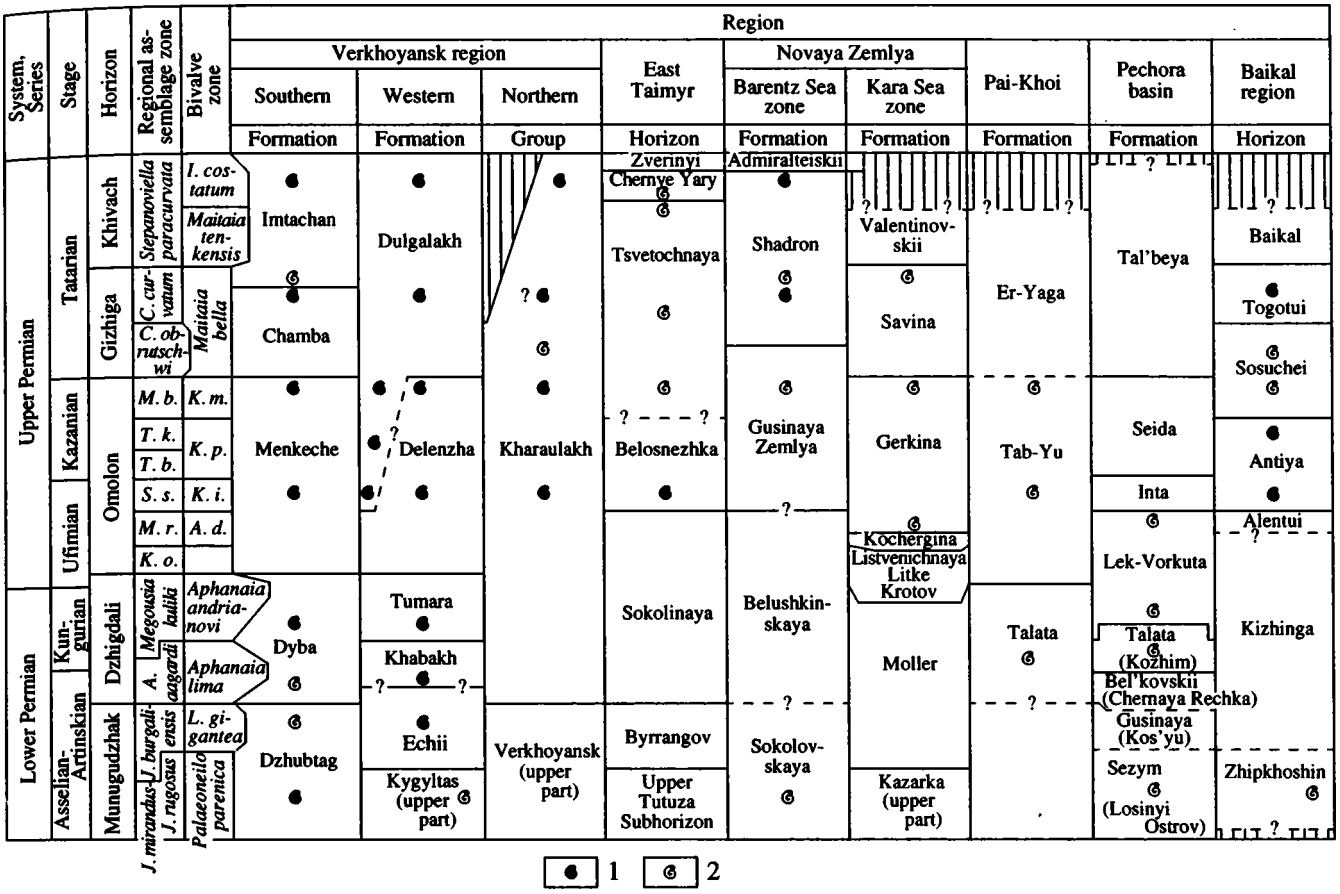

Fig. 5. Bivalve-based correlation of the Boreal Permian deposits: (1) index species; (2) zonal elements (for abbreviations see Fig. 2).

lya and some in Taimyr, the Pai-Khoi, Pechora basin, northern Russian platform, Kolguev Island, and Kanin Peninsula.

The bivalve-based correlation between the sections of northeastern Asia and those of remote (extraboreal) regions (the Tethys, North America, New Zealand, Australia) is still difficult and conventional due to well-known paleogeographic factors and inadequate bivalve studies. However, at present, some correlative levels can be outlined (Fig. 6).

The first correlative level (*P. parenica* Zone) may be established within the Nura-Nura Member of the Pool Sandstone of the Canning Basin and in the Fossil Cliff Formation of the Perth Basin in Western Australia, where *Myophosa subarbithrata* (Dick.) was described. These deposits contain "*Anthraconeilo*" sp. nov. very similar to *Palaeoneilo parenica* Biak (Dickins, 1963).

The second correlative level outlined is within the lower Liveringa Formation (the Lightjack Member) of the Canning Basin and the Baker and Coolkilya formations of the Carnarvon Basin. These deposits yielded the bivalve assemblages described by Dickins (1956, 1963) and contain many species similar to those of the assemblage of the *dilatata* Zone in association with the ammonoids *Daubichites, Agathiceras*, and *Popanoceras* (Glenister and Furnish, 1961).

At the same level or slightly higher, there is the Letham Formation of New Zealand, which contains "*Atomodesma*" *obliquatum* Water. (Waterhouse, 1963). The similar forms "*At.*" *pauchoicum* Gus. et Murom. and *Aphanaia stepanovi* (Murom.) are known from the Tab-Yu Formation of the Pai-Khoi (Astaf'eva, 1993) and from the lower Omolon Horizon and its analogues in northeastern Asia (the *inoceramiformis* Zone), respectively.

The *multiformis* Zone may be correlated with the upper Branxton Formation of New South Wales in eastern Australia, which contains the form described by Waterhouse (1979) as *Maitaia gigantea* (Kon.) very similar to some specimens of *Maitaia varvarae* Biak. from the Omolon massif and the Sea of Okhotsk region.

The lower part of the *bella* Zone (*Merismopteria permiana* Beds) may be recognized in the Ferntree Mudstone of Tasmania, where Dickins (1981) described *Merismopteria* sp. similar to *M. permiana* (Kul.). Probably, the entire *bella* Zone is correlative with the *Trabeculatia trabeculum* Zone corresponding to the upper sandstone beds of the Tramway Formation

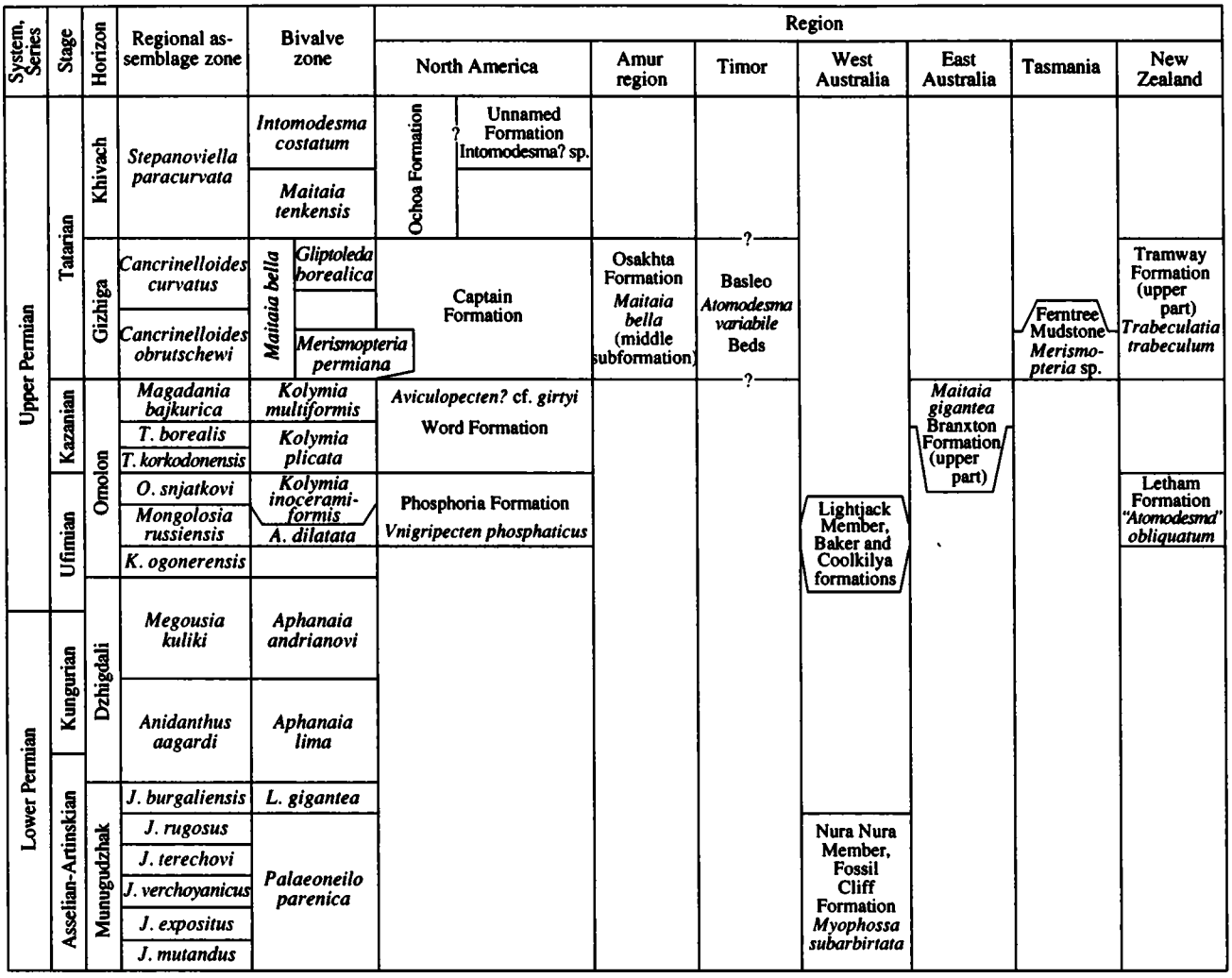

Fig. 6. Permian bivalve-based correlations between northeastern Asia and extraboreal regions.

of New Zealand (Waterhouse, 1963, 1976, 1979). These index species demonstrate some identical morphological features, such as a thickened anterior wall of the shell and the shell shape and sculpture, and can be considered vicarious.

Probably, the *bella* Zone can be also recognized in Timor Island, where *Atomodesma variabile* Wan. (Wanner, 1922) was described. In the northern Verkhoyansk region, this species is associated with forms morphologically similar to *M. bella* Biak. In the Amur region, I identified *M. bella* in association with *Timorites* in the middle of the Osakhta Formation (Kotlyar, 1997).

In the Glass Mountains of North America, the *dilatata* and *inoceramiformis* zones may be distinguished within the Phosphoria Formation on the basis of *Vnigripecten phosphaticus* (Girty) similar to *Vrigripecten* sp. of the Omolon massif. The *multiformis* Zone of the Omolon massif, which yields the pectinids *Aviculopecten?* cf. *girtyi* Newell and *A.?* cf. *gryphus* Newell characteristic of the Word Formation (Newell, 1938), most likely corresponds to the upper part of this formation. Rather conventionally, the *costatum* Zone may be distinguished within the siltstones of the unnamed formation of Nevada (the Elko County) according to occurrence of *Intomodesma?* sp. (Kauffman and Runnegar, 1975). Because the upper part of this zone in the Omolon massif yields *Euchondria* aff. *paucicostata* Yin described from Changxingian in southeast China (Yin, 1982), we can expect a possible analogue of the zone in this region as well.

CONCLUSION

This article summarizes my studies on the Permian bivalve biostratigraphy of northeastern Asia. The zonation suggested, especially its lower and uppermost (the *costatum* Zone) parts need to be refined and modified. Further investigations should be focused on revision of bivalves from other regions in order to elucidate their

time successions with the help of some additional biostratigraphic studies. This especially concerns the stratotypes of the regions.

ACKNOWLEDGMENTS

The work was partly supported by the Russian Foundation for Basic Research, project no. 97-05-65864.

Reviewers V.G. Ganelin and A.S. Alekseev

REFERENCES

Andrianov, V.I., *Permskie i nekotorye kamennougol'nye ammonity Severo-Vostoka Azii* (Permian and Some Carboniferous Ammonites of Northeastern Asia), Novosibirsk: Nauka, 1985.

Astaf'eva, M.M., *Permskie inoceramopodobnye dvustvorchatye molluski Rossii* (Permian Inoceram-like Bivalves of Russia), Moscow: Nauka, 1993.

Astaf'eva, M.M. and Astaf'eva-Urbaitis, K.A., Stages in Development of the Boreal Permian Bivalves, in *Permskaya sistema: Voprosy stratigrafii i razvitiya organicheskogo mira* (The Permian System: Problems of Stratigraphy and Organic Evolution), Kazan: Kazan Univ., 1988, pp. 3–11.

Biakov, A.S., Abstracts of Papers, *30th Int. Geol. Congr., Beijing, China, 4–14 Aug. 1996*, Beijing, 1996, vol. 2, p. 82.

Byakov, A.S., Stratigraphic Significance of Permian Inoceram-like Bivalves in the Northeastern USSR, in *Stratigrafiya i paleontologiya fanerozoya Severo-Vostoka SSSR* (Phaneozoic Stratigraphy and Paleontology of the Northeastern USSR), Magadan: Sev.-Vost. Kompl. Nauch.-Issled. Inst. Dal'nevost. Nauch. Center, Akad. Nauk SSSR, 1988, pp. 60–65.

Byakov, A.S., Beds with Bivalves, in *Opornyi razrez permi Omolonskogo massiva* (The Permian Reference Section of the Omolon Massif), Leningrad: Nauka, 1990, pp. 127–133.

Byakov, A.S., Beds with Fauna and Bivalve Assemblages from Permian Reference Sections of the Southeastern Omolon Massif, in *Materialy po geologii i poleznym iskopaemym Severo-Vostoka SSSR* (Materials on the Geology and Mineral Deposits of the Northeastern USSR), Magadan: Magadan Knizh. Izd., 1991a, pp. 122–128.

Byakov, A.S., Permian Bivalve Zonation of the Northeastern USSR, in *Permskaya sistema Zemnogo shara* (Permian System of the Globe), Sverdlovsk: Ural. Otd. Akad. Nauk SSSR, 1991b, p. 26.

Byakov, A.S., Permian Stratigraphy and Bivalves of the Kolyma River Basin, *Cand. Sci. (Geol.–Min.) Dissertation*, Moscow: Paleontol. Inst. Acad. Sci. USSR, 1991c.

Byakov, A.S., Permian Inoceram-like Mollusks of Genus *Intomodesma* Popow, *Paleontol. Zh.*, 1991d, no. 4, pp. 120–123.

Byakov, A.S., New Species of Permian Inoceram-like Bivalves from the Northeastern USSR, *Paleontol. Zh.*, 1992, no. 1, pp. 27–37.

Byakov, A.S., Main Evolutionary Stages of Permian Inoceram-like Bivalves from Northeastern Asia and Detailed Permian Correlations in the Boreal Region, in *Problemy evolyutsii permskoi morskoi bioty* (Problems of Permian Marine Biota Evolution), Moscow: Paleontol. Inst. Ross. Akad. Nauk, 1995, pp. 11–13.

Byakov, A.S., Permian Ctenodont Bivalves of Northeastern Russia, *Paleontol. Zh.*, 1998, no. 2, pp. 30–33.

Byakov, A.S., Two New Zonal Index Species of Late Permian Inoceram-like Bivalves of Northeastern Asia, *Paleontol. Zh.*, 1999, no. 3, pp. 13–16.

Byakov, A.S. and Vedernikov, I.L., Permian Stratigraphy of Northeastern Surrounding Structures of the Omolon Massif, the Central and Southeastern Ayan-Yuryakh Anticlinorium, *Preprint of Southeastern Joint Research Inst., Far East Branch, USSR Acad. Sci.*, Magadan, 1990, p. 69.

Chuvashov, B.I., Molin, V.A., Kanev, G.P., and Chermnykh, V.A., Lower and Upper Terrigenous Permian, in *Permskaya sistema Zemnogo shara. Putevoditel' geologicheskikh ekskursii* (The Permian System of the Globe: Guide to Geological Excursions), Sverdlovsk: Ural. Otd. Akad. Nauk SSSR, 1991, pp. 23–50.

Ciriacks, K.W., Permian and Eotriassic Bivalves of the Middle Rockies, *Bull. Am. Mus. Nat. Hist.*, 1963, vol. 125, no. 1.

Dickins, J.M., Permian Pelecypods from the Carnarvon Basin, Western Australia, *Bull. Bur. Miner. Resour. Geol. Geophys.* (Aust.), 1956, no. 29.

Dickins, J.M., Permian Pelecypods and Gastropods from Western Australia, *Bull. Bur. Miner. Resour. Geol. Geophys.* (Aust.), 1963, no. 63.

Dickins, J.M., A Permian Invertebrate Fauna from the Warwick Area, Queensland, *Bull. Bur. Miner. Resour. Geol. Geophys.* (Aust.), 1981, no. 209.

Ganelin, V.G., Upper Paleozoic Biostratigraphy and Brachiopods of the Kolyma–Omolon Massif, *Cand. Sci. (Geol.–Min.) Dissertation*, Moscow, Geol. Inst., USSR Acad. Sci., 1973.

Ganelin, V.G., The Taimyr–Kolyma Subarea, *Tr. Vses. Geol. Inst., Nov. Ser.*, 1984, vol. 286, pp. 111–142.

Ganelin, V.G., Byakov, A.S., and Karavaeva, N.I., The Permian Biostratigraphy of the Omolon Massif, in *Opornyi razrez permi Omolonskogo massiva* (The Permian Reference Section of the Omolon Massif), Leningrad: Nauka, 1990, pp. 102–117.

Ganelin, V.G. and Karavaeva, N.I., Stratigraphic Section of the Dzhigdali, Omolon, Gizhiga, and Khivach Horizons of the Permian of the Northeastern USSR, in *Materialy po geologii i poleznym iskopaemym Severo-Vostoka SSSR* (Materials on Geology and Mineral Deposits of the Northeastern USSR), Magadan: Magadan Knizh. Izd., 1977, pp. 23–28.

Girty, G.H., Fauna of the Phosphate Beds of the Park City Formation in Idaho, Wyoming, and Utah, *Bull. US Geol. Surv.*, 1910, vol. 436, pp. 1–82.

Glenister, B.F. and Firnish, W.M., The Permian Ammonoids of Australia, *J. Paleontol.*, 1961, vol. 35, no. 4, pp. 673–736.

Grunt, T.A., *Atiridy Russkoi platformy* (Atiriids of the Russian Platform), Moscow: Nauka, 1980.

Gus'kov, V.A., The Lower–Upper Permian Boundary Defined by Marine Bivalves, in *Permskaya sistema: Voprosy stratigrafii i razvitiya organicheskogo mira* (The Permian System: Problems of Stratigraphy and Organic Evolution), Kazan: Kazan Univ., 1988, pp. 11–15.

Gus'kov, V.A., Pukhonto, S.K., and Yatsuk, I.E., Upper Permian Deposits of the Northeastern Pai-Khoi, *Sov. Geol.*, 1980, no. 2, pp. 68–75.

Harland, W.B., Cox, A.V., Llewellyn, P.G., *et al.*, *A Geologic Time Scale*, Cambridge: Cambridge Univ., 1982. Translated under the title *Shkala geologichskogo vremeni*, Moscow: Mir, 1985.

Kaufmann, E.G. and Runnegar, B., *Atomodesma* (Bivalvia) and Permian Species of the United States, *J. Paleontol.*, 1975, vol. 49, no. 1, pp. 23–51.

Karavaeva, N.I., Beds with Foraminifers, in *Opornyi razrez permi Omolonskogo massiva* (The Permian Reference Section of the Omolon Massif), Leningrad: Nauka, 1990, pp. 118–126.

Kotlyar, G.V., Correlative Reference Levels of the Permian, *Stratigr. Geol. Korrelyatsiya*, 1997, vol. 5, no. 2, pp. 35–50.

Kotlyar, G.V., Zakharov, Yu.D., Bogdan, V.K., *et al.*, *Pozdnepermskii etap evolyutsii organicheskogo mira. Dzhul'finskii i dorashamskii yarusy SSSR* (The Late Permian Stage of the Organic Evolution: Dzhulfian and Dorashamian Stages of the USSR), Leningrad: Nauka, 1983.

Kotlyar, G.V., Popeko, L.I., Oleksiv, B.I., and Afanas'ev, M.N., New Data on the Upper Permian Biostratigraphy of the Borzya Depression in the East Baikal Region, in *Stratigrafiya dokembriya i fanerozoya Zabaikal'ya i yuga Dal'nego Vostoka* (Precambrian and Phanerozoic Stratigraphy in the Baikal Region and Southern Part of the Far East), Khabarovsk, 1990, pp. 122–124.

Kuznetsov, V.V. Permian Bivalves of the Verkhoyansk Region and Their Stratigraphic Significance, *Cand. Sci. (Geol.–Min.) Dissertation*, Yakutsk: Yakutsk Geol. Department, 1972.

Kulikov, M.V., Permian Mollusks of the USSR, in *Biostratigraficheskii sbornik* (Collection of Biostratigraphic Articles), Leningrad: Nedra, 1967, pp. 114–135.

Kulikov, M.V., Some Rare Representatives of Mollusks from the Lower Kazanian Deposits of the Russian Platform, *Dokl. Akad. Nauk SSSR*, 1978, vol. 241, no. 1, pp. 177–180.

Kurushin, N.I., Solov'eva, N.A., Nekrasov, A.I., *et al.*, New Data on Permian Biostratigraphy and Lithology of the Western Verkhoyansk Region, *Dokl. Ross. Akad. Nauk*, 1996, vol. 348, no. 2, pp. 223–227.

Leven, E.Ya., Bogoslovskaya, M.F., Ganelin, V.G., *et al.*, Reorganization of Marine Biota during the Mid-Early Permian Epoch, *Stratigr. Geol. Korrelyatsiya*, 1996, vol. 4, no. 1, pp. 61–70.

Likharev, B.K., *Fauna permskikh otlozhenii Kolymskogo kraya* (Permian Fauna of the Kolyma Region), Leningrad: Akad. Nauk SSSR, 1934.

Lobanova, O.V. and Lutkevich, E.M., Description of Species: Class Bivalvia, in *Polevoi atlas permskoi fauny i flory Severo-Vostoka SSSR* (Field Atlas of the Permian Fauna and Flora of the Northeastern USSR), Magadan: Magadan Knizh. Izd., 1970, pp. 42–63.

Logan, A., Permian Bivalvia of Northern England, *Paleontogr. Soc. India*, 1967, vol. 121, no. 518, pp. 1–72.

Maslennikov, D.F., Late Permian Lamellibranchia of the Northern Region, *Tr. Tsentr. Nauch.–Issled. Geologorazved. Inst.*, 1935, no. 29, pp. 1–124.

Muromtseva, V.A., Bivalve Mollusks, in *Permskie otlozheniya Novoi Zemli* (Permian Deposits of Novaya Zemlya), Leningrad: Nauka, 1981, pp. 26–51.

Muromtseva, V.A. and Gus'kov, V.A., *Permskie morskie otlozheniya i dvustvorchatye mollyuski Sovetskoi Arktiki* (Permian Marine Deposits and Bivalves of the Soviet Arctic), Leningrad: Nedra, 1984.

Nakazawa, K. and Newell, N.D., Permian Bivalves of Japan, *Mem. Fac. Sci. Kyoto Univ., Ser. Geol. Mineral.*, 1968, vol. 35, no. 1, pp. 1–108.

Newell, N.D., Late Paleozoic Pelecypods: Pectinacea, *State Geol. Surv. Kansas*, 1938, vol. 10, pp. 1–123.

Newell, N.D., Permian Pelecypods of East Greenland, *Medd. Groenl. Komm.*, 1955, vol. 110, no. 4, pp. 1–36.

Opornyi razrez permi Omolonskogo massiva (The Permian Reference Section of the Omolon Massif), Leningrad: Nauka, 1990.

Permskie otlozheniya Novoi Zemli (The Permian Deposits of Novaya Zemlya), Leningrad: Nauka, 1981.

Popov, Yu.N., Some Permian Pelecypods, Gastropods, and Ammonites of the Verkhoyansk Region, in *Sbornik statei po paleontologii i biostratigrafii* (Collection of Articles on Paleontology and Biostratigraphy), Leningrad: Nedra, 1957, pp. 45–60.

Resheniya 2-go mezhvedomstvennogo regional'nogo stratigraficheskogo soveshchaniya po dokembriyu i fanerozoyu Severo-Vostoka SSSR 1974–1975 (Resolutions of the 2nd Interdepartmental Regional Conf. on Precambrian and Phanerozoic Stratigraphy of the Northeastern USSR, 1974–1975), Magadan: Magadan Knizh. Izd., 1978.

Shtukenberg, A.A., The General Geological Map of Russia. Sheet 127, *Tr. Geol. Kom.*, 1898, vol. 16, no. 1, pp. 198–297.

Solomina, R.V. and Preobrazhenskaya, E.N., On the Permian Stratigraphic Scheme of Taimyr, *Stratigr. Geol. Korrelyatsiya*, 1993, vol. 1, no. 2, pp. 13–25.

Stratigraficheskii kodeks (The Stratigraphic Code), St. Petersburg: Vseross. Geol. Inst., 1992.

Ustritskii, V.I., Late Paleozoic History of the Northeastern USSR, in *Verkhnii paleozoi Severo-Vostoka SSSR* (The Upper Paleozoic of the Northeastern USSR), Leningrad: Nauch.–Issled. Inst. Geol. Arctic., 1975, pp. 54–75.

Wanner, C. Die Gastropoden und Lamellibranchiaten der Dyas von Timor, *Palaeontol. Timor*, 1922, vol. 18, no. 18, pp. 1–82.

Waterhouse, J.B., New Zealand Species of the Permian Bivalve *Atomodesma* Beyrich, *Palaeontol.*, 1963, vol. 6, Pt. 4, pp. 699–717.

Waterhouse, J.B., World Correlation for Permian Marine Faunas, *Pap. Dep. Geol. Univ. Queensland*, 1976, vol. 7, no. 2, pp. 1–232.

Waterhouse, J.B., New Members of the *Atomodesmina* (Bivalvia) from the Permian of Australia and New Zealand, *Pap. Dep. Geol. Univ. Queensland*, 1979, vol. 9, no. 1, pp. 1–22.

Yin, H.F., Uppermost Permian (Changxingian) Pectinacea from South China, *Riv. Ital. Paleontol. Stratigr.*, 1982, vol. 88, no. 3, pp. 337–385.

Zavodovskii, V.M., Brief Review of the Permian Stratigraphy of the Northeastern USSR, in *Polevoi atlas permskoi fauny i flory Severo-Vostoka SSSR* (Field Atlas of the Permian Fauna and Flora of the Northeastern USSR), Magadan: Magadan Knizh. Izd., 1970, pp. 5–21.

Stratigraphy and Geological Correlation, Vol. 8, No. 1, 2000, pp. 49–59. Translated from Stratigrafiya. Geologicheskaya Korrelyatsiya, Vol. 8, No. 1, 2000, pp. 55–65.
Original Russian Text Copyright © 2000 by Shevyrev.
English Translation Copyright © 2000 by MAIK "Nauka/Interperiodica" (Russia).

The Lower Boundary of the Triassic and Its Correlation in Marine Sediments: Article 2. Boreal Sections of the Basal Triassic and Their Correlation with the Permian–Triassic Boundary Deposits of the Tethys

A. A. Shevyrev

Paleontological Institute, Russian Academy of Sciences, Profsoyuznaya ul. 123, Moscow, 117647 Russia

Received October 20, 1997

Abstract—The lower boundary of the Triassic should be placed at the base of the *Otoceras* Beds. In the boreal sections, these beds yield ammonite species of the *Otoceras concavum* and *O. boreale* zones. The upper part of the *boreale* Zone is an equivalent of the *O. woodwardi* Zone in the Himalayas, where it approximately corresponds to the conodont *Hindeodus parvus* Zone. The Permian–Triassic boundary, which is traditionally coordinated with the base of the *woodwardi* Zone, is easily traceable in the Tethyan sections but poorly correlative in the Boreal region. The boundary becomes more convenient and universal when placed at the base of the *concavum* Zone and its analogues. Everywhere, the *woodwardi* and *concavum* zones are separated from the underlying Permian beds by a stratigraphic hiatus. At present none of the sections suggested can be recommended as the Global Boundary Stratotype Section and Point for the lower Triassic boundary.

Key words: *Upper Permian, Lower Triassic, Boreal sections, faunal assemblages, ammonitic zones, correlation.*

In my previous article (Shevyrev, 1999), I described the Permian–Triassic boundary sections of the Tethyan basins. These sections, demonstrating a wide spectrum of lithological and biostratigraphic distinctions, can be divided into two main groups: some of them include the uppermost Permian beds and lack the lowermost Triassic strata, whereas the other sections incorporate the basal Triassic beds but lack the uppermost Permian horizons. In this article, I consider sections of the respective boundary deposits in the Boreal region and their correlation with those of the Tethys.

ARCTIC CANADA

The Lower Triassic siltstones, mudstones, and sandstones of the Blind Fiord Formation are exposed in northern Axel Heiberg and northwestern Ellesmere islands (the Queen Elizabeth Islands). The rocks have three members: Confederation Point (100 m thick), Smith Creek, and Swartfjeld (Embry, 1986). Each member begins with mudstone beds and is crowned with siltstone layers. The lower member includes the ammonite *Otoceras concavum–O. boreale* (basal mudstones), *Ophiceras commune*, and *Bukkenites strigatus* (green siltstones) zones equivalent in total range to the Griesbachian Stage (Tozer, 1965, 1967, 1994). The stratotype of the stage and three its zones (*concavum, boreale*, and *strigatus*) are located in the Griesbach River basin of Axel Heiberg Island. The stratotype of the *commune* Zone is considered to be an analogue of the upper *Ophiceras* Beds in Kap Stosch of eastern Greenland.

In Canada, the lower zone is known only from the stratotype area, where it contains *Otoceras gracile* Tozer and *O. concavum* Tozer. Mudstone beds of the Blind Fiord Formation rest here on the Permian Degerboels Formation, which is attributed to the Wordian Stage on the basis of brachiopod fauna (Nassichuk *et al.*, 1972; Thorsteinsson, 1974). The first occurrence level of Triassic ammonites is recorded 12 m above the top of the Degerboels Formation (Fig. 1). At a level of 32.9–36.6 m above the base of the Griesbachian stratotype, there appear specimens of *O. boreale* (the *boreale* Zone). On Ellesmere Island, this guide species is associated with *Hypophiceras gracile* (Spath) and *Vishnuites kummeli* Tozer. The *concavum* and *boreale* zones span the range of the lower Griesbachian Substage.

The reference section of the next *commune* Zone is located on Axel Heiberg Island, where *Ophiceras greenlandicum* Spath, *O. commune* Spath, *P. sakuntala* Spath, *Discophiceras wordiei* (Spath), and *Wordieoceras wordiei* (Spath) were respectively found at the levels of 53.3, 54.2, 55.5, 57.3, and 65.2 m above the base of the Blind Fiord Formation. On Ellesmere Island, this assemblage also includes *Tompophiceras extremum* (Spath). In the Griesbachian stratotype, *Bukkenites macilentus* Tozer, *B. nitidus* Tozer, *B. strigatus* (Tozer), and *Wordieoceras wordiei* (Spath) have their first occurrence levels within the interval of 65.5–150 m

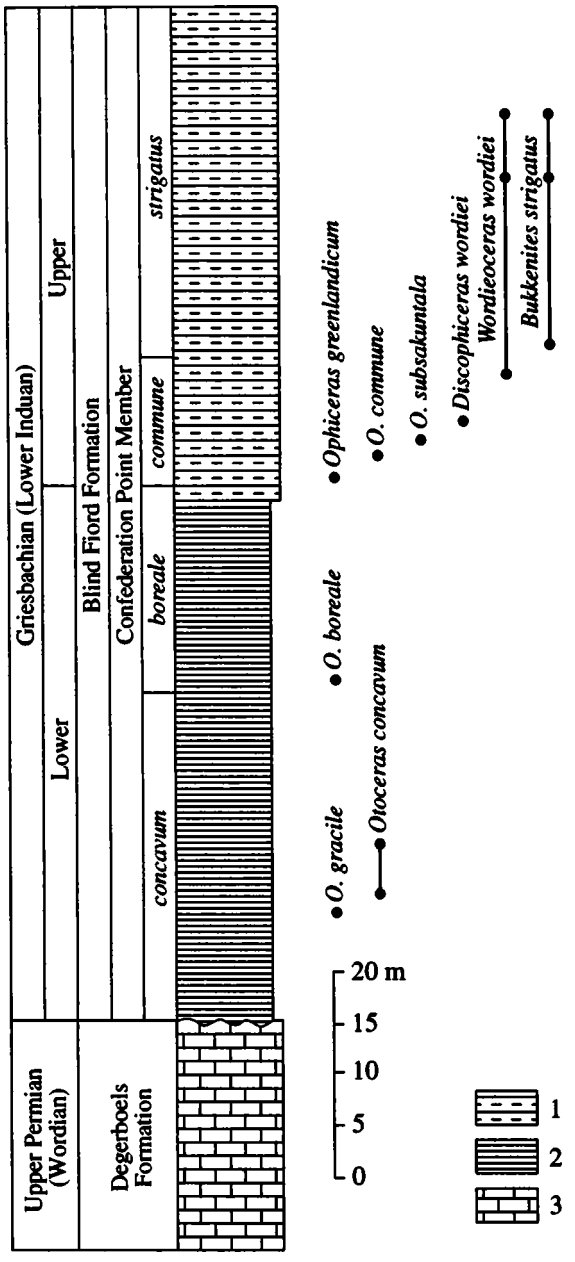

Fig. 1. The Permian–Triassic boundary section on Axel Heiberg Island (after Tozer, 1965, 1967, 1994): (1) siltstone; (2) mudstone; (3) limestone.

above the Blind Fiord Formation base. These ammonites mark the *strigatus* Zone, which, together with the *commune* Zone, represents the upper Griesbachian Stage.

EASTERN GREENLAND

Marine Triassic deposits are exposed along the eastern coast of Greenland (Kap Stosch, Traill Island, Jameson Land, and Scoresby Land). They are represented by conglomerate, sandstone, and mudstone beds of the Wordie Creek Formation overlying, with a hiatus, the Permian shales of the Foldvik Creek (or Schuchert Dal) Formation. The formation is still vaguely dated. Teichert and Kummel (1972, 1976) assumed that the uppermost Permian horizons are missing in eastern Greenland. Stemmerick and Piasecki (1991) from the Greenland Geological Survey assume that the Upper Permian beds (up to the Tatarian Stage inclusive) belong to the Schuchert Dal Formation, but biostratigraphic evidence supporting their opinion has not been presented.

The most complete Triassic sections (640 m thick) are located in the Kap Stosch area. In the 1920s–1930s, English and Danish expeditions collected abundant Early Triassic ammonites and bivalves described by Spath (1930, 1935). In the Wordie Creek Formation, he recognized eight biostratigraphic levels characterized by different ammonitic assemblages: the lower (1) and upper (2) *Glyptophiceras* Beds; the lower (3) and upper (4) *Ophiceras* Beds; the lower, middle, and upper (5–7) *Vishnuites* Beds; and the *Proptychites* Beds (8).

This scheme by Spath was modified by Trümpy (Grasmück and Trümpy, 1969; Trümpy, 1969), who suggested another ammonite zonation consisting of six units: (1) the *Hypophiceras triviale* Zone with *Otoceras* sp. and *H. triviale* (Spath); (2) the *Hypophiceras martini* Zone with *H. martini* Trümpy; (3) the *Metophiceras subdemissum* Zone with *Otoceras boreale* Spath, *Ophiceras commune* Spath, *O. spathi* Trümpy, *Metophiceras subdemissum* (Spath), *Hypophiceras minor* (Spath), *H. gracile* (Spath), *Tompophiceras extremum* (Spath), *Discophiceras compressum* Spath, *Vishnuites striatus* (Spath), and *V. paradigma* (Trümpy); (4) the *Ophiceras commune* Zone with *Hypophiceras minor, H. gracile, Ophiceras greenlandicum* Spath, *O. commune* Spath, *O. subsakuntala* (Spath), *Discophiceras subkyokticum* (Spath), and *D. wordiei* (Spath); (5) the *Vishnuites decipiens* Zone with *Ophiceras transitorium* Spath, *O. kilenense* Spath, *O. leptodiscus* Spath, *Proptychites grandis* Spath, *Wordieoceras wordiei* (Spath), and *W. decipiens* (Spath); and (6) the *Proptychites rosenkrantzi* Zone with *Proptychites anomalus* Spath, *P. rosenkrantzi* Spath, and *P. intermedius* Spath. The zonation is based on the succession recorded in the Wegener Halvö site (Jameson Land) located 250 km to the south of Kap Stosch. The four lower zones suggested by Trümpy correspond to both *Glyptophiceras* Beds and the lower and upper *Ophiceras* Beds of Spath, while the two upper zones are considered correlative to the *Vishnuites* and *Proptychites* Beds (Fig. 2).

According to Trümpy, the upper distribution limit of *O. boreale* is confined to the *subdemissum* Zone. The peculiar ammonite assemblage of this zone includes some genera (*Ophiceras, Discophiceras* and *Tompophiceras*) that were found at a higher stratigraphic level than that of *Otoceras* forms in the Canadian Arctic sections. Accordingly, Trümpy made an attempt to subdivide the *aubdemissum* Zone and to recognize its

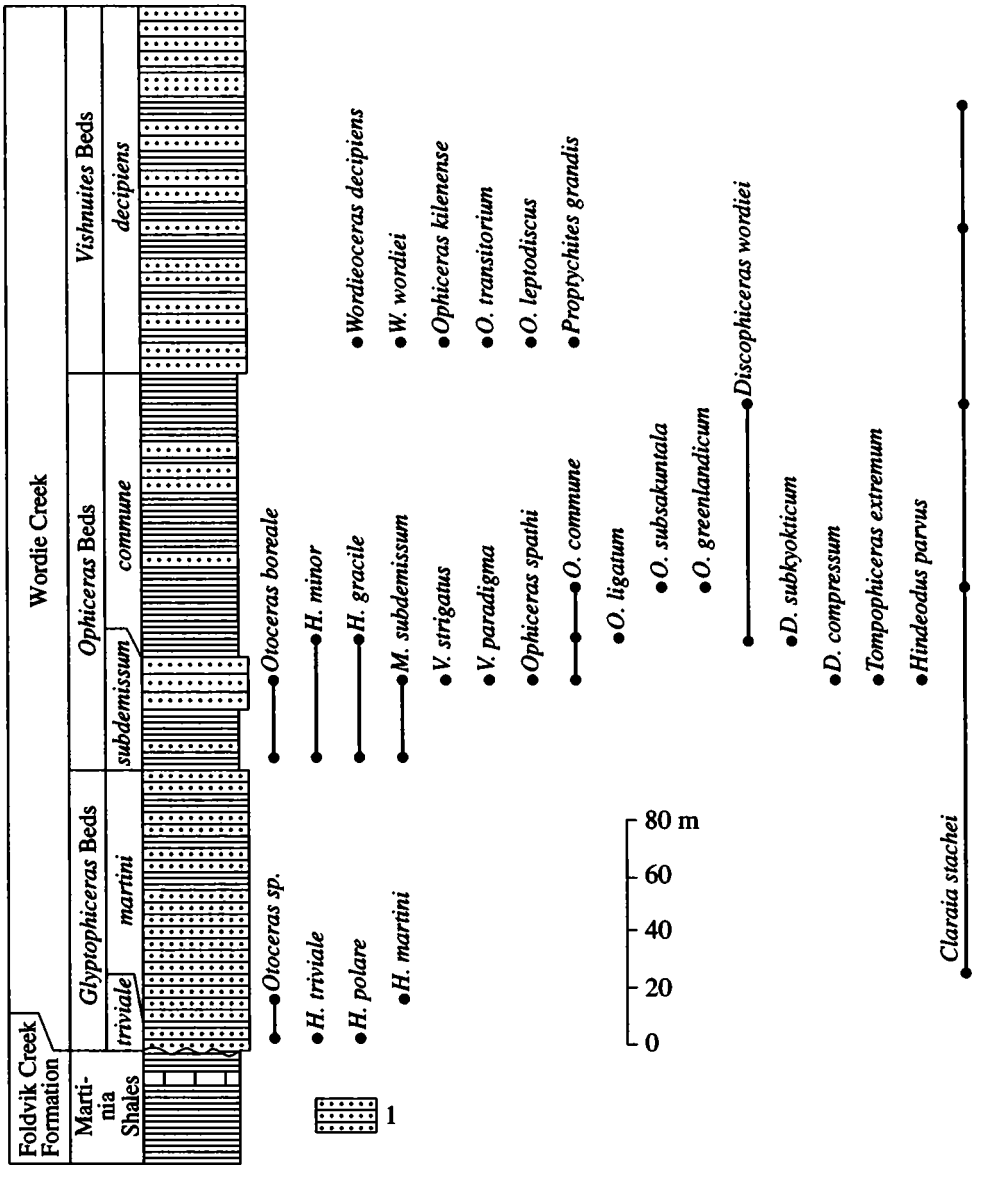

Fig. 2. The Permian–Triassic boundary section in Eastern Greenland (after Grasmück and Trümpy, 1969; Trümpy, 1969; Teichert and Kummel, 1972, 1976): (1) sandstone (other symbols as in Fig. 1).

upper part as the *Ophiceras spathi* Subzone, in which the guide species is associated with *Tompophiceras* aff. *pascoei* (Spath), *Vishnuites paradigma, Hypophiceras glacile*, and rare *Ophiceras commune* in the Walter Martin Bjerg site and with *Otoceras boreale* elsewhere.

In contrast to other boreal regions, that of eastern Greenland is distinguished by abnormally high diversity of Late Permian and Early Triassic conodonts. They were collected by Teichert and Kummel (1972, 1976) from the Kap Stosch section, and Sweet (1976) studied and described them. Kozur *et al.*, (1996) recently revised this conodont collection. However, their results are not well known, except for the fact that the lower *Otoceras* Beds (probably, the *triviale* and *martini* zones) contain *Hindeodus typicalis* (Sweet), *Clarkina* cf. *carinata* (Clark), *C. subcarinata* (Sweet), and *C.* cf. *changxingensis* (Wang et Wang), while the upper *Otoceras* Beds (the *subdemissum* Zone) bear *Hindeodus latidentatus* (Kozur, Mostler et Rahimi-Yazd), *Clarkina carinata*, and some other forms. The *Ophiceras* Beds (the *spathi* or *commune* Subzone) mark the first occurrence level of very primitive *Hindeodus parvus* (Kozur et Pjatakova).

SPITSBERGEN

In this archipelago, the Lower Triassic section begins with mudstone and siltstone beds of the Vardebukta Formation (Buchan *et al.*, 1965). At Lusitania Creek (the southern coast of the Sasenfjorden, western Spitsbergen), the mudstone beds of this formation over-

lie the sandstone layers of the Selender Formation (the Kazanian–lower Tatarian, according to Ustritskii, 1983) without any visible sign of a hiatus. The lower part of the mudstone member yielded single specimens of *Otoceras boreale* (Fig. 3, Member 1). Six meters above its base, there was found a concretion with abundant ammonites *O. boreale, Tompophiceras nielseni* (Spath), *Ophiceras spathi* Trümpy, *O.* cf. *compressum* Spath., *O. kochi* Spath *Vishnuites paradigma* (Trümpy), and *V. oxynotus* (Spath); they associate with the rare bivalves *Promyalina* cf. *degeeri* (Lindgr.) and *Unionites* cf. *breviformis* Spath, and also with the gastropods *Bellerophon borealis* Spath (Korchinskaya and Vavilov, 1987). The conodont assemblage of *Clarkina carinata* (Clark), *Enantiognathus ziegleri* (Diebel), *Neohindeodella nevadensis* (Müller), and *Ozarkodina* sp. was also described from this level (Dagys and Korchinskaya, 1987, 1989). Two meters above, the overlying siltstones (Member 2) yielded poorly preserved but abundant *O. boreale* forms and single specimens of *Hypophiceras gracile* (Spath), *Ophiceras* sp., *Promyalina* sp., and *Bellerophon borealis*. Fragments of *Proptychites rosenkrantzi* Spath and *P.* cf. *simplex* Spath were found in concretions and a siltstone matrix 25 m above the upper boundary of *Otoceras* Beds.

Another section on the eastern Recherchefjorden coast exposes Triassic deposits resting on siliceous sandstone and siltstone layers of the Kap Starostin Formation (the Ufimian Stage, according to Ustritskii, 1983; or the Kungurian and Dzhulfian stages, according to Nakamura *et al.*, 1987). The Verdebukta Formation of this section consists of two (Selmaneset and Siksaken) members (Nakazawa *et al.*, 1990). The lower member (35 m thick) is composed of mudstone enclosing calcareous siltstone and fine-grained sandstone interbeds. Its conformable contact with the Kap Starostin Formation is marked by a clay bed (Fig. 3). The level at 12–14 m above this bed yielded abundant bivalves *Claraia stachei* Bitt and the rare ammonite species *Tompophiceras* cf. *nielseni* (Korchinskaya and Vavilov, 1987). Immediately above this level, similar mudstone beds contain impressions of *Otoceras boreale* and the rare *Tompophiceras* sp. and *Claraia stachei*.

The Siksaken Member (68 m thick) overlying the previous one predominantly consists of coarser grained deposits. It is composed of siltstones or fine-grained sandstones intercalated with clayey shales and, in the middle part, with limestone interbeds. The lower half of the member bears the bivalves *Promyalina degeeri* and *Unionites fassaensis* (Wissmann). In the middle part, Polish paleontologists Gazdzicki and Trammer (1977) found *Vavilovites* aff. *sverdrupi* Tozer, which was later identified by Korchinskaya (1986) as a new species *V. spitsbergensis*. The described section is remarkable due to the fact that *Claraia stachei* and *Tompophiceras* cf. *nielseni* show their first appearance under the *Otoceras* Beds, i.e., beneath their usual position. Upsection, *Claraia* forms associate with *O. boreale*.

SIBERIA

The basal Triassic deposits are most widespread in the eastern Verkhoyansk region (the Vostochnaya Khandyga and Tompo river basins), where the ammonite *Otoceras concavum, O. boreale, Tompophiceras pascoevi, T. morphaeos*, and *Wordieoceras secipiens* zones spanning the entire lower Induan Substage can be recognized (Dagys and Ermakova, 1993, 1996; Dagys, 1994b).

Hypostratotypes of two lower ammonite zones are situated at the Setorym River (upper reaches of the Vostochnaya Khandyga River), where siltstone and sandstone layers of the Imtachan Formation (the Kazanian Stage) are overlain, without any visible sign of unconformity, by siltstone and mudstone beds of the Nekuchan Formation (Dagys *et al.*, 1986). The lower mudstone beds bear flattened calcareous–clayey concretions (Member 1, thickness 12 m) and belong to the *concavum* Zone (Fig. 4). Ammonites *Otoceras concavum* Tozer, bivalves *Palaeonucula aldanensis* Kurushin, and nautiloids *Tomponautilus setorymi* Sobolev were found at the level of 0.6–1.2 m above the base of this zone. Upsection, there is a mudstone interval with siltstone interbeds and frequent horizons of calcareous–clayey concretions (Member 2, thickness 7.5 m) containing *Otoceras boreale* and *Palaeonucula aldanensis*. The overlying fine-grained sandstones (Member 3, thickness 0.8 m), and mudstones with concretion interbeds (Member 4, thickness 29.5 m) yield *Otoceras* ex gr. *boreale*. The last three members constitute the *boreale* Zone.

Stratotypes of the overlying *pascoei*, and *morphaeos* zones, as well as the hypostratotype of the lower Induan *decipiens* Zone, are situated at the Lekeer River (the Tompo River basin). The mudstone beds with *O. boreale* are overlain here by mudstone layers with interbeds of calcareous concretions (Member 5, thickness 2.5 m) containing *Tompophiceras pascoei* (Spath), *T. extremum* (Spath), *T. nielseni* (Spath), *Hypophiceras gracile* (Spath), and *Promyalina schamarae* (Bittner). The enclosing deposits are referred to the *pascoei* Zone.

Upsection, there are exposed mudstone beds (Member 6, thickness 1.5 m) analogous to those of Member 5 and containing *Tompophiceras morphaeos* (Popow) and *T. extremum* (Spath). Upward in the section, there is the following succession of rocks: mudstones with interbeds of coalesced calcareous–clayey concretions (Member 7, thickness 7 m) enclosing *Hypophiceras minor* (Spath); mudstones with siltstone interbeds and concretions (Member 8, thickness 41 m); alternating mudstone and sandstone beds (Member 9, thickness 19 m); and mudstones with a clayey conglomerate horizon and small concretions at the base (Member 10, thickness 32 m), which contain *Metophiceras subdemissum* (Spath) and *Tompophiceras* sp. The interval lying above is covered with talus. Members 6–11 represent the *morphaeos* Zone. The section is crowned by

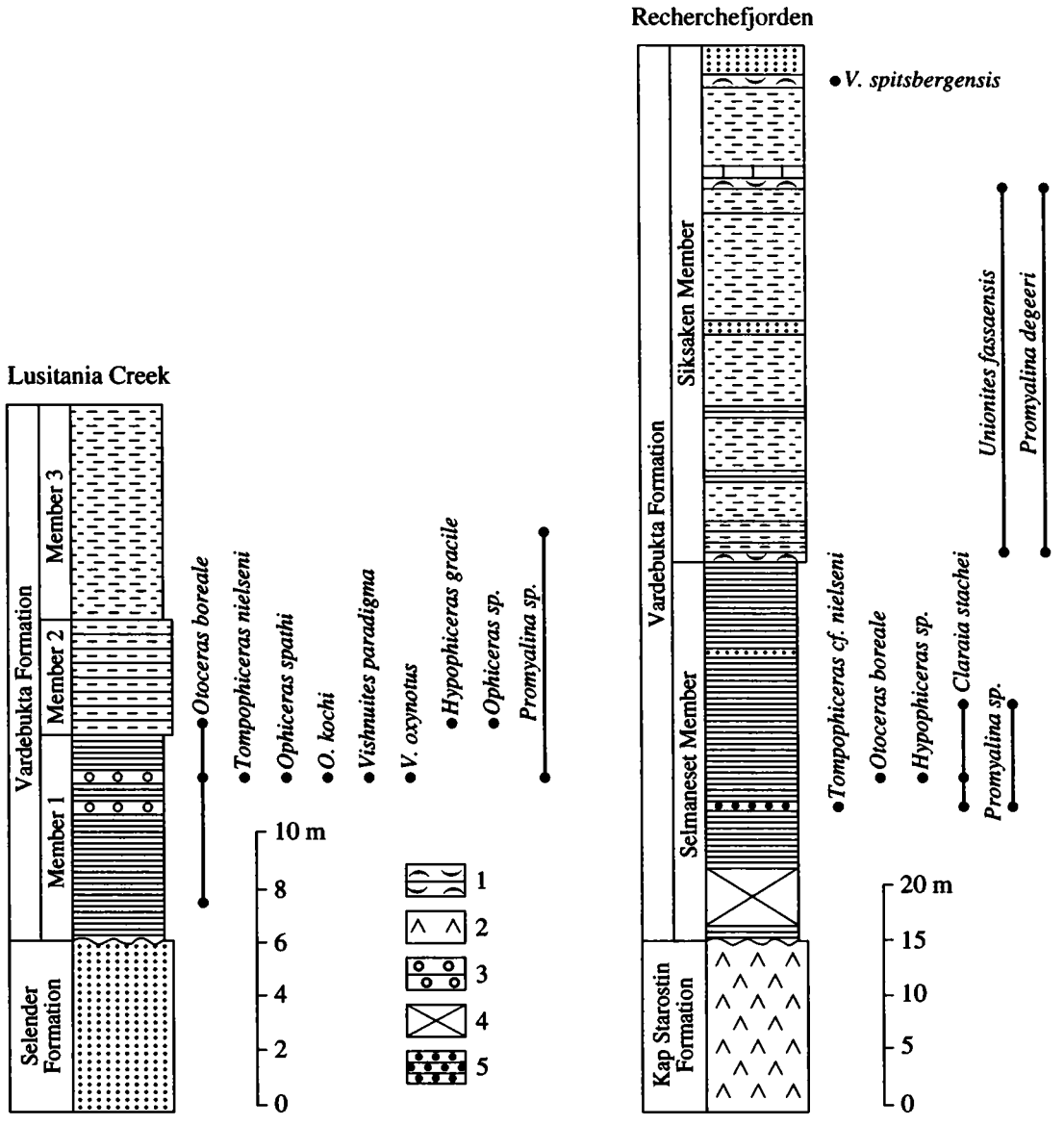

Fig. 3. The Permian–Triassic boundary section in West Spitsbergen Island (after Korchinskaya and Vavilov, 1987; Nakazawa *et al.*, 1990): (1) coquina; (2) siliceous sandstone; (3) bed with concretions; (4) debris; (5) conglomerate (other symbols as in Figs. 1 and 2).

mudstones with siltstone interbeds and rare concretion horizons (Member 12, thickness 25 m) containing *Wordieoceras decipiens* (Spath) and *Promyalina* sp. (the *decipiens* Zone).

One more ammonite zonation is suggested by Zakharov (1978, 1986, 1994) on the basis of ammonite distribution patterns in exposures at the Setorym River. According to his data, *O. concavum* occurs together with *O. boreale* in the lower part of the Nekuchan Formation (0.7–7.0 m above its base). Accordingly, Zakharov considers the lower part of the *Otoceras* stratigraphic range as an equivalent of the lower *boreale* Subzone. He reported on the occurrence of conodonts *Hindeodus typicalis* and *Clarkina* cf. *changxingensis* at a level of 5 m above the formation base. In the upper part of the *Otoceras* distribution interval, *O. boreale* was found in association with *Tompophiceras pascoei* and *Ophiceras* sp. (the upper *boreale* Subzone).

CORRELATION OF THE PERMIAN–TRIASSIC BOUNDARY BEDS

My attempt to analyze the described sections in terms of their correlation is presented below. The first important fact is that the Triassic base is marked by the first occurrence of the genus *Otoceras*, i.e., by the *Otoceras* Beds and their chronological equivalents.

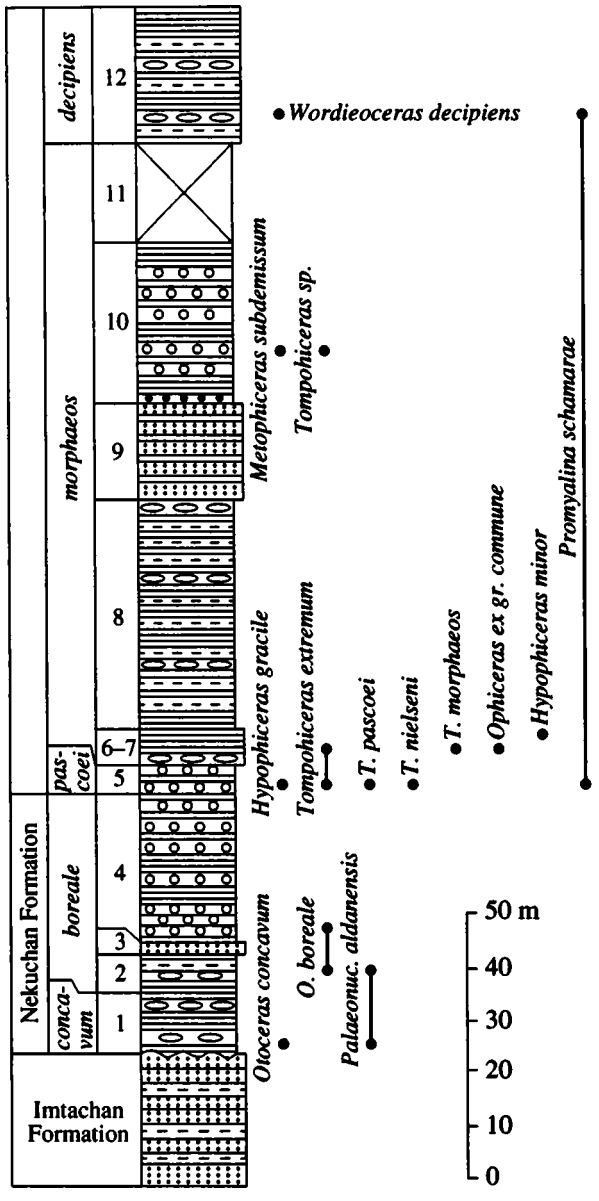

Fig. 4. The Permian–Triassic boundary section in the eastern Verkhoyansk region (after Dagys *et al.*, 1986; Dagys and Ermakova, 1993, 1996; Dagys, 1994b; symbols as in Figs. 1–3).

Boreal sections, where the lower Induan ammonite zonation is easily recognizable, will be considered first.

In the Arctic islands of Canada, the lower Griesbachian deposits unconformably resting on the Wordian Degerboels Formation include the *concavum* and *boreale* zones (Fig. 1). The *concavum* Zone only contains two *Otoceras* species, while in the *boreale* Zone, the guide species was found together with *Hypophiceras gracile* and *Vishnuites kummeli*. The upper Griesbachian deposits begin with the *commune* Zone, where *Ophiceras, Discophiceras, Tompophiceras*, and *Wordieoceras* appear for the first time.

In eastern Greenland, the Triassic basal beds correspond to the *triviale* and *martini* zones (Fig. 2). Due to the occurrence of *Otoceras* sp. ind. shells similar to those of *O. boreale* (Spath, 1935), these local zones may be correlated with the *boreale* Zone of Canada. Dagys and Dagys (1988) are also in favor of this correlation. Trümpy (1969, p. 83) reported on a shell of *Otoceras* sp. found in the *martini* Zone of Traill Island. This form has a flattened ventral lobe suggesting its similarity to *O. concavum*. On this basis, the *triviale* and *martini* zones may be correlated with the *concavum* Zone, exactly as it was done by Trümpy (1969, p. 110, Table 2). In eastern Greenland, *O. boreale* is mainly characteristic of the overlying *subdemissum* Zone, which, therefore, correlates well with the *boreale* Zone of Canada (table). However, these zones cannot be considered as equivalents, because the upper part of the *subdemissum* Zone (the *spathi* Subzone) contains some genera (*Ophiceras, Discophiceras, Tompophiceras*), which appear above the *Otoceras* Beds in Canada. The succeeding *commune* Zone of Greenland is an equivalent of the *commune* zone of Canada.

The *Otoceras* Beds of Spitsbergen, especially those at Lusitania Creek (Fig. 3), which span the *boreale* Zone interval, are similar in their fossil content to the *subdemissum* Zone of eastern Greenland and can be considered as an equivalent of the latter (table). The *concavum* Zone seems to have no analogues in Spitsbergen.

In the eastern Verkhoyansk area, the *concavum, boreale, pascoei, morphaeos*, and *decipiens* zones of the lower Induan can be recognized (Fig. 4). Two lower zones can be correlated with corresponding zones in Canada. The *pascoei* and *morphaeos* zones correlate well with the Canadian *commune* Zone (table) owing to the presence of the genus *Tompophiceras*. The first occurrence level of *Wordieoceras* forms in the uppermost beds of the *commune* Zone allows the latter to be correlated with the lower *decipiens* Zone.

All the boreal sections lack the uppermost Permian deposits of the Changxingian Stage. The Triassic begins with either the *concavum* Zone or the *boreale* Zone. The upper part of the latter frequently yields *Ophiceras* species locally associated with *Hindeodus parvus*.

The Permian–Triassic boundary deposits of the Tethys are the next to be analyzed.

The Triassic lower boundary is vaguely positioned in the South Alpine sections. Up to the mid-1980s, the Permian–Triassic chronostratigraphic boundary was considered as corresponding to the lithostratigraphic boundary separating the Bellerophon and Werfen formations, with allowance for a hiatus between them (Assereto *et al.*, 1973). However, comprehensive investigations of the South Alpine sections revealed the occurrence of fusulinids and Permian brachiopods in the lower Tesero Horizon, which is the basal one in the Werfen Formation. Owing to these findings, the Triassic lower boundary was displaced to a higher level (Broglio Lorida *et al.*, 1988; Neri and Pasini, 1985;

Pasini, 1985; Noé, 1987, 1988). At present many Alpine stratigraphers place the boundary between the middle and upper parts of the Tesero Horizon, thus dividing the last occurrence of Permian microfossils and the first occurrence of Triassic bivalves, which associate, however, with Permian brachiopods. As ammonites have not been found, their zonation in the South Alpine boundary deposits is unknown. Data on conodonts from these deposits are very contradictory. For instance, Kozur *et al.*, (1996) believe that, in the Dolomites, *Hindeodus parvus* appears in the lower part of the Mazzin Member, i.e., above the Tesero Horizon. In the Carnic Alps, this conodont species was found in the upper part of the Tesero Horizon penetrated by the Gartnerkofel borehole and also in the basal part of the same horizon exposed in the neighboring Reppwand Cliff (Schönlaub, 1991). According to Kozur *et al.*, (1996), these contradictions are the result of misidentification of the advanced *H. latidentatus* form classed in the Carnic Alps with *H. parvus*. If so, the lower part of the Mazzin Member can be correlated with the upper part of the *boreale* Zone (table).

In the Transcaucasia, the *Paratirolites* Beds of the Akhura Formation are overlain by red-brown mudstones and marls of the Karabaglyar Formation bearing *Pleuronodoceras occidentale* and *Xenodiscus jubilaearis*. The deposits are attributed to the *occidentale* Zone of the uppermost Dorashamian Stage. The lower part of the *Claraia* Beds lying above yielded conodonts *H. parvus*, marking the upper part of the *boreale* Zone. Upward in the section, there are ammonites of the genus *Ophiceras* and conodonts *Isarcicella isarcica*, which suggest correlation of the enclosing deposits with the *tibeticum* Zone of the Himalayas (table).

In Central Iran, the *Paratirolites* limestones of the Hambast Formation are overlain by basal beds of barren clayey shales of the Elikah Formation. According to the stratigraphic position, the shale beds are analogues of the mudstone layers of the *occidentale* Zone in the Transcaucasia; and hence, they can be dated back to the Permian. The overlying stromatolitic limestones with *Hindeodus parvus* and *Hypophiceras* sp. correspond to the *woodwardi* Zone of the Himalayas or to the upper part of the *boreale* Zone. Higher in the section, beds with *Ophiceras, Claraia*, and *I. isarcica* characterize the range of the *isarcica* Zone corresponding to the ammonite *tibeticum* Zone (table).

In the West Pakistan sections, the Permian–Triassic boundary is inside the basal Kathwai Member of the Mianwali Formation. The lower part of the member with Permian brachiopods, bryozoans, and foraminifers represents the Changxingian Stage. Lower beds in the middle part of the member bear *Ophiceras connectens* and conodonts of the *parvus–minutus* Zone; they can be correlated with the ammonite *woodwardi* Zone, while the overlying beds with *O. connectens* and conodonts of the *isarcica–parvus* Zone may correspond to the ammonite *tibeticum* Zone (table).

In the Guryul Ravine of Kashmir, the Permian–Triassic boundary is placed inside Member E at the base of the Khunamuh Formation. The lower part of this member (Unit E_1, Beds 47–51) yields Permian brachiopods, ammonites *Hypophiceras?* sp., and bivalves *Claraia bioni*; it is referred to either the Upper Permian or the Lower Triassic. Japanese geologists, who studied this section, initially correlated the lower unit with the *Paratirolites* Beds (Nakazawa *et al.*, 1975, Table 13). Later, taking into consideration the presence of *Hypophiceras?* sp. and *C. bioni*, Nakazawa (1993) identified Unit E_1 as the *Hypophiceras?* sp. Zone of the basal Triassic. This correlation scheme was supported by Kapoor (1996). However, correct identification of poorly preserved ammonites from this unit is difficult, and they may belong to Permian xenodiscids. I conventionally correlate Unit E_1 with the lower part of the Kathwai Member of West Pakistan and consider it as corresponding to the Changxingian Stage (table). The middle part of Member E (Unit E_2, Beds 52–59) likely represents the *woodwardi* Zone, as it yields the guide species of this zone. This species coexists with *Hindeodus parvus* and *Ophiceras sakuntala* (Nakazawa *et al.*, 1975). For some reason, however, Nakazawa (1993) later changed the first occurrence of the last species, placing it in the *Ophiceras* Beds. The lower beds in the upper part of Member E (Unit E_3, Beds 60–64), where *O. tibeticum* was found in association with diverse *Claraia* forms and *I. isarcica*, are correlated with the ammonite *tibeticum* Zone and the conodont *isarcica* Zone.

In the central Himalayas, where the *Otoceras* beds were originally distinguished, rock outcrops along the Lilang (Spiti) mountain pass demonstrate the classic biostratigraphic zonation of the basal Triassic. Here, the Permian Kuling Shales are separated by a conglomerate bed from massive limestones with *Otoceras woodwardi, Anotoceras nala*, and *Ophiceras sakuntala* (the *woodwardi* Zone), which underlie flaggy limestones with *O. tibeticum* and *Claraia* shells (the *tibeticum* Zone). Both zones contain *Hypophiceras himalayanum* and *Episageceras dalailamae*. Owing to the presence of the genus *Ophiceras*, the *woodwardi* Zone of this section can be correlated with the upper part of the *boreale* Zone (table).

In the section near the Selong Settlement in southern Tibet, the Permian–Triassic boundary coincides with the boundary between the Selong and Kangshare formations. The upper portion of the Selong Formation, consisting of coral limestones and *Waagenella* Beds with tabulates, rugoses, bryozoans, and brachiopods, is referred to the Permian but probably not to the uppermost part of this system. The Kangshare Formation begins with the limestone beds bearing *Otoceras latilobatum* (Bed 20) and *O. woodwardi* (Bed 21). Nakazawa (1992) and Yin (1993) consider the *O. latilobatum* Beds to be an analogue of the *concavum* Zone. However, as correctly noted by Dagys (1994a), *O. latilobatum* differs from *O. concavum* in a roof-shaped ventral lobe and therefore is more similar to *O. woodwardi*. For

Interregional correlation of marine Permian–Triassic boundary deposits

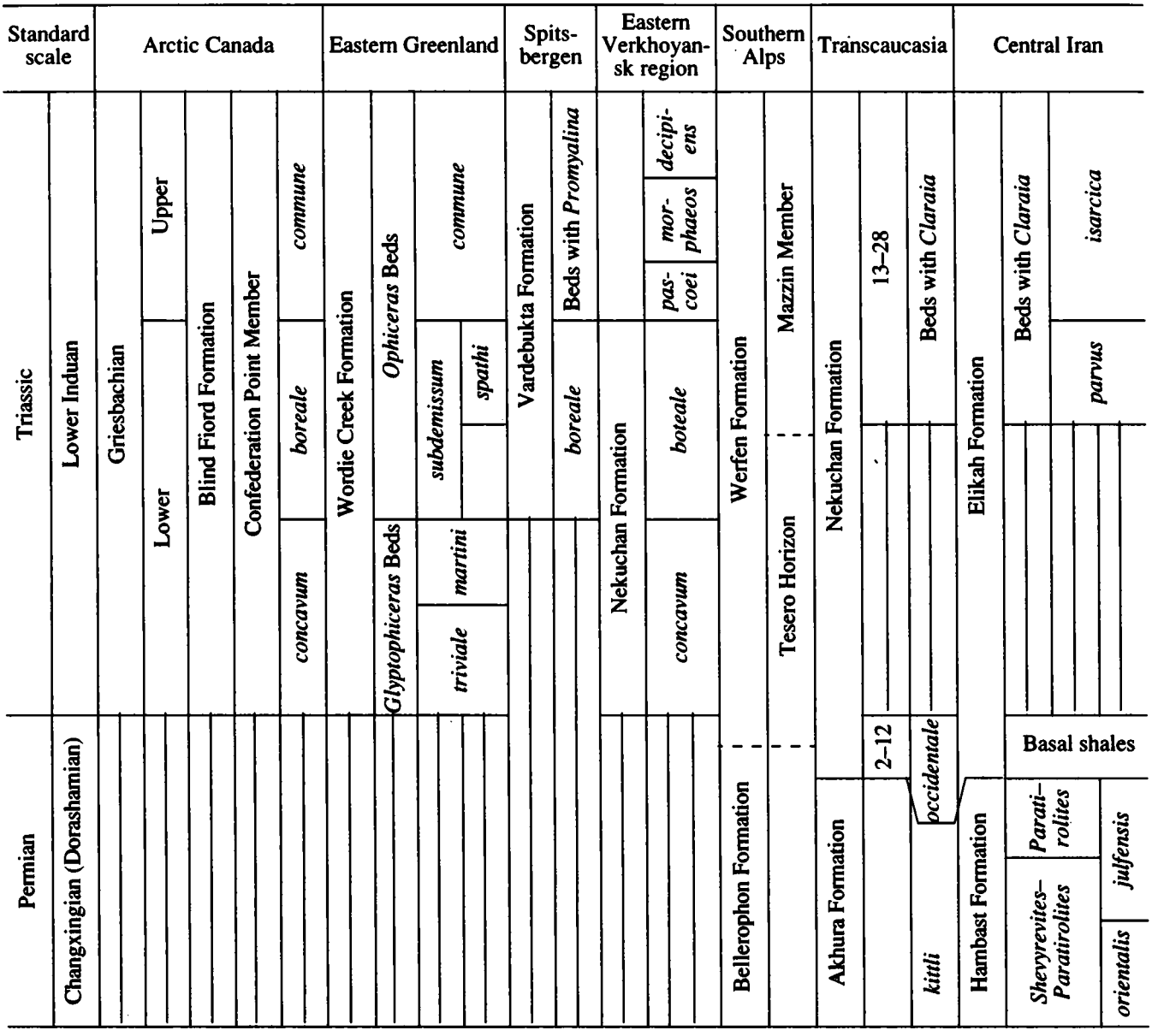

this reason, layers with *O. woodwardi* and *O. latilobatum* Beds lying stratigraphically below should be referred together to the *woodwardi* Zone. It is also necessary to mention that representatives of the genus *Ophiceras* have not been found in this zone of the Selong section, in contrast to the Himalayan sections of India. These forms appear only in the overlying *Ophiceras* Beds. According to its paleontological characteristics, the *woodwardi* Zone should be considered as a full equivalent of the *boreale* Zone (table).

In the Shangsi section (Sichuan Province), the position of the Triassic lower boundary is a subject of debates. Beds 24–27, which crown the Dalong Formation, contain the ammonite assemblage of *Pseudogastrioceras, Pleuronodoceras, Rotodiscoceras, Pseudotirolites, Lopingoceras, Huananoceras*, and *Changsingoceras* forms attributable to the uppermost Changxingian Stage. The overlying Feixianguan Formation begins with clays (Bed 28a), where Chinese paleontologists found an assemblage of mixed Permian (*Pseudogastrioceras* and *Pseudotirolites*) and Triassic (*Hypophiceras, Metophiceras*, and *Tompophiceras*) ammonites. However, the poorly preserved ammonites are not easily identifiable. *Pseudogastrioceras*, characterized by a peculiar spiral sculpture, is definitely present amid them. Forms with big marginal cusps, which were identified by Chinese paleontologists as representatives of the genus *Tompophiceras*, most likely belong to the genus *Paratirolites*. Other taxa, such as *Hypophiceras* and *Metophiceras*, may repre-

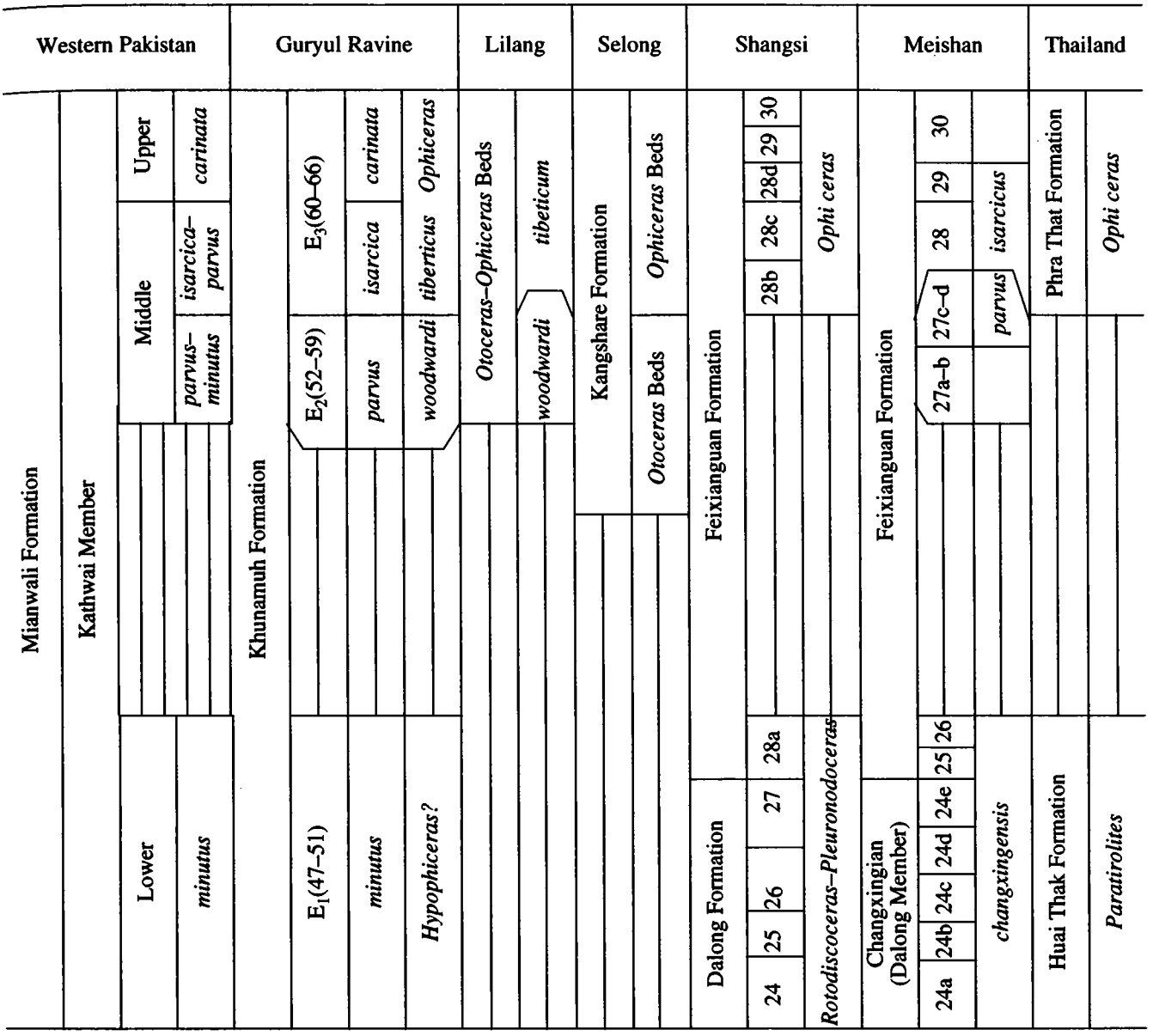

sent Permian xenodiscids. On this basis, Bed 28a with the listed ammonites should correspond to the upper Changxingian Substage. Bed 28c with *Otoceras* sp. represents the *tibeticum* Zone, which also includes Bed 28b with abundant *Claraia* shells (table).

The Meishan section, which is insistently suggested as the Global Stratotype Section and Point for the Triassic lower boundary, is worthy of special attention. The Meishan Member crowning the Changxing Formation contains an association of fusulinids and other foraminifers, Permian brachiopods, ammonites (*Pseudogastrioceras, Pleuronodoceras*, and *Rotodiscoceras*), and conodonts (*Clarkina carinata, C. changxingensis*, and *C. deflecta*). It is beyond doubt that the Meishan Member belongs to the upper Changxingian. Above, there are transitional beds of white and black clays (Beds 25 and 26) basal in the Yinkeng Formation. Their ages are unclear. The white clay beds are barren of guide fossils. The black beds bear brachiopods *Cathaysia, Crurithyris, Neochonetes, Araxathyris*, bivalves *Peribositra*, and conodonts *Clarkina changxingensis, C. deflecta, C. carinata, C. meishanensis*, and *Hindeodus latidentatus*. They also yielded the ammonites *Otoceras?* sp., *Hypophiceras* cf. *martini, Metophiceras* sp., *Tompophiceras* sp., *Pseudogastrioceras* sp., and *Pseudosageceras* sp. (Wang, 1984). As in the Shangxing section, these species represent a mixed assemblage of Permian and Triassic forms. *Pseudogastrioceras* with a spiral sculpture is a typical representative of the Changxingian biota. *Otoceras, Hypophiceras*, and

Metophiceras forms are characteristic of the basal Triassic. *Tompophiceras* is the Boreal genus usually occurring at a higher stratigraphic level, and *Pseudosageceras* species appear only in the upper Induan deposits in all other sections of the world. The surprising composition of the assemblage is a result of misidentification of poorly preserved ammonites, whose shells are deformed and lack visible lobe ribs. Presumable *Otoceras* forms of this assemblage may be representatives of araxoceratids; *Paratirolites* seems to be taken for *Tompophiceras* and *Shevyrevites* for *Metophiceras*. There is no difference between *Hypophiceras* and Permian xenodiscids. Dagys, who earlier analyzed the ammonites under consideration, came to the same conclusion (Dagys and Dagys, 1988). Therefore, I am inclined to attribute the lower transitional beds 25 and 26, together with the Meishan Member, to the upper Changxingian Stage. Beds 27c and 27d, where the earliest *H. parvus* forms were identified, and analogous beds below (27a and 27b) can be correlated with the *woodwardi* Zone of the Himalayas or with the upper part of the *boreale* Zone (table). Beds 28–30, where *Ophiceras* species and *I. isarcica* appear, belong to the *tibeticum* Zone.

The correlation of the Permian–Triassic boundary deposits of Thailand presents no difficulties. The upper part of the Huai Thak Formation with ammonites *Paratirolites, Tapashanites*, and *Pseudogastrioceras* corresponds to the uppermost Changxingian beds. The Phra That Formation containing *Ophiceras* and *Claraia* is an equivalent of the *tibeticum* Zone (table).

CONCLUSION

From the analysis of interregional correlations of the Permian–Triassic boundary beds, we can arrive at the disappointing conclusion that the continuous marine sections of this interval appear to be unavailable (table).

The Boreal sections exhibit marine deposits of the basal Triassic. Regretfully, they are separated everywhere from Permian deposits by a stratigraphic hiatus. In contrast, there are complete and continuous Upper Permian successions (the Dorashamian, or Changxingian Stage) in the Tethyan region but the Lower Triassic deposits (equivalents of the *concavum* Zone and of the lower *boreale* Subzone) are missing in the majority of the sections. The Meishan section, which is presumed to be the Global Stratotype Section and Point for the Triassic lower boundary, is not an exception. The transitional beds at the base of the Yinkeng Formation yield a mixed faunal assemblage containing only Permian ammonites and should be assigned to the Changxingian Stage. The overlying deposits with *Hindeodus parvus* can be correlated with an upper part of the *boreale* Zone. The hiatus is probably less significant in the Selong section, where the Triassic ammonite zonation likely begins with the lower part of the *boreale* Zone.

The South Alpine sections probably include the continuous sequence of Permian–Triassic boundary beds, but the latter lack ammonites; and reliable correlation of these beds with ammonite zones is impossible.

At present, we do not know a section that would be acceptable as the Global Stratotype Section and Point of the Triassic lower boundary. Therefore, we must be patient and continue the search.

ACKNOWLEDGMENTS

The work was supported by the Russian Foundation for Basic Research, project no. 96-05-64984.

Reviewers A.S. Alekseev and A.G. Konstantinov

REFERENCES

Assereto, R., Bosellini, A., Fantini Sestini, N., and Sweet, W.C., The Permian–Triassic Boundary in the Southern Alps (Italy), *Mem. Can. Soc. Petr. Geol.*, 1973, no. 2, pp. 176–199.

Broglio Loriga, C., Neri, C., Pasini, M., and Posenato, M., Marine Fossil Assemblages from Upper Permian to Lowermost Triassic in the Western Dolomites (Italy), *Mem. Geol. Ital.*, 1988, vol. 34, pp. 5–44.

Buchan, S.H., Challinor, A., Harland, W.B., and Parker, J.R., The Triassic Stratigraphy of Svalbard, *Skr. Norsk Polarinst.*, 1965, vol. 135, pp. 1–92.

Dagys, A.A. and Korchinskaya, M.V., First Findings of Conodonts in the *Otoceras* Beds of Svalbard, in *Boreal'nyi trias* (The Boreal Triassic), Moscow: Nauka, 1987, pp. 110–113.

Dagys, A.A. and Korchinskaya, M.V., Triassic Conodonts of Svalbard, in *Verkhnii paleozoi i trias Sibiri* (The Upper Paleozoic and Triassic of Siberia), Novosibirsk: Nauka, 1989, pp. 109–121.

Dagys, A.S., Correlation of the Lowermost Triassic, *Albertiana*, 1994a, vol. 14, pp. 38–44.

Dagys, A.S., Lower Triassic Stage, Substage and Zonal Scheme of Northeastern Asia, *Mem. Geol.*, (Lausanne), 1994b, no. 22, pp. 15–23.

Dagys, A.S. and Dagys, A.A., Biostratigraphy of the Lowermost Triassic and the Boundary between Paleozoic and Mesozoic, *Mem. Soc. Geol. Ital.*, 1988, vol. 34, pp. 313–320.

Dagys, A.S., Dagys, A.A., Kazakov, A.M., *et al.*, The Lower Induan Biostratigraphy of the Eastern Verkhoyansk Region, in *Biostratigrafiya mezozoya Sibiri i Dal'nego Vostoka* (The Mesozoic Biostratigraphy of Siberia and the Far East), Novosibirsk: Nauka, 1986, pp. 21–31.

Dagys, A.S. and Ermakova, S.P., A Detailed Biostratigraphic Scheme of the Boreal Lower Triassic, *Stratigr. Geol. Korrelyatsiya*, 1993, vol. 1, no. 2, pp. 26–36.

Dagys, A.S. and Ermakova, S.P., Induan (Triassic) Ammonoids from Northeastern Asia, *Rev. Paleobiol.*, 1996, vol. 15, no. 2, pp. 401–447.

Embry, A.F., Stratigraphic Subdivision of the Blind Fiord and Bjorne Formations (Lower Triassic), Sverdrup Basin, Arctic Islands, *Pap. Geol. Surv. Can.*, 1986, no. 86-1B/1, pp. 329–340.

Gazdzicki, A. and Trammer, J., The Sverdrupi Zone in the Lower Triassic of Svalbard, *Acta Geol. Polon.*, 1977, vol. 27, no. 3, pp. 349–356.

Grasmück, K. and Trümpy, R., Triassic Stratigraphy and General Geology of the Country around Fleming Fjord (East Greenland), *Medd. Groenl.*, 1969, vol. 168, no. 2, pp. 6–71.

Kapoor, H.M., The Guryul Ravine Section, Candidate of the Global Stratotype Section and Point of the Permo-Triassic Boundary, *Palaeozoic–Mesozoic Boundary: Candidates of the Global Stratotype Section and Point of the Permo-Triassic Boundary*, Wuhan: China Univ. Geosci. Press, 1996, pp. 99–110.

Korchinskaya, M.V., Biostratigraphy of the Induan Stage of Spitsbergen, in *Geologiya osadochnogo chekhla arkhipelaga Shpitsbergen* (Geology of the Sedimentary Cover of the Spitsbergen Archipelago), Leningrad: Sevmorgeologiya, 1986, pp. 77–93.

Korchinskaya, M.V. and Vavilov, M.N., Early Induan Ammonoids of Spitsbergen, in *Problemy biostratigrafii permi i triasa Vostoka SSSR* (Problems of the Permian and Triassic Biostratigraphy of the Eastern USSR), Vladivostok: Dal'nevost. Nauchn. Tsentr Akad. Nauk SSSR, 1987, pp. 64–73.

Kozur, H., Ramovs, A., Wang, Gh., and Zakharov, Yu.D., The Importance of *Hindeodus parvus* (Gonodonta) for the Definition of the Permian–Triassic Boundary and Evaluation of the Proposed Sections for a Global Stratotype Section and Point (GSSP) for the Base of the Triassic, *Geologija*, 1996, vols. 37–38, pp. 173–213.

Nakamura, K., Kimura, G., and Winsnes, T.S., Brachiopod Zonation and Age of the Permian Kap Starostin Formation (Central Spitsbergen), *Polar Res.*, 1987, no. 5, pp. 207–219.

Nakazawa, K., Permian–Triassic Boundary, *Albertiana*, 1992, vol. 10, pp. 25–30.

Nakazawa, K., Stratigraphy of the Permian–Triassic Transition and the Paleozoic–Mesozoic Boundary, *Bull. Geol. Surv. Jpn.*, 1993, vol. 44, no. 7, pp. 42–44.

Nakazawa, K., Kapoor, H.M., Ishii, K., *et al.*, The Upper Permian and the Lower Triassic in Kashmir, India, *Mem. Fac. Sci. Kyoto Univ., Ser. Geol. Miner.*, 1975, vol. 42, pp. 1–106.

Nakazawa, K., Suzuki, H., Kumon, F., and Winsnes, T.S., Scientific Results of the Japanese Geological Expedition to Svalbard, 1986, in *The Japanese Scientific Expeditions to Svalbard, 1983–1988*, Tokyo: Kyoikusha, 1990, pp. 181–214.

Nassichuk, W.W., Thorsteinsson, R., and Tozer, E.T., Permian–Triassic Boundary in the Canadian Arctic Archipelago, *Bull. Can. Petrol. Geol.*, 1972, vol. 20, no. 4, pp. 651–658.

Neri, C. and Pasini, M., A "Mixed Fauna" at the Permian–Triassic Boundary, Tesero Section, Western Dolomites (Italy), *Boll. Soc. Paleontol. Ital.*, 1985, vol. 23, no. 1, pp. 113–117.

Noé, S., Facies and Paleogeography of the Marine Upper Permian and of the Permian–Triassic Boundary in the Southern Alps (Bellerophon Formation, Tesero Horizon), *Facies*, 1987, vol. 16, pp. 89–142.

Noe, S., Foraminiferal Ecology and Biostratigraphy of the Marine Upper Permian and of the Permian–Triassic Boundary in the Southern Alps (Bellerophon Formation, Tesero Horizon), *Rev. Paleobiol*, 1988, vol. 2, pp. 75–88.

Pasini, M., Biostratigrafia con i Foraminiferi del limite formazione a Bellerophon-formazione di Werfen fra Recoaro e la Val Badia (Alpi meridionali), *Riv. Ital. Paleontol. Stratigr.*, 1985, vol. 90, no. 4, pp. 481–513.

Schönlaub, H.P., The Permian–Triassic of the Gartnerkofel-1 Core (Carnic Alps, Austria): Conodont Biostratigraphy, *Abh. Geol. Bundesanst.* (Austria), 1991, no. 45, pp. 79–98.

Shevyrev, A.A., The Lower Boundary of the Triassic and Its Correlation in Marine Sediments. Article 1: The Boundary Sections of the Tethys, *Stratigr. Geol. Korrelyatsiya*, 1999, vol. 7, no. 2, pp. 14–27.

Spath, L.F., The Eotriassic Invertebrate Fauna of East Greenland, *Medd. Groenl.*, 1930, vol. 83, no. 1, pp. 3–90.

Spath, L.F., Additions to the Eotriassic Invertebrate Fauna of East Greenland, *Medd. Groenl.*, 1935, vol. 98, no. 2, pp. 3–115.

Stemmerik, L. and Piasecki, S., The Upper Permian of East Greenland: A Review, *Zentralbl. Geol. Palaéontol.*, 1991, no. 4, pp. 825–837.

Sweet, W.C., Conodonts from the Permian–Triassic Boundary Beds at Kap Stosch, East Greenland, *Medd. Groenl.*, 1976, vol. 197, no. 5, pp. 51–54.

Teichert, C. and Kummel, B., Permian–Triassic Boundary in the Kap Stosch Area, East Greenland, *Bull. Can. Petrol. Geol.*, 1972, vol. 20, no. 4, pp. 659–675.

Teichert, C. and Kummel, B., Permian–Triassic Boundary in the Kap Stosch Area, East Greenland, *Medd. Groenl.*, 1976, vol. 197, no. 5, pp. 3–54.

Thorsteinsson, R., Carboniferous and Permian Stratigraphy of Axel Heiberg Island and Western Ellesmere Island, Canadian Arctic Archipelago, *Bull. Geol. Surv. Can.*, 1974, no. 224, pp. 1–115.

Tozer, E.T., Lower Triassic Stages and Ammonoid Zones of Arctic Canada, *Pap. Geol. Surv. Can.*, 1965, no. 63–12, pp. 1–14.

Tozer, E.T., A Standard for Triassic Time, *Bull. Geol. Surv. Can.*, 1967, no. 156, pp. 1–103.

Tozer, E.T., Canadian Triassic Ammonoid Faunas, *Bull. Geol. Surv. Can.*, 1994, no. 467, pp. 1–663.

Trümpy, R., Lower Triassic Ammonites from Jameson Land (East Greenland), *Medd. Groenl.*, 1969, vol. 168, no. 2, pp. 77–116.

Ustritskii, V.I., The Stage Scale for the Boreal Permian, in *Paleontologicheskoe obosnovanie raschleneniya paleozoya i mezozoya arkticheskikh raionov SSSR* (Paleontological Substantiation of Subdivision of the Arctic Paleozoic and Mesozoic Deposits of the USSR), Leningrad: Sevmorgeologiya, 1983, pp. 16–38.

Wang, Y., Earliest Triassic Ammonoid Faunas from Jiangsu and Zheejiang and Their Bearing on the Definition of Permo-Triassic Boundary, *Acta Palaeontol. Sin.*, 1984, vol. 23, no. 3, pp. 257–269.

Yin, H., A Proposal for the Global Stratotype Section and Point (GSSP) of the Permian–Triassic Boundary (Chinese Working Group on the Permian–Triassic Boundary), *Albertiana*, 1993, vol. 11, pp. 4–30.

Zakharov, Yu.D., *Rannetriasovye ammonoidei Vostoka SSSR* (The Early Triassic Ammonoids of the Eastern USSR), Moscow: Nauka, 1978.

Zakharov, Yu.D., Macroevolution and the Major Boundaries in the Phanerozoic, *Eclogae Geol. Helv.*, 1986, vol. 79, no. 1, pp. 227–235.

Zakharov, Yu.D., Proposals on Revision of the Siberian Standard for the Lower Triassic and Candidate Stratotype Section and Point for the Induan–Olenekian Boundary, *Albertiana*, 1994, vol. 14, pp. 44–51.

Metophiceras forms are characteristic of the basal Triassic. *Tompophiceras* is the Boreal genus usually occurring at a higher stratigraphic level, and *Pseudosageceras* species appear only in the upper Induan deposits in all other sections of the world. The surprising composition of the assemblage is a result of misidentification of poorly preserved ammonites, whose shells are deformed and lack visible lobe ribs. Presumable *Otoceras* forms of this assemblage may be representatives of araxoceratids; *Paratirolites* seems to be taken for *Tompophiceras* and *Shevyrevites* for *Metophiceras*. There is no difference between *Hypophiceras* and Permian xenodiscids. Dagys, who earlier analyzed the ammonites under consideration, came to the same conclusion (Dagys and Dagys, 1988). Therefore, I am inclined to attribute the lower transitional beds 25 and 26, together with the Meishan Member, to the upper Changxingian Stage. Beds 27c and 27d, where the earliest *H. parvus* forms were identified, and analogous beds below (27a and 27b) can be correlated with the *woodwardi* Zone of the Himalayas or with the upper part of the *boreale* Zone (table). Beds 28–30, where *Ophiceras* species and *I. isarcica* appear, belong to the *tibeticum* Zone.

The correlation of the Permian–Triassic boundary deposits of Thailand presents no difficulties. The upper part of the Huai Thak Formation with ammonites *Paratirolites, Tapashanites*, and *Pseudogastrioceras* corresponds to the uppermost Changxingian beds. The Phra That Formation containing *Ophiceras* and *Claraia* is an equivalent of the *tibeticum* Zone (table).

CONCLUSION

From the analysis of interregional correlations of the Permian–Triassic boundary beds, we can arrive at the disappointing conclusion that the continuous marine sections of this interval appear to be unavailable (table).

The Boreal sections exhibit marine deposits of the basal Triassic. Regretfully, they are separated everywhere from Permian deposits by a stratigraphic hiatus. In contrast, there are complete and continuous Upper Permian successions (the Dorashamian, or Changxingian Stage) in the Tethyan region but the Lower Triassic deposits (equivalents of the *concavum* Zone and of the lower *boreale* Subzone) are missing in the majority of the sections. The Meishan section, which is presumed to be the Global Stratotype Section and Point for the Triassic lower boundary, is not an exception. The transitional beds at the base of the Yinkeng Formation yield a mixed faunal assemblage containing only Permian ammonites and should be assigned to the Changxingian Stage. The overlying deposits with *Hindeodus parvus* can be correlated with an upper part of the *boreale* Zone. The hiatus is probably less significant in the Selong section, where the Triassic ammonite zonation likely begins with the lower part of the *boreale* Zone.

The South Alpine sections probably include the continuous sequence of Permian–Triassic boundary beds, but the latter lack ammonites; and reliable correlation of these beds with ammonite zones is impossible.

At present, we do not know a section that would be acceptable as the Global Stratotype Section and Point of the Triassic lower boundary. Therefore, we must be patient and continue the search.

ACKNOWLEDGMENTS

The work was supported by the Russian Foundation for Basic Research, project no. 96-05-64984.

Reviewers A.S. Alekseev and A.G. Konstantinov

REFERENCES

Assereto, R., Bosellini, A., Fantini Sestini, N., and Sweet, W.C., The Permian–Triassic Boundary in the Southern Alps (Italy), *Mem. Can. Soc. Petr. Geol.*, 1973, no. 2, pp. 176–199.

Broglio Loriga, C., Neri, C., Pasini, M., and Posenato, M., Marine Fossil Assemblages from Upper Permian to Lowermost Triassic in the Western Dolomites (Italy), *Mem. Geol. Ital.*, 1988, vol. 34, pp. 5–44.

Buchan, S.H., Challinor, A., Harland, W.B., and Parker, J.R., The Triassic Stratigraphy of Svalbard, *Skr. Norsk Polarinst.*, 1965, vol. 135, pp. 1–92.

Dagys, A.A. and Korchinskaya, M.V., First Findings of Conodonts in the *Otoceras* Beds of Svalbard, in *Boreal'nyi trias* (The Boreal Triassic), Moscow: Nauka, 1987, pp. 110–113.

Dagys, A.A. and Korchinskaya, M.V., Triassic Conodonts of Svalbard, in *Verkhnii paleozoi i trias Sibiri* (The Upper Paleozoic and Triassic of Siberia), Novosibirsk: Nauka, 1989, pp. 109–121.

Dagys, A.S., Correlation of the Lowermost Triassic, *Albertiana*, 1994a, vol. 14, pp. 38–44.

Dagys, A.S., Lower Triassic Stage, Substage and Zonal Scheme of Northeastern Asia, *Mem. Geol.*, (Lausanne), 1994b, no. 22, pp. 15–23.

Dagys, A.S. and Dagys, A.A., Biostratigraphy of the Lowermost Triassic and the Boundary between Paleozoic and Mesozoic, *Mem. Soc. Geol. Ital.*, 1988, vol. 34, pp. 313–320.

Dagys, A.S., Dagys, A.A., Kazakov, A.M., *et al.*, The Lower Induan Biostratigraphy of the Eastern Verkhoyansk Region, in *Biostratigrafiya mezozoya Sibiri i Dal'nego Vostoka* (The Mesozoic Biostratigraphy of Siberia and the Far East), Novosibirsk: Nauka, 1986, pp. 21–31.

Dagys, A.S. and Ermakova, S.P., A Detailed Biostratigraphic Scheme of the Boreal Lower Triassic, *Stratigr. Geol. Korrelyatsiya*, 1993, vol. 1, no. 2, pp. 26–36.

Dagys, A.S. and Ermakova, S.P., Induan (Triassic) Ammonoids from Northeastern Asia, *Rev. Paleobiol.*, 1996, vol. 15, no. 2, pp. 401–447.

Embry, A.F., Stratigraphic Subdivision of the Blind Fiord and Bjorne Formations (Lower Triassic), Sverdrup Basin, Arctic Islands, *Pap. Geol. Surv. Can.*, 1986, no. 86-1B/1, pp. 329–340.

Gazdzicki, A. and Trammer, J., The Sverdrupi Zone in the Lower Triassic of Svalbard, *Acta Geol. Polon.*, 1977, vol. 27, no. 3, pp. 349–356.

Grasmück, K. and Trümpy, R., Triassic Stratigraphy and General Geology of the Country around Fleming Fjord (East Greenland), *Medd. Groenl.*, 1969, vol. 168, no. 2, pp. 6–71.

Kapoor, H.M., The Guryul Ravine Section, Candidate of the Global Stratotype Section and Point of the Permo-Triassic Boundary, *Palaeozoic–Mesozoic Boundary: Candidates of the Global Stratotype Section and Point of the Permo-Triassic Boundary*, Wuhan: China Univ. Geosci. Press, 1996, pp. 99–110.

Korchinskaya, M.V., Biostratigraphy of the Induan Stage of Spitsbergen, in *Geologiya osadochnogo chekhla arkhipelaga Shpitsbergen* (Geology of the Sedimentary Cover of the Spitsbergen Archipelago), Leningrad: Sevmorgeologiya, 1986, pp. 77–93.

Korchinskaya, M.V. and Vavilov, M.N., Early Induan Ammonoids of Spitsbergen, in *Problemy biostratigrafii permi i triasa Vostoka SSSR* (Problems of the Permian and Triassic Biostratigraphy of the Eastern USSR), Vladivostok: Dal'nevost. Nauchn. Tsentr Akad. Nauk SSSR, 1987, pp. 64–73.

Kozur, H., Ramovs, A., Wang, Gh., and Zakharov, Yu.D., The Importance of *Hindeodus parvus* (Gonodonta) for the Definition of the Permian–Triassic Boundary and Evaluation of the Proposed Sections for a Global Stratotype Section and Point (GSSP) for the Base of the Triassic, *Geologija*, 1996, vols. 37–38, pp. 173–213.

Nakamura, K., Kimura, G., and Winsnes, T.S., Brachiopod Zonation and Age of the Permian Kap Starostin Formation (Central Spitsbergen), *Polar Res.*, 1987, no. 5, pp. 207–219.

Nakazawa, K., Permian–Triassic Boundary, *Albertiana*, 1992, vol. 10, pp. 25–30.

Nakazawa, K., Stratigraphy of the Permian–Triassic Transition and the Paleozoic–Mesozoic Boundary, *Bull. Geol. Surv. Jpn.*, 1993, vol. 44, no. 7, pp. 42–44.

Nakazawa, K., Kapoor, H.M., Ishii, K., *et al.*, The Upper Permian and the Lower Triassic in Kashmir, India, *Mem. Fac. Sci. Kyoto Univ., Ser. Geol. Miner.*, 1975, vol. 42, pp. 1–106.

Nakazawa, K., Suzuki, H., Kumon, F., and Winsnes, T.S., Scientific Results of the Japanese Geological Expedition to Svalbard, 1986, in *The Japanese Scientific Expeditions to Svalbard, 1983–1988*, Tokyo: Kyoikusha, 1990, pp. 181–214.

Nassichuk, W.W., Thorsteinsson, R., and Tozer, E.T., Permian–Triassic Boundary in the Canadian Arctic Archipelago, *Bull. Can. Petrol. Geol.*, 1972, vol. 20, no. 4, pp. 651–658.

Neri, C. and Pasini, M., A "Mixed Fauna" at the Permian–Triassic Boundary, Tesero Section, Western Dolomites (Italy), *Boll. Soc. Paleontol. Ital.*, 1985, vol. 23, no. 1, pp. 113–117.

Noé, S., Facies and Paleogeography of the Marine Upper Permian and of the Permian–Triassic Boundary in the Southern Alps (Bellerophon Formation, Tesero Horizon), *Facies*, 1987, vol. 16, pp. 89–142.

Noe, S., Foraminiferal Ecology and Biostratigraphy of the Marine Upper Permian and of the Permian–Triassic Boundary in the Southern Alps (Bellerophon Formation, Tesero Horizon), *Rev. Paleobiol*, 1988, vol. 2, pp. 75–88.

Pasini, M., Biostratigrafia con i Foraminiferi del limite formazione a Bellerophon-formazione di Werfen fra Recoaro e la Val Badia (Alpi meridionali), *Riv. Ital. Paleontol. Stratigr.*, 1985, vol. 90, no. 4, pp. 481–513.

Schönlaub, H.P., The Permian–Triassic of the Gartnerkofel-1 Core (Carnic Alps, Austria): Conodont Biostratigraphy, *Abh. Geol. Bundesanst.* (Austria), 1991, no. 45, pp. 79–98.

Shevyrev, A.A., The Lower Boundary of the Triassic and Its Correlation in Marine Sediments. Article 1: The Boundary Sections of the Tethys, *Stratigr. Geol. Korrelyatsiya*, 1999, vol. 7, no. 2, pp. 14–27.

Spath, L.F., The Eotriassic Invertebrate Fauna of East Greenland, *Medd. Groenl.*, 1930, vol. 83, no. 1, pp. 3–90.

Spath, L.F., Additions to the Eotriassic Invertebrate Fauna of East Greenland, *Medd. Groenl.*, 1935, vol. 98, no. 2, pp. 3–115.

Stemmerik, L. and Piasecki, S., The Upper Permian of East Greenland: A Review, *Zentralbl. Geol. Palaéontol.*, 1991, no. 4, pp. 825–837.

Sweet, W.C., Conodonts from the Permian–Triassic Boundary Beds at Kap Stosch, East Greenland, *Medd. Groenl.*, 1976, vol. 197, no. 5, pp. 51–54.

Teichert, C. and Kummel, B., Permian–Triassic Boundary in the Kap Stosch Area, East Greenland, *Bull. Can. Petrol. Geol.*, 1972, vol. 20, no. 4, pp. 659–675.

Teichert, C. and Kummel, B., Permian–Triassic Boundary in the Kap Stosch Area, East Greenland, *Medd. Groenl.*, 1976, vol. 197, no. 5, pp. 3–54.

Thorsteinsson, R., Carboniferous and Permian Stratigraphy of Axel Heiberg Island and Western Ellesmere Island, Canadian Arctic Archipelago, *Bull. Geol. Surv. Can.*, 1974, no. 224, pp. 1–115.

Tozer, E.T., Lower Triassic Stages and Ammonoid Zones of Arctic Canada, *Pap. Geol. Surv. Can.*, 1965, no. 63–12, pp. 1–14.

Tozer, E.T., A Standard for Triassic Time, *Bull. Geol. Surv. Can.*, 1967, no. 156, pp. 1–103.

Tozer, E.T., Canadian Triassic Ammonoid Faunas, *Bull. Geol. Surv. Can.*, 1994, no. 467, pp. 1–663.

Trümpy, R., Lower Triassic Ammonites from Jameson Land (East Greenland), *Medd. Groenl.*, 1969, vol. 168, no. 2, pp. 77–116.

Ustritskii, V.I., The Stage Scale for the Boreal Permian, in *Paleontologicheskoe obosnovanie raschleneniya paleozoya i mezozoya arkticheskikh raionov SSSR* (Paleontological Substantiation of Subdivision of the Arctic Paleozoic and Mesozoic Deposits of the USSR), Leningrad: Sevmorgeologiya, 1983, pp. 16–38.

Wang, Y., Earliest Triassic Ammonoid Faunas from Jiangsu and Zheejiang and Their Bearing on the Definition of Permo-Triassic Boundary, *Acta Palaeontol. Sin.*, 1984, vol. 23, no. 3, pp. 257–269.

Yin, H., A Proposal for the Global Stratotype Section and Point (GSSP) of the Permian–Triassic Boundary (Chinese Working Group on the Permian–Triassic Boundary), *Albertiana*, 1993, vol. 11, pp. 4–30.

Zakharov, Yu.D., *Rannetriasovye ammonoidei Vostoka SSSR* (The Early Triassic Ammonoids of the Eastern USSR), Moscow: Nauka, 1978.

Zakharov, Yu.D., Macroevolution and the Major Boundaries in the Phanerozoic, *Eclogae Geol. Helv.*, 1986, vol. 79, no. 1, pp. 227–235.

Zakharov, Yu.D., Proposals on Revision of the Siberian Standard for the Lower Triassic and Candidate Stratotype Section and Point for the Induan–Olenekian Boundary, *Albertiana*, 1994, vol. 14, pp. 44–51.

Stratigraphy and Geological Correlation, Vol. 8, No. 1, 2000, pp. 60–76. Translated from Stratigrafiya. Geologicheskaya Korrelyatsiya, Vol. 8, No. 1, 2000, pp. 66–82.
Original Russian Text Copyright © 2000 by Zubakov.
English Translation Copyright © 2000 by MAIK "Nauka/Interperiodica" (Russia).

The Pliocene of the Pontic–Caspian Region and Its Correlation

V. A. Zubakov

Center of International Cooperation on Environmental Problems, Russian Academy of Sciences, nab. Kutuzova 14, St. Petersburg, 191187 Russia

Received February 24, 1998; in final form, August 30, 1998

To Elena Nikolaevna Ananova, Galina Ivanovna Karmishina, Natal'ya Alekseevna Lebedeva, and Varvara L'vovna Yakhimovich, four devoted scientists, who contributed much to Pontic–Caspian stratigraphy.

Abstract—Relationships between traditional Pontic–Caspian Pliocene units (Pontian, Kimmerian, and Kuyalnikian regional stages of the Black Sea region and Pontian and Akchagylian regional stages of the Caspian region) and the Messinian, Zanclean, Piacenzian, and Gelasian stages of the Mediterranean are considered. The ranges and boundaries of the units are shown to be inconsistent. It is concluded that the regional Pontic–Caspian type boundaries maximum correlative to those of the standard Mediterranean scale and, consequently, new regional stages should be introduced for the Pontic–Caspian region. It is proposed to change the Pontian boundaries and introduce new regional units: Panagian (= Eoakchagylian), Polovetsian (= Akchagylian *s. str.*), and Polivadinian stages with their boundaries correlated to geomagnetic field reversals and dated back to 7.2, 5.2, 3.5, and 2.5 Ma, respectively.

Key words: *Pontic–Caspian Pliocene, stages of general scale, correlation: Pontian = Messinian, Akchagylian = (Zanclean, Gelasian).*

INTRODUCTION

The Pontic–Caspian sections represent a cornerstone of the Cenozoic stratigraphic scale of Russia. Due to the peculiar geological history of the Pontic–Caspian region, Russian Cenozoic stratigraphy had to be self-sufficient, because methods of direct correlation with the standard Mediterranean scale were inaccessible. Problems of correlation of the Pontic–Caspian and Mediterranean stratigraphic units were and remain a subject of considerable discussion and disagreement. As a result, the Upper Cenozoic scale of Russia is now autonomous and poorly comparable with the international scale; and stratigraphic materials published in Russia are almost completely ignored by foreign researchers.

The epoch of self-sufficient regional stratigraphic scales terminated when methods of radiometric dating, and geomagnetic correlation in particular, became available to geological practice. The current development of stratigraphy is marked by expansion of the Mediterranean Upper Cenozoic stratigraphic scale over the globe. By its recent resolutions, the Regional Committee on the Mediterranean Neogene Stratigraphy (RCMNS) revised the content of the Pliocene stages and introduced them into the standard scale using an essentially new methodological basis. The Interdepartmental Stratigraphic Committee (ISC) of Russia has to urgently revise the Pontic–Caspian Pliocene scheme, traditionally used in this country and divided into Pontian, Akchagylian, Kimmerian, and Kuyalnikian regional stages, on order to correlate it with the new international Neogene scale.

Main objectives of this work are as follows: (1) to compare the traditional Pontic–Caspian and new Mediterranean scales; (2) to review the principles used in the standard Cenozoic scale; and (3) to suggest a correlation scheme for reference sections of the Black Sea–Caspian Sea region with the Messinian, Zanclean, Piacenzian, and Gelasian stages, the new standard boundaries of which are approved by the RCMNS.

After this paper had been submitted for publication, it was subsequently revised with due regard for results of discussions of the problem at the April session (1998) of three Cenozoic commissions of the ISC; reviewer's recommendations; and critical analysis in the preprint by Chumakov (2000), who kindly lent me his manuscript.

1. MODERN METHODOLOGY FOR PERFECTING THE STANDARD NEOGENE STRATIGRAPHIC SCALE

The Neogene stratigraphic scale, whose main features were outlined as early as the 19th century, was persistently under revision, because the accuracy of geochronological methods that register synchronous events progressively advanced. Magnetostratigraphic and climatostratigraphic, particularly isotopic, methods

are among those that developed most intensely. Their application in stratigraphy is realized either through the theoretical introduction of specialized stratigraphic scales or through empirical improvement of the general stratigraphic scale on the basis of so-called event or causal (in terms of M.A. Krasilov) stratigraphy. The verification of the standard stratigraphic scale on the basis of events that are particularly evident in its Upper Cenozoic portion was closely associated with attempts to impart a global status to the latter. The traditional development of the Tertiary and Quaternary stratigraphy resulted in the appearance of many local scales poorly comparable to one another. Nowadays, we observe the opposite tendency. The detailed standard climatoisotopic scale of the Quaternary is now supplemented with the standard bio-climato-magnetostratigraphic scale of the Messinian and Pliocene.

Attempts to impart global status to the Messinian–Pliocene portion of the standard scale and to improve its event basis are grounded on the introduction of type boundaries (limitotypes), which correspond to standard synchronization levels with their physical age objectively evaluated and recognizable based on close biological reference points.[1] Four biogeomagnetic limitotypes of this kind were suggested by the RCMNS to be a basis for depicting new boundaries of the Upper Neogene stages. I myself applied a similar biogeomagnetic method of stratigraphic synchronization long ago and in 1974 suggested the composite Pontic–Caspian scheme, where the specific units *seasons* were used to correlate sections characterized by paleomagnetic parameters. Under this term, I understood "...biomagnetostratigraphic subdivisions, where the magnetization polarity is predominantly of the opposite sign relative to the neighboring intervals, ... and rocks have individual paleontological characteristics... The combination of paleomagnetic and paleontological data *doubles* not only the reliability of correlation but also *doubles* the resolution potential of scale, allowing seven seasons to be distinguished instead of three–four biostratigraphic zones" (*Geokhronologiya SSSR...*, 1974, p. 284).

Actually, the biogeomagnetic limitotypes and seasons can be used in correlation practice only after a thorough biostratigraphic analysis and, what is particularly important, after the uninterrupted magnetostratigraphic subdivision of regional reference sections. Progress like this is now being achieved in the Mediterranean Neogene stratigraphy reviewed in many publications (Zubakov and Borzenkova, 1983; Berggren *et al.*, 1985, 1995; Semenenko, 1987; Zubakov, 1990; Hilgen, 1991; Benson and Rakis-El Bied, 1991a, 1991b). During the Soviet period, the Pliocene stratigraphy of the Pontic–Caspian region was also elaborated to a high level. The continuous paleomagnetic subdivision of sections in regions of the Black and Caspian seas was a routine procedure at that time. Therefore, the Pontic–Caspian region is ready more than any other for section subdivision based on selected biomagnetostratigraphic type boundaries like those in the Mediterranean region.

What is the essence of the new practice of substantiating stages based on biogeomagnetic limitotypes? In this case, we advance further in recognition from registration units, which require the stratotype (geological body) of the taxon range (these were, in fact, the Pontic–Caspian regional stages and units of the Mediterranean scale prior to their last revision), to correlation units, where only the boundaries representing synchronization signals are important (e.g., *Ritmostratigraficheskie podrazdeleniya*, 1978, p. 26). For instance, the Messinian regional stage was previously considered as a synonym of the evaporite–diatomite formation known only in the Mediterranean basin. At present, in terms of limitotype, it is the event-stratigraphic unit of the standard scale, which recorded global consequences of the maximum shield glaciation in Antarctica and Patagonia. About 25 years ago, researchers discussed which of two events, the Maud Rise Glaciation or Messinian Salinity Crisis, was the cause and which was the consequence (Ryan *et al.*, 1974); but now, when both events are well dated and studied, the responsibility of the Messinian crisis for shield glaciation in the southern hemisphere is beyond question (see below).

Similarly, the Zanclean transgression, which was thought to be related only to strike-slip tectonic movements within the Alboran plate (ideas of 1973), is now interpreted in terms of global event stratigraphy, as a global interglacial glacioeustatic transgression.

The modern standard stratigraphic scale empirically acquires the event content primarily because of the parallel development of particularly specialized stratigraphic classifications and scales, such as magneto- and climatostratigraphic scales, and, naturally, of different biozonations. For instance, there is rapid progress in the development of astronomical–climatic scales. They first represented an empirical tool that appeared in the form of oxygen-isotope stages recognized after investigation of deep-water sediments by isotopic methods. At present, the scale includes more than 100 stages corresponding to orbital cycles by Milankovitch, which are 100000, 40000, and 20000 years long and can now be measured by using astronomical methods. A real breakthrough in Pliocene rhythmostratigraphy is the discovery and analysis of eccentricity rhythms lasting 413000 years. Mathematical calculation of changes in the Earth's orbital parameters (precession, axis inclination relative to the ecliptic, and eccentricity) during the past 500 m.y., i.e., as far back as to the Ordovician, was performed recently by Berger *et al.* (1982) and showed that only the eccen-

[1] The term limitotype was proposed by H. Erban in 1971 (*Ritmostratigraficheskie podrazdeleniya*, 1978); the concept, but not the term itself, is widely used in the RCMNS materials.

tricity rhythms (100000, 413000, and 1200000 years long) remained almost invariable in the past.

It is essential that these rhythms are manifested in moisture variations and that, consequently, they are in genetic relation with changes in oceanic circulation. It is not incidental that all biozones are aliquot parts of eccentricity rhythms. In my previous article (Zubakov, 1999), I showed that, during the last 7 m.y., organic life responded to climatic changes by recurrent regular phases of cycles 413000 years long. This is an appropriate basis for elaborating the astronomically calibrated climatic scale of the Messinian–Pliocene interval, i.e., for metering the "inner clocks of the biosphere," where organic life responds to globally synchronous climatic–hydrological changes. Elements of the aforementioned cycle ("superclimathem") can now serve as an independent criterion for global correlation.

There are even more exciting possibilities. As is known, the eccentricity variations substantially change the amplitude of precession rhythms, which control, via monsoon rainfalls and Nile discharge, sapropel accumulation in the Mediterranean basin. Based on this mechanism, Hilgen (1991a, 1991b) developed a method for astronomical–climatic dating of sapropel horizons with the accuracy of 1000–2000 years. Taken together, the empirical method of biomagnetic limitotypes and astronomical–climatic dating represent a tool for interregional correlation of high precision. This methodological basis is a promising elaboration of the uniform standard stratigraphic scale of global events of the Messinian–Pliocene interval.

2. DATA FOR GENERAL COMPARISON OF THE TRADITIONAL PONTIC–CASPIAN STRATIGRAPHIC SCALE WITH STANDARD PLIOCENE STAGES OF THE MEDITERRANEAN

Due to limited space in the article, the graphic form is most appropriate for presentation of results of the comparative analysis. Fig. 1 demonstrates the most representative Miocene–Pliocene reference section of the Pontic–Caspian region, which is subdivided into paleomagnetic zones, and where limitotypes are established for three of the four stages under consideration. The section is located between the Panagiya and Zheleznyi Rog (near Zelenskii) capes on the southern coast of the Taman' Peninsula; below it is referred to as the Taman' section. The paleomagnetic study of opposite limbs of a single syncline was carried out between 1978 and 1981 (Semenenko and Pevzner, 1979; Ananova *et al.*, 1985; unfortunately, results of the first work are published only in a graphic and very generalized form: see Fig. 14 in Semenenko, 1987). Nevertheless, one can see in both cases the almost identical Kimmerian successions with four ore horizons and a hiatus spanning the interval of *Moquicardium* Beds with *Paradacna deformis* and also the Pontian regiostage divided into Odessa and Bosporus horizons, which are separated by a hiatus corresponding to the interval of Portafer Beds with *Congeria subrhomboidea*. Both hiatuses (Fig. 1) coincide with section intervals of normal polarity. However, paleomagnetic interpretation of the Taman' section assumes two versions.

According to the first of them, Chron 5 is correlative with the *Moquicardium* Beds, whereas according to the second one, it spans the interval of Portafer Beds. Semenenko and Pevzner (1979) accepted the first variant. In different periods of my activity, I supported different viewpoints. Initially, I was disposed toward the second one, because it easily explains why V.M. Trubikhin and A.L. Chepalyga (see Muratov and Nevesskaya, 1986) correlated the so-called "condensed Pontian" with the lower part of the Matuyama Chron in the Romanian sections, where the hiatus is at the level of Chron 5 and the Portafer Beds. Reasoning in this manner, I plotted Fig. 2, where the interpretation of magnetic zones proposed by Veklich (1982) for the magnificent section of the Crimean thrust formation near the settlement of Lyubimovka is changed and the pedological Sevastopol' complex is significantly wider in range. Later, however, I preferred another variant (Fig. 1); and now I believe that the Bel'bek loess (Fig. 2, column VI) should be at the level of Chron 5, but not at that of Chron 7. Nonetheless, there are insufficient data to correctly place Chron 5 in sections of the Black Sea region. It is not incidental that Chumakov (2000), who quoted my Figure 2 from this article and, choosing the second interpretation, correlated the Portafer Beds with Chron 5. In Fig. 3, the principal one for the present article, I show both variants for the Black Sea region.

Now, let us turn to a comparison of the Pontic–Caspian and Mediterranean schemes. In order to demonstrate the event–climatic essence of the Mediterranean stage standard, Fig. 3 includes two other regional schemes: one for the western Atlantic with adjacent areas of North America and Antarctica, and another characteristic of Iceland. In these regions, the interval of geological history between 7.5 and 1.8 Ma is distinctly divided into three epochs corresponding to two shield glaciations in the southern and northern hemispheres, which were separated by the interglacial period. The time limits of these glaciations (necessary dates are rather abundant now) accords with the special climatostratigraphic scale I calibrated on the basis of astronomical calculations by Berger (1992), and also with the soil–loess scale of Ukraine (Veklich, 1982), both shown in the right side of the figure. Correlation of all events will be considered below after analysis of the ranges and boundaries of stratigraphic units of the Pontic–Caspian and Mediterranean scales.

A comparison of both scales leads to the following conclusions: (1) The Pontian Stage in the Black Sea regional scale is the initial one of the Pliocene, whereas the Messinian, its probable analogue in the Mediterranean scale, is the terminal unit of the Miocene. (2) According to the first variant, the difference between

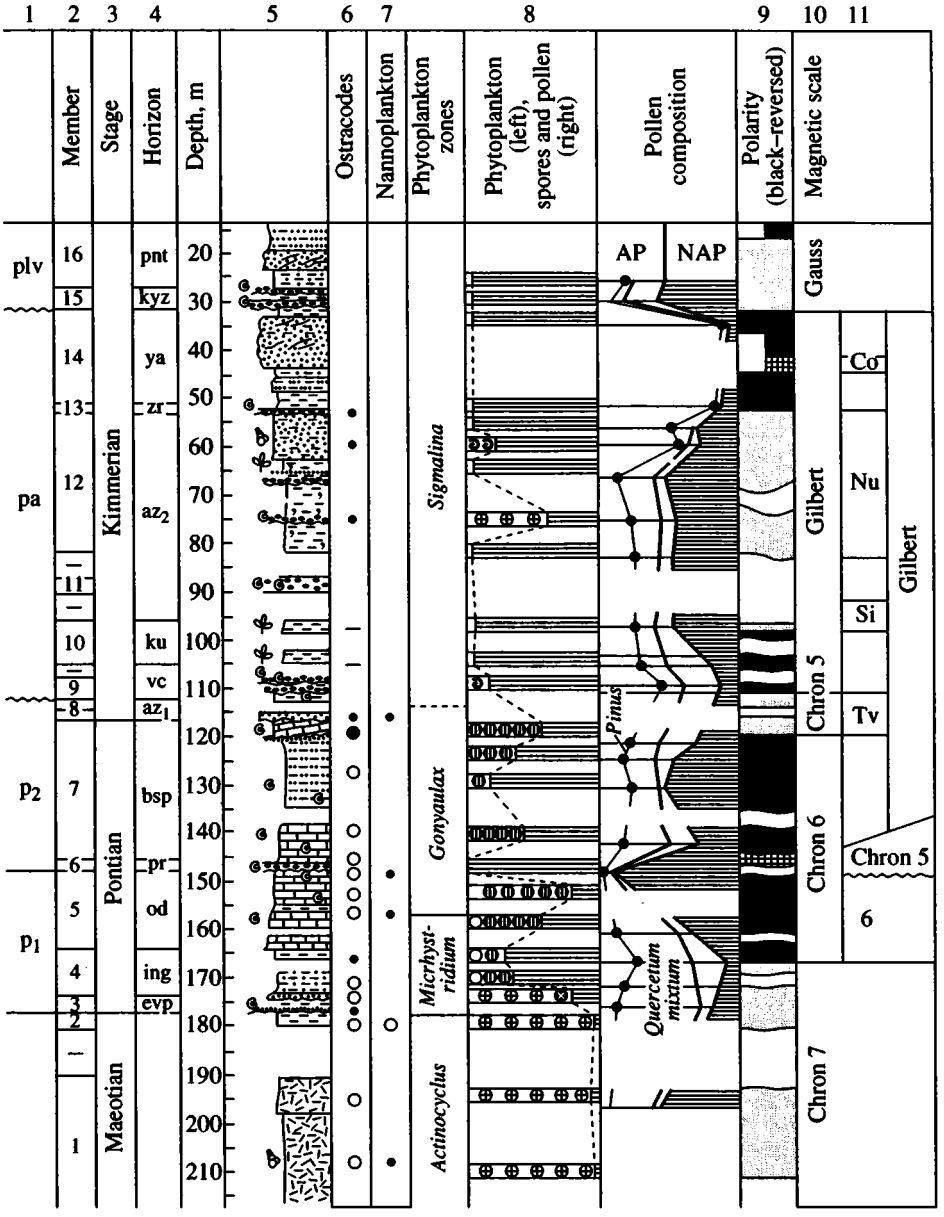

Fig. 1. The section near the Kutrya Ravine illustrating the proposed limitotypes of the Black Sea regional analogues of four stages in the Miocene–Pliocene standard scale. (1) Black Sea regional analogues of the Mediterranean standard stages, namely (p_1) upper Tortonian Pontian ("Novorossiisk"), (p_2) Messinian Pontian with (pa) Panagian regional stage (= Gelasian Stage) and (plv) Polovetsian regional stage (= Piacenzian Stage). (2) Member nos. in the section after Zubakov (see Ananova *et al.*, 1985). (3) Regional stages of the traditional Russian scale. (4) Horizons and beds: (evp) Evpatoriya climatic horizon with *Abra* and *Parvenius* forms, Tortonian phytoplankton, and pollen of *Quercus* and *Zelkova*; (ing) Ingulets climatic horizon with erratic pebbles, dinoflagellates, and coniferous pollen (cooling event); (od) Odessa climatic horizon with *Valenciennius* sp. and last *Micrhystridium* species; (pr) Portafer climatic horizon with *Congeria subromboidea* and erosional hiatus; bsp, Bosporus climatic horizon with *Paradacna abichi*; (az_1) basal Azov ferruginous sands; (mc) *Moquicardium* Beds with *P. deformis*; ku, Kutrya Beds with foraminifers and macroremains of aqueous plants; (az_2) upper Azov (Panagian) Beds with Zanclean immigrants; (zr) Zheleznyi Rog Beds (erosion event); (ya) amber sands and varves with *Pinus* pollen (cooling event); (kyz) Kyzaul ore-beach horizon with coquina of thermophilic mollusks (erosion event); pnt, Pantikapei Beds. (5) Lithology (symbols as in Fig. 2) and the depth of stripping, m. (6) Ostracodes after V.I. Pavlovskaya (Ananova *et al.*, 1985). (7) Nanoplankton after M.G. Ushakova and S.A. Lyul'eva (see text). (8) Phytoplankton (acritarchs), spores, and pollen after E.N. Ananova. (9) Magnetic polarity zones after V.I. Remizovskii. (10) First variant of interpretation (ultimate). (11) Second variant of interpretation (preliminary).

ranges of the Pontian Stage in the Caspian and Black Sea regions is 1.4 m.y. (3) The Kimmerian regional stage corresponds to two, or even three (in the first variant), stages of the Mediterranean scale; i.e., from the point of view of event stratigraphy, it represents an eclectic stratigraphic taxon. (4) The Akchagylian

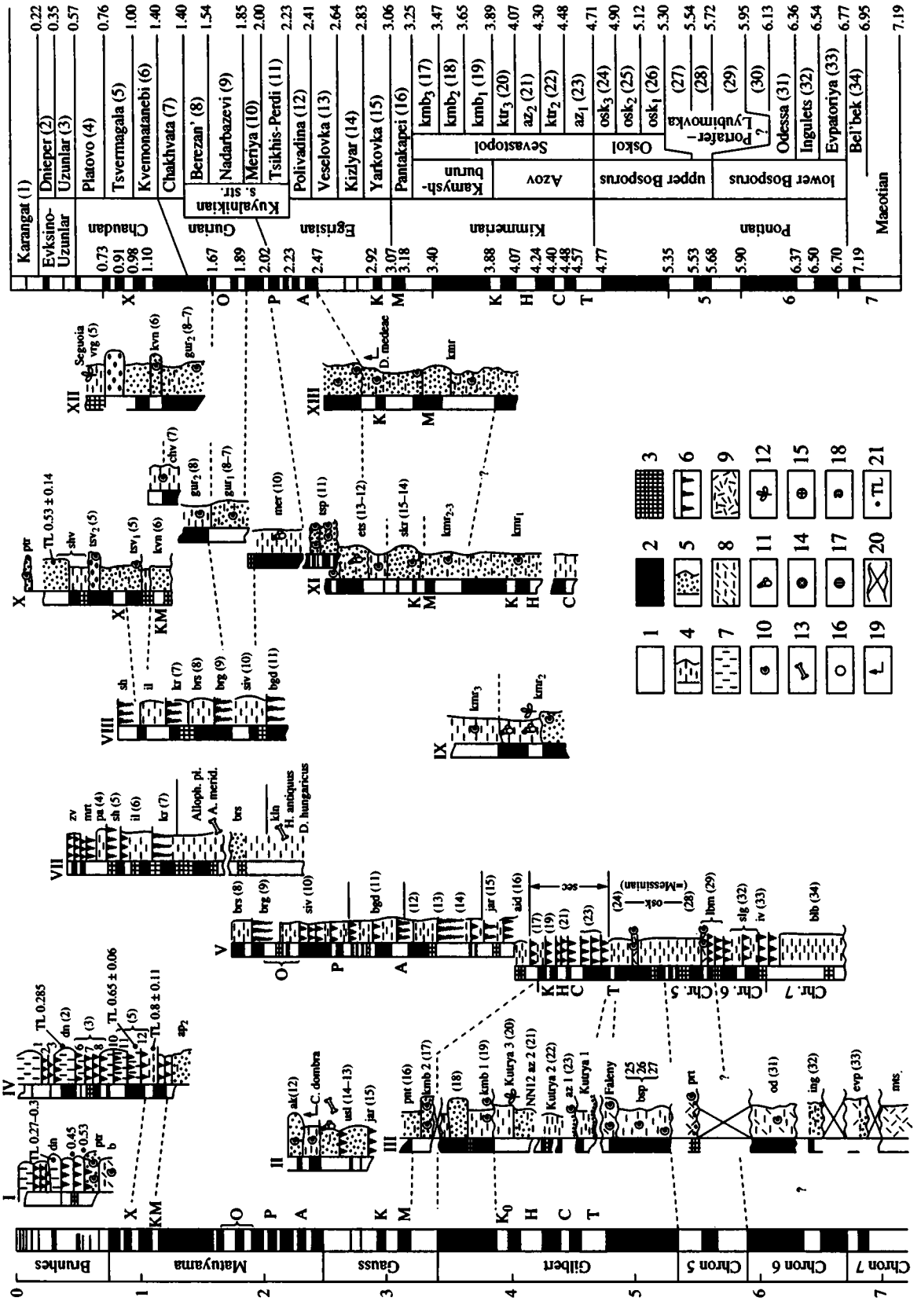
Karangat (1)
Dnieper (2)
Uzunlar (3)
Platovo (4)
Tsvermagala (5)
Kvemonatanebi (6)
Chakhvata (7)
Berezan' (8)
Nadarbazevi (9)
Meriya (10)
Tsikhis-Perdi (11)
Polivadina (12)
Veselovka (13)
Kizlyar (14)
Yarkovka (15)
Pantakapei (16)
Evksino-Uzunlar
Chaudan
Gurian
Kuyalnikian s. str.
Egrisian
Kimmerian
Karamysh-burun
Azov
Sevastopol
upper Bosporus
Oskol
lower Bosporus
Portaferr–Lyubimovka
Pontian
Maeotian
Brunhes
Matuyama
Gauss
Gilbert
Chron 5
Chron 6
Chron 7

regional stage corresponds to the entire Pliocene of the Mediterranean scale. (5) The Kuyalnikian, like the Egrisian regional stage (Taktakishvili, 1984) spans the upper half of the Piacenzian and the lower half of the Gelasian. (6) The registration–historical essence of regional stages of the Pontic–Caspian scale does not correspond to the event–correlation significance of the last four Neogene stages in the standard stratigraphic scale, and this is an obstacle to correct understanding of stratigraphic information that is coded by respective indices of traditional Russian regional stages in publications and maps.

The situation implies that fundamental revision of the Russian Pontic–Caspian regional scale is unavoidable. The question is, in what manner should it be revised? Should we replace our stratigraphic taxons with the unified Mediterranean, now global, stages and accept their nomenclature? Or would it be better to keep our own regional Pontic–Caspian stages, though with new limitotypes approaching as closely as possible to those of the Mediterranean scale? I prefer the second way. It is clear that when calibrating our regional stages on the basis of geomagnetic reversals authorized by the RCMNS we must correlate them simultaneously with the local Pontic–Caspian events and outline local biological reference points. Thus, a certain disagreement between the Pontic–Caspian subdivisions and Mediterranean standard units is unavoidable in any correlation scheme. One thing is important here—the disagreement should be insignificant and acceptable from the practical standpoint. In other words, the unique geological history of the Pontic–Caspian region should be inset into the global succession of bio-magneto-climatic-hydrologic events in order to obtain a satisfying correlation scheme.

3. EVENT CORRELATION OF PONTIC-CASPIAN, MEDITERRANEAN AND NORTH ATLANTIC REGIONS WITHIN THE TIME INTERVAL 7.5–1.7 Ma

The suggested correlation is based on four bio-magneto-stratigraphic limitotypes selected to represent the lower boundaries of four stages in the international stratigraphic scale. In Fig. 3, they are shown by thick arrows.

Pontian–Messinian Correlation

In 1979, a commission headed by M. Colalongo proposed to consider the first event of cryophilic fauna migration into the Mediterranean Sea as marking the base of the Messinian Stage (the event is recorded, for instance, by the appearance of foraminifer species *Globorotalia conomiozea* in the Falconaria section of Sicily). The proposal was approved by the RCMNS. This limitotype corresponds to the appearance level of the ostracod assemblage with *Agrenocythere pliocenica*, which coincides with the middle of Chron 6n in the Bou-Regreg section of Morocco (Benson *et al.*, 1991a, b). At present, Chron 6, whose base and top are dated back to 7.37 and 6.93 Ma, respectively, is subdivided into Subchrons $6n_1$, $6n_2$, and $6n_3$ (Berggren *et al.*, 1995). Therefore, when radiometric data are taken into consideration, the age of the lower Messinian boundary must be estimated as ranging from 7.1 to 7.26 Ma.

These dates are younger than those restricting the age of the Maud Rise Glaciation that initiated, according to my compilations (Zubakov and Borzenkova, 1983, 1990; Zubakov, 1990), not later than 7.4 Ma. The Patagonian glaciation followed this event 6.5 Ma ago during superclimathem 32 (Mercer and Sutter, 1982). Thus, the "Messinian Salinity Crisis," as D. Rio called the process of salt evaporation in the drying Messinian basin, which was particularly intense during the second half of the Gauss Chron, is 0.6 and 1.3 Ma younger than the Patagonian and Maud Rise glaciations, respectively. Consequently, the salinity crisis could not be a response to these glaciations as was previously thought (Ryan *et al.*, 1974). According to computer simulations, the volume of the Antarctica ice shield exceeded the present one by a factor of 1.8 during the Patagonian glaciation peak. According to Mayewski (1975), the value corresponds a sea-level drop of 108 m (the current ice volume in the Antarctica is equal to an ocean-wide water layer of 59 m).

The late Tortonian basin was connected with the Atlantic via two wide, though shallow (about 100–50 m) Rif and Betic seaways (the depth of the Strait of Gibraltar is 300 m). Therefore, isolation of the Mediterranean Sea and its transformation into the closed Lago Mare could have happened without tectonic movements.

Fig. 2. Paleomagnetic data for Pliocene reference sections on the Black Sea coast (Zubakov, 1990). Interpretation of magnetic polarity zones according to the second variant (Fig. 1). Polarity: (1) normal, (2) reversed, (3) anomalous. Lithology: (4) clay, (5) sand, (6) buried soil, (7) loess, (8) limestone, (9) diatomite. Organic remains: (10) marine mollusks, (11) freshwater mollusks, (12) plant detritus, (13) mammals, (14) dinoflagellates, (15) marine diatoms, (16) phytoplankton of the *Micrhystridium* genus characteristic of the Tortonian and Tripoli Formation, (17) phytoplankton characteristic of the Messinian, (18) freshwater phytoplankton of the *Sigmalina* genus characteristic of the Pliocene, (19) first occurrence level; (20) erosion; (21) thermoluminescence dates. Samples studied by V.V. Kochegura and V.I. Remizovskii.

Reference sections: Taman' (Zubakov, 1990): (I) Tuzla Cape, (II) Veselovka–Polivadina Ravine, (III) Panagiya Cape–Zheleznyi Rog, (IV) Tsokur Liman, Crimea and Odessa (Veklich, 1982; Tret'yak *et al.*, 1987; Zubakov, 1990): (V) Beregovka, (VI) Lyubimovka, (VII) Kryzhanovka; Crimea and Abkhaziya (Zubakov, 1990): (VIII) Kamyshburun, (IX) Duaba; Georgia (Zubakov, 1990): (X) Tsvermagala, (XI) Gogoreti and Meriya, (XII) Gora River, (XIII) Khvarbeti; (XIV) climatic horizons and their numbers (in brackets); (XV) estimated age, Ma (Zubakov, 1990).

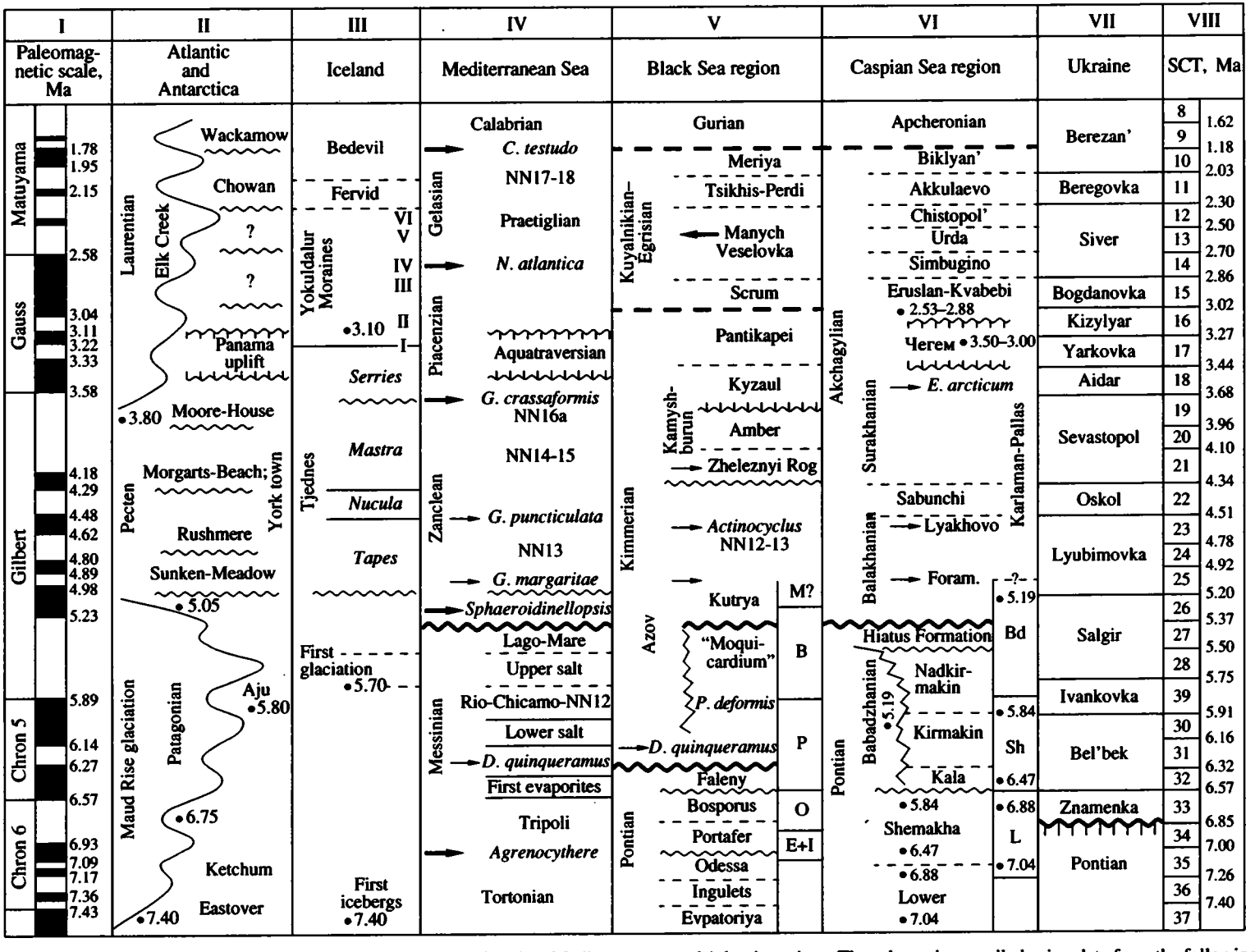

Fig. 3. Correlated magnetic–climatostratigraphic events in the Pontic–Caspian, Mediterranean, and Atlantic regions. The scheme is compiled using data from the following works: (I) Berggren *et al.*, 1995; (II) Cronin, 1991a; Coats *et al.*, 1992; Hodell and Warnke, 1991; Dowsett *et al.*, 1994; Krantz, 1991; Mayewski, 1975; Mercer and Sutter, 1982; Webb and Harwood, 1991; (III) Gladenkov *et al.*, 1978; Cronin, 1991b; Einarsson *et al.*, 1967, 1978; (IV) Berggren *et al.*, 1985, 1995, Catalano *et al.*, 1978; Cita, 1976, 1979; Cita and Colombo, 1979; Cita and Corselli, 1990; Müller and Schrader, 1989; Rio *et al.*, 1984, 1994; Ryan *et al.*, 1974; Selli *et al.*, 1975; Suc and Zagwijn, 1983; Steininger and Papp, 1979, Chumakov, 1974; (V) Muratov and Nevesskaya, 1986; Zubakov, 1990; Semenenko, 1987; Taktakishvili, 1984; (VI) Muratov and Nevesskaya, 1986; Nevesskaya and Trubikhin, 1984; Alizade *et al.*, 1972; Bludorova *et al.*, 1985; Zhidovinov *et al.*, 1995; Zubakov, 1990; Zubakov and Kochegura, 1971; Ismail-Zade *et al.*, 1967; Trubikhin, 1977; Yakhimovich *et al.*, 1981, 1984; (VII) Veklich, 1982, Pevzner, 1986; Tret'yak *et al.*, 1987; (VIII) Zubakov, 1990, 2000; Zubakov and Borzenkova, 1990.

According to the first version considered above, the base of the Pontian stage in the Taman' section is placed inside Chron 7 (Fig. 1); and thus, the Ingulets cooling, when the northern part of the Pontian sea, as was established long ago (Andrusov, 1928, 1965), was covered by ice in winter, appears to be synchronous with the beginning of the Maud Rise glaciation 7.43 Ma ago.

The Evpatoriya, Ingulets, and probably Odessa horizons (the *Tortonian Pontian* in Fig. 4) should be included, according to this variant, in the Maeotian, but not in the Pontian, Stage. In the second variant (Fig. 3), the base of the Pontian exactly corresponds to Subchron 6n, whereas the fission-track dates obtained for the lower Pontian of the Caspian region (7.04–6.88 Ma; Chumakov *et al.*, 1992) are close in age to this subchron. Thus, the problem of the Messinian boundaries in the Pontic–Caspian region cannot yet be solved unambiguously. Most likely, the limitotype of 7.1–7.2 Ma approved by the RCMNS (Berggren *et al.*, 1995) corresponds to the base of the Portafer Beds, which span three or four climathems in Mingrelya (Taktakishvili, 1984). However, it is still necessary to show that they correspond to Subchron 6n. Nonetheless, I believe that the polarity reversal between Chrons 6 and 7, which is 7.43 Ma old and coincided with the Ingulets cooling or with the beginning of the Maud Rise glaciation and mountainous glaciation in Greenland, is of great significance for planetary event correlation.

The first half of the Messinian terminates with the so-called "transit phase" of the Atlantic nanoplankton assemblage with *Discoaster quinqueramus* (Zone NN 11). Benson *et al.*, (1991) correlate this event with the beginning of Subchron 5r (6.27–6.14 Ma), whose entire range corresponds to SCT 31. This species was supposedly distinguished (see below) by S.A. Lyul'eva in samples collected by me from the lower Azov ore horizon, i.e., in the exactly coeval layer (Fig. 1, Member 9), where the Mediterranean *Sigmalina* genus of phytoplankton also makes its first appearance (Ananova *et al.*, 1985). It is important that this stratigraphic interval, which I refer, following Gabuniya (1948), to the *Moquicardium* Beds, is above the Bosporus Pontian Stage, being separated from the latter by ferruginous sands overlying the Faleny Horizon and characterized, similarly to the latter, by normal polarity. The occurrence of *D. quinqueramus* and first *Sigmalina* forms at the base of the *Moquicardium* Beds, which are washed out of the Taman' section, is consistent with the first variant of the interpretation (Fig. 1). In contrast, this event is absolutely incompatible with the second variant, according to which *D. quinqueramus* should be found under the Bosporus Beds (see in Benson *et al.*). Chumakov (2000) tries to find a way out by using the hypothesis of long survival of *D. quinqueramus* in the Pliocene. In this case, however, it is necessary to assume that this zonal (NN 11) species survived till the Thvera Subchron 4.98 Ma ago. In contrast to the generally accepted date, this 900000-year-long delay in extinction of *D. quinqueramus* is difficult to imagine, particularly when we take into account that the second half of the Messinian corresponds already to Zone NN 12, where the index species is *C. tricorniculatus*.

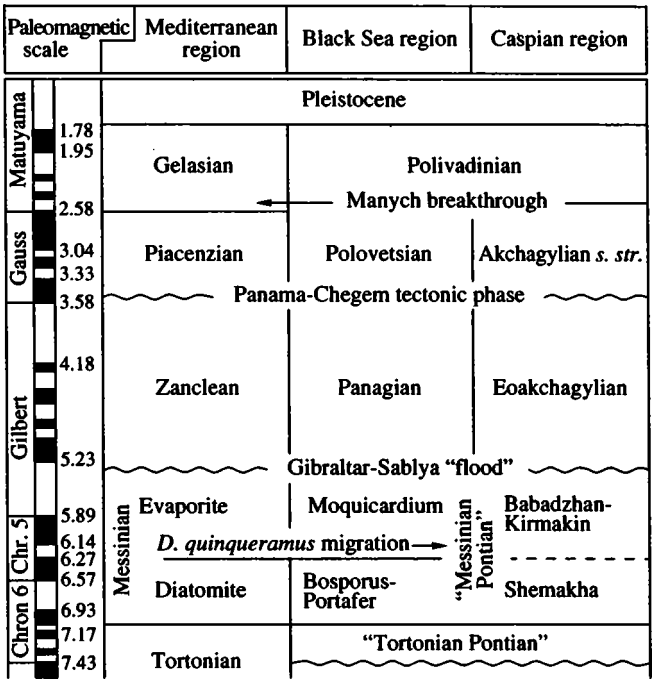

Fig. 4. Proposed regional stages of the Pontic–Caspian region and their correlation with stages of the standard stratigraphic scale (compiled using the first variant of interpretation of paleomagnetic chrons, Fig. 1).

The evaporite portion of the Messinian Stage comprises an interval from SCT 30 to SCT 28. The other half of the Messinian (between 600 and 700 ka) is represented only by the Gessososolifera Formation displaying the rhythmic alternation of the following rock types: marine sediments with foraminifers (*Globigerina multiloba* included); wattenschlick with desiccation cracks; beach pebblestone; stromatolite mats; salt and gypsum horizons with selenite crystals; shallow-water marl with Pannonian–Pontian fauna, including ostracods *Cyprideis djaffarovi* and mollusks of *Congeria, Limnocardium, Dreissena*, and other genera; and deep water marl bearing benthic foraminifers *Elphidium* and *Ammonia*, brachiopods *Terebratulina*, and the stenohaline sea grass *Posidonia oceanica*, which dwells at a depth of 30 m and never occurs in a redeposited state. According to Catalano *et al.* (1978), all these indications suggest an intermittent water influx from the Atlantic Ocean, the periodic draining of the basin, and its subsequent filling with freshened (salinity of 5–10 to 20‰) waters from the Pannonian and Pontian basins, which also periodically drained.

There are 11 cyclothems distinguished as corresponding to 41-kyr glacial–interglacial cycles. They are

recorded in two evaporite horizons (evidently corresponding to cryogenic SCT 30 and 28), which are divided by deep-water Rio-Chicamo diatomite formation with the Atlantic fauna including corals (Müller and Schrader, 1989). The top of these interglacial beds with normal polarity encloses remains of mammals of the Turolian type (site Krivelente 6), which allows these sediments to be correlated with the warm SCT 29. The sea level was 25 m higher at that time compared with the present one, as it is evident from the K–Ar age for palagonite in lavas from the Barranco volcano (the Aju site, Canary Islands), whose flows reached the shore (Meco and Stearns, 1981).

What was the ocean's response to the Messinian Salinity Crisis? As was correctly noted before (Ryan *et al.*, 1974), about 6% of the total salt volume from the water mass of the Messinian basins was evaporated during the time interval 500–700 ka. This stimulated processes of sea ice formation and, thus, resulted in a sharp acceleration of the Antarctica and Patagonia glaciation. The event (SCT 28) corresponds to the second $\delta^{13}C$ excursion in oceanic waters (the first one coincides with SCT 34).

Thus, the event stratigraphy of the Messinian and Pontian ages was controlled by the history of shield glaciation in the southern hemisphere. As is calculated, the Mediterranean Sea could dry up completely in a period as short as 1500 years; and within the period of 300–400 years, its level would fall by 500 m provided the sea was isolated (*Messinian Evaporites...*, 1978). The Messinian basin was 5–6 times shallower than the present-day Mediterranean Sea. Consequently, the intermittent renewal of water environs in the basin was possible only in the case of alternating water influx from the Atlantic (during interglacials) and Pontian (during glacials) basins. The influx from the latter is evident from the high bromine content in the evaporite horizons.

The aforesaid makes the event–stratigraphic correlation between Pontian and Messinian sections (Zubakov, 2000) understandable. The first Pontian ostracod assemblage in the Messinian basin is recorded at the base of Chron 5 in the Cuevas-del-Alman Zora, Fortuna, and Vera sections of Spain (Benson *et al.*, 1991a, 1991b), i.e., in the interval of SCT 32. If we follow the first correlation scheme, the respective beds are correlative to Faleny Horizon ostracod coquina of the Black Sea region, where it marks an erosion zone (Karmishina, 1975), whereas the second variant suggests their correlation with the lower Portafer Beds bearing *Congeria flexuosa*. Thus, both variants of correlation are acceptable. Abundant Pontian immigrants occurring in sections of Andalusia within the upper half of Chron 5 (SCT 30) are also explicable in both scenarios. As for the most abundant finds of Pontian fauna characteristic of the Lago Mare Formation corresponding to the Matuyama Chron, they are inexplicable in the second variant of the paleomagnetic data interpretation. According to the latter, the Pontian basin of that time (SCT 29 and 28) accumulated the well-preserved Bosporus Beds, whose thickness grew to a maximum in this period. According to the first variant, this time interval of the Pontian was characterized by accumulation of the *Moquicardium* Beds corresponding, on the contrary, to a period of maximum erosion.

Both variants appear to be applicable to correlation of the Pontian interval in the Caspian sections with the Messinian. At first glance, the second variant is more consistent with the Messinian geological history, being supported, in addition, by fission-track dating results (Chumakov *et al.*, 1982). However, paleomagnetic data conflict with both reported fission-track dates and, correspondingly, with this variant. According to paleomagnetic measurements (Ismail-Zade *et al.*, 1967), all five formations in the lower part of the productive complex of the Apsheron Peninsula reveal, as shown in Fig. 3, normal polarity (Chron 5) and rest on the Pontian strata with reversed magnetization. The Pontian should begin here with the Shemakha Horizon. Data indicating normal polarity of the horizon are still unknown.

The correlation performed between the Messinian and Pontian leads to the following conclusions:

(1) The Pontian regional stage is the only one in the Pontic–Caspian region that is more or less correlative with the Messinian Stage, provided that this regional stage includes the *Moquicardium* Beds of the Kimmerian, as was assumed long ago (Eberzin, 1940). The *Moquicardium* Beds known only in Abkhaziya (Gabunia, 1948) represent an equivalent of the evaporite formation that was eroded and redeposited in the Messinian basin.

(2) The unit-by-unit correlation of Pontian and Messinian intervals is now at the updating stage. Summing up the advantages and disadvantages of both variants of paleomagnetic interpretation of the Taman' section, I may state that the first one is preferable. In this case, however, the Pontian regional stage becomes 300–400 ka longer than the Messinian. This means that either almost the entire Novorossiisk Substage with *Micrhystridium* and *Cymatosphaera* genera of the Mediterranean phytoplankton (Fig. 1) should be excluded from the Pontian, or the RCMNS should make a decision and accept the reversal between Chrons 6 and 7 (7.43 Ma old) as the limitotype of the Messinian instead of the middle level of Chron 6n authorized now. This variant is favored by the fission-track date of 7.5 ± 0.45 Ma measured in tuff from the Tortonian–Messinian boundary layer in Sicily (Cita and Colombo, 1979).

(3) Prior to an ultimate choice between the considered variants of detailed event correlation for the Messinian and Pontian stages, it is necessary to undertake the following actions: (a) investigate the *Moquicardium* and Portafer sections in Abkhaziya using the bed-by-bed sampling method for paleomagnetic and nanoplankton analyses; (b) confirm or refute

the possible presence of the normal polarity zone at the top of the Maeotian (Fig. 1, interval of 160–195 m), which should be there according to the second correlation variant; and (c) confirm or refute the correlation between the Shemakha Beds and Chron 5, which is suggested in the second variant.

The Miocene–Pliocene Boundary in the Pontic–Caspian Region

Following the proposal by Cita (see Ryan *et al.*, 1974), the contact between the Trubi Formation in the Capo Rossello section of southern Sicily and erosion surface of the Arenazzolo alluvial sands is accepted to be the Miocene–Pliocene boundary. According to calculations by Hilgen (1991) based on an astronomically calibrated succession of climatic events, this boundary is dated back to 5.33–5.32 Ma. The formation period of the Arenazzolo Sands is estimated to be about 1500 years (? V.Z.). The Zanclean transgression commenced as early as the glacial period (SCT 26), when the narrow but deep (300 m) faulted trough of the Strait of Gibraltar was formed as a result of tectonic collision in inner areas of the Alboran plate. The initiated "flood" quickly leveled the water surface in the Messinian Basin and Atlantic Ocean for 26000 years. The lower glacial member accumulated during the Zanclean transgression (5.28 Ma old) corresponds to the *Sphaeroidinellopsis* Acme-Zone and is marked by the first occurrence of tropical foraminiferal species *Sphaeroidinellopsis dehistens*. The appearance of the latter seems to be paradoxical; but it is explicable, because the water temperature in the Messinian basin was higher than in the ocean, despite the fact that it was flooded during the glacial period.

Thus, the limitotype of the Zanclean Stage corresponds to a past hydrological event that occurred 110 k.y. prior to the early Thvera reversal (5.23 Ma). Of course, the Black Sea flooding could have been asynchronous with respect to the event recorded by the limitotype be the Capo-Rossello section, because the former could have been delayed due to the Tunisia–Sicily threshold as Cita and Colombo (1979) assumed. However, this is only a hypothesis. In the Caspian region, the boundary between pebblestone beds of the "Hiatus" Formation, the facies analogue of the Arenazzolo Sands in Sicily and Balkhan Formation in the productive deposits of the Apsheron Peninsula, also lies immediately under the base of the interval of the Cochiti–Thvera Subchrons (Zubakov, 1990, Fig. 5.2-2). Therefore, the Miocene–Pliocene boundary in the Black Sea region could also be distinguished as the "limitotype" of the event stratigraphy.

In his article, Chumakov (2000) writes that "the Miocene–Pliocene boundary in the Black Sea region is at the base of the Azov Beds of the Kimmerian Stage. The Azov Beds recorded events of the "instant" Zanclean transgression and surface leveling in the World Ocean and Mediterranean Sea..." Chumakov's analysis is wholly based on the Taman' reference section (Fig. 1). Discussing the buried soil that divides the Pontian and Kimmerian stages with a hiatus 100–150 ka long, he notes that shells of *P. deformis* rest on the soil surface but unfortunately does not specify the polarity sign of the deposits underlying the latter. As is seen from Fig. 1, the *Moquicardium* Beds transformed into soil (here I agree with Chumakov) rest upon the reversed/normal polarity boundary, i.e., on the erosion surface. Here, I should mention first that not only myself, but also Semenenko and Pevzner (1979), consider the normal polarity zone as representing Chron 5. Second, absolutely all researchers, beginning from Andrusov (1928, 1965), correlate the angular unconformity at the base of the Azov sands with the base of the Kimmerian Stage. In this section, these ferruginous sands overlying the Faleny Beds are less than 1 m thick, although there are sections where their thickness is up to few dozen meters. The aforementioned angular unconformity is located at the very base of Chron 5 and is, consequently, about 6.5 Ma old; i.e., it is 1.2 m.y. older than the Miocene–Pliocene boundary in the Capo Rossello section. If the normal polarity zone of the sands is considered as corresponding to the Thvera Subchron (the second possibility considered by Chumakov), the angular unconformity and, correspondingly, the base of the Kimmerian should be dated back to 5.1–5.15 Ma and would be 180000–230000 years younger. Accordingly, I conclude that the base of the Azov Beds cannot represent the required paralimitotype of the Miocene–Pliocene boundary in any case.

In my opinion, this status can be suggested for the base of the Kutrya Beds (Fig. 1, Member 10) overlying the buried ore soil with *P. deformis*. First, *Sigmalina* forms and *D. quinqueramus* occur either in or under this soil. Thus, the hiatus interrelated with the soil is not 100000–150000 years long as Chumakov believes but 800000. In the 20-m-thick Kutrya Beds, E.N. Ananova also found single specimens of *Sigmalina (Sigmopollis)*, a Zanclean phytoplankton from the Mediterranean region, which indicates the marine origin of the beds. The spore and pollen spectrum in the Kutrya Beds is rich in herbaceous (34–35%) and small-leaved arboreal (*Betula, Alnus, Salix*) pollen. The beds also yield macroremains of aquatic plants *Typha, Potomogeton*, and *Nuphar*. These data are consistent with the glacial age of the *Sphaeroidinellopsis* Acme-Zone in the Mediterranean region. Additional extremely important evidence in favor of marine origin of clay composing the Kutrya Beds was reported by Karmishina (1975, p. 30), who wrote when describing sections in the Kerch' Strait: "The Pontian–Kimmerian boundary layer of dark gray clay encloses abundant foraminifers *Bolivina aksaica* and more scarce *Elphidium stellatum* of the Akchagylian type in association with more widespread *Ammonia beccarii* and *Elphidium incertum*."

Back in 1975, the Zanclean water influx event into the Black Sea had not been even hypothesized. Deep-sea drilling in the Black Sea (Leg 42B) was conducted

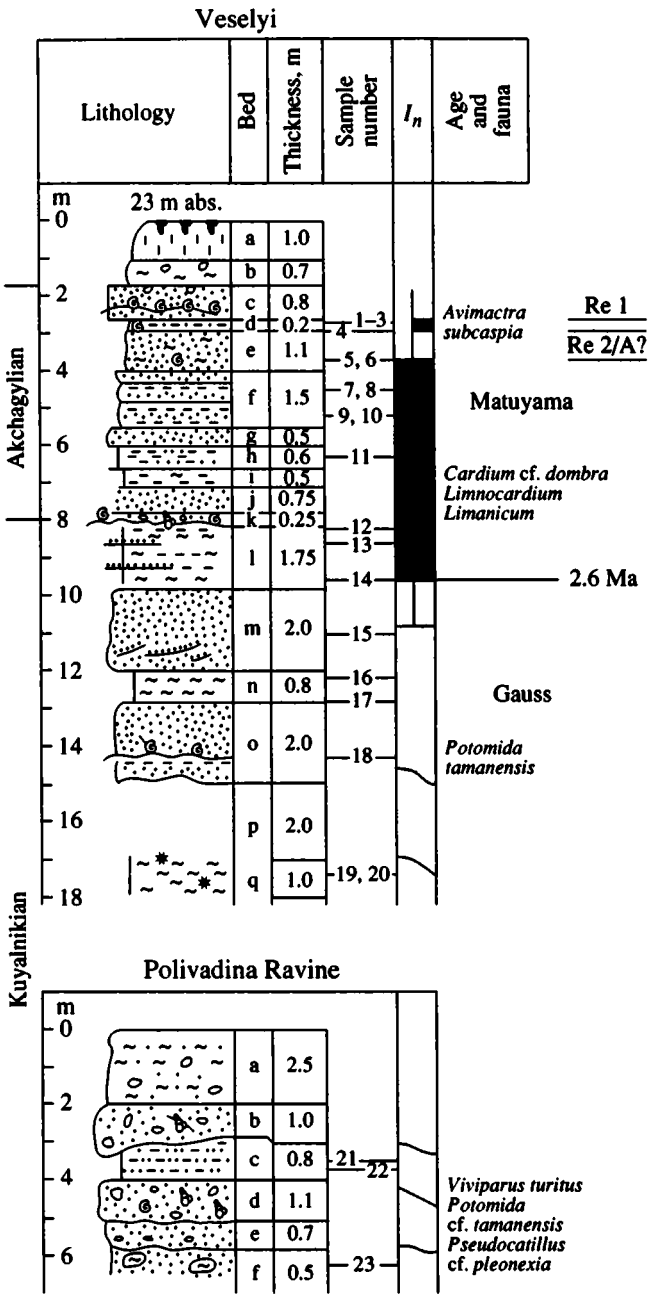

Fig. 5. The Akchagylian Reference section (stratotype of the Polivadian regional stage) in the Veselovka–Polivadina Ravine, Taman' Peninsula (data from *Geokhronologiya SSSR...*, 1974; symbols as in Fig. 2).

in 1977, and all the problems related to interpretation of its results, extremely ambiguous and requiring special consideration, appeared only in 1978 (Ross and Neprochnov, 1978; Hoe, 1978). Naturally, the hypothesis of fauna migration from the Caspian Sea was quite logical at that time. Nevertheless, I should emphasize that Karmishina was the first to discuss the idea of sea water ingression in the Black Sea region during the early Kimmerian.

Correlation between the Zanclean, Kimmerian, and Akchagylian Intervals

The first occurrence level of *Globorotalia margaritae* in the Mediterranean sections used to be correlated with the beginning of the glacioeustatic period of the Zanclean transgression (Ryan *et al.*, 1974). According to an astronomically calibrated climatic scale, this event was variably dated back to 5.97, 5.11, and 5.2 Ma (Hilgen, 1991; Berggren *et al.*, 1995). Duration of the eustatic wave at the time of transgression was 1.6 million years, thus spanning four cycles of the "link" rank.

What is the global succession of Zanclean events in the standard scale? In Antarctica, corresponding pebblestone beds with *Pecten* shells (*Chlamys andersoni, Ch. tuftsensis*, and others) are situated at about 600 m above the sea level. These deposits, as well as the *Sirius* moraine, are intruded by volcanic cones lacking ice abrasion signs and yielding K–Ar dates ranging from more than 4.2 to 3.7 Ma (Mayewski, 1975). In Patagonia, the ice shield was eliminated 5.05 Ma ago (Mercer and Sutter, 1982). Thus, the duration of the *Pecten Superinterglacial* was at least 1.35 m.y.

The sea level rise in response to thawing of the Antarctic ice shield is estimated to range from 44 (Orlemans, 1982) to 60–70 m (Haq *et al.*, 1987). In the Canary Islands, the relevant transgression is recorded in deposits bearing tropical mollusks *Strombus coronatus* and *Gryphaea virleti*, and overlying lava flows with the K–Ar date of 4.25 ± 0.44 Ma (Meco and Stearns, 1981). In the Tjednes Group of northern Iceland, corresponding deposits are represented by two zones with the southern Boreal genera *Tapes* and *Mactra*; zones hosting two coal seams are separated by the so-called "Bardarsson Cryomere" (Gladenkov, 1978).

Morphologically, the consequences of the event are best expressed on the North American coast, where the transgression left the enormous erosional Orangeburg or Yorktown Scarp 85 m high. According to American researchers, the scarp includes four terraces (Fig. 3), unfortunately of unknown age. Based on the faunal remains, Cronin (1991) estimated that the age could be 3 or 4 Ma, although, according to the revised chronology of biological reference points (Hilgen, 1991; Berggren *et al.*, 1995), it is at least 0.5 Ma older. For instance, the first occurrence of foraminifer species *Globorotalia puncticulata* is recorded at the levels of 4.55 Ma (Hilgen, 1991) and even 4.8 Ma, above the Sidufjall Subchron (Berggren *et al.*, 1995). This allows the four Yorktown levels to be correlated with SCT 25 (Sunken-Meadow terrace), 23 (Rushmere terrace), 21 (Morgarts-Beach terrace), and 19–17 (Moore-House terrace). Karmishina (1975), Lyul'eva (see Semenenko and Lyul'eva, 1982), and Ananova were first to recognize fossils indicative of the Zanclean transgression in the Black Sea sections. Ananova discovered the Mediterranean diatoms *Actinocyclus ehrenbergi* and phytoplankton form *Sigmalina* in samples collected by me from normally magnetized layers of the Taman' section

correlative with the Sidufjall Subchron (Fig. 1). Simultaneously, I donated to Lyul'eva, who worked together with Semenenko at that time, a large collection of samples (about a hundred). However, Semenenko has never informed me about the results of their study, which was published (Semenenko and Lyul'eva, 1982) without any reference to my collection and, naturally, without a precise stratigraphic allocation, although the published data were sensational. I would like to cite here how Semenenko (1987, p. 157) "allocated Lyul'eva's finds" in his book. He writes: "in Cape Zheleznyi Rog, the transition level from the Azov Horizon to the Kimmerian Kamyshburun strata, i.e., from the relatively deep- to shallow-water sediments marking the Kimmerian transgression, yielded characteristic nanofossils *Ceratolithus* ex gr. *acutus* Gartner et Bukry and *Ceratolithus* ex gr. *rugosus* Bruml. et Wilcoz." And nothing else is added. The section description, even if very schematic, or any graphic representation are missing, although the two nanofossil forms in question represent the guide species of the NN 12 and NN 13 zones and are extremely important for controlling the whole Kimmerian–Zanclean correlation. Fig. 14, the principal one in Semenenko's book, shows only indices "NN 11" and "NN 12–13" against an empty interval, where the section of Cape Zheleznyi Rog should be continued from the Pontian to Kimmerian.

Of course, I supplemented my collection with a section description where the polarity chrons were indicated and the index "NN 12–13" is placed almost correctly in Fig. 14 by Semenenko. Nonetheless, I should mention the following. The two guide forms of the indicated zones could have originated from the basal part of Member 12, where Ananova discovered the peak abundance of the Zanclean phytoplankton form *Sigmalina* and diatom *Actinocyclus eherenbergi*, i.e., from the interval of the Sidufjall, but not Thvera Subchron (this is clear from Fig. 1). In the ocean, the boundary between zones NN 12 and 13 was later dated back to 4.82 Ma by Rodde on the basis of K–Ar dates and thus correlated with the same Sidufjall Subchron (Berggren *et al.*, 1985).

One of the most enigmatic events in Caspian Sea history has been debated for over a century. This is the appearance of the Akchagylian fauna of distinct Mediterranean affinity in this closed basin. According to the opinion formulated long ago by Andrusov (1928, 1965) and now shared by the majority of Russian researchers, most decisively by Fedorov (1986), this fauna is autochthonous and represents the transformed Sarmatian and late Maeotian relics that survived the Pontian Age in refuges somewhere in the eastern Caspian region. The alternative hypothesis, according to which the Akchagylian fauna penetrated into the Caspian Sea from the Arctic via the Kama seaway, was initially (in 1936) proposed by Kovalevskii (1944) and recently supported by Yakhimovich *et al.* (1981, 1984) and Sidnev (1985). Based on finds of the brackish-water forms in the Van Lake area, Chepalyga put forward in 1980 a hypothesis of the "Turkish" route used by the Akchagylian fauna. According to this hypothesis, which was outlined in a brief manner (Zubakov, 1990; Zubakov and Borzenkova, 1990), scarce initial elements of the Akchagylian fauna represented Zanclean immigrants that penetrated into the Black Sea during the early Kimmerian via the formerly existing Kuban'–Terek seaway. I suggest naming it the Sablya seaway after the Sablya River, a tributary of the Kuma River, where Lebedeva (1978) described the Akchagylian section in the Kuban'–Kuma interfluve at an altitude of 200 m. Now, this hypothesis can be substantiated by the event correlation in a vast region from the Atlantic coast to the Ufa estuary.

Thus, the large *Pecten*–Yorktown-Zanclean interglacial period includes four eustatic phases corresponding to the 413-ka-long eccentricity cycles. Peaks of these phases coincide with small interglacials of the Tyrrhenian (Eemian) type (Zubakov, 1999). Correlation of these four phases in the west–east direction is given below (Fig. 3).

The first phase corresponding to the SCT 25 of link-type cycling (Zubakov, 1999) is dated as the middle one of the Thvera Subchron (5.08–5.07 Ma); in other words, it coincides with the first occurrence level of *Globorotalia margaritae* in the Mediterranean sections. In the Atlantic, it is represented by the Sunken-Meadow terrace, whose age is estimated to be 5.1–4.8 Ma (Krantz, 1991), and corresponds to the basal part of the *Tapes* Zone (underlain by lava that yielded the K–Ar date of 5.3 Ma). In the Black Sea region, the event is recorded in sediments bearing foraminifers *Cassidulinita prima* and *Bolivina aksaica* (Karmishina, 1975) and in Member 11 of the Azov Horizon, the upper ore–beach site (Fig. 1). In the Caspian region, the first eustatic phase corresponds to the middle of the Balakhna Formation, where, according to available data (Alizade *et al.*, 1972; Karmishina (1975), the freshwater Pontian fauna is replaced by the brackish-water Akchagylian fauna with benthic foraminifers of the *Bolivina, Cassidulina,* and *Ammonia* genera and also with ostracods of the *Prolimnocythere* (*P. tenuireticulata* and others), *Aglaiocypris, Caspiollina, Liventalina, Citherissa,* and other genera.

Ananova and Lyul'eva first established the second eustatic phase that is marked by index species of the NN 13 Zone in the Black Sea region. Later, I named it the Panagian transgression. In the Atlantic region, the phase corresponds to the level of the Rushmere terrace, whereas in the Caspian region, it is correlated with the Pallas–Karlaman transgression. The commencement of the phase corresponds to the Sidufjall Subchron, and its cessation is attributed to the first half of the Nunivak Subchron (4.8–4.55 Ma). Probably, SCT 23 corresponds to the period when mollusks of the *Cardium, Avimactra, Clessiniola,* and *Potamides* genera penetrated into the Caspian Sea and formed the ancestral core of the Akchagylian fauna (Chel'tsov, 1968; Mura-

tov and Nevesskaya, 1986; Danukalova, 1990). The peculiar "*Clessiniola*" assemblage is characteristic of deposits accumulated during the first stage of the Pallas transgression (Zhidovinov *et al.*, 1995). It is important that the commencement of the Karlaman transgression in the northern Caspian region corresponds exactly to the Sidufjall and Nunivak subchrons, as established in the Nikolaevka and Lyakhovo borehole sections.

Consequently, it is clear that organisms related to the Zanclean transgression reached the Urals region not later than 4.8 Ma ago. Some data indicate that the opening of the Bering Strait and the phenomenal invasion of Pacific fauna into the North Atlantic via the ice-free Arctic Ocean happened within the normal-polarity interval of the Nunivak Subchron (Gladenkov *et al.*, 1991). In other words, the SCT 23 represents a thermal peak of the early Pliocene transgression and, correspondingly, of the entire Antarctic *Pecten–Sirius* Interglacial (Webb and Harwood, 1991). This conclusion is also favored by the maximum decrease in the frequency of the Kharmatan winds that transported dust from the Sahara to the Atlantic Ocean at that time (Tiedemann *et al.*, 1994). The estuarine zone of Mediterranean basins of the Zanclean time extended along the Kinel' valley to Bashkortostan.

The third phase of the eustatic transgression (SCT 21) corresponding to the Cochiti Subchron (4.29–4.18 Ma) is marked by the foraminiferal species *Globorotalia puncticulata*, whose first occurrence level in oceanic sections is dated back to 4.55 Ma (Hilgen, 1991). *Globorotalia puncticulata* is characteristic of the North Atlantic water mass and indicates a significant temperature drop in the Atlantic during the SCT 22. The "Bardarsson Cryomere" or *Nucula* Zone of the Tjednes Group in Iceland (Gladenkov, 1978) is evidently related to this cooling. In North America, this phase is marked by the origin of the Morgarts-Beach terrace; and in Iceland, it corresponds to the base of the *Mactra* Zone. In the Black Sea region, the phase is correlative with the Zheleznyi Rog (First Kamyshburun) Horizon of the Taman' section (Fig. 1, Member 13), where I.M. Gubkin found *Cardium* sp. amid abundant molluscan fauna. The inference is indirectly supported by the occurrence of *Cerastoderma dombra* in the upper member of the Pallas Formation stratotype penetrated by Borehole 40 in the northern Caspian region (Zhidovinov *et al.*, 1995).

The last, less distinct phase of the Yorktown–Zanclean transgression responsible for development of the 25-m-high Moore-House terrace on the American coast corresponds to the interval inside which the limitotype of the Piacenzian Stage is distinguished. In the Black Sea region, this event is recorded at the top of the Kamyshburun ore horizon (Fig. 1, Member 15) resting on the erosion surface of sediments corresponding to the Gauss–Matuyama reversal (3.58 Ma). The paleontological characteristic of the horizon is equivocal. The composition of the molluscan assemblage (20 species, *Didacna ponticapaeae* and *D. tamanensis* included) and species gigantism reveal the thermophilic affinity of this fauna. However, the *Pinus–Picea* type of spore and pollen spectrum indicates, in the opinion of Ananova (1985), a cooling event. All these data provide grounds to consider the fourth eustatic phase of the early Pliocene transgression as spanning a significant time interval with a transition climate (SCT 19, 18, and 17; 3.96–3.27 Ma). Once in the last superclimathem, evidently not later than 3.5 Ma ago, the Caspian region welcomed "northern guests:" Boreal foraminifers *Cribroelphidium heterocameratum* Volosh., *Elphidium arcticum* Cushman, and *Globigerina* sp.; ostracods *Leptocythere litica* Liv., *Limnocythere vara* Liep., and others; and sea grass species *Zostera nana* (Yakhimovich *et al.*, 1981, p. 47). Evidently, this was a time when seals could penetrate into the Caspian Sea. Climatic cooling is also evident from the first occurrence of pollen and spores of mountain tundra plants in the upper Karlaman Beds of Bashkortostan. In my opinion, this was SCT 18 (or 16), whereas in the scheme by Veklich (1982), the event is named the Aidar cooling.

Let us summarize the results of the Zanclean–Akchagylian correlation. Sections in all the considered areas (Atlantic, Black Sea, and Caspian regions) reveal an interval about 1.6 m.y. long corresponding to the Yorktown transgression in the United States coast and to the *Pecten–Sirius* transgression recorded on the Antarctic coast. The rhythmic structure of this immense interstadial (two cycles 826 ka long and four 413 ka long) is recorded in oceanic and continental sections. For instance, according to Suc and Zagwijn (1983), the Brunssumian Phytoage, whose whole range corresponds to the Zanclean Stage, is divisible like the Tjednes Group into two parts separated by the Brunssum cooling event. A similar sequence of events is recorded in the loess–soil formation of Ukraine (Veklich, 1982), where the Lyubimovka and Sevastopol' complexes of buried soils are divided by the Oskol loess (Fig. 3), as shown by paleomagnetic data (Tret'yak *et al.*, 1987). One can hypothesize that, in the Caspian region, the 826-ka-long cycles are reflected in the lithology of the Akchagylian part of the productive deposits and their Sabuncha Formation most likely corresponds to the cryogenic SCT. In general, the Zanclean Age corresponds in the Caspian region to the Karlaman (Yakhimovich *et al.*, 1981) and Pallas (Zhidovinov *et al.*, 1995) transgressions. I call this Akchagylian interval the *Eoakchagylian*. It seems that this name is most convenient in terms of nomenclature succession. Simultaneously, I propose to call an analogue of the Zanclean Stage in the Black Sea region the Panagian regional stage and to accept the base of the Kutrya Beds in the Taman' section as representing the limitotype of the latter (Fig. 1).

A Possible Analogue of the Piacenzian Stage in the Pontic–Caspian Region

Since the criteria and principles of subdivision of the Akchagylian, Kimmerian, and Kuyalnikian regional stages are vague, the idea of distinguishing analogues of the Piacenzian and Gelasian stages in the Pontic–Caspian region is particularly important. The RCMNS selected the Gilbert–Gauss magnetic reversal (3.58 Ma) marking the first occurrence level of the cold-resistant foraminifer *Globorotalia crassaformis* in the Mediterranean Sea as the type boundary of the updated Piacenzian Stage. The indicated event is now dated back to 3.6 Ma (Berggren *et al.*, 1995). The respective boundary is nearly at the base of the *Serripes* Zone in the Tjednes Group, which includes Sceif lavas (the interval of reversed magnetization) attributable either to the Matuyama Chron (Einarsson *et al.*, 1967) or to the Mammoth Subchron (Cronin, 1991b; the entire section becomes 0.5 m.y. younger in this case). The *Serripes groenlandicus* Zone yields the molluscan species that migrated into the ice-free Arctic basin during the SCT 23 via the opened Bering Strait and one million years later reached Iceland and England.

In the scale of "links" (Zubakov, 1990, 1999), the limitotype of the Piacenzian Stage coincides with the cryogenic SCT 18 (3.68–3.52 Ma) that activated glaciation in the southern hemisphere (Scott glaciation) and resulted in the advance of piedmont glaciers toward Viedma Lake in the Patagonian Andes (Mercer and Sutter, 1982). Data from the northern hemisphere point to the commencement of permanent glaciation in the Wrangel mountainous massif (see review in Zubakov, 1990; Zubakov and Borzenkova, 1990) and Greenland. This event in the northern hemisphere appears to be related to a phase of tectonic uplift in the Alpine–Himalayan belt, which was most intense in the Pliocene (Khain and Balukhovskii, 1993). It is also important that, during the thermal SCT 17 (3.5 Ma ago), the Panama Isthmus closed (Coats *et al.*, 1992), and the event changed the whole system of deep oceanic circulation. This considerably activated the Gulf Stream and also the cold Labrador and Irminger countercurrents. The increased climatic contrasts in the North Atlantic favored ice sheet growth. The overall uplift in the Alpine system, particularly in the Himalayas and Tibet, drastically changed the atmospheric circulation between 3.5 and 3.0 Ma and provoked monsoon activity.

Thus, the essence of the Piacenzian Age consisted in active tectonic events and enhanced global atmospheric and oceanic circulation, whose patterns are quite well reviewed by Barash *et al.*, (1989, pp. 244–249). In the Mediterranean, this tectonic phase is known as the Acquatraversan Phase, which lasted from 3.5 to 2.5 Ma (Azzaroli *et al.*, 1983), whereas in the Caucasus, it is termed the Chegem tectonic phase dated by M.M. Arakelyants back to the period of 3.5–3.0 to 2.2 Ma (*Geokhronologiya SSSR*, 1974). Lava extrusions and activation of erosion-related mud-flow processes resulted in the closure of the Sablya Seaway not later than 3.5 Ma ago. As a result, the Caspian basin, a former gulf of the Mediterranean Sea, turned into spacious brackish-water lake that existed for about one million years.

I suggest restricting the event analogues of the Piacenzian Stage in the Pontic–Caspian region to the limitotype corresponding to the level of the Gilbert–Gauss magnetic reversal (3.58 Ma). The base of the Kyzaul (Second Kamyshburun) Horizon in the easily accessible coastal Taman' section located between Panagiya and Zheleznyi Rog capes (Fig. 1, Member 15) may represent the limitotype of the Piacenzian Stage in the Black Sea region. This unit is proposed to be termed the Polovetsian regional stage, which would comprise the upper part of the Kimmerian and the lower part of the Kuyalnikian (Egrisian) regional stages together with the Veselovka Beds. For the Caspian region, it would be useful to keep the name Akchagylian *s. str.* for the coeval regional stage, if it would be possible to avoid confusion with the Akchagylian regional series of the Neogene.

A Possible Analogue of the Gelasian Stage in the Pontic–Caspian region

The upper part of the Piacenzian Stage was proposed by RCMNS to be considered as the autonomous Gelasian (after Gela in Sicily) Stage, the third one in the standard Pliocene scale. Its type boundary corresponds to the Gauss–Matuyama magnetic reversal in the Sante-Nicolo section (Rio *et al.*, 1984, 1994). This limitotype recorded penetration of *Neogloboquadrina atlantica* into the Mediterranean Sea dated 2.72 Ma ago (Hilgen, 1991). The main event of the stage consists in a transition to shield glaciation in the northern hemisphere.

I suggest the *Polivadinian regional stage* (named after the Polivadina Ravine near the settlement of Veselovka in the Taman' Peninsula) as an analogue of the Gelasian Stage in the Pontic–Caspian region. The Polivadina Ravine section includes the so-called "Akchagylian of Taman'" (Eberzin, 1940) and shows records of the onset of the Manych drainage event in the Caspian Sea.

During its million-year-long isolation, the Caspian Sea increased in dimensions by factor of 2 or 3, and the "Lesser Akchagylian basin" that occupied an area in Turkmenistan around the Kopet-Dagh (Trubikhin, 1977) during the episode of the Kaena Subchron was then transformed into the "Greater Akchagylian basin" spread along the Kinel' River valley to the lower courses of the Kama River (Yakhimovich *et al.*, 1981; Bludorova and Filicheva, 1985; Sidnev, 1985). The lake level presumably rose 80–90 m above sea level (an exact estimate is impossible because of neotectonic dislocations). During this period, descendants of scarce Zanclean immigrants amid the Caspian mollusks and

microfauna evolved into the peculiar Akchagylian fauna (Chel'tsov, 1968), whose diversity was very low according to Danukalova (1990), who investigated these fossils.

Reaching the high level (80 or 90 m higher than before), the Greater Akchagylian lake (sea basin) broke through the meridional Zunda–Tolga uplift that served as a watershed between rivers flowing along the Manych depression into the Black and Caspian seas. The timing of the Manych breakthrough was estimated by me together with V.V. Kochegura using the paleomagnetic data on the Veselovka–Polivadina Ravine section (Fig. 5), the best Akchagylian section in the Black Sea region (*Geokhronologiya SSSR...*, 1974). The first occurrence level of *Cardium dombra*, which marks the onset of Caspian water penetration into the Black Sea, is recorded here 1.5 m above the Gauss–Matuyama reversal. This allows us to date the breakthrough of Caspian waters, using the sedimentation rate calculated relative to the overlying interval of normal polarity (attributable either to the Reunion or Argentina subchrons), as an event that happened 2.490 ± 40 ka ago (calibration versus the updated scale). As a result of the breakthrough, the level of the Caspian basin gradually lowered, although it was almost two times greater in dimensions and included areas of the Black and Aegean seas, because deposits in northern coastal areas of the latter yielded the typical Akchagylian fauna (Muratov and Nevesskaya, 1986; Semenenko, 1987).

CONCLUSION

(1) The analyzed data on the problem under consideration showed that the traditional Pliocene subdivisions (stages and horizons) of the Pontic–Caspian region are incompatible with standard units of the late Neogene scale approved by the RCMNS.

(2) In their state of knowledge, as well as in the level of detailed and complex magneto-bio-chronometric subdivision, the reference sections of the Pontic–Caspian region are as good as the Mediterranean ones; and the Pontic–Caspian regional scale based on same event-bio-magnetic principles can easily be incorporated into the Neogene standard stratigraphic scale (Fig. 4).

(3) The Pontian regional stage is the only one in the Pontic–Caspian region that represents an almost complete analogue of the Messinian Stage, provided that it also includes the *Moquicardium* Beds of the Kimmerian. Nonetheless, the unit-by-unit correlation of the regional Pontian stage and standard Messinian stage is still ambiguous and should be verified. The base of the Portafer Beds in Abkhaziya most likely corresponds to the Messinian limitotype (Chron 6n), but this requires substantiation as well.

(4) The Miocene–Pliocene boundary approved by the RCMNS as coinciding with the base of the *Sphaeroidinellopsis* Acme-Zone (5.32 Ma) corresponds in the Black Sea region to the base of the Kutrya Beds bearing foraminifers and unconformably overlying the erosion surface of the normally magnetized *Moquicardium* Beds with *Paradacna deformis* and (?) *Discoaster quinqueramus*. Naturally, the conclusion needs further testing.

(5) The problem of correlation of the Pontic–Caspian sequences with three stages of the standard Pliocene scale can be solved only if three regional stages, namely, the Panagian–Eoakchagylian, Polovetsian, and Polivadinian (names are conditional), are introduced as regional analogues of the Zanclean, Piacenzian, and Gelasian stages, respectively. Type boundaries of these regional stages can be established in the easily accessible sections of the Taman' Peninsula.

(6) The event-bio-geomagnetic correlation of four glacioeustatic phases of the immense Early Pliocene transgression spread from the Atlantic coast to Bashkortostan helps solve the problem of the Akchagylian fauna origin and puts forward the problem of depicting the shape and evolution of the Sablya (Kuban'–Terek) Seaway, which was an important part of the Mediterranean basin during the Zanclean time.

ACKNOWLEDGMENTS

The work was supported by the George Soros Foundation (grant MT-9000), the Russian Foundation for Basic Research (project 97-058-65545), and by the Joint George Soros and RFBR Foundation (grant MT-9300).

Reviewer Yu.B. Gladenkov

REFERENCES

Alizade, K.A., Asadullaev, E.M., Pashaly, N.V., *et al.*, The Pliocene and Quaternary Systems, in *Geologiya SSSR, T. 47: Azerbaidzhanskaya SSR* (The Geology of the USSR, vol. 47: Azerbaijani SSR), Moscow: Nedra, 1972, pp. 178–203.

Ananova, E.N., Volkova, N.S., Zubakov, V.A., *et al.*, New Data on the Mio-Pliocene Reference Section near Taman', Black Sea Region, *Dokl. Akad. Nauk SSSR*, 1985, vol. 284, no. 4, pp. 925–928.

Andrusov, N.I., Recent Studies on Pliocene Deposits in Southern Russia, *Azerb. Neft. Khoz.*, 1928, nos. 6–7.

Andrusov, N.I., *Izbrannye trudy* (Selected Works), 3 vols., Moscow: Akad. Nauk SSSR, 1961–1965.

Barash, M.S., Blyum, N.S., Burmistrova, I.I., *et al.*, *Neogen-chetvertichnaya paleookeanologiya* (The Neogene–Quaternary Paleoceanology), Moscow: Nauka, 1989.

Benson, R.H. and Rakis-El Bied, R., Biodynamics, Saline Giants, and Late Miocene Catastrophism, *Carbonates and Evaporites*, 1991a, vol. 6, no. 2, pp. 127–168.

Benson, R.H., Rakis-El Bied, K., and Bonaduce, G., An Important Current Reversal in the Riftian Corridor at the Tortonian–Messinian Boundary, *Paleoceanography*, 1991b, vol. 6, no. 1, pp. 164–192.

Berger, A., Loutre, M.F., and Laskar, J., Stability of the Astronomical Frequencies over the Earth's History for Paleoclimate Studies, *Science*, 1992, vol. 255, pp. 560–565.

Berggren, W.A., Kent, D.V., Swisher, C.C., and Aubry, M.-P., A Revised Cenozoic Geochronology and Chronostratigraphy, *SEPM*, 1995, no. 54, pp. 129–211.

Berggren, W.A., Kent, D.V., and Van Couvering, L.A., The Neogene. Chronology of the Geological Record, *Mem. Geol. Soc. London*, 1985, no. 10, pp. 141–260.

Bludorova, E.A. and Filicheva, N.L., *Opornye razrezy Kazanskogo Povolzh'ya* (Reference Sections in the Volga Region near Kazan), Kazan: Kazan Univ., 1985.

Chel'tsov, Yu.G., On the Phylogeny of Akchagylian Cardidae and Mactridae, in *Tr. XII Ses. Vses. Paleontol. O–va* (Proc. XII Conference Vses. Paleontol. Society), Leningrad: Nauka, 1968, pp. 73–81.

Chumakov, I.S., Lower Miocene of the Mediterranean Sea as the Facies of an Instant Transgression, *Byull. Mosk. O–va Ispyt. Prir., Otd. Geol.*, 1974, vol. 49, no. 2, pp. 1–144.

Chumakov, I.S., *Stratigr.. Geol. Korrelyatsiya* (in press).

Chumakov, I.S., Byzova, S.L., and Ganzei, S.S., *Geokhronologiya i korrelyatsiya pozdnego kainozoya Paratetisa* (Late Cenozoic Geochronology and Correlation of the Paratethys), Moscow: Nauka, 1992.

Cita, M.B., Planktonic Foraminiferal Biostratigraphy of the Mediterranean Neogene, in *Progress in Micropaleontology*, New York, 1976, pp. 47–68.

Cita, M.B., Lacustrine and Hypersaline Deposits in the Desiccated Mediterranean and Their Bearing on Paleoenvironment and Paleoecology, in *Deep Drilling Results in the Atlantic Ocean*, Washington, 1979, pp. 402–419.

Cita, M.B. and Colombo, L., Sedimentation in the Latest Messinian at Capo Rossello, *Sedimentology*, 1979, vol. 26, pp. 497–522.

Cita, M.B. and Corselli, C., Messinian Paleogeography and Erosional Surfaces in Italy: An Overview, *Palaeogeogr. Palaeoclimatol. Palaeoecol.*, 1990, vol. 77, pp. 67–82.

Coats, A.G., Jackson, J.B., Colling, L., *et al.*, Closure of the Isthmus of Panama, *Bull. Geol. Soc. Am.*, 1992, vol. 104, pp. 814–828.

Cronin, T.M., Late Neogene Marine Ostracoda from Tjornes, Iceland, *J. Paleontol.*, 1991a, vol. 65, no. 5, pp. 167–194.

Cronin, T.M., Pliocene Shallow Water Paleoceanography of the North Atlantic Ocean Based on Marine Ostracoda, *Quat. Sci. Rev.*, 1991b, vol. 10, nos. 2–3, pp. 87–106.

Danukalova, G.A., Bivalves and the Akchagylian Stratigraphy, *Abstract of Cand. Sci. (Geol.–Mineral.) Dissertation*, Moscow, Inst. of Paleontology, 1990.

Dowsett, H., Thompson, R., Barren, J., Cronin, T., *et al.*, Joint Investigation of the Middle Pliocene Climate: PRISM Paleoenvironmental Reconstructions, *Global and Planetary Change*, 1994, vol. 9, pp. 169–195.

Eberzin, A.G., Middle and Upper Pliocene of the Black Sea Region, in *Stratigrafiya SSSR* (Stratigraphy of the USSR), Moscow: Akad. Nauk SSSR, 1940, vol. 12, pp. 477–566.

Einarsson, T. and Albertsson, K., The Glacial History of Iceland during the Past Three Million Years, *Phil. Trans. R. Soc. London*, 1978, vol. 317, pp. 637–644.

Einarsson, T., Hopkins, D.M., and Doell, R.R., The Stratigraphy of Tjornes, Northern Iceland and the History of the Bering Land Bridge, in *The Bering Land Bridge*, Hopkins, D., Ed., Stanford, 1967, pp. 312–341.

Excursion Guidebook. The Neogene–Quaternary Boundary. II Symposium, Bologna, 1975, Selli, R., Ed., Bologna, 1975.

Fedorov, P.V., Problems Concerning the Akchagylian, in *Kontinental'nyi verkhnii pliotsen Chernomorsko-Kaspiiskoi oblasti* (Continental Upper Pliocene of the Black Sea–Caspian Area), Moscow: Nauka, 1986, pp. 69–76.

Gabuniya, L.K., The Azov Horizon in Guriya, *Izv. Akad. Nauk Gruz. SSR*, 1948, vol. 9, no. 1, pp. 42–44.

Geokhronologiya SSSR. T. 3. Noveishii etap (Geochronology of the USSR, vol. 3: Recent Epoch), Zubakov, V.A., Ed., Leningrad: Nedra, 1974.

Gladenkov, Yu.B., *Morskoi verkhnii kainozoi severnykh raionov* (Marine Upper Cenozoic of Northern Regions), Moscow: Nauka, 1978.

Gladenkov, Yu.B., Barinov, K.B., Basilian, A.B., and Cronin, T.M., Stratigraphy and Paleoceanography of Pliocene Deposition of Karaginsky Island, Eastern Kamchatka, *Quat. Sci. Rev.*, 1991, vol. 10, nos. 2/3, pp. 239–245.

Haq, B.U., Hardenbol, J., and Vail, P.R., Chronology of Fluctuating Sea Levels since the Triassic, *Science*, 1987, vol. 235, pp. 1156–1167.

Hilgen, F.J., Astronomical Calibration of Gauss to Matuyama Sapropels in the Mediterranean and Implication for the Geomagnetic Polarity Time Scale, *Earth Planet. Sci. Lett.*, 1991a, vol. 104, nos. 2/4, pp. 226–244.

Hilgen, F., Extensive Approximation of the Astronomically Calibrated Time Scale to the Miocene–Pliocene Boundary, *Earth Planet. Sci. Lett.*, 1991b, vol. 107, pp. 349–368.

Hodell, D.A. and Warnke, D.A., Climate Evolution of the Southern Ocean during the Pliocene Epoch from 4.8 to 2.6 Myr Ago, *Quat. Sci. Rev.*, 1991, vol. 10, nos. 2/3, pp. 205–214.

Hsü, K.J., Correlation of Black Sea Sequences, *Initial Rep. Deep Sea Drill. Project*, Washington: US Gov. Print. Off., 1978, vol. 42, part 2, pp. 482–497.

Ismail-Zade, T.A. and Aliev, A.I., Correlation of Middle Pliocene Sections of Oil-Bearing Deposits in Azerbaijan and Some Paleogeographic Problems, *Izv. Akad. Nauk Azerb. SSR. Ser. Nauk Zemle.*, 1967, nos. 3–4, pp. 151–160.

Karmishina, G.I., *Ostrakody pliotsena yuga Evropeiskoi chasti SSSR* (Pliocene Ostracods from the Southern Part of the European USSR), Saratov: Saratov Univ., 1975.

Khain, V.E. and Balukhovskii, A.N., *Istoricheskaya geotektonika. Mezozoi i kainozoi* (Historical Geotectonics: Mesozoic and Cenozoic), Moscow: Aviar, 1993.

Kovalevskii, S.A., The Great Akchagylian Transgression and Its Contribution to the Formation of the Oil-Producing Deposits, *Izv. Azerb. Fil. Akad. Nauk SSSR*, 1944, no. 5, pp. 11–27.

Krantz, D.E., A Chronology of Pliocene Sea-Level Fluctuations: the US Middle Atlantic Coastal Plain Record, *Quat. Sci. Rev.*, 1991, vol. 10, nos. 2–3, pp. 163–174.

Lebedeva, N.A., *Korrelyatsiya antropogenovykh tolshch Ponto-Kaspiya* (Correlation of Anthropogene Deposits in the Pontic–Caspian Region), Moscow: Nauka, 1978.

Mayewski, P.A., Glacial Geology and Late Cenozoic History of the Transantarctic Mountains, Antarctica, *Rep. Inst. Polar Studies*, 1975, no. 56, pp. 1–168.

Meco, J. and Stearn, C.E., Emergency of Littoral Deposits in the Eastern Canary Islands, *Quat. Res.*, 1981, vol. 15, no. 2, pp. 199–208.

Mercer, J.H. and Sutter, J.F., Late Miocene–Earliest Pliocene Glaciation in Southern Argentina, *Palaeogeogr. Palaeoclimatol. Palaeoecol.*, 1982, vol. 38, pp. 185–206.

Messinian Evaporites in the Mediterranean, Catalano, R., Ruggieri, G., and Sprovieri, R., Eds., *Mem. Geol. Soc. Ital.*, 1978, vol. 16, pp. 1–358.

Müller, D.W. and Schrader, H., Diatoms of the Fortuna Basin, Southern Spain: Evidence for the Intra-Messinian Inundation, *Paleoceanography*, 1989, vol. 4, no. 1, pp. 75–86.

Milanovskii, E.E. and Koronovskii, N.V., The Nizhnii Chegem Volcanic Region, *Vestn. Mosk. Univ., Ser. 4: Geol.*, 1969, no. 4, pp. 15–19.

Nevesskaya, L.A. and Trubikhin, V.M., Late Pliocene–Early Pleistocene History of the Caspian Basin and Its Molluscan Fauna, in *Antropogen Evrazii* (The Anthropogene of Eurasia), Moscow: Nauka, 1984, pp. 19–33.

Pevzner, M.A., Middle Miocene–Pliocene Stratigraphy of Southern Europe, *Abstract of Doctoral (Geol.-Mineral.) Dissertation*, Moscow, Inst. of Geology, 1986.

Rio, D., Sprovieri, R., and Di Stefano, E., The Gelasian Stage: A Proposal of a New Chronostratigraphic Unit of the Pliocene Series, *Riv. Ital. Paleontol. Stratigr.*, 1994, vol. 100, no. 1, pp. 103–124.

Rio, D., Sprovieri, R., and Thunell, R., Pliocene–Lower Pleistocene Chronostratigraphy: A Reevaluation of Type Sections, *Bull. Geol. Soc. Am.*, 1984, vol. 103, no. 8, pp. 1049–1058.

Ritmostratigraficheskie podrazdeleniya (Rhythmostratigraphic Units), Leningrad: Vses. Geol. Inst., 1978.

Ross, D.A., Neprochnov, Y.P., and Supko, P.R., *et al.*, *Initial Reports of Deep Sea Drilling Project*, Washington: US Gov. Print. Off., 1978, vol. 42, part. 2.

Ryan, W.B.F., Cita, M.B., Rawson, D.M., *et al.*, A Paleomagnetic Assignment of Neogene Stage Boundaries and the Development of Isochronous Datum Planes between the Mediterranean, the Pacific and Indian Oceans, *Riv. Ital. Paleontol. Stratigr.*, 1974, vol. 80, pp. 631–688.

Semenenko, V.N., *Stratigraficheskaya korrelyatsiya verkhnego miotsena i pliotsena Vostochnogo Paratetisa i Tetisa* (Stratigraphic Correlation between Upper Miocene and Pliocene Deposits of Eastern Paratethys and Tethys), Kiev: Naukova Dumka, 1987.

Semenenko, V.N. and Lyul'eva, S.A., *Problemy pryamoi korrelyatsii verkhnego miotsena* (Problems of Direct Correlation of Upper Miocene), Kiev: Naukova Dumka, 1982.

Semenenko, V.N. and Pevzner, M.A., Correlation of the Pontic–Caspian Upper Miocene and Pliocene Deposits by Biostratigraphic and Paleomagnetic Methods, *Izv. Akad. Nauk SSSR, Ser. Geol.*, 1979, no. 1, pp. 5–15.

Sidnev, A.V., *Istoriya razvitiya gidrograficheskoi seti pliotsena v Predural'e* (Pliocene History of the River System Development in the Urals Region), Moscow: Nauka, 1985.

Steininger, F.F. and Papp, A., Current Biostratigraphic and Radiometric Correlation of Late Miocene Central Paratethys Stages and Mediterranean Stages and the Messinian Event in the Paratethys, *Newslett. Stratigr.*, 1979, vol. 8, no. 2, pp. 100–110.

Stratigrafiya SSSR. Neogenovaya sistema (Stratigraphy of the USSR. The Neogene System), Muratov, M.V. and Nevesskaya, L.A., Eds., 2 vols., Moscow: Nedra, 1986.

Sue, J.-P. and Zagwijn, W.H., Plio-Pleistocene Correlations between the Northwestern Mediterranean Region and Northwestern Europe according to Recent Biostratigraphic and Paleoclimatic Data, *Boreas*, 1983, vol. 12, no. 3, pp. 153–166.

Taktakishvili, I.G., *Biostratigrafiya pliotsena Zapadnoi Gruzii* (Pliocene Biostratigraphy of Western Georgia), Tbilisi: Metsniereba, 1984.

Tiedemann, R., Sarnthein, M., and Shackleton, N.J., Astronomic Time Scale for the Pliocene Atlantic 18 and Dust Flux Records of Ocean Drilling Program Site 659, *Paleoceanography*, 1994, vol. 9, no. 4, pp. 619–638.

Tret'yak, A.N., Shevchenko, A.I., Dudkin, V.P., and Vigilyanskaya, L.I., *Paleomagnitnaya stratigrafiya opornykh razrezov pozdnego kainozoya yuga Ukrainy* (Paleomagnetic Stratigraphy of the Upper Cenozoic Reference Sections in Southern Ukraine), Kiev: Inst. Geofiz., 1987.

Trubikhin, V.M., *Paleomagnetizm i stratigrafiya akchagyl'skikh otlozhenii Zapadnoi Turkmenii* (Paleomagnetism and Stratigraphy of the Akchagylian Deposits in Western Turkmenistan), Moscow: Nauka, 1977.

Veklich, M.F., *Paleoetapnost' i stratotipy pochvennykh formatsii verkhnego kainozoya* (Upper Cenozoic Stages and Stratotypes of Soil Formations), Kiev: Naukova Dumka, 1982.

Webb, P.H. and Harwood, D.M., Late Cenozoic History of the Ross Embayment Antarctica, *Quat. Sci. Rev.*, 1991, vol. 10, nos. 2–3, pp. 215–233.

Yakhimovich, V.L., Nemkova, F.I., Suleimanova, L.K., *et al.*, *Pliotsen i pleistotsen Volgo-Ural'skoi oblasti* (The Pliocene and Pleistocene of the Volga–Urals Area), Moscow: Nauka, 1981.

Yakhimovich, V.L. and Suleimanova, F.I., The Pliocene–Lower Pleistocene Magnetostratigraphic Section in the Extraglacial Area of the Urals, *Byull. Komis. Izuch. Chetvert. Perioda*, 1984, no. 51, pp. 47–51.

Zhidovinov, N.Ya., Fedkovich, Z.N., and Kovalenko, N.D., New Data on Stratigraphy of the Upper Pliocene and Eopleistocene of the Lower Volga and Northern Caspian Sea Region, *Stratigr. Geol. Korrelyatsiya*, 1995, vol. 3, no. 1, pp. 73–80.

Zubakov, V.A., *Global'nye klimaticheskie sobytiya neogena* (The Global Neogene Climatic Events), Leningrad: Gidrometeoizdat, 1990.

Zubakov, V.A., *Vodn. Res.* (in press).

Zubakov, V.A. and Borzenkova, I.I., *Paleoklimaty pozdnego kainozoya* (Late Cenozoic Climates), Leningrad: Gidrometeoizdat, 1983.

Zubakov, V.A. and Borzenkova, I.I., Global Paleoclimate of the Late Cenozoic, in *Developments in Paleontology and Stratigraphy*, Amsterdam: Elsevier, 1990.

Zubakov, V.A. and Kochegura, V.V., Magnetostratigraphic Subdivision of the Middle–Upper Pliocene of the Apsheron Peninsula and Northern Ciscaucasia, *Problemy korrelyatsii noveishikh otlozhenii Severa Evropy* (Problems of Correlation of Recent Deposits in Northern Europe), Leningrad: Vses. Geogr. O-vo, 1971, pp. 3–12.

Stratigraphy and Geological Correlation, Vol. 8, No. 1, 2000, pp. 77–83. Translated from Stratigrafiya. Geologicheskaya Korrelyatsiya, Vol. 8, No. 1, 2000, pp. 83–89.
Original Russian Text Copyright © 2000 by Vangengeim, Pevzner.
English Translation Copyright © 2000 by MAIK "Nauka/Interperiodica" (Russia).

Biometric Dating of Elephants of the *Archidiskodon–Mammuthus* Lineage

E. A. Vangengeim and M. A. Pevzner

Geological Institute, Russian Academy of Sciences, Pyzhevskii per. 7, Moscow, 109017 Russia

Received May 13, 1998; in final form, June 29, 1998

Abstract—Using the biometric dating of lamellar frequency in the last upper molars of the *Archidiskodon–Mammuthus* elephant lineage, the age of the Liventsovka, Sinyaya Balka, Tiraspol' (Russia), Süssenborn, Mosbach (Germany), Ilford, Balderton (Great Britain), Dolni Vestonice, and Předmosti (Czech Republic) localities is determined. The localities are correlated with the oxygen-isotope stages and regional stratigraphic scales. The ^{14}C date of 29600 ± 600 years available for mammoth remains from the Balderton locality is concordant with the biometric age of this site.

Key words: *Europe, Pliocene, Quaternary, biometric dating, elephants of the mammoth lineage.*

INTRODUCTION

This work was aimed at absolute age determination by the biometric method using teeth of elephants of the *Archidiskodon–Mammuthus* phyletic lineage from a series of European localities. As indicated earlier (Pevzner and Vangengeim, 1994), the lamellar frequency in the 10-cm-long interval of the last upper molar is one of the evolutionarily important characteristics of elephants from this lineage. The time-dependent changes in this parameter develop according to the area cotangent law, permitting absolute age determination of bone remains and, consequently, of their host localities.

MATERIALS AND METHODS

Since the lamellar frequency is a highly variable parameter leading to an erroneous age determination, we consider only localities that yielded tooth series consisting of at least ten teeth (see the table). These localities are associated with different genetic types of deposits. For instance, the Liventsovka (Rostov region, Russia), Tiraspol' (Moldova), Süssenborn, Mosbach (Germany), Ilford, and Balderton (Great Britain) localities occur in alluvial sediments; the upper Paleolithic Dolni Vestonice and Předmosti (Czech Republic) sites are known in the sedimentary cover deposits; and the Sinyaya Balka locality (Krasnodar region, Tamanskii Peninsula, Russia) is buried in mudflow sediments. In some localities, we know the concrete lamellar parameter for each tooth, whereas only the extreme and mean values of this characteristic have been published in the literature for others. The mean value is supplemented in most cases with the mean square deviation.

Defects of the analyzed material consist of the following: first, we used tooth measurements made by different researchers, who used somewhat different methods; second, the degree of tooth wear, which strongly affects the minimum and mean characteristic values, is missing in almost all the publications. As a result, the mean lamellar parameters for teeth from the same collection studied by different authors are not identical. The lamellar frequency of strongly worn teeth is considerably lower than that of slightly worn specimens. Thus, the minimum and mean characteristic values used in the calculations turned out to be understated. Accordingly, in determining tooth ages by the biometric method, when data on degree of tooth wear are unavailable, the dates obtained should be considered as the maximum possible, i.e., not older than the estimated value.

Errors in determination of the mean parameter depend, on the one hand, on the number of measurements, and on the other, on the variability of the parameter itself. The great variability of the lamellar frequency of the studied elephants most likely results not only from intraspecific variability, but also from the fact that the measured tooth series represent heterochronous burials. The accumulation of mammal remains in the localities of alluvial sediments and Paleolithic sites could span a considerable time interval.

Liventsovka locality. We used the measurement results for 30 teeth of *Archidiskodon gromovi* from this locality, which have been kindly donated by Garutt (see the table).

Sinyaya Balka locality. The lamellar frequency values of *Archidiskodon meridionalis tamanensis* are calculated using the plot by Dubrovo (1963, Fig. 1).

Tiraspol' and Süssenborn localities. Dubrovo (1971, Table 11) reported only on the extreme and mean lamellar frequency values for *A. trogontherii*, missing data necessary for calculating the mean square

Lamellar frequency in the 10-cm-long interval of the upper last molars (M^3) of *Archidiskodon–Mammuthus* elephants and biometric ages of the studied localities

Locality	*n*	lim	$M \pm m$	δ	δ/M%	*T*	*k*
Liventsovka (1)	30	3.25–5.5	4.5 ± 0.09	0.48	10.67	2.419	+0.258 –0.223
Sinyaya Balka (2)	45	4.5–6.5	5.5 ± 0.08	0.53	9.64	0.947	+0.066 –0.060
Tiraspol' (3)	19	5.0–8.5	6.1 ± 0.15	0.65*		0.589	+0.072 –0.063
Süssenborn (3)	130	4.0–8.25	6.35 ± 0.06	0.67*		0.486	+0.022 –0.021
Mosbach (4)	14	5.9–8.3	7.11 ± 0.21	0.80	11.25	0.276	+0.047 –0.039
(5)	18	5.83–8.74	6.99 ± 0.16	0.66	9.44	0.302	+0.038 –0.034
Ilford (6)	11	7.6–9.6	8.7 ± 0.25	0.83	9.54	0.082	+0.019 –0.015
Dolni Vestonice (7)	26	7.4 ± 12.2	9.4 ± 0.22	1.12	11.91	0.044	+0.011 –0.009
Balderton (5)	19	7.67 ± 12.17	9.72 ± 0.29	1.25	12.86	0.032	+0.011 –0.009
Předmosti (8)	34	8.1 ± 12.3	9.89 ± 0.18	1.08	10.90	0.027	+0.006 –0.005
(7)	30	7.5 ± 11.9	9.60 ± 0.17	0.93	9.69		
(5)	43	7.61 ± 11.8	9.45 ± 0.15	1.01	10.69		

Note: *n* is number of teeth; lim is the extreme values of lamellar frequency; *M* is the mean value of lamellar frequency; *m* denotes the mean square error of *M* determination; δ is the mean square deviation of *M* values; *T* is age in Ma; and *k* is the mean square error of age determination in Ma (for explanations of figures marked by an asterisk, see the text). Data used for calculations are from the following sources: (1) measurements of V.E. Garutt; (2) Dubrovo (1963); (3) Dubrovo (1971); (4) Guenther (1968); (5) Lister and Brandon (1991); (6) Lister (1993); (7) Aver'yanov *et al.* (1995); (8) Musil (1968).

deviation (δ) and mean square error (*m*). For these localities, the mean square errors in age determination (*k*) presented in the table should be considered as most probable only. They are calculated from δ values (marked by asterisks in the table) using δ/M = 11.62%, which is the average value for all other localities.

Mosbach locality (major bone bed). Data on *A. trogontherii* are evaluated using the graph published by Guenther (1968, Fig. 4), who also presented values of LLQ index for 14 M^3 from the depth range of 12.5–18 m. We converted the index to a lamellar frequency in a tooth interval 10 cm long. The parameter obtained is similar to those of 18 teeth from this locality calculated by Lister and Brandon (1991, Table 1).

Ilford locality. The extreme and mean values together with the mean square errors are calculated for 11 teeth of *Mammuthus primigenius* using the graph of Lister (1993, Fig. 6).

Dolni Vestonice locality. The extreme and mean parameters for 26 teeth of *Mammuthus primigenius* and the mean square errors have been published by Aver'yanov *et al.* (1995), who discussed the measurement results of E.V. Urbanas.

Balderton locality. Lister and Brandon (1991) calculated the extreme and mean parameters together with δ value for 19 teeth of *M. primigenius* from this locality.

Předmosti locality. In this case, we used the measurement results (Musil, 1968,Table 43 a, b) for 34 out of 40 teeth of *M. primigenius*, which display a wearing degree of 1–(1–2)–(1–3)–(1–4) and have presumably been recovered from the major cultural bed. In our calculations, we ignored data on strongly worn teeth, which considerably understate the mean lamellar frequency value (M). For instance, M for 34 teeth is 9.89, but for 40 teeth, six strongly worn specimens included, this value decreases to 9.53.

Somewhat different data on mammoth teeth from the Předmosti locality were reported by Aver'yanov *et al.* (1995) and by Lister and Brandon (1991). The

extreme lamellar frequency values are similar in both publications, but lower than that estimated by Musil. Correspondingly, the mean parameter is also lower (see the table and Fig. 1). These understated values may indicate that strongly worn teeth were present in the analyzed series.

Data on the Liventsovka, Sinyaya Balka, and Předmosti localities (Fig. 2) were used as reference points for determining the locality positions on the area cotangent curve and for scale calibration along the X (time) and Y (morphological evolutionary parameter) axes.

An age of 2.4 Ma, the average between 2.6 Ma (the Gauss-Matuyama boundary) and 2.2 Ma (age of the Psekups locality), was adopted for the Liventsovka locality.[1] The mean parameter for this locality is 4.5. The Sinyaya Balka locality is dated back to 0.95 Ma, which corresponds to the mean age of the Taman' faunal assemblage (Vangengeim *et al.*, 1991); the respective mean parameter is 5.5. The cultural bed of the Předmosti site yielded the ^{14}C age of 26.5 ka (Svoboda, 1990); for this site, the mean parameter is 9.89.

Using the above data, we obtain the following formula:

$$T = 1.62\frac{0.141e^{0.623M}+1}{0.141e^{0.623M}-1} - 1.6427 \text{ m.y.},$$

which is used to calculate ages of localities (T) and the mean square age error (k) (see the table).

GEOLOGICAL POSITION OF LOCALITIES AND DISCUSSION

In general, the age determinations obtained by the biometric method agree with the present notion of stratigraphic succession of the studied localities.

The Liventsovka locality in a sandy quarry is on the right bank of the Don River in the neighborhood of Rostov-on-Don. The quarry exhibits the 20 to 25-m-thick sequence of gravelly, sandy, and clayey deposits of the high Don terrace, which overlie the Sarmatian limestones. Small mammal remains occur throughout the sequence (Aleksandrova, 1976); large mammal remains, including those of the elephants *Archidiskodon gromovi* Garutt et Alexeeva, are associated with the lower part of the alluvial sediments. The whole alluvial sequence is reversibly magnetized.

The Sinyaya Balka locality is situated on the northern coast of the Tamanskii Peninsula, 18 km west of Temryuk. Mammal remains, mainly those of the ele-

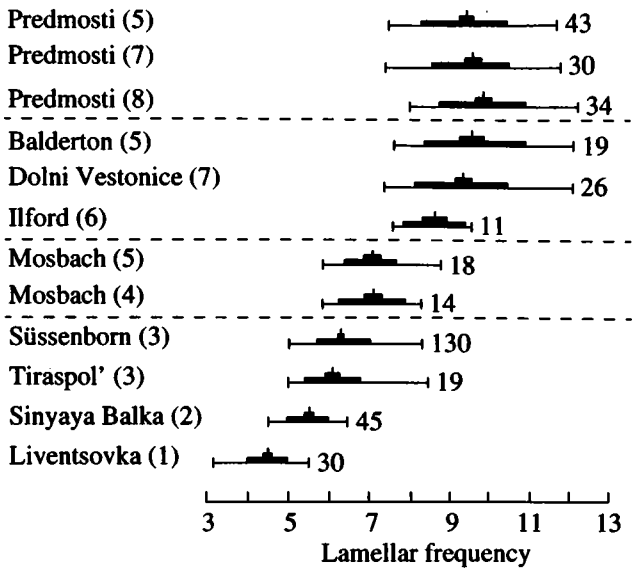

Fig. 1. Lamellar frequency in the 10-cm-long interval of upper last molars (M^3) of elephants from the studied localities. Line bars show the variability range; long rectangles correspond to δ and short ones to m; vertical line bars signify M; figures in parentheses denote the source of information; figures to the right of symbols are equal to n (see note to the table).

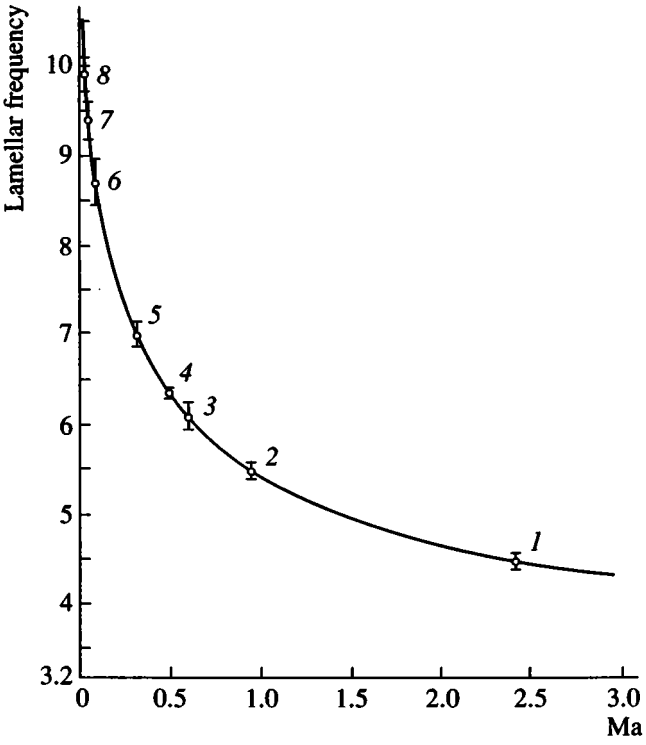

Fig. 2. Position of M^3 of elephants from the studied localities on the area cotangent curve. Vertical bars denote range of the mean square error m; localities: (1) Liventsovka; (2) Sinyaya Balka; (3) Tiraspol'; (4) Süssenborn; (5) Mosbach; (6) Ilford; (7) Dolni Vestonice; (8) Balderton; (9) Předmosti.

[1] The age of the Psekups locality is determined according to its position in the magnetochronological scale. Previously, it was dated back to 2.15 Ma (Vangengeim *et al.*, 1990) based on the dates 1.91 Ma for the Olduvai Subchron lower boundary and 2.48 Ma for the Gauss-Matuyama boundary. Older ages adopted for these boundaries in the latest magnetochronological scales correspondingly change the age of the Psekups locality. The same reason is responsible for the older age of the Liventsovka locality as compared to that reported by Pevzner and Vangengeim (1994).

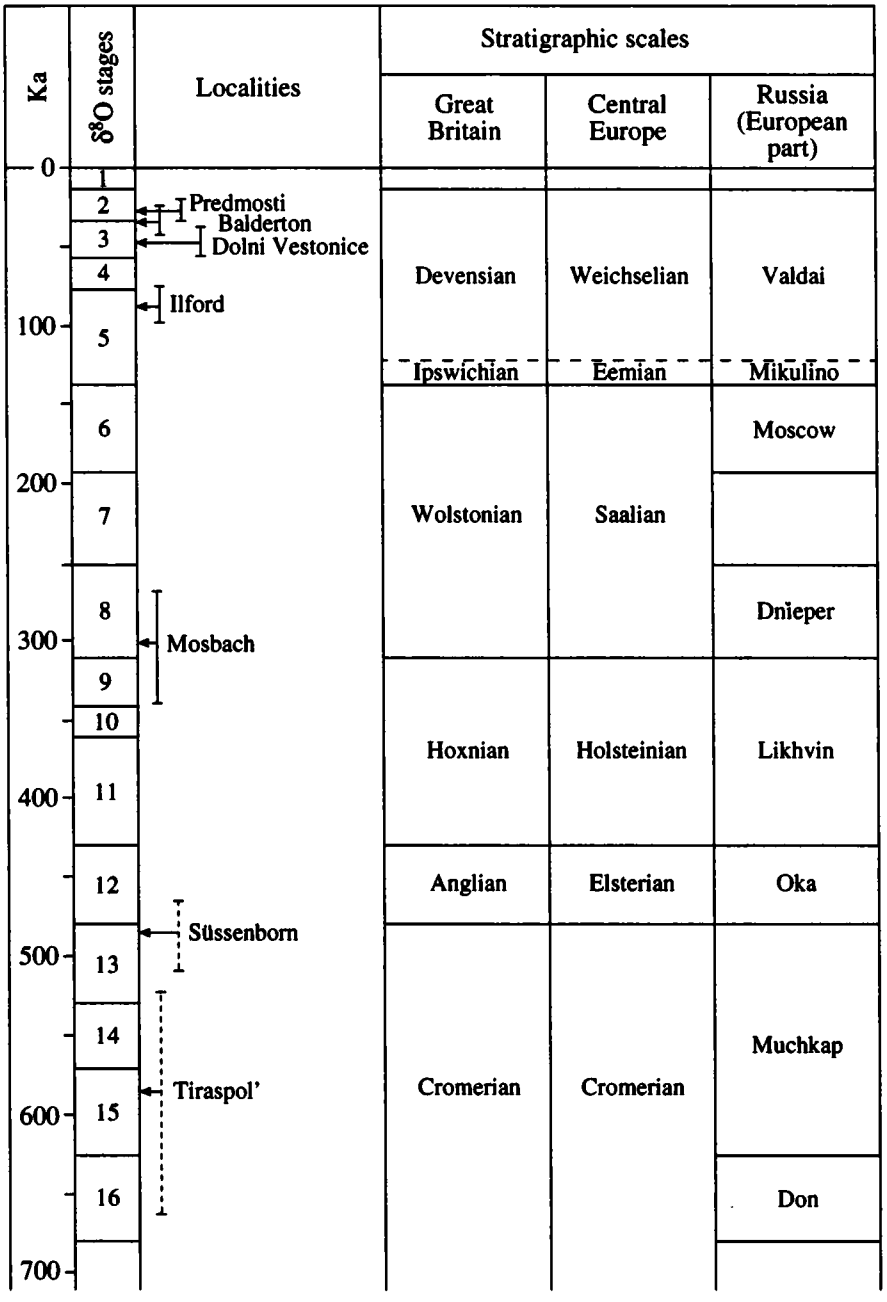

Fig. 3. Stratigraphic position of localities. Oxygen-isotope stages are those by Shackleton (1995); arrows and vertical bars indicate, respectively, the inferred age of localities and mean square error of age determination (solid for calculated and dashed for probable).

phants *A. meridionalis tamanensis* Dubrovo, occur in the bone breccia filling an ancient gully that cuts the marine Kuyal'nik Clay.

Since these two localities were taken for the reference points, their biometric ages are outside of the discussion.

The Tiraspol' (Kolkotova Balka) locality is associated with alluvial deposits 10–12 m thick, composing terrace VI of the Dniester River in Tiraspol'. The direct correlation of these sediments with glacial horizons is impossible, and their radiometric dates are unknown. Different researchers place the bone bed stratigraphically above the Don moraine (Nikiforova, 1982; Agadzhanyan, 1992) or just below it (Nikiforova and Aleksandrova, 1991; Markova, 1992). Most of them correlate the Don moraine (Don Horizon) with oxygen-isotope stage 16 (0.680–0.625 Ma). The biometric age of 0.589 Ma allows us to correlate the locality with oxygen-isotope stage 15 (0.625–0.570 Ma), i.e., to place it stratigraphically above the Don Horizon (Fig. 3). This strati-

graphic position of the Tiraspol' locality is confirmed by data on small mammals.

According to Agadzhanyan (1992), small mammalian fauna from localities underlying the Don moraine includes two rooted voles *Mimomys pusillus* and *M. intermedius*. The *gregaloides* morphotype dominates, along with scarce morphotypes *hintoni* and *arvaloides*, among the *Pitymys* remains. Steppe lemmings are represented by morphotypes intermediate between *Prolagurus pannonicus* and *Lagurus transiens*. The small mammalian fauna from localities above the Don moraine is characterized by the presence of a single *Mimomys* species, namely, *M. intermedius*, and also by the predominance of the *arvaloides* morphotype in the *Pitymys* populations and of *Lagurus transiens* among Lagurini forms.

In the Tiraspol' locality (Aleksandrova, 1976), only *M. intermedius* exemplifies the rooted voles, the *arvaloides* morphotype dominates among *Pitymys* species, and Lagurini are represented by *Lagurus transiens* and *Prolagurus posterius*. Such a composition enables fauna correlation with localities overlying the Don moraine.

The Süssenborn locality near Weimar is associated with alluvial sediments of the upper terrace system of the Ilm River. Alluvium enclosing the major bone bed with *Archidiskodon trogontherii* Pohl. is overlain by the Elsterian till. Kahlke dated this locality as corresponding to the Elsterian I (*Das Pleistozan von Süssenborn*, 1969). Most researchers correlate the Elsterian glaciation with oxygen-isotope stage 12 dated back to 0.480–0.430 Ma. The biometric age of the locality of 0.486 Ma suggests that the major bone bed of Süssenborn is correlative with the end of oxygen-isotope stage 13 or, with due regard for possible error, with the beginning of stage 12. The composition of mammalian fauna does not contradict this correlation. The assemblage includes the cryophilic *Ovibos* and *Rangifer* taxa along with predominant steppe forms.

The Tiraspol' and Süssenborn faunas are very similar in taxonomic composition, despite the absence of cold-resistant forms in the former, and can be considered as very close in age. The available dating results show that the Süssenborn fauna is about 100000 years younger than the Tiraspol' assemblage.

The Mosbach locality is associated with alluvial deposits of the Rhine River terrace in the vicinity of Wiesbaden.

The major bone bed of the locality ("gray Mosbach") was placed at different stratigraphic levels between the Cromerian III and Holsteinian (Brunacker *et al.*, 1977; Kahlke, 1975; Koenigswald and Tobien, 1987; Fejfar, 1976). Lister (1993) estimated that the Mosbach site, like that of Süssenborn, is 0.5–0.6 Ma old. However, according to the species composition, the Mosbach fauna is indubitably younger than that of Süssenborn. Many lineages of mammals, for instance, those of rhinoceroses and horses, are represented by more advanced forms in the Mosbach assemblage. As a representative of small mammals, the genus *Arvicola* occurs in the Mosbach fauna, whereas the Süssenborn assemblage includes its direct ancestor *Mimomys savini*.

According to its biometric age (about 0.300 Ma), the Mosbach locality is close to the boundary between oxygen-isotope stages 9 and 8; i.e., it corresponds to the Holsteinian–Saalian boundary. The Mosbach fauna bearing *Macaca* and *Hippopotamus* is indicative of warm interglacial conditions, which enable its correlation with the Holsteinian Interglacial. Geologic data also do not contradict the high stratigraphic position of the bone bed within the Holsteinian (near the boundary with the Saalian). Koenigswald and Tobien (1987, p. 234) noted that there is no lithologic hiatus between the major bone bed and the overlying Mosbach Bed III. The upper Mosbach horizon already includes remains of primigenoid elephant and glutton *Gulo gulo*. Sedimentological and faunal data on the Mosbach Horizon III point to a cool or cold climate and, therefore, to the forthcoming glaciation.

The Ilford locality is situated on the left bank of the Reading River (lower reaches of the Thames River). It is associated with alluvial deposits of the middle terrace of the Thames River (Sutclife, 1986). There is no agreement among researchers with respect to the locality age. It was once attributed to the Ipswichian (Mitchell *et al.*, 1973; Clayton, 1977) and then to the second part of the Ipswichian (Stuart, 1982) or to the interglacial phase between the Hoxnian and Ipswichian, i.e. to the warm stage within the Wolstonian (Sutclife, 1986). Using the amino acid epimerization method, Lister (1993) dated it back to 200 ka.

We estimate the biometric age of the Ilford locality as corresponding to 82 ka. This date agrees with Stuart's reference to the second half of the Ipswichian, if we consider the latter in a broad sense as an analogue of oxygen-isotope stage 5. Even with due regard for the estimated error (+19000 years), the date excludes the possibility of placing the locality at the beginning of the Ipswichian (stage 5e), much less to the pre-Ipswichian time.

The mammalian fauna of the Balderton locality was recovered from the 7 to 8-m-thick sandy-gravel deposits exposed in a series of quarries within the area of about 40 km^2 in the interfluve of the Trent and Witham rivers between Newark and Lincoln. Most remains are collected by workers from conveyer belts by work in the quarries. The bones are presumably from the lower part of the section.

Until recently, the age of the deposits was estimated to be the Devensian. Afterward (Brandon and Sumbler, 1991; Lister and Brandon, 1991; Lister, 1993), the sediments were attributed to the Wolstonian, correlated with oxygen-isotope stage 6 and dated back to 140–150 ka. These conclusions are based on geomorphological considerations, lithofacies analysis, and on age

determinations by the electron spin resonance and amino acid epimerization methods.

Lister pointed out that the Balderton mammoth is morphologically very close to the Wurm mammoths from central Europe and, in particular, from Předmostí. The difference between the age of Balderton and central European mammoths, which were at a close evolutionary stage, he explained by the fact that "...in northwest Europe at least, *Mammuthus* had completed its evolution by the penultimate cold stage" (Lister and Brandon, 1991, p. 141), i.e., more than 100000 years earlier than in central Europe. However, from a biological standpoint, it is difficult to admit such an evolutionary advancement of one species in a single distribution area, especially bearing in mind the panmixis phenomenon.

The Balderton biometric age is 32 + 11/–9 ka. This date indicates middle Devensian age for the remains and is distinctly inconsistent with the age determination of 140 ka accepted by Lister. This contradiction could be resolved by means of the ^{14}C dating of mammoth remains, because our result is within the potential limits of the method. After our request, Lister kindly donated a fragment of a mammoth limb bone from the Balderton Quarry 4e for radiocarbon analysis. The analysis was made by L.D. Sulerzhitskii at the laboratory of the Geological Institute, Russian Academy of Sciences. The obtained date of 29600 ± 600 years (GIN8743) agrees well with the biometric age of the locality and excludes the possibility that the Balderton mammoth is older than the middle Wurm mammoths from central Europe. Consequently, the accelerated evolution of species in northwestern Europe should also be discredited. According to Sulerzhitskii, the dating result is valid, because the ^{14}C concentration in the sample is considerably greater than could be due to carbon contamination during burial or during the age measurement procedure.

The Dolni Vestonice locality in southern Moravia is the late Paleolithic site of the Pavlovian industry. It is associated with the uppermost part of the soil (Paudorf, Stillfried B) and overlying loess horizon (Ivanova, 1965). The soil yielded the following ^{14}C dates: 28990 ± 1400, 29940 ± 300, and 28300 ± 300 years. Radiocarbon dates of 25820 ± 170, 26730 ± 250, and 26000 ± 350 years are known for the lower part of the loess horizon (Kozlowski, 1990).

According to the geological records and industrial typology, the Dolni Vestonice locality is similar to the Předmostí site. Both localities have been considered as identical in age. However, the minimum and mean values of the lamellar frequency in mammoth teeth (M^3) from the Dolni Vestonice locality are substantially lower than these parameters reported for the Předmostí site.

The biometric age of the locality in question is 43 + 10/–9 thousand years and differs considerably from the ^{14}C dates. Even with due regard for measurement errors, this date is older than those obtained on the basis of the radiocarbon method. The discrepancy between age determinations is understandable if strongly worn teeth have been included in the statistics. This, as stated above, decreases the mean parameter and thus increases the age.

The late Paleolithic Předmostí locality (Pavlovian culture) at the Morava River near Prerov is associated with the basal part of the young loess horizon. The ^{14}C age of the cultural layer of the site is about 26.5 ka (Svoboda, 1990). This date was used as the third reference point.

CONCLUSION

All the obtained biometric dates should be considered as indicating the maximum possible age, because almost all cited publications lack data on the wearing degree of teeth. When included in statistical analysis, the parameters of strongly worn teeth substantially decrease the mean values of the lamellar frequency, and we obtain an older age.

Time intervals between individual localities could be determined with a higher accuracy, if one researcher could perform measurements in all instances.

The biometric dating of the oldest Liventsovka locality does not essentially change the age accepted at present, since the biometric age is calculated with a large error. The age of the Sinyaya Balka locality was formerly adopted as equal to 0.95 Ma, i.e., to the average value between 1.1 and 0.8 Ma (the time span of the Taman' faunal assemblage). Our calculations allow us to reduce the possible time limit of the locality from 1 to 0.9 Ma, leaving the same mean value of the age.

The Tiraspol', Süssenborn, and Mosbach localities similar in composition of the mammal assemblages were formerly considered as close in age; namely, the Tiraspol' and Süssenborn sites were assumed to be of the same age and somewhat older than the Mosbach locality. Our investigations infer that the Tiraspol' locality is the oldest one, probably about 600 ka old. The Süssenborn site is 100000 years younger, and the Mosbach locality is about 200000 years younger than the latter.

Our dating results for the Ilford and Balderton localities are distinctly inconsistent with those reported recently by English researchers. They refine the former age determinations. The biometric age of the Balderton site agrees well with the new ^{14}C date obtained for the bone sample from this locality.

Reviewers V.I. Zhegalo and Yu.B. Gladenkov

REFERENCES

Agadzhanyan, A.K., Pleistocene Stages of Small Mammal Development in Central Areas of the Russian Plain, in *Stratigrafiya i paleogeografiya chetvertichnogo perioda Vostoch-*

noi Evropy (Quaternary Stratigraphy and Paleogeography of Eastern Europe), Moscow: Inst. Geogr. Ross. Akad. Nauk, 1992, pp. 37–49.

Aleksandrova, L.P., *Gryzuny antropogena evropeiskoi chasti SSSR* (Anthropogene Rodents of the European Part of the USSR), Moscow: Nauka, 1976.

Aver'yanov, A.O., Vartanyan, S.L., and Garutt, V.E., Small Mammoth *Mammuthus primigenius vrangelensis* Garutt, Averianov et Vartanyan, 1993, from Vrangel Island (Northeastern Siberia), *Tr. Zool. Inst. Ross. Akad. Nauk*, 1995, vol. 263, pp. 184–199.

Brandon, A. and Sumbler, M.G., The Balderton Sand and Gravel: Pre-Ipswichian Cold Stage Pluvial Deposits near Lincoln, England, *J. Quat. Sci.*, 1991, vol. 6, pp. 117–138.

Brunnacker, K., Tobien, H., and von der Brelie, G., Pliozän und Altestpleistozän in der Bundesrepublik Deutschland - Ein Beitrag zur Neogene/Quartar Grenze, *Giorn. Geol.*, 1977, Ser. 2a, vol. 41, nos. 1–2, pp. 131–163.

Clayton, K.M., River Terraces, in *British Quaternary Studies*, Shotto, F.W., Ed., Oxford: Clarendon, 1977, pp. 153–168.

Das Pleistozän von Süssenborn, *Palaontol. Abh., Abt. A*, 1969, vol, 3, issue 314, pp. 367–788.

Dubrovo, I.A., New Data on the Taman' Vertebrate Fauna, *Byull. Mosk. O–va Ispyt. Prir., Otd. Geol.*, 1963, vol. 38, no. 6, pp. 94–99.

Dubrovo, I.A., Order Proboscidea. Proboscideans. Family Elephantidae Gray, 1821, in *Pleistotsen Tiraspolya* (The Pleistocene of Tiraspol), Chisinau: Shtiintsa, 1971, pp. 92–108.

Fejfar, O., Plio-Pleistocene Mammal Sequence, in *Project 73/1/24: Quaternary Glaciations in the Northern Hemisphere. IUGS–UNESCO Int. Geol. Correlation Program*, Prague, 1976, pp. 351–366.

Guenther, E.W., Elefantenbackenzäne aus den Mosbacher Sanden, *Mz. Naturw. Arch.*, 1968, no. 7, pp. 55–73.

Ivanova, I.K., *Geologicheskii vozrast iskopaemogo cheloveka* (Geological Age of Fossil Man), Moscow: Nauka, 1965.

Kahlke, H.D., The Macro-Faunas of Continental Europe during the Middle Pleistocene: Stratigraphic Sequence and Problems of Intercorrelation, *After Australopithecines*, Butzer, K.W. and Isaac, G.L., Eds., Chicago, 1975, pp. 309–374.

Koenigswald von, W. and Tobien, H., Bemerkungen zur Altersstellung der Pleistozänen Mosbach-Sande bei Wiesbaden, *Geol. Jahrb. Hessen*, 1987, no. 115, pp. 227–237.

Kozlowski, J.K., Northern Central Europe c. 18000 BP, *The World at 18000 BP*, Softer, O. and Gamble, C., Eds., London: Unwin Hyman, 1990, vol. 1, pp. 204–227.

Lister, A., Patterns of Evolution in Quaternary Mammal Lineages, in *Evolutionary Patterns and Processes*, London: Linn. Soc. London, 1993, pp. 72–93.

Lister, A. and Brandon, A., A Pre-Ipswichian Cold Stage Mammalian Fauna from the Balderton Sand and Gravel, Lincolnshire, *J. Quat. Sci.*, 1991, vol. 6, pp. 139–157.

Markova, A.K., Pleistocene Microtheriofauna of Eastern Europe, in *Stratigrafiya i paleogeografiya chetvertichnogo perioda Vostochnoi Evropy* (Quaternary Stratigraphy and Paleogeography of Eastern Europe), Moscow: Inst. Geogr. Ross. Akad. Nauk, 1992, pp. 50–94.

Mitchell, G.F., Penny, L.F., Shotton, F.W., and West, R.G., A Correlation of Quaternary Deposits in the British Isles, *Spec. Rep. Geol. Soc. London*, 1973, no. 4, pp. 1–99.

Musil, R., Die Mammutmolaren von Předmosti (CSSR), *Palaontol. Abh., Abt. A*, 1968, vol. 3, issue 1, pp. 1–192.

Nikifirova, K.V., The General Stratigraphic Scale for the Upper Pliocene and Quaternary (Anthropogene) of the USSR, in *Stratigrafiya SSSR. Chetvertichnaya sistema*, (Stratigraphy of the USSR: Quaternary System), Moscow: Nedra, 1982, part 1, pp. 120–128.

Nikifirova, K.V. and Aleksandrova, L.P., Stratigraphy, Chronology, and Correlation of European and North American Events of the Late Pliocene and Anthropogene in Relation to Changes in Geosphere and Biosphere, in *Paleogeografiya i biostratigrafiya pliotsena i antropogena* (Paleogeography and Biostratigraphy of the Pliocene and Anthropogene), Moscow: Geol. Inst. Ross. Akad. Nauk, 1991, pp. 99–123.

Pevzner, M.A. and Vangengeim, E.A., Some General Features of Mammalian Evolution, *Stratigr. Geol. Korrelyatsiya*, 1994, vol. 2, no. 6, pp. 3–9.

Shackleton, N.J., New Data on the Evolution of Pliocene Climatic Variability, *Paleoclimate and Evolution with Emphasis on Human Origins*, Vrba, E.S., Denton, G.H., Partridge, T.C., and Burckle, L.H., Eds., Yale: Yale Univ. Press, 1995, pp. 242–248.

Stuart, A.J., *Pleistocene Vertebrates in the British Isles*, London: Longman, 1982.

Sutclife, A.J., *On the Track of Ice Age Mammals*, London: Brit. Mus. Nat. Hist., 1986.

Svoboda, J., Moravia during the Upper Pleniglacial, *The World at 18000 BP*, Soffer, O. and Gamble, C., Eds., London: Unwin Hyman, 1990, vol. 1, pp. 193–203.

Vangengeim, E.A., Pevzner, M.A., and Tesakov, A.S., Magneto- and Biostratigraphic Investigations in the Stratotype Region of the Psekup Mammalian Fauna, *Byull. Komis. Izuch.. Chetvert. Perioda*, 1990, no. 59, pp. 81–93.

Vangengeim, E.A., Vekua, M.L., Zhegallo, V.I., *et al.*, Position of the Taman' Faunal Assemblage in the Stratigraphical and Magnetochronological Scales, *Byull. Komis. Izuch. Chetvert. Perioda*, 1991, no. 60, pp. 41–52.

Stratigraphy and Geological Correlation, Vol. 8, No. 1, 2000, pp. 84–98. Translated from Stratigrafiya. Geologicheskaya Korrelyatsiya, Vol. 8, No. 1, 2000, pp. 90–105.
Original Russian Text Copyright © 2000 by Derevyanko, Devyatkin, Simakova, Olsen, Kulikov, Gnibedenko.
English Translation Copyright © 2000 by MAIK "Nauka/Interperiodica" (Russia).

The Tsagan-Agui Cave (Mongolia): Pleistocene Stratigraphy, Archeology, and Paleoecology

A. P. Derevyanko,* E. V. Devyatkin, A. N. Simakova,** J. Olsen,*** O. A. Kulikov,**** and Z. N. Gnibedenko******

* *Institute of Archeology and Ethnography, Siberian Division, Russian Academy of Sciences, pr. akademika Lavrent'eva 17, Novosibirsk, 630090 Russia*

** *Geological Institute, Russian Academy of Sciences, Pyzhevskii per. 7, Moscow, 109017 Russia*

*** *University of Arizona, Tuscon, 85721 USA*

**** *Moscow State University, Vorob'evy gory, Moscow, 111899 Russia*

Received December 29, 1997; in final form, April 13, 1998

Abstract—First results on stratigraphy, archeology, and paleoecology in the Tsagan-Agui Cave (Mongolia) are discussed. The palynological analysis along with radiothermoluminescence and magnetostratigraphic dating allowed the stratigraphic units to be defined in the stratified sequence of cave deposits and the archeological complexes to be dated. The archeological complexes of the Tsagan-Agui Cave are correlated with those from the Flint Valley and Narin-Gol open-air sites.

Key words: *stratigraphy, archeology, palynology, paleoclimate, paleoecology.*

The stratigraphy and archeology of the Upper Cenozoic (Pliocene–Pleistocene) geological sequence in the Inner Asian arid belt have been insufficiently studied so far. This primarily concerns Mongolia, where pertinent studies were mainly carried out in central and northern areas of this spacious region (Devyatkin, 1981; *Pozdnii kainozoi...*, 1989). For instance, archeological investigations of the Orkhon River terraces (Mal'tyn-Am, Orkhon 1 and 2) in the Khangai Ridge revealed detailed Late Pleistocene–Holocene geoarcheology and climatostratigraphy (Derevyanko *et al.*, 1992). A summarizing monograph dedicated to the Paleolithic and Neolithic of the Mongolian Altai also includes materials on the Late Cenozoic stratigraphy and paleogeography of Mongolia (Derevyanko *et al.*, 1990).

In the Gobi region of Mongolia, abundant archeological finds are known from sites of the open-air type. Their geomorphological confinement to particular terraces allows one to reconstruct the succession of heterochronous archeological complexes, but it is impossible to determine without a thorough study of stratified sites the geological and geochronological ages of the stone cultures and, correspondingly, to understand the paleoecology of the ancient human habitation. The study of cave sections using different geological and archeological methods is a promising approach. The Tsagan-Agui karst cave was first visited in 1988–1989 (Derevyanko *et al.*, 1995) and then thoroughly studied in 1995–1996 in the course of the Russian–Mongolian–American expedition (Derevyanko *et al.*, 1996). The present paper discusses the geological structure and stratigraphy of the cave deposits in the Tsagan-Agui area, as well as the results of palynological, magnetostratigraphic, radiothermoluminescence, paleoclimatic, and archeological studies.

In contrast to China, where geological–archeological studies in caves have been in progress for several decades, similar investigations in the Gobi areas of Mongolia began only recently. For instance, in the Tsenkher Cave of the Mongolian Altai, Okladnikov (1981) discovered petroglyphs, most prominent among which are drawings of mammoth and ostrich. This allowed him to refer the oldest human habitation in this cave to at least the late Paleolithic, although no excavations were carried out in the cave proper.

During the 1970s and 1980s, the joint Soviet–Mongolian biological expedition investigated caves in the Mongolian Gobi (Dinesman *et al.*, 1989). They discovered approximately a dozen caves and benches, which where excavated to a depth of about 1.5 m, usually down to the collapse horizon. Analysis of the lithology and composition of fossil plant and animal communities allowed these researchers to draw the conclusion that cryogenesis was atypical of the terminal Pleistocene–Holocene characterized by several alternating pluvial and arid phases, when climate was relatively warm in general but less arid than it is now.

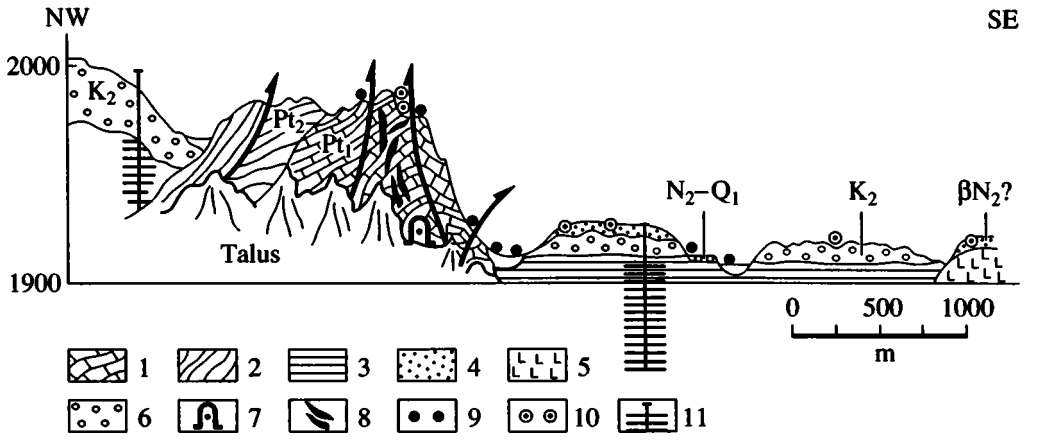

Fig. 1. Geological cross section in the Tsagan-Agui Cave area (compiled by E.V. Devyatkin): (1) limestone (Pt_1); (2) sandstone and volcanics (Pt_2); (3) red and variegated clays with detritus and pebbles (K_1); (4) pebblestone of high terraces (N_2^3–Q_1); (5) basalt (βN_2); (6) pebblestone, boulders, and sandstone (K_2); (7) Tsagan-Agui Cave; (8) flint veins in the Proterozoic sequence; (9) Late Paleolithic flint artifacts; (10) "pebble" artifacts; (11) boreholes.

In our study, E.V. Devyatkin was responsible for structural analysis of the Tsagan-Agui Cave and surroundings and also for general interpretation of all relevant geological materials. Particular analytical procedures were carried out by A.N. Simakova (palynology), Z.N. Gnibedenko (magnetostratigraphy), V.S. Zazhigin (paleontology), O.A. Kulikov (RTL-dating), and O.B. Parunin (isotopic analysis of calcite). Archeological materials presented here are after Derevyanko *et al.* (1996), supplemented with an additional interpretation of analytical data.

GEOLOGICAL AND GEOMORPHOLOGICAL STRUCTURE OF THE TSAGAN-AGUI CAVE AREA

The Tsagan-Agui Cave is located on the southern slope of the Gobi Altai southwest of the Dzun-Bogd-Ula Ridge; the site coordinates are 44°42′32″N and 101°10′8″ (Derevyanko *et al.*, 1996). The highest point of a small ridge, where the cave is located, is at an altitude of 1980 m (Mt. Khukh-Obo). The oldest deposits constituting the bulk of the ridge are Proterozoic in age and represent two lithological units. The lower unit up to 1000 m thick corresponds to light-colored marmorized limestones with lentils and interbeds of siliceous rocks, whereas the upper one (more than 800 m thick) consists of dark metasandstones, siltstones, metavolcanics, and schists. Younger rocks of the area are attributed to the Mesozoic. The Lower Cretaceous rocks are represented by brown-red to green detrital–sandy clays and gritstones intercalated with strongly weathered pebbly and rubble interbeds. These deposits fill depressions, are more than 100 m thick, and outcrop at the terrace socles. The Upper Cretaceous sequence of conglomerate, cobblestone, pebble, and sand beds is up to 200 m thick. Conglomerates are large-pebbled, almost unaltered; pebbles are composed of quartz, sandstone, and metamorphic rocks. The sedimentary cover of the beds extends from the Baga-Bogd and Ikhe-Bogd Mountains southward to the Trans-Altai Gobi. Transverse blocks of the Altai Ridge slope are embedded into these deposits.

The youngest rocks of the Cenozoic succession are divided into several heterochronous sequences. The upper Pliocene(?)–lower Pleistocene deposits compose terraces (up to 30 m high) fragmentarily preserved along large dry drainage valleys (sairs in Mongolian). They consist of boulders and pebbles of reworked Upper Cretaceous deposits and are exposed along valleys extending southward into the Gobi and northward into the Valley of Lakes. The oldest "pebble" complex of archeological finds of the "Narin-Gol" type is associated with these terraces (Derevyanko *et al.*, 1990).

Slopes of the ridge are covered with proluvial aprons of coarse detrital and boulder deposits. Along dry valleys, they form low enclosed terraces of three levels, which are up to 10 m high at the ridge foot and almost join each other south of the latter. The clastic material mainly consists of limestone, sandstone, and schist; it also includes reworked pebbles of Upper Cretaceous rocks. The age of these terraces ranges from the middle (third terrace) to late (two lower terraces) Pleistocene. Proluvial aprons at the ridge foot and surface levels of the terraces yield the younger "Sair" archeological complex represented by flint artifacts similar to those from the Tsagan-Agui Cave. The general geological–geomorphological situation in the Tsagan-Agui Cave area is shown in Figure 1.

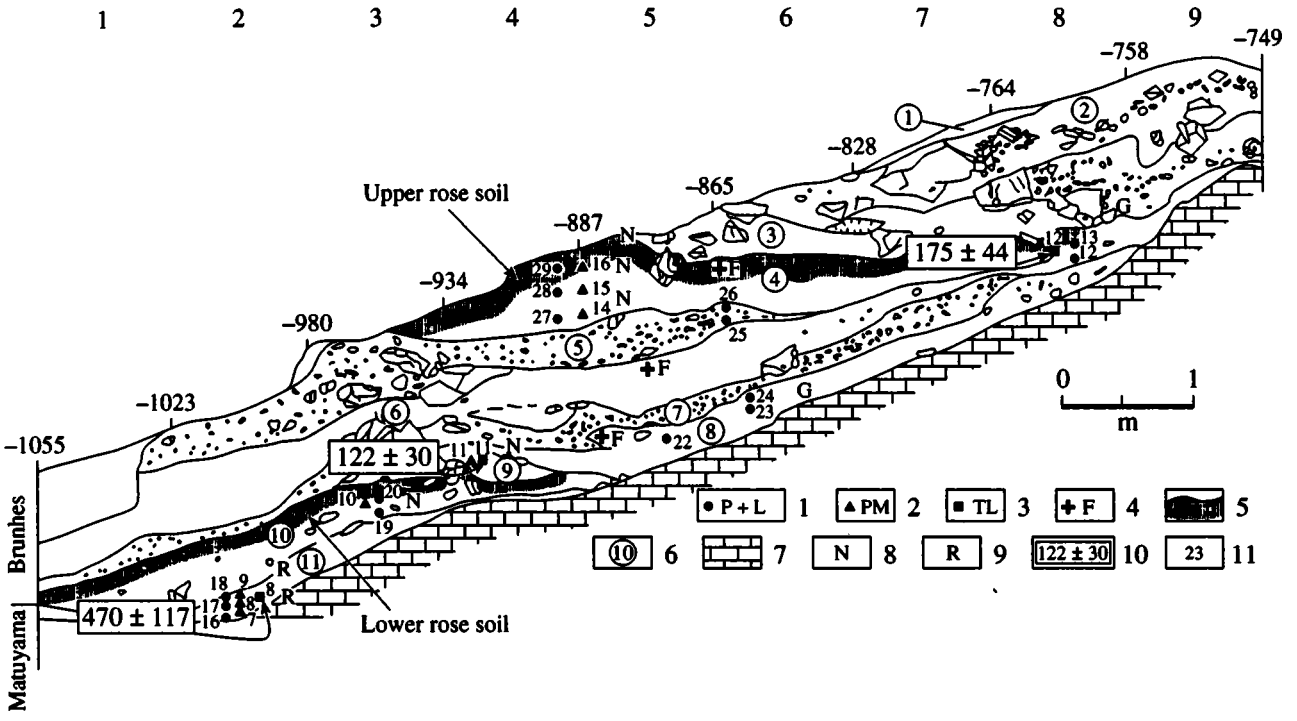

Fig. 2. Longitudinal cross section of the Tsagan-Agui Cave entrance area (after Derevyanko *et al.*, 1996 with modifications) and sites of samples used in this study: (1) palynological and lithological samples; (2) samples for paleomagnetic analysis; (3) samples for the RTL dating; (4) mammalian remains; (5) fossil soil; (6) archeological beds; (7) limestone; (8) samples with normal (N) polarity; (9) samples with reversed (R) polarity; (10) RTL dates, ka; (11) sample number.

GEOLOGICAL STRUCTURE OF THE TSAGAN-AGUI CAVE

The cave is located on the left (eastern) slope of a sair crosscutting a small ridge composed of limestone. The sair follows a fault system dipping southward (the dip angle is up to 70°) and is clearly of the karst origin. The cave entrance slowly rises toward its central room and coincides with the surface of the second sair terrace. The cave is 38 m long; its mouth is 5.3 m wide and 4.6 m high; the height of the central room (the Great Grotto) amounts to 10–12 m.

The cave deposits were recovered from one longitudinal excavation stretching from the entrance toward the main cave chamber and from one test pit in the center of the cave. A description of the recovered beds (from the base upward) is given bellow.

The near-entrance section (Figs. 2, 3; description by Devyatkin from the base upward):

Bed 11: dark red to orange-yellow sandy clay enclosing rare fragments (up to 0.5 cm) of loose limestone and displaying inclined bedding (parallel to underlying limestone). This brightly colored bed of fine clay occurs almost everywhere at the limestone surface, even when the latter dips steeply. When the surface of the limestone flattens, the bed thickness increases to 0.25 m due to the partial erosion of underlying sediments.

It can be assumed that the bed represents a peculiar result of weathering of the cave limestone top. In bedrock depressions, the deposits appear to have been transported and redeposited by water, as it is evident from the thin horizontal bedding. The formation of the bed is apparently related to the elevated moisture in the cave. The RTL age is 470 ± 117 ka.

Bed 10 corresponds to the "lower rose" soil developed in the top part of Bed 11; further inside the cave (up from the excavation), the soil rests directly on limestone. The basal part of the bed is enriched in limestone fragments, thus representing the clastic horizon; clasts are also scattered throughout the bed. The bed is distinguished only near the entrance to the cave. Its upper part (soil proper) is light rose in color, massive, and shows an admixture of dispersed carbonate, which forms vertical rounded and branching concretions responsible for almost vertical jointing in the uppermost soil horizon. The total thickness of the bed is 50 cm, and that of the fossil soil is 15 cm.

Bed 9 corresponds to a small (up to 1.2–1.3 m) lentil composed of limestone fragments embedded into a sandy–gravelly matrix. Some limestone blocks are up to 0.7 m across. Locally, the top part of the bed encloses a gray gravelly intercalation with dispersed carbonates, which is about 10 cm thick. This is probably a result of superimposed soil-forming processes. The RTL age is 122 ± 30 ka.

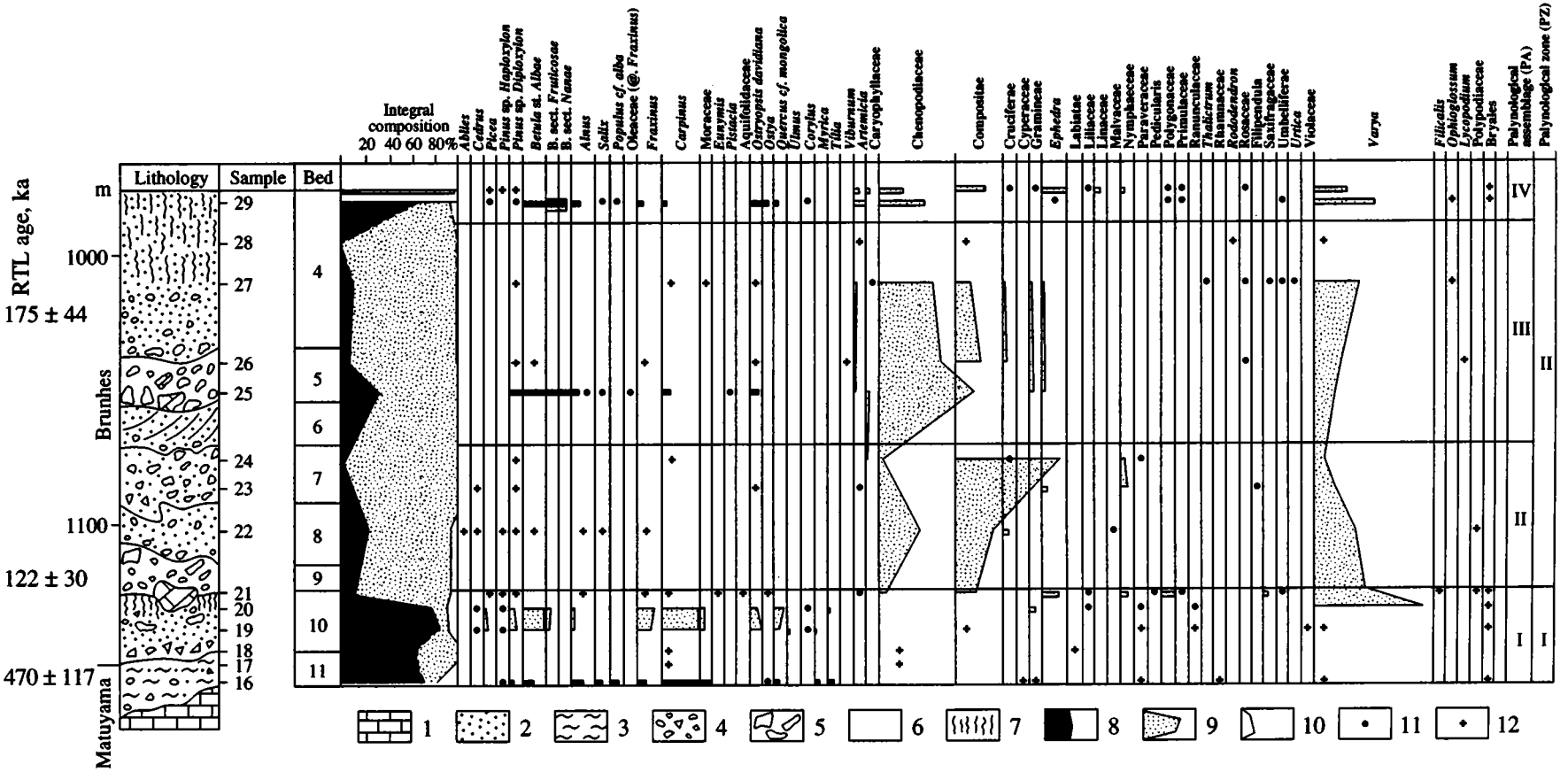

Fig. 3. Palynological diagram for deposits recovered in the entrance area of the Tsagan-Agui Cave (plotted by A.N. Simakova): (1) limestone; (2) sand; (3) clay; (4) clastic material; (5) limestone blocks; (6) proluvial deposits; (7) fossil soil; (8) abundance of arboreal–frutescent pollen (%); (9) abundance of herbaceous–fruticulose pollen (%); (10) abundance of spores; (11) single grains; (12) pollen and spores of low abundance rate.

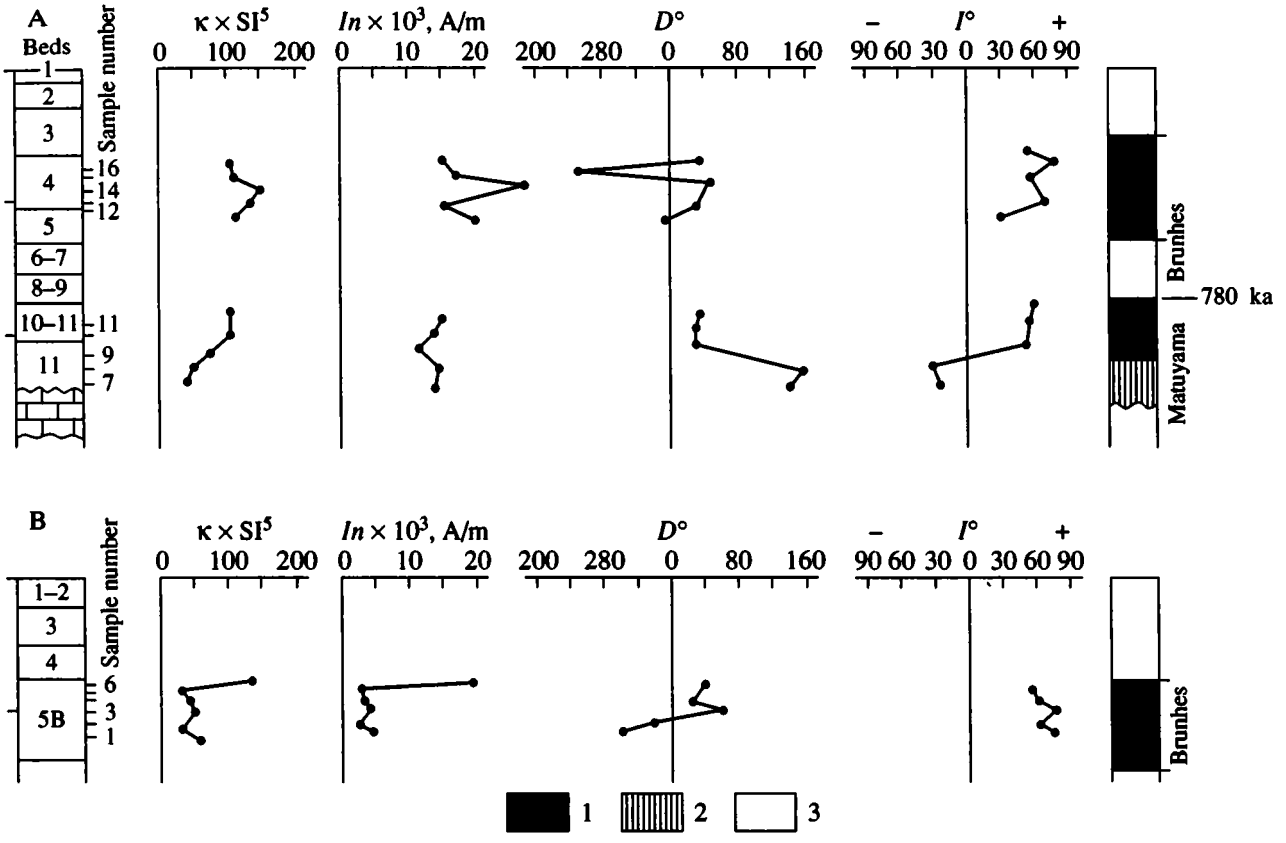

Fig. 4. Paleomagnetic cross-sections of deposits in the Tsagan-Agui Cave (compiled by G.N. Gnibedenko). (A) Longitudinal cross-section near the northern wall of entrance area; (B) cross section of the lower grotto in the entrance area: (1) normal polarity; (2) reversed polarity; (3) intervals where polarity is unknown.

Bed 8: gray coarse-grained sand with inclined bedding; the bed contains fragments of platy limestones oriented parallel to the bedding planes. The basal part of the bed is enriched in large limestone clasts and fragmented calcite crystals. The bed yields small black bones of rodents (*Lepus* sp., *Ochotona* sp., *Citellus* sp.) and birds. In the cave entrance area, Bed 8 with erosion marks overlies the beds 9 and 10. Inside the cave, it rests directly on limestone and encloses coarser detritus.

The bed formation is probably related to removal of clastic material from the cave by water streams.

Bed 7 of blocky–detrital deposits dips toward the cave entrance. Limy blocks up to 25 cm across are angular, chaotically oriented, and mixed with abundant small fragments of sinter and crystalline calcite. Near the entrance, there is a large (75 cm across) limestone block truncating the bed. The bed, pinching out in the right internal part of the excavation, is 70 cm thick at the left side of the excavation near the entrance. These deposits are of gravitational–sliding (seismogravitational) origin and record a collapse of the cave walls and ceiling, fragments of which slid downward.

Bed 6 of gray sand encloses separate limestone blocks and detritus in its basal part; sandy material envelopes large rock fragments along the bed inclination. The wash-type sand is fairly well sorted and deposited by water streams. In the right part of the excavation (close to the cave entrance), sand overlies the previous bed; the bed 6 is missing inside the cave. The bed enclose bones of mammalian taxa *Equus* sp. and *Ochotona* sp.

Bed 5 corresponds to a lentil of limestone detritus and boulders. Near the entrance, the latter are up to 50 cm across. Boulders are chaotically oriented and angular. Like in the Bed 7, the coarse clastic material is mixed with abundant broken calcite crystals usually concentrated in the basal part. Near the cave entrance, the bed is up to 60 cm thick and overlies the previous layer, but it wedges out inside the cave.

In its structure and texture along the strike, this bed is similar to the Bed 7 and also represents gravitational-sliding (seismogravitational) deposits. Both beds were formed by clastic material when the cave shelter near the entrance collapsed.

Bed 4 is of a complex structure. In the right upper part of the excavation, it consists of red, very fine-bedded clay enveloping, like in Bed 11, the bedrock limestone. Near the entrance, the bed lacks the inclined bedding patterns, shows the vertical jointing and fracturing, and contains small limestone fragments enclosed

in a sandy loam matrix, thus being similar to the fossil soil of Bed 10. In the topmost part, there are rounded, vertically oriented and branching carbonate segregations of the soil type (up to 1 cm across). The bed coloration is generally rose, locally yellowish rose, presumably due to the washout of bedded dark red clay and subsequent pigmentation of the soil. Sometimes the top part of this "upper" rose soil shows flattened horizons of carbonatization (up to 10 m thick). The bed yields flint artifacts and bones of small mammals (*Citellus* sp., *Ochotona* sp., *Lepus* sp., *Allactaga* sp.) and birds. The RTL date for the upper part of the bed is 175 ± 44 ka.

Bed 3, inclining outward, consists of large angular limestone blocks (up to 50–60 cm across) often covered by druses of crystalline calcite. The basal part of the bed (up to 10 m thick) contains calcite clasts. The matrix consisting of sand and sandy loam is massive and slightly calcareous; its most fine-grained portions (lentils and inclusions) resemble loess, which, however, always contains small limy detritus. The boundary with the overlying bed is obscure. The thickness is up to 50 cm. The loess-like material is most likely of eolian origin.

Bed 2 is similar to the previous stratum but is richer in large limestone blocks irregularly merged into the massive, slightly calcareous matrix of pale yellow loess-like loam with limestone detritus. The thickness is up to 50 cm. Beds 2 and 3 extend from the entrance to the central part of the cave.

Bed 1 of recent, slightly humified soil is fragmentarily preserved at the surface near the cave entrance. Its thickness is 10 cm.

Section of the central test pit in the main chamber along its southern wall (Fig. 5; description by Devyatkin from the base upward):

Bed 13: gray to greenish gray soft clay and loam showing frequent alternation of thin sandy (1–2 mm) and clayey (2–3 mm) laminas. Sediments were clearly deposited by water streams; the rhythmical sedimentary bedding is probably seasonal. The apparent thickness to the pit bottom is 20 cm.

Bed 12 resembles the previous one, but is more sandy in composition and consists of alternating bluish to greenish clayey and coarse-grained sandy laminas. The basal part of the bed is composed of inequigranular sands with small (10 × 15 cm) lentils of gray and greenish gray clay and loam. Some lentils are composed of small-sized subangular limestone gravel. There are also alien fragments of quartzite, quartz, black metamorphic schist, and metasandstone (some of them are rounded). The fragments are up to 10–12 cm across.

The occurrence of alien rocks suggests that they have been transported from a ridge composed of these rocks via channels opening inside the cave. The RTL age is 520 ± 130 ka.

Bed 11 shows alternation of dove-colored to greenish clay laminas and yellowish to reddish coarse-grained sand lentils. Rusty intercalations occur throughout the bed. In addition, there are small alluvial pebbles. The upper boundary of the bed is distinct, whereas the lower one is less clear. The RTL age is 490 ± 123 ka. The thickness is 30–100 cm.

Bed 10: coarse-grained sand with rusty patches and inclusions of variable-size clasts of calcite crystals. It includes a sliding horizon composed of broken blocks of crystalline rocks. The thickness is 0–30 cm.

Bed 9: coarse-grained sand with abundant detritus and rare small pebbles of alien rocks. The bed is light yellow with reddish shading. It was observed only in the northeastern wall of the pit between two large blocks.

Bed 8: bluish gray clay with an insignificant admixture of small-sized clastic material. The upper boundary of the bed is relatively even, whereas the lower one dips steeply toward the right wall of the cave. The thickness varies from zero to 75 cm.

Bed 7: grayish yellow sand with abundant clastic material and rare small alluvial pebbles. The bed dips steeply and becomes thinner toward the entrance. Its boundaries with overlying and underlying beds are distinct. The thickness is 5–50 cm.

Bed 6 of rusty sand with clay inclusions of the same coloration encloses limestone fragments, which are less abundant than in beds 8 and 9. Coloration is spotty, ocherous in general. The thickness is up to 20 cm.

Bed 5 has a distinct undulating lower boundary. It is composed of gray homogenous loam with obscure bedding and scattered fragments (3–5 cm across) of alien rocks: schist, sandstone, limestone, and calcite. The RTL age is 227 ± 57 ka.

Although the deposits of beds 5–7 contain clastic material, they are probably related in origin to flooding events in the central part of the cave. Structural features of these deposits suggest that they were subsequently squeezed out to fill the space between the slid rock fragments (beds 8 and 9). Saturation of the sediments with water (beds 5–7) resulted in their pliable deformation. None of the known signs of cryogenic structures has been observed.

Bed 4 of dark gray loamy sand is enriched in clastic material represented mostly by angular limestone fragments (up to 0.3 m across) and also by calcite grains. The bed represents the third (from the base) horizon of gravitational–sliding deposits.

Bed 3 of loam and sand is darker than Bed 4. It is massive, 15–20 cm thick, and encloses limestone and calcite fragments.

Bed 2: light gray compact massive loam with limestone fragments in the basal part. The upper part of the bed exhibits rounded spots (up to 1 cm across) and inclusions of white carbonates (an ancient soil horizon?). The thickness is 10–15 cm.

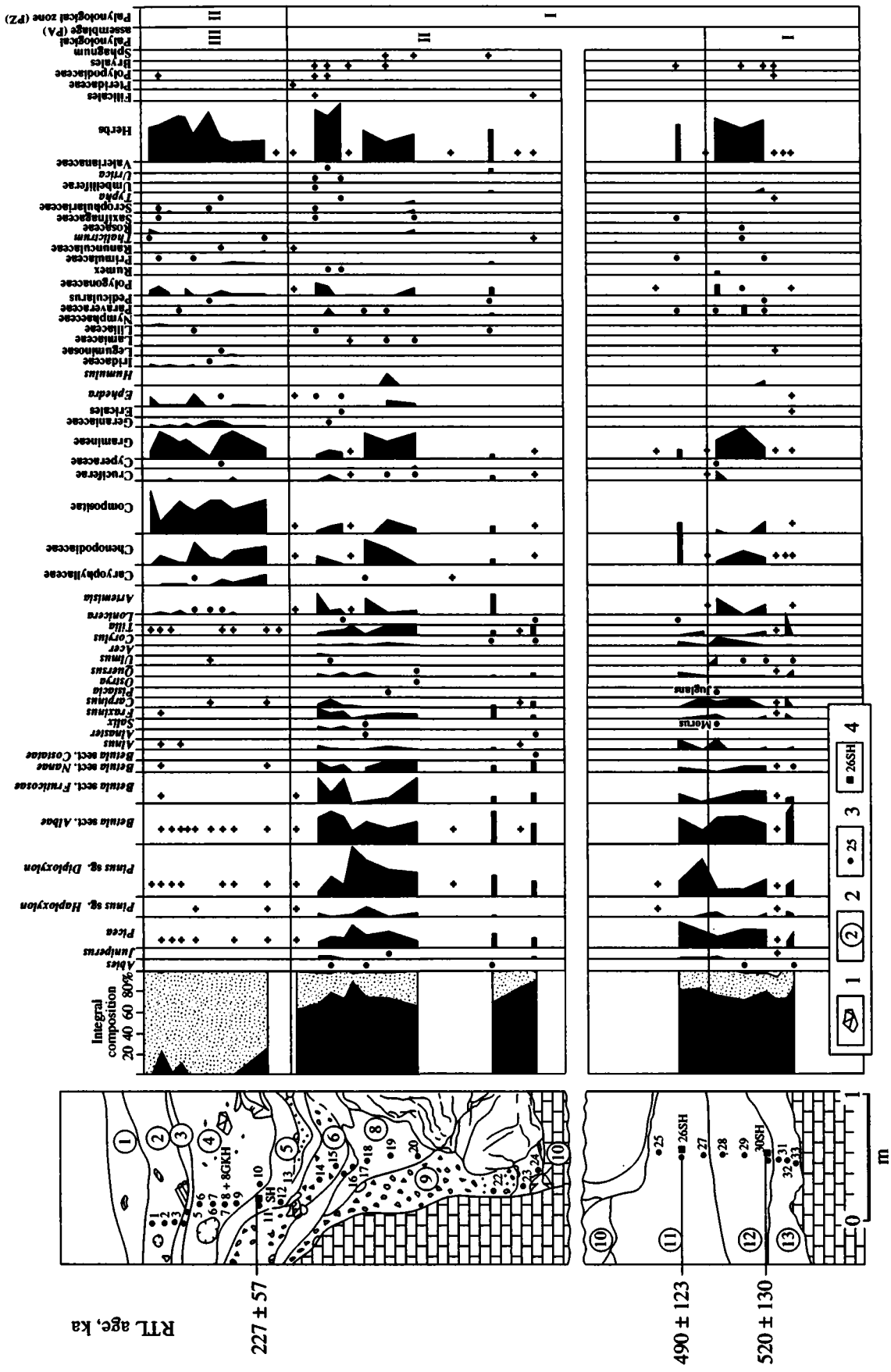

Fig. 5. Palynological diagram for deposits recovered in the main chamber pit, the central part of the Tsagan-Agui Cave (plotted by A.N. Simakova): (1) large limestone blocks; (2) bed number; (3) number of sample for the spore–pollen analysis; (4) number of sample dated by the RTL method (other symbols as in Fig. 3).

Bed 1: dark loam with inclusions of charcoal of the Historical Time and ceramic fragments. It actually represents the top of Bed 2. The thickness is 5–10 cm.

ANALYTICAL INVESTIGATIONS OF DEPOSITS FROM THE TSAGAN-AGUI CAVE

More than 100 samples collected from deposits of the Tsagan-Agui Cave have been analyzed in order to understand the succession of archeological finds and to interpret paleoecological data. The results obtained are partly presented in the paper.

Paleomagnetic analysis of rock samples collected by Devyatkin was performed by Z.N. Gnibedenko. The samples characterize the most fine-grained sediments, namely, clays and sandy loams of the northern and southern walls of the near-entrance longitudinal excavation, where sliding and gravitational processes did not disturb the beds. In total, 16 samples (5 × 5 cm in size) were analyzed. Samples 1–6 are from the lower (southern) grotto near the entrance, and samples 7–16 exemplify rocks of the northern wall in the cave entrance area (Fig. 4).

The preliminary stage of the paleomagnetic study was aimed at the obtaining magnetic and paleomagnetic characteristics of cave deposits in order to detect the Matuyama–Brunhes reversal (730 ka ago) and the fine structure of the paleomagnetic record.

The total collection used for paleomagnetic studies included 50 rock cubes (2.4 × 2.4 × 2.4 cm) cut from oriented samples. The magnetic susceptibility of the rocks (χ) and remanent magnetization were measured using the KLY-2 and ION-1 instruments, respectively. To remove the secondary magnetization, Aparin's system of equipment for thermal demagnetization (vertical modification) and a device for demagnetization in an alternating magnetic field (an original construction of the Institute of Geology and Geophysics) were used.

The studied clay, sandy loam, and fossil soil samples, all representing slightly magnetized rocks, differ from each other in magnetic properties. The magnetic susceptibility of the rocks varies from 30 to 155×10^{-5} SI. Some samples of the lower and upper rose soils yielded values outside this interval owing to their high χ values ($100–150 \times 10^{-5}$ SI). The NRM values correlate in detail with changes in magnetic susceptibility. Bed 5B is heterogeneous with respect to magnetic characteristics. The upper part of the bed (sample 6) is characterized by higher χ and Jn values (135×10^{-5} SI and 20×10^{-3} A/m, respectively) compared with its lower part, where χ is $30–60 \times 10^{-5}$ SI and Jn is 3.5×10^{-3} A/m. It is probable that such variations in magnetic parameters are related to the influence of climatic changes. The NRM direction was established using the Zijderveld temperature diagrams. The NRM is usually represented by a low-temperature and a high-temperature component, whose directions only slightly differ from each other. The low-temperature component, viscous in nature, is subordinate and disappears at a temperature of 100–200°C. After this step of demagnetization, samples show no changes in Jn direction during the whole thermal step up to 600°C. According to preliminary measurements, the NRM direction in samples from both sections of the entrance area (those of the lower grotto northern wall) is normal, which is characteristic of the Brunhes Chron. After the demagnetization procedures (temporal and thermal), the magnetic polarity direction in deposits of the lower grotto remained normal, whereas samples 7 and 8 from Bed 11 of the northern wall section area showed reversed polarity. It is probable that these samples correspond to the upper part of the Matuyama Chron.

Interpretation of magnetic data with due account for the results of palynological, lithological, radiothermoluminescence, and archeological studies allow us to suggest that the indicated samples mark the boundary interval between the Brunhes and Matuyama Chrons. Accordingly, the age of red deposits from the basal part of the near-entrance section of the Tsagan-Agui Cave is close to 0.7 Ma.

The palynological analysis of samples collected by Devyatkin was carried out by A. N. Simakova. Palynological characteristics are obtained for deposits of the northern wall of the near-entrance excavation and for those recovered in the test pit inside the main chamber of the Tsagan-Agui Cave. As the cave is located in the Gobi Altai area of the Central Asian arid belt (Vostokova *et al.*, 1995), the region is characterized by the following succession of climatic zones: deserts and semideserts, steppes and areas of cryoxerophitic herbaceous vegetation. The average annual temperature in the region is positive; the average temperature of the coldest month is −18°C, and that of the warmest month amounts to +23.3°C. The maximum precipitation is characteristic of summer, mainly July and August. The total annual precipitation is about 112–133 mm/year (Vostokova *et al.*, 1995).

According to the analysis of subfossil palynological spectra performed by E.M. Malaeva (*Pozdnii kainozoi...*, 1989), rainfall redistributes pollen most intensely near the lower boundary of the forest zone and in the upper part of the steppe zone. In central areas of the steppe zone, the abundance of pollen that is derived from forest areas and recorded in the most recent palynological spectra significantly decreases. As is shown (Krupenina, 1985), the present spore–pollen spectra in the forest–steppe zone are characterized by both high and insignificant proportions of arboreal pollen (forest- and steppe-type spectra, respectively). Therefore, all the information recorded in the fossil spore–pollen spectra should be used, with due account for the genesis of deposits and regional geomorphology, in order to determine the paleozones of vegetation.

The subfossil spectrum of a sample collected in the sair of the Tsagan-Agui Cave is dominated by herbaceous pollen (84%). Most abundant is pollen of Com-

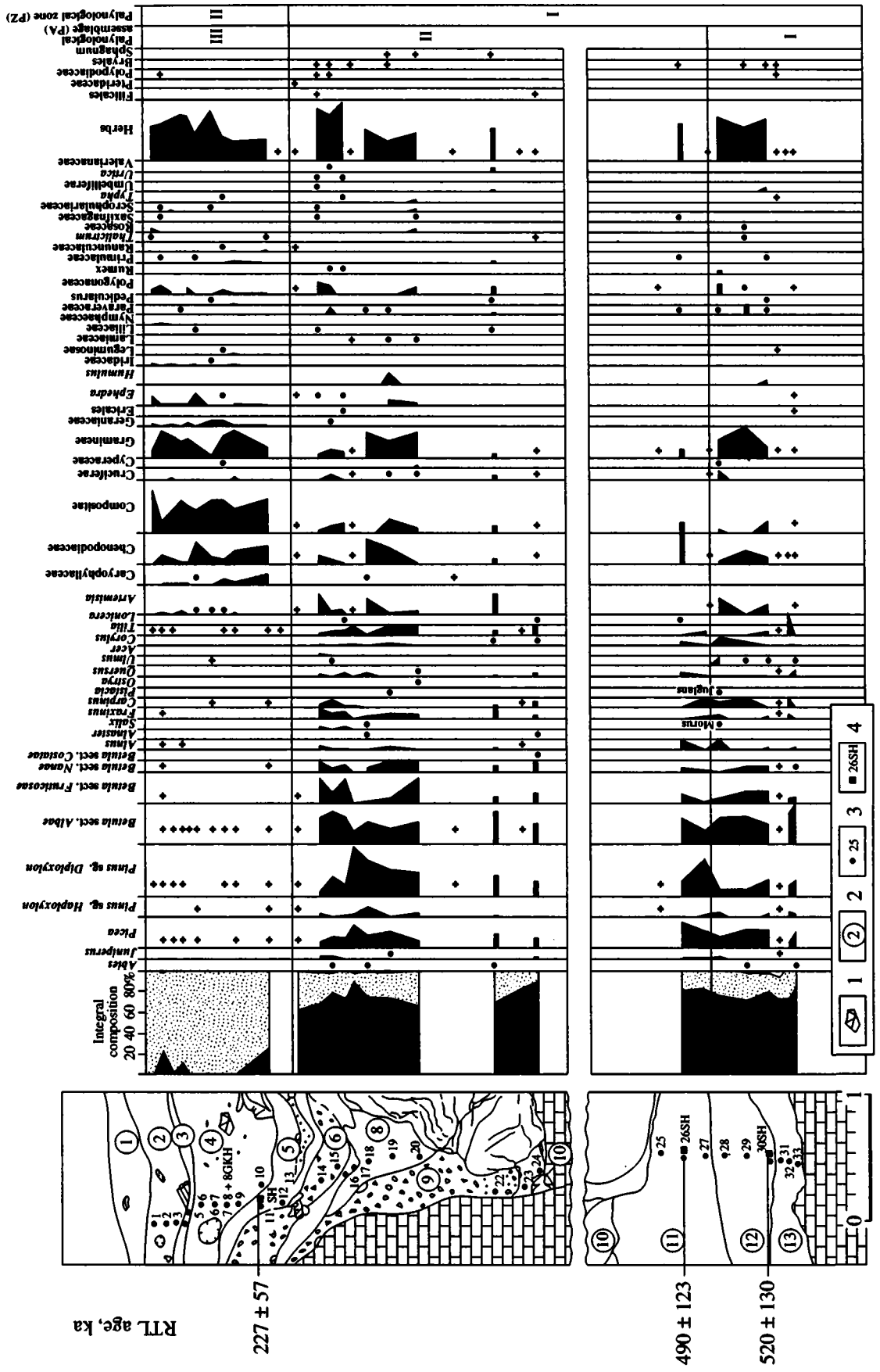
Palynological zone (PZ)
Palynological assemblage (PA)
Palynological Sphagnum Bryales Polypodiaceae Pteridaceae Filicales Herbs Valerianaceae Urtica Umbelliferae Typha Scrophulariaceae Saxifragaceae Cosmeae Thalictrum Ranunculaceae Primulaceae Rumex Polygonaceae Pedicularis Paraveratrum Nymphaeaceae Liliaceae Labiatae Leguminosae Iridaceae Humulus Ephedra Ericales Geraniaceae Gramineae Cyperaceae Cruciferae Compositae Chenopodiaceae Caryophyllaceae Artemisia Lonicera Tilia Corylus Acer Ulmus Quercus Ostrya Fraxinus Ptilacia Carpinus Salix Fraxinus Alnaster Alnus Betula sect. Costatae Betula sect. Nanae Betula sect. Albae Betula sect. Fruticosae Pinus sg. Diploxylon Pinus sg. Haploxylon Picea Juniperus Abies
Integral composition
20 40 60 80%
Juglans
Morus
1 2 3 4 25 26SH
RTL age, ka
227 ± 57
490 ± 123
520 ± 130
m

Fig. 5. Palynological diagram for deposits recovered in the main chamber pit, the central part of the Tsagan-Agui Cave (plotted by A.N. Simakova): (1) large limestone blocks; (2) bed number; (3) number of sample for the spore–pollen analysis; (4) number of sample dated by the RTL method (other symbols as in Fig. 3).

Bed 1: dark loam with inclusions of charcoal of the Historical Time and ceramic fragments. It actually represents the top of Bed 2. The thickness is 5–10 cm.

ANALYTICAL INVESTIGATIONS OF DEPOSITS FROM THE TSAGAN-AGUI CAVE

More than 100 samples collected from deposits of the Tsagan-Agui Cave have been analyzed in order to understand the succession of archeological finds and to interpret paleoecological data. The results obtained are partly presented in the paper.

Paleomagnetic analysis of rock samples collected by Devyatkin was performed by Z.N. Gnibedenko. The samples characterize the most fine-grained sediments, namely, clays and sandy loams of the northern and southern walls of the near-entrance longitudinal excavation, where sliding and gravitational processes did not disturb the beds. In total, 16 samples (5 × 5 cm in size) were analyzed. Samples 1–6 are from the lower (southern) grotto near the entrance, and samples 7–16 exemplify rocks of the northern wall in the cave entrance area (Fig. 4).

The preliminary stage of the paleomagnetic study was aimed at the obtaining magnetic and paleomagnetic characteristics of cave deposits in order to detect the Matuyama–Brunhes reversal (730 ka ago) and the fine structure of the paleomagnetic record.

The total collection used for paleomagnetic studies included 50 rock cubes (2.4 × 2.4 × 2.4 cm) cut from oriented samples. The magnetic susceptibility of the rocks (χ) and remanent magnetization were measured using the KLY-2 and ION-1 instruments, respectively. To remove the secondary magnetization, Aparin's system of equipment for thermal demagnetization (vertical modification) and a device for demagnetization in an alternating magnetic field (an original construction of the Institute of Geology and Geophysics) were used.

The studied clay, sandy loam, and fossil soil samples, all representing slightly magnetized rocks, differ from each other in magnetic properties. The magnetic susceptibility of the rocks varies from 30 to 155×10^{-5} SI. Some samples of the lower and upper rose soils yielded values outside this interval owing to their high χ values ($100–150 \times 10^{-5}$ SI). The NRM values correlate in detail with changes in magnetic susceptibility. Bed 5B is heterogeneous with respect to magnetic characteristics. The upper part of the bed (sample 6) is characterized by higher χ and Jn values (135×10^{-5} SI and 20×10^{-3} A/m, respectively) compared with its lower part, where χ is $30–60 \times 10^{-5}$ SI and Jn is 3.5×10^{-3} A/m. It is probable that such variations in magnetic parameters are related to the influence of climatic changes. The NRM direction was established using the Zijderveld temperature diagrams. The NRM is usually represented by a low-temperature and a high-temperature component, whose directions only slightly differ from each other. The low-temperature component, viscous in nature, is subordinate and disappears at a temperature of 100–200°C. After this step of demagnetization, samples show no changes in Jn direction during the whole thermal step up to 600°C. According to preliminary measurements, the NRM direction in samples from both sections of the entrance area (those of the lower grotto northern wall) is normal, which is characteristic of the Brunhes Chron. After the demagnetization procedures (temporal and thermal), the magnetic polarity direction in deposits of the lower grotto remained normal, whereas samples 7 and 8 from Bed 11 of the northern wall section area showed reversed polarity. It is probable that these samples correspond to the upper part of the Matuyama Chron.

Interpretation of magnetic data with due account for the results of palynological, lithological, radiothermoluminescence, and archeological studies allow us to suggest that the indicated samples mark the boundary interval between the Brunhes and Matuyama Chrons. Accordingly, the age of red deposits from the basal part of the near-entrance section of the Tsagan-Agui Cave is close to 0.7 Ma.

The palynological analysis of samples collected by Devyatkin was carried out by A. N. Simakova. Palynological characteristics are obtained for deposits of the northern wall of the near-entrance excavation and for those recovered in the test pit inside the main chamber of the Tsagan-Agui Cave. As the cave is located in the Gobi Altai area of the Central Asian arid belt (Vostokova *et al.*, 1995), the region is characterized by the following succession of climatic zones: deserts and semideserts, steppes and areas of cryoxerophitic herbaceous vegetation. The average annual temperature in the region is positive; the average temperature of the coldest month is −18°C, and that of the warmest month amounts to +23.3°C. The maximum precipitation is characteristic of summer, mainly July and August. The total annual precipitation is about 112–133 mm/year (Vostokova *et al.*, 1995).

According to the analysis of subfossil palynological spectra performed by E.M. Malaeva (*Pozdnii kainozoi...*, 1989), rainfall redistributes pollen most intensely near the lower boundary of the forest zone and in the upper part of the steppe zone. In central areas of the steppe zone, the abundance of pollen that is derived from forest areas and recorded in the most recent palynological spectra significantly decreases. As is shown (Krupenina, 1985), the present spore–pollen spectra in the forest–steppe zone are characterized by both high and insignificant proportions of arboreal pollen (forest- and steppe-type spectra, respectively). Therefore, all the information recorded in the fossil spore–pollen spectra should be used, with due account for the genesis of deposits and regional geomorphology, in order to determine the paleozones of vegetation.

The subfossil spectrum of a sample collected in the sair of the Tsagan-Agui Cave is dominated by herbaceous pollen (84%). Most abundant is pollen of Com-

positae (25%), Chenopodiaceae (18%) and *Ephedra* (18%). Common also is pollen of *Artemisia*, Caryophilaceae, and Linaceae. Arboreal pollen represented by single grains of *Pinus* and *Picea* is poorly preserved, probably transported from the Khangai Highland. The modern-day spore–pollen spectrum corresponds to semidesert steppe landscapes of the region, where climate is very arid.

The excavation along the northern wall near the entrance in the Tsagan-Agui Cave (Fig. 3). Spore–pollen spectra were analyzed in 14 samples collected from Beds 11, 10, 8, 7, 5, and 4. They are characterized by the low pollen content, and all spores and pollen show a moderate preservation degree. Samples 28 (Bed 4) and 18 (Bed 11) are virtually barren of spores and pollen. In other samples, their total content was sufficient to calculate proportions and to plot spore–pollen diagrams using the standard method of V.P. Grichuk.

As a result of testing different methods of maceration of spores and pollen (cavitational, alkaline, and pyrophosphatic), we selected the following procedure. Decarbonatization of the samples was performed in hot hydrochloric acid (HCl), and the residue was elutriated from fine particles in sodium pyrophosphate ($NaHPO_4$). Organic remains were separated in a heavy liquid with a specific weight of 2.2 g/cm^3; elimination of the silicate fraction, if needed, was performed using hydrofluoric acid (HF) and acetolysis. Redeposited Cretaceous pollen is present in three samples (sample 25, Bed 5; sample 23, Bed 7; and sample 22, Bed 8).

The analysis of spore–pollen diagrams (Fig. 3) reveals two palynological zones (PZ) and four palynological assemblages (PA). The first palynological zone includes one palynological assemblage (I) macerated from Beds 11 and 10. The second palynological zone corresponds to Beds 8 and 7, Bed 5, and the basal part of Bed 4, which yielded palynological assemblages II, III, and IV, respectively.

Palynological assemblage I is dominated by arboreal and frutescent pollen (67–87%). Most abundant is pollen of deciduous taxa *Carpinus* (up to 39%), *Fraxinus* (up to 14%), *Ostryopsis davidiana* (up to 9%), *Quercus mongolica* (up to 7%), and *Betula* sect. *Albae* (up to 18%). Pollen of *Cedrus, Picea*, and *Pinus* represents coniferous plants. Exotics of modern Mongolia are represented by pollen grains of *Carpinus, Fraxinus, Myrica, Ostrya*, and *Tilia*. The herbaceous group includes single pollen grains of Chenopodiaceae, Cyperaceae, Liliaceae, Paraveraceae, Ranunculaceae, and Violaceae. Spores are missing except for single Bryales grains.

This composition of spore–pollen spectra suggests the past development of mixed broad-leaved and coniferous broad-leaved forests in the region. The climate of that time was humid and relatively warm, with precipitation exceeding 400–500 mm/year and winter temperatures above –18°C. The described floral assemblage may indicate that the host deposits are not younger than the middle Pleistocene (according to the European scale), because pollen of *Ostrya* and *Myrica* never occurs in younger deposits of Mongolia in contrast to that of other of deciduous forms (*Pozdnii kainozoi...*, 1989). This conclusion is supported by the paleomagnetic and RTL data.

The second palynological zone is marked by a sharp decrease in abundance of arboreal pollen and by a preponderance of Chenopodiaceae and Compositae in the herbaceous group. Vegetation of this period was characterized by contrasting dynamic changes in plant communities.

Palynological assemblage II shows a noticeable decrease in abundance of arboreal and frutescent pollen and also contrasting variations in the general spectra composition. The herbaceous pollen content ranges here from 72 to 98%. Spores are virtually absent. The arboreal–frutescent group is represented by pollen of *Pinus* sg. *Diploxylon, Carpinus, Ostryopsis* and by single grains of *Alnus, Salix, Pistacia,* and *Betula*, and *Fraxinus*. Compositae forms prevail amid herbaceous pollen (up to 85%). Usual components of spore–pollen spectra are also Chenopodiaceae (up to 32%), Cruciferae (up to 6%), *Ephedra* (up to 21%), and Polygonaceae (up to 10%) associated with less abundant pollen of Liliaceae, Nymphaeceae, and Umbelliferae. The spectrum includes spores of *Filicales*, Polypodiaceae, Lycopodiaceae, and Bryales.

Spore–pollen spectra of palynological assemblage II correspond to arid environments of steppe landscapes. Distribution areas of forest vegetation are sharply reduced, and this plant community became less diverse. The number of deciduous forms decreased in the arboreal group. The climate of that time was relatively arid, though more humid than it is now.

Palynological assemblage III is dominated by herbaceous and frutescent pollen (68–92%). Its characteristic feature consists in a sharply increased content of Chenopodiaceae (up to 75%) and reduced abundance of Compositae (up to 21%). Pollen of *Artemisia*, Cruciferae, Gramineae, and *Ephedra* is present here in association with that of *Thaictrum*, Rosaceae, Saxifragaceae, Umbelliferae, and *Urtica*. The coniferous group includes only pollen of *Pinus* sg. *Diploxylon* (up to 79%); and single pollen grains of *Alnus, Carpinus, Viburnum*, Moraceae, and *Fraxinus* represent deciduous forms. The composition of spore–pollen spectra indicates a preponderance of steppe ecosystems and landscapes, where coniferous broad-leaved and meadow formations were subordinate. The climate of this stage became noticeably more arid and slightly colder than that corresponding to palynological assemblage II.

Beds 8, 7, 5, and the basal part of Bed 4, which yield palynological assemblages II and III, are estimated to be as old as the second half of the middle–late Pleis-

tocene, because the respective arid epochs were characterized by significant development of forest formations incorporating a series of forms (*Abies, Picea*, Oleaceae, Moraceae, *Pistacia, Tilia*, and *Viburnum*) missing now from vegetation of the area.

Palynological assemblage IV is recorded from the upper part of Bed 4. The arboreal and frutescent pollen, mostly that of *Betula* sect. Albae (37%) and *Betula* sect. Fruticose (17%), represents 67% of the assemblage. Pollen of *Alnus, Picea, Pinus, Fraxinus, Quercus*, and *Ostryopsis* is constantly present. Pollen of *Salix* and *Corylus* occurs as single grains. The herbaceous and fruticulose groups mainly consist of Chenopodiaceae (36%) and *Artemisia* (8%) associated with subordinate *Ephedra*, Polygonaceae, and Umbelliferae. Spores represent taxa *Ophyoglossum* and Bryales.

Palynological assemblage IV probably corresponds to the development period of steppe ecosystems. The period was marked by a wide distribution of *Artemisia*–Chenopodiaceae formations. The belt of coniferous–birch forests with an insignificant admixture of broad-leaved forms was characteristic at that time of mountains. The phytocoenoses in question most likely existed under conditions of a relatively humid and warm climate. The age of the upper Bed 4 can be estimated as corresponding to the late Pleistocene. This is supported by the fact that, according to results of studies at the floodplain levels, pollen of deciduous *Alder, Corylus, Ulmus*, and *Tilia* occurred in some northern river valleys of Mongolia until the Subboreal period of the Holocene (Malaeva and Murzaeva, 1987).

The formation period of deposits recovered in excavations shows the general trend of increasing aridity and progressing continental properties of the climate that was associated with distinct climatic fluctuations (arid–humid). Two distinguished periods of humid climate correspond to the formation intervals of rose soils of Beds 10 and 11, and of the upper part of Bed 4.

The test pit in the main chamber of the Tsagan-Agui Cave (Fig. 5). Among 33 samples selected for palynological analysis, only 5 samples from Beds 13, 11, 9, and 5 appeared to be virtually barren of spores and pollen. Other samples yielded, according to calculation results, from 150 to 313 grains of spores and pollen. Single reworked spores and pollen grains are registered in Beds 4, 5, and 8.

The plotted spore–pollen diagrams revealed two palynological zones, which sharply differ from each other in the general composition of pollen spectra. Two palynological assemblages from Beds 6–13, which consist of abundant arboreal pollen and show predominance of broad-leaved forms but no contrasting changes in plant communities, characterize the first palynological zone.

Palynological assemblage I from Beds 12 and 13 is dominated by arboreal and frutescent pollen (75–90%). Most abundant is pollen of *Pinus* (up to 25%), *Picea* (up to 35%), and arboreal birch species (up to 28%). Pollen of broad-leaved *Alnus* (up to 15%), *Carpinus* (up to 10%), *Quercus mongolica* (up to 4%), *Ulmus* (up to 6%), *Corylus* (up to 8%), *Tilia* (up to 22%) is another characteristic component of the assemblage. Pollen of Moraceae, *Lonicera*, and *Juglans* occurs here as single grains. Gramineae, Chenopodiaceae, *Artemisia*, and Paraveraceae are preponderant taxa of the herbaceous and fruticulose groups.

This composition of spore–pollen spectra suggests the past existence of well-developed forest communities in the mountains and of wormwood–gramineous formations around the study area. The climate of that time was more humid than it is now and relatively warm. The high content of arboreal pollen, including that of broad-leaved forms and single pollen grains of *Juglans*, allow us to consider Beds 12 and 13 as older in age than the late Pleistocene.

Palynological assemblage II characterizes spore–pollen spectra of Beds 6–11, where arboreal pollen is preponderant. Most abundant is pollen of *Picea* (up to 50%), *Pinus* (up to 24%), and *Betula* (up to 55%). Pollen of *Abies, Alder, Ulmus, Carpinus, Acer, Quercus, Tilia*, and *Lonicera* is also present in the beds. Moraceae and *Juglans* became extinct at this level. The herbaceous formation also changed its composition, because Gramineae and *Artemisia* are somewhat less abundant here and Chenopodiaceae become dominant. These taxa coexisted with Compositae and Polygonaceae and also with Umbelliferae, *Thalictrum*, Valerianaceae, Cyperaceae, and *Typha* exemplified by single pollen grains. The diversity of spores increases, and Polypodiaceae and *Sphagnum* appear in the sporogenous group.

The composition of above spore–pollen spectra is indicative of progressive cooling and relatively high humidity of the climate. This is evident from indications of widening forest areas rich in coniferous forms and from the increased content of pollen of frutescent taxa *Betula* and *Salix*. The presence of *Typha* and Cyperaceae pollen allows an assumption that still and slowly flowing waters existed near the cave at that time.

Palynological assemblage III from Beds 2–5 is marked by preponderance of herbaceous pollen (75%). The arboreal–frutescent group is represented in this case by rare pollen of *Picea, Pinus*, and *Betula* in association with single pollen grains of *Alnus, Fraxinus, Carpinus*, and *Tilia*. It should be noted that some pollen grains look reworked. Gramineae, Compositae, Chenopodiaceae, *Ephedra*, and Polygonaceae prevail amid the herbaceous taxa. All this indicates a sharp reduction of arboreal forms and the virtual disappearance of broad-leaved forest-forming species.

At the same time, the study area was mainly occupied by steppe formations. Forests, which mostly consisted of coniferous small-leaved forms and were considerably reduced in area, still existed in the mountains nearby. The climate was significantly arid. The deposits

bearing the third palynological assemblage are dated back to the middle–late Pleistocene.

It should be noted that the described succession of palynological assemblages from the cave recorded two major stages of vegetation development. Different phytocoenoses of the stages reflected sharp changes in climate aridity. On the basis of spore–pollen spectra, one may suggest that deposits corresponding to the first palynological zone and adjacent to the northern near-entrance wall of the cave are older that those in the pit. It is also possible that the content of arboreal and frutescent pollen is overestimated in the first palynological zone distinguished in the central test pit. This site located inside the cave far from the entrance was reliably sheltered from direct pollen precipitation and more completely reflects the composition of the surrounding zonal vegetation. In addition, the arboreal pollen could be redeposited to a certain extent, if we take into consideration the complex stratification of the deposits and their gravitational and indentation structures produced when sediments squeezed into underlying deposits.

On the basis of magnetostratighraphic data and the position of the Matuyama–Brunhes reversal at the top of Bed 11 (the entrance area of the cave), the first palynological assemblage of this section is dated back to the lower middle Pleistocene (older than 0.73 Ma). Palynological assemblages I and II from the central test pit may be younger than, or partly synchronous (in the basal part of the section) to, the previous one. The uppermost beds of both sections recovered by excavations near the entrance and in the central part of the cave are attributed to the upper Pleistocene–basal Holocene.

Inasmuch as the cave is located in the southern part of Mongolia, which is almost unstudied with respect to palynology, direct correlation of the studied sections with those from other Mongolian regions is impossible. It is probable, for instance, that some representatives of the broad-leaved flora became extinct due to cooling in northern Mongolia earlier than in southern areas, where steppe and desert landscapes could have appeared later. This agrees with the similarity of the studied spore–pollen spectra, which are presumably of the middle Pleistocene age, with palynological assemblages of the late Pliocene deposits in northern Mongolia (the Khangai and Khantei ridges) and with those of the middle Pleistocene sediments deposited in the high plains and depressions of southeastern Mongolia (*Pozdnii kainozoi...*, 1989).

In general, the cave deposits accumulated under the influence of persistent dynamic changes in composition of the mountainous forest belt, when the climate was more humid than at present. The belt existed during the entire Pleistocene. Forest–steppe and meadow–steppe phytocoenoses represented the vegetation zones of the piedmont areas of the Gobi Altai. From the base upward, the studied section recorded the aridity increase, the growing contrast of the climate, and compositional impoverishment of the plant assemblages. According to both palynological and lithological data, "cold" periglacial types of spectra have not been recorded

Radioisotopic studies were performed by O.B. Parunin at the Laboratory of Recent Deposits and Pleistocene Paleogeography, Faculty of Geography, Moscow State University. Fragments of calcite crystals collected from the basal portion of Bed 7 near the northern wall of the cave entrance area (gravitational horizon) yielded the radiocarbon date of 42 ka (MSU–LUU9), which seems to be too big for the data obtained by this method. Two factors may be responsible for this: (1) Calcite could have been crystallized from the $CaCO_3$ solution derived from older limestones, and this resulted in the age overestimation. (2) The calcite formation time exceeds the maximum determination limit of the radiocarbon method. In any case, the date obtained is meaningless for the age interpretation of sediments enclosing calcite

Radiothermoluminescence (RTL) analysis was performed by O.A. Kulikov at the Laboratory of Radiation Monitoring, Environment Radioactivity and RTL Dating, Moscow State University. Samples collected by Devyatkin for the analysis are from the sections of the northern (TL-8, 11, 12) and southern parts of the entrance area (TL-1, 4, 6) and from the central test pit (TL–11P 26P, 30P) of the Tsagan-Agui Cave (Table 1). The sampling sites are shown in Figs. 3–5.

The dating procedure has been described earlier (Vlasov and Kulikov, 1988). The monomineral quartz fraction representing the RTL-detector (paleodosimeter) was extracted from selected samples to determine afterward the total accumulated RTL. The thermoluminescence curve of a paleodosimeter usually represents a superposition of elementary peaks of different sensitivities relative to the absorbed dose and different thermoluminescence parameters. One of the stages during RTL age determination is aimed at defining an elementary peak in the thermal range of 230–260°C. To discriminate the elementary peaks, we used the modified Alentsev method (Vlasov *et al.*, 1980). The defined elementary peak in the thermoluminescence curve of the paleodosimeter was used for subsequent irradiation and calibration.

The calibration procedure consists in determining the dosing dependence of an elementary peak in order to measure the dose of ionizing radiation accumulated by the paleodosimeter (quartz) in the host sediments under natural environments. The calibration was performed by means of superposition of successive doses from a gamma-radiation source on the natural dose accumulated by the analyzed sample. Further, the functional relation between the total radiothermoluminescence measured in the laboratory as the RTL sum and the dose absorbed by the detector (quartz) in natural environments was determined. Determination of the

energy accumulation in the paleodosimeter is the main task in the RTL dating procedure. The latter is a source of significant errors in age determination.

Almost all the available techniques of RTL dating are based on the linear dependence of energy accumulation in the paleodosimeter, i.e., the linear equation relating the total accumulated luminescence and absorbed irradiation dose. We established that the linear equation describes approximately how the RTL of solid paleodosimeters depends on irradiation doses, and only the initial part of the curve (1–10%) can be used for the analysis. This approach to the determination of RTL age limits is substantially different from traditional methods accepted in other countries. For instance, the maximum age determinable by our approach is 1–1.5 Ma, whereas the value usually accepted in foreign approaches is 150–200 ka.

The following conclusions can be drawn on the basis of the results obtained (Table 1):

(1) The age range of the cave deposits spans a significant geochronological interval (more than 500 ka), thus being in agreement with paleomagnetic and palynological data.

(2) The RTL dates for the pit section of the Great Grotto are in the normal succession with respect to the superposition of the dated samples. Samples 11 and 12 from the entrance area yielded approximately the same age with due account for measurement errors.

In our opinion, the obtained RTL dates are reliable in general. They are controlled by the results of other methods and can be used for the geochronological interpretation of stratigraphic and archeological successions.

Archeological materials from the Tsagan-Agui Cave were obtained during the field work of 1995 and later (Derevyanko and Petrin, 1995; Derevyanko *et al.*, 1996). All excavations and pits in the Tsagan-Agui Cave were studied in a bed-by-bed manner to find archeological materials. On the basis of techno–typological features, three archeological complexes of artifacts different in age are defined at present.

Complex 1 is represented by a small amount of archeological stone artifacts (74 specimens) and originates from the upper part of cave deposits (Beds 1–3 of the entrance area and Beds 1 and 2 recovered in the pit inside the main chamber). The age of the complex is estimated to be the terminal Paleolithic–Neolithic.

Complex 2 (241 artifacts) originates from the middle part of the cave deposits (Beds 4–6 of the entrance area and Beds 1 and 2 recovered in the pit inside the main chamber). The RTL age of the upper part of Bed 4 in the entrance area (the upper rose soil) is 175 ± 44 ka, and that of Bed 5 in the main chamber is 277 ± 57 ka. Artifacts of this complex "show fairly clear Levallois-type patterns, though with some features characteristic of technologies transitional to the late Paleolithic" (Derevyanko *et al.*, 1996, p. 27). The age of the complex is estimated to be the Mousterian and the late Mousterian–transitional to the late Paleolithic in the upper part of the beds.

Table 1. RTL dates for deposits of the Tsagan-Agui Cave

Sample and bed number	Laboratory index	RTL age, ka
Northern edge		
Tl-8 (Bed 8)	RTL-800	470 ± 117
Tl-11 (Bed 11)	RTL-801	122 ± 30
Tl-12 (Bed 12)	RTL-802	175 ± 44
Central pit		
Tl-26SH (Bed 11)	RTL-803	490 ± 123
Tl-11SH (Bed 5)	RTL-804	227 ± 57
Tl-30SH (Bed 12)	RTL-805	520 ± 130
Southern edge		
Tl-1 (Bed 6)	RTL-922	131 ± 35
Tl-4 (Bed 4)	RTL-921	126 ± 32
Tl-6 (Bed 2)	RTL-923	7 ± 3

Complex 3 (295 artifacts) originates from Beds 7–9 in the entrance area and from Beds 9–13 recovered in the pit inside the main chamber. The RTL age of Bed 9 in the entrance area is 122 ± 30 ka and that of Beds 11 and 12 in the main chamber ranges from 490 ± 123 and 520 ± 130 ka, but the last dates should be verified. Based on the results of a techno–typological analysis of artifacts, it is assumed that the complex characterizes "the early Mousterian epoch and probably the younger period" (Derevyanko *et al.*, 1996, p. 28).

We suspect that an older complex of the Tsagan-Agui Cave can be distinguished in addition. It is related to red sediments recovered in the southern wall of the excavation near the cave entrance, where a large pebble core with a single flake removal surface was found. It is quite probable that "this artifact belongs to the pre-Acheulian time" (Derevyanko *et al.*, 1996, p. 68). Olsen (1997, p. 106) also reported that the lower part of the same section yielded "a small collection of stone tools, including a bifacial flat–convex hand axe and single pebble core with a striking platform; the same deposits also enclose microfossils and charcoal..."

Actually, the red sand and clay enclosing the artifacts are similar in lithology to pre-Quaternary sediments. The RTL dates (131 ± 35 and 126 ± 32 ka) for these sediments recovered near the southern wall of the cave are evidence against their old age. The sediments themselves and the found artifacts appear to be redeposited from the pebblestone cover developed northward. This cover is promising for *in situ* finds of the oldest archeological complex.

When considering the ages of archeological complexes from the Tsagan-Agui Cave (Derevyanko and Petrin, 1995) and the RTL dates obtained, we should note the following.

bearing the third palynological assemblage are dated back to the middle–late Pleistocene.

It should be noted that the described succession of palynological assemblages from the cave recorded two major stages of vegetation development. Different phytocoenoses of the stages reflected sharp changes in climate aridity. On the basis of spore–pollen spectra, one may suggest that deposits corresponding to the first palynological zone and adjacent to the northern near-entrance wall of the cave are older that those in the pit. It is also possible that the content of arboreal and frutescent pollen is overestimated in the first palynological zone distinguished in the central test pit. This site located inside the cave far from the entrance was reliably sheltered from direct pollen precipitation and more completely reflects the composition of the surrounding zonal vegetation. In addition, the arboreal pollen could be redeposited to a certain extent, if we take into consideration the complex stratification of the deposits and their gravitational and indentation structures produced when sediments squeezed into underlying deposits.

On the basis of magnetostratighraphic data and the position of the Matuyama–Brunhes reversal at the top of Bed 11 (the entrance area of the cave), the first palynological assemblage of this section is dated back to the lower middle Pleistocene (older than 0.73 Ma). Palynological assemblages I and II from the central test pit may be younger than, or partly synchronous (in the basal part of the section) to, the previous one. The uppermost beds of both sections recovered by excavations near the entrance and in the central part of the cave are attributed to the upper Pleistocene–basal Holocene.

Inasmuch as the cave is located in the southern part of Mongolia, which is almost unstudied with respect to palynology, direct correlation of the studied sections with those from other Mongolian regions is impossible. It is probable, for instance, that some representatives of the broad-leaved flora became extinct due to cooling in northern Mongolia earlier than in southern areas, where steppe and desert landscapes could have appeared later. This agrees with the similarity of the studied spore–pollen spectra, which are presumably of the middle Pleistocene age, with palynological assemblages of the late Pliocene deposits in northern Mongolia (the Khangai and Khantei ridges) and with those of the middle Pleistocene sediments deposited in the high plains and depressions of southeastern Mongolia (*Pozdnii kainozoi...*, 1989).

In general, the cave deposits accumulated under the influence of persistent dynamic changes in composition of the mountainous forest belt, when the climate was more humid than at present. The belt existed during the entire Pleistocene. Forest–steppe and meadow–steppe phytocoenoses represented the vegetation zones of the piedmont areas of the Gobi Altai. From the base upward, the studied section recorded the aridity increase, the growing contrast of the climate, and compositional impoverishment of the plant assemblages. According to both palynological and lithological data, "cold" periglacial types of spectra have not been recorded

Radioisotopic studies were performed by O.B. Parunin at the Laboratory of Recent Deposits and Pleistocene Paleogeography, Faculty of Geography, Moscow State University. Fragments of calcite crystals collected from the basal portion of Bed 7 near the northern wall of the cave entrance area (gravitational horizon) yielded the radiocarbon date of 42 ka (MSU–LUU9), which seems to be too big for the data obtained by this method. Two factors may be responsible for this: (1) Calcite could have been crystallized from the $CaCO_3$ solution derived from older limestones, and this resulted in the age overestimation. (2) The calcite formation time exceeds the maximum determination limit of the radiocarbon method. In any case, the date obtained is meaningless for the age interpretation of sediments enclosing calcite

Radiothermoluminescence (RTL) analysis was performed by O.A. Kulikov at the Laboratory of Radiation Monitoring, Environment Radioactivity and RTL Dating, Moscow State University. Samples collected by Devyatkin for the analysis are from the sections of the northern (TL-8, 11, 12) and southern parts of the entrance area (TL-1, 4, 6) and from the central test pit (TL–11P 26P, 30P) of the Tsagan-Agui Cave (Table 1). The sampling sites are shown in Figs. 3–5.

The dating procedure has been described earlier (Vlasov and Kulikov, 1988). The monomineral quartz fraction representing the RTL-detector (paleodosimeter) was extracted from selected samples to determine afterward the total accumulated RTL. The thermoluminescence curve of a paleodosimeter usually represents a superposition of elementary peaks of different sensitivities relative to the absorbed dose and different thermoluminescence parameters. One of the stages during RTL age determination is aimed at defining an elementary peak in the thermal range of 230–260°C. To discriminate the elementary peaks, we used the modified Alentsev method (Vlasov *et al.*, 1980). The defined elementary peak in the thermoluminescence curve of the paleodosimeter was used for subsequent irradiation and calibration.

The calibration procedure consists in determining the dosing dependence of an elementary peak in order to measure the dose of ionizing radiation accumulated by the paleodosimeter (quartz) in the host sediments under natural environments. The calibration was performed by means of superposition of successive doses from a gamma-radiation source on the natural dose accumulated by the analyzed sample. Further, the functional relation between the total radiothermoluminescence measured in the laboratory as the RTL sum and the dose absorbed by the detector (quartz) in natural environments was determined. Determination of the

energy accumulation in the paleodosimeter is the main task in the RTL dating procedure. The latter is a source of significant errors in age determination.

Almost all the available techniques of RTL dating are based on the linear dependence of energy accumulation in the paleodosimeter, i.e., the linear equation relating the total accumulated luminescence and absorbed irradiation dose. We established that the linear equation describes approximately how the RTL of solid paleodosimeters depends on irradiation doses, and only the initial part of the curve (1–10%) can be used for the analysis. This approach to the determination of RTL age limits is substantially different from traditional methods accepted in other countries. For instance, the maximum age determinable by our approach is 1–1.5 Ma, whereas the value usually accepted in foreign approaches is 150–200 ka.

The following conclusions can be drawn on the basis of the results obtained (Table 1):

(1) The age range of the cave deposits spans a significant geochronological interval (more than 500 ka), thus being in agreement with paleomagnetic and palynological data.

(2) The RTL dates for the pit section of the Great Grotto are in the normal succession with respect to the superposition of the dated samples. Samples 11 and 12 from the entrance area yielded approximately the same age with due account for measurement errors.

In our opinion, the obtained RTL dates are reliable in general. They are controlled by the results of other methods and can be used for the geochronological interpretation of stratigraphic and archeological successions.

Archeological materials from the Tsagan-Agui Cave were obtained during the field work of 1995 and later (Derevyanko and Petrin, 1995; Derevyanko *et al.*, 1996). All excavations and pits in the Tsagan-Agui Cave were studied in a bed-by-bed manner to find archeological materials. On the basis of techno–typological features, three archeological complexes of artifacts different in age are defined at present.

Complex 1 is represented by a small amount of archeological stone artifacts (74 specimens) and originates from the upper part of cave deposits (Beds 1–3 of the entrance area and Beds 1 and 2 recovered in the pit inside the main chamber). The age of the complex is estimated to be the terminal Paleolithic–Neolithic.

Complex 2 (241 artifacts) originates from the middle part of the cave deposits (Beds 4–6 of the entrance area and Beds 1 and 2 recovered in the pit inside the main chamber). The RTL age of the upper part of Bed 4 in the entrance area (the upper rose soil) is 175 ± 44 ka, and that of Bed 5 in the main chamber is 277 ± 57 ka. Artifacts of this complex "show fairly clear Levallois-type patterns, though with some features characteristic of technologies transitional to the late Paleolithic" (Derevyanko *et al.*, 1996, p. 27). The age of the complex is estimated to be the Mousterian and the late Mousterian–transitional to the late Paleolithic in the upper part of the beds.

Table 1. RTL dates for deposits of the Tsagan-Agui Cave

Sample and bed number	Laboratory index	RTL age, ka
Northern edge		
Tl-8 (Bed 8)	RTL-800	470 ± 117
Tl-11 (Bed 11)	RTL-801	122 ± 30
Tl-12 (Bed 12)	RTL-802	175 ± 44
Central pit		
Tl-26SH (Bed 11)	RTL-803	490 ± 123
Tl-11SH (Bed 5)	RTL-804	227 ± 57
Tl-30SH (Bed 12)	RTL-805	520 ± 130
Southern edge		
Tl-1 (Bed 6)	RTL-922	131 ± 35
Tl-4 (Bed 4)	RTL-921	126 ± 32
Tl-6 (Bed 2)	RTL-923	7 ± 3

Complex 3 (295 artifacts) originates from Beds 7–9 in the entrance area and from Beds 9–13 recovered in the pit inside the main chamber. The RTL age of Bed 9 in the entrance area is 122 ± 30 ka and that of Beds 11 and 12 in the main chamber ranges from 490 ± 123 and 520 ± 130 ka, but the last dates should be verified. Based on the results of a techno–typological analysis of artifacts, it is assumed that the complex characterizes "the early Mousterian epoch and probably the younger period" (Derevyanko *et al.*, 1996, p. 28).

We suspect that an older complex of the Tsagan-Agui Cave can be distinguished in addition. It is related to red sediments recovered in the southern wall of the excavation near the cave entrance, where a large pebble core with a single flake removal surface was found. It is quite probable that "this artifact belongs to the pre-Acheulian time" (Derevyanko *et al.*, 1996, p. 68). Olsen (1997, p. 106) also reported that the lower part of the same section yielded "a small collection of stone tools, including a bifacial flat–convex hand axe and single pebble core with a striking platform; the same deposits also enclose microfossils and charcoal..."

Actually, the red sand and clay enclosing the artifacts are similar in lithology to pre-Quaternary sediments. The RTL dates (131 ± 35 and 126 ± 32 ka) for these sediments recovered near the southern wall of the cave are evidence against their old age. The sediments themselves and the found artifacts appear to be redeposited from the pebblestone cover developed northward. This cover is promising for *in situ* finds of the oldest archeological complex.

When considering the ages of archeological complexes from the Tsagan-Agui Cave (Derevyanko and Petrin, 1995) and the RTL dates obtained, we should note the following.

Complex 1 (terminal late Paleolithic–Neolithic) is without RTL dates and can be reliably dated using the radiocarbon method.

Complex 2 (middle—late Mousterian and transition to the late Paleolithic) is dated by the RTL method back to 175 ± 44 and 122 ± 30 ka (the entrance area). The latter date needs to be verified. In the main chamber, the upper horizons of the complex are dated as 227 ± 57 ka old.

Complex 3 (early Mousterian and transition to the older time), or rather its lower part (Beds 10 and 11) recovered in the main chamber, is dated by the RTL method back to 490 ± 123 and 520 ± 130 ka. Taking into consideration these old dates, the complex cannot be of the Mousterian age. Most likely, the dates characterize an older complex correlative on the basis of lithology with the lower part of the section in the entrance area, where the RTL data obtained is 470 ± 117 ka, and presumably with other deposits of the entrance grotto lacking such dates so far. It is important that the RTL dates for Complex 2 (middle–late Mousterian) are close to the dates of 280 ± 56, 224 ± 45, and 155 ± 31 ka measured for Beds 21 and 22 in the Denisova Cave known in the Altai Ridge. This supports the assumption that the Mousterian in the Altai–Sayan region and Mongolia is older than elsewhere (Derevyanko *et al.*, 1992).

These old artifacts are probably similar to those from the "Narin-Gol" pebble complex from high terraces and to the heavily abraded tools of the Flint Valley attributed to the pre-Mousterian epoch (Derevyanko *et al.*, 1990, 1996).

The age of the deposits from the Tsagan-Agui Cave is based on all stratigraphic, palynological, paleomagnetic, radiothermoluminescence, and archeological data available at present for the entrance area and main chamber of the cave. Despite the small thickness of the cave deposits, they span a significant stratigraphic interval, presumably ranging from the lower Pleistocene to Holocene; i.e., their formation period started 0.7 Ma ago at least and lasted from the late Matuyama Chron throughout the Brunhes Chron. It would be logical to assume that not all the events of this geochronological period have been recorded in the section displaying complex stratification and incorporating gravitational–sliding horizons. Therefore, direct correlation of the section with any stratigraphic scheme would be premature.

The archeological data allow us to distinguish three heterochronous artifact complexes: (1) the terminal Paleolithic–Neolithic; (2) the middle–late Mousterian and transitional to the late Paleolithic; and (3) the early Mousterian and transitional to the older period. The future recognition of additional very old complex (pre-Acheulian or early Acheulian) is also possible.

The problem of correlation of the stratified Tsagan-Agui site with other archeological sites of the open-air type is rather difficult. We took into consideration several criteria when correlating them. The geological–geomorphological position of sites on river terraces or proluvial aprons offers an opportunity to define the relative succession of different archeological complexes on the basis of terrace ages. The complexes are discriminated using the technological–typological features of stone flaking. Considering these features together with the eolian abrasion degree of artifacts, we may outline a succession of heterochronous archeological industries. The direct arrangement of the open-air sites into a stratigraphic succession is possible only on the basis of their correlation with stratified sites of the Tsagan-Agui type. Our version of such a correlation is shown in Table 2.

The following **succession of geological and geomorphological events** can be outlined:

(1) The uplift of frontal ridges of the Gobi Altai during the Pliocene–Pleistocene triggered the formation of a system of erosional valleys displaying a complex of high pebble–boulder terraces mainly composed of reworked Upper Cretaceous deposits. As is evident from palynological data, the climate of that time was relatively warm and humid, and many streams ran across the region. Similar coeval terraces are known in the southern slope of the Khangai Ridge between the Baidarik and Tatsin-Gol rivers and also in the Burunkhurai depression near the piedmonts of the Mongolian Altai.

(2) The oldest archeological pebble complex, Narin-Gol (Acheulian or pre-Acheulian according to Derevyanko *et al.*, 1991), is confined to the surface levels of high terraces. Artifacts of this age also occur on flat tops of the ridge within the distribution area of Upper Cretaceous conglomerates. In contrast to younger complexes, the oldest one includes elongated sandstone, siltstone, and quartz pebbles with flake removal surfaces at one or two ends or on their elongated sides. These tools resemble hammer-stones and large side-scrapers. There are also rough cores with one or two flake removal surfaces. They are heavily abraded on both flaked and non-flaked pebble surfaces. The surface of the pebble tools is rusty and ferruginous.

(3) The ridge uplift along faults continued throughout the Quaternary period. At this stage, flint veins and interbeds, which subsequently served as the main source of materials for the stone industry, became exposed on the ridge slopes.

(4) Development of the karst caves during the most humid Pliocene–early Pleistocene time, antecedent erosion of the ridges, and accumulation of the basal portion of the cave deposits represented by red-colored karst sediments.

(5) Formation of karst hollows and caves within the ridge extended over the whole Quaternary Period, when the climate was more humid than at present. This is evident from palynological data and can be suspected on the basis of fluvial facies in the central section of the cave and two fossil soils in the entrance area. It seems

Table 2. Correlated stratified and open-air archeological complexes and their geological age

Age			Stratified complexes	Open-air complexes	
geological		archeological	Tsagan-Agui Cave	Flint Valley	Narin-Gol River
0.01		Neolithic			
Brunhes	late Pleistocene	late Paleolithic	Complex 1, late Paleolithic–Neolithic	unabraded complex, late Paleolithic	
		middle Paleolithic	Complex 2, late Mousterian	slightly abraded complex, Mousterian	
	middle Pleistocene		Complex 3, early Mousterian, the lower part is probably older		
0.7		early Paleolithic		heavily abraded complex, pre-Mousterian	
Matuyama	early Pleistocene		Complex 4 (?), Acheulian or older	?	Narin-Gol (pebble) complex, early Acheulian or pre-Acheulian

that the cave was persistently connected via a system of fractures and vertical channels with the ridge surface, thus being open to atmospheric precipitation. Structural features related to cryogenesis have not been observed, and processes of this kind cannot be admitted for the period in question.

(6) As is evident from palynological data, the climate was significantly different from the present-day extremely arid conditions and remained relatively favorable for ancient human habitation during the entire Pleistocene. This was the main factor responsible for human expansion into the Mongolian Gobi areas over a long period.

(7) Flint artifacts (made of the material from veins located 50–100 m upward in the sair and on the ridge surface) occur in variable concentrations within the sedimentary section near the cave entrance and in its central part. Their age is estimated to be the Mousterian–late Paleolithic; the lower part of the section may be older.

(8) There are at least four horizons of gravitational-sliding deposits distinguished in the cave section. They reflect the influence of past earthquakes that occurred in the area during the Quaternary period (the magnitude of present earthquakes is 9–10 or more). These coarse clastic deposits were formed during the collapse phases of cave walls, ceiling, and shelter (in the entrance area) and cannot be considered a result of climatic events. Seismogenic collapses could have dammed the dry sair to form temporary lakes. In this case, sandy and clayey lacustrine deposits could have penetrated into the entrance area of the cave.

(9) Two horizons of rose soil are indications of either the humid climate or the cave's proximity to the flooded sair streams. Accordingly, they suggest the general pluvial climatic regime of the Quaternary time in this part of the Mongolian Gobi.

(10) The "loess-like" sediments in the upper part of the near-entrance section can be interpreted as a result of the enhanced aridity at that time and eolian transport of dusty material into the cave from the ridge slopes and bottoms of small piedmont depressions of the Gobi Altai.

(11) Three terraces up to 10 m high are situated in the Tsagan-Agui sair near its exit area from the ridge. Flint artifacts from the surface of these terraces resemble those of the cave complex and appear to be completely or partly coeval with the latter. Artifacts of this time have a fresh surface. The composition of the source material for the artifacts (flint) and their fresh surface substantially differ them from those of the Pebble Complex.

The young stratigraphic complex is that of the Neolithic time, corresponding to sandy deposits in large sairs. It is characteristic of areas flooded during the Holocene, i.e., of the short-lived (in the geological sense) lakes and streams of the Shabarak-Usu type. The complex seems to be heterochronous, but the stages of its development during the Holocene will likely be distinguished after additional comprehensive study.

Thus, the first thorough study of the Tsagan-Agui Cave of Mongolia using different investigation methods revealed a succession of geological and archeological events recorded in the sedimentary section of this unique object. The results elucidate paleoclimatic peculiarities and paleoecology of the ancient human habitation and offer a new approach to correlation between the open-air and stratified sites.

ACKNOWLEDGMENTS

The field work of 1995 and analytical processing of materials were financially supported by the following institutions: the Institute of Archeology and Ethnography, Siberian Division, Russian Academy of Sciences; the Venner-Gren Foundation for Anthropological Research; the L.S.B. Leakey Foundation, the University of Arizona (Tuscon); and the Russian Foundation for Basic Research (project no. 96-05-64552). We express our gratitude to all these organizations.

Reviewers Z.A. Abramova and M.N. Alekseev

REFERENCES

Derevyanko, A.P., Devyatkin, E.V., Petrin, V.T., and Semeihan, T., New Discovery of the Lower Paleolithic in Mongolia and Its Geological–Geomorphological Position, in *The INQUA Int. Symposium on Stratigraphy and Correlation of Quaternary Deposits of the Asian and Pacific Regions*, CCOP Tech. Secretariat, 1991, pp. 119–132.

Derevyanko, A.P., Dorzh, D., Vasilevskii, R.S., *et al.*, *Paleolit i neolit Mongol'skogo Altaya* (The Paleolithic and Neolithic of the Mongolian Altai), Novosibirsk: Inst. Arkheol. Sib. Otd. Ross. Akad. Nauk, 1990.

Derevyanko, A.I., Laukhin, S.A., Kulikov, O.A., *et al.*, The First Middle Pleistocene Dates for the Paleolithic in the Altai Mountais, *Dokl. Akad. Nauk*, 1992, vol. 326, no. 3, pp. 497–501.

Derevyanko, A.P., Nikolaev, S.V., and Petrin, V.G., *Geologiya, stratigrafiya, paleogeografiya paleolita Yuzhnogo Khangaya* (Paleolithic Geology, Stratigraphy, and Paleogeography of the Southern Khangai), Novosibirsk: Inst. Arkheol. Sib. Otd. Ross. Akad. Nauk, 1992.

Derevyanko, A.P., Olsen, J., *et al.*, *Arkheologicheskie issledovaniya Rossiisko-Mongol'sko-Amerikanskoi ekspeditsii v Mongolii v 1995 g.* (Archaeological Investigations of the Russian–Mongolian–American Expedition in Mongolia, 1995), Novosibirsk: Inst. Arkheol. Sib. Otd. Ross. Akad. Nauk, 1996.

Derevyanko, A.P. and Petrin, V.T., *Issledovanie peshchernogo kompleksa Tsagan-Agui na yuzhnom fase Mongol'skogo Altaya v Mongolii* (Studies of the Tsagan-Agui Cave Complex in the Southern Termination of the Mongolian Altai, Mongolia), Novosibirsk: Inst. Arkheol. Sib. Otd. Ross. Akad. Nauk, 1995.

Devyatkin, E.V., *Kainozoi Vnutrennei Azii (stratigrafiya, geokhronologiya, korrelyatsiya)* (The Cenozoic of Inner Asia: Stratigraphy, Geochronology, and Correlation), Moscow: Nauka, 1981.

Dinesman, L.G., Kiseleva, N.K., and Knyazeva, A.V., *Istoriya stepnykh ekosistem Mongol'skoi Narodnoi Respubliki* (History of Steppe Ecosystems in the Mongolian People's Republic), Moscow: Nauka, 1989.

Krupenina, L.A., Palynological Studies of the Pliocene–Quaternary Deposits in Northern Mongolia, in *Palinologiya chetvertichnogo perioda* (Palynology of the Quaternary Period), Moscow: Nauka, 1985, pp. 68–95.

Malaeva, E.M. and Murzaeva, V.E., The North Mongolian Holocene, *Izv. Akad. Nauk SSSR, Ser. Geogr.*, 1987, no. 2, pp. 69–73.

Okladnikov, A.P., *Paleolit tsentral'noi Azii* (The Paleolithic of Central Asia), Novosibirsk: Nauka, 1981.

Olsen, J., New Data on Earliest Phases of Colonization in Eastern Asia, in *Chelovek zaselyaet planetu. Materialy simpoziuma "Pervichnoe rasselenie chelovechestva"* (Man Occupies the Planet. Proc. Symp. "The Earliest Human Settlements"), Moscow: Inst. Geogr. Ross. Akad. Nauk, 1997, pp. 97–108.

Pozdnii kainozoi Mongolii (stratigrafiya i paleogeografiya) (The Late Cenozoic of Mongolia: Stratigraphy and Paleogeography), Logachev, N.A., Ed., Moscow: Nauka, 1989.

Vlasov, V.K., Karpov, N.A., and Tarasov, M.Yu., A Model of Accumulation of Ion–Emission Energy by Solid Dosimeters, *Tekh. Fiz.*, 1980, vol. 50, no. 10, pp. 2141–2145.

Vlasov, V.K. and Kulikov, O.A., *Radiotermolyuministsentnyi metod datirovaniya rykhlykh otlozhenii. Metodicheskoe posobie* (Thermoluminescence Dating of Unconsolidated Deposits), Moscow: Mosk. Gos. Univ., 1988.

Vostokova, E.A., Gunin, P.D., Rachkovskaya, E.M., *et al.*, *Ekosistemy Mongolii* (Mongolian Ecosystems), Moscow: Nauka, 1995.

Stratigraphy and Geological Correlation, Vol. 8, No. 1, 2000, pp. 99–102. Translated from Stratigrafiya. Geologicheskaya Korrelyatsiya, Vol. 8, No. 1, 2000, pp. 106–109.
Original Russian Text Copyright © 2000 by Gladenkov.
English Translation Copyright © 2000 by MAIK "Nauka/Interperiodica" (Russia).

Early Paleogene Mollusks of Kamchatka: Assemblages and Paleogeographic Environment

Yu. B. Gladenkov

Geological Institute, Russian Academy of Sciences, Pyzhevskii per. 7, Moscow, 109017 Russia

Received March 29, 1998; in final form, April 6, 1998

Key words: *mollusks, Paleogene, Kamchatka, beds, local zones, horizons, paleogeography.*

INTRODUCTION

In contrast to abundant data on Eocene, Oligocene and Neogene molluscan assemblages of Kamchatka, which are well described and analyzed in a series of monographs and articles, information about the early Paleogene mollusks from this region is limited (Krishtofovich, 1947; Devyatilova and Volobueva, 1981; and others). Only scarce, poorly preserved specimens and their impoverished assemblages are characterized. Their dating is conventional to a great extent. In addition, the stratigraphy of the enclosing deposits is insufficiently understood.

In the 1980s and 1990s, researchers from the Geological Institute of the Russian Academy of Sciences thoroughly studied the Lower Paleogene deposits of Kamchatka. Materials obtained are used as a basis for the new regional stratigraphic scale and characterize the Paleogene fossil assemblages. V.N. Sinel'nikova and I studied collected mollusks representing the oldest forms of the Paleogene malacofauna in Kamchatka, Sakhalin, and Koryak Upland. The comprehensive paleontological investigations of the sections (floral remains were studied by Chelebaeva and foraminifers, by Benyamovskii and Stupin) controlled the dating results based on mollusks. The molluscan assemblages and their stratigraphic positions are characterized below.

Stratigraphy. Problems of the Paleogene stratigraphy were considered in detail by Gladenkov *et al.*, (1997). The Lower Paleogene deposits in Kamchatka, which correspond to a large sedimentational cycle, are unconformably overlain with a hiatus by the middle Eocene deposits (the Snatol and Kovachina horizons). The basal Paleogene beds are likely in conformable contact with the underlying Cretaceous deposits, but the situation is not entirely clear. Two lower Paleogene groups were recognized in the region. The lower Ulevenei Group is mostly exposed in the Tigil' region (the central part of West Kamchatka), and the upper Chemurnaut Group is characteristic of the Penzhina region (the northwestern part of West Kamchatka). The lower group corresponds to the Ulevenei Horizon (continental and less frequent marine deposits more than 1000 m thick). The stratigraphic positions of sporadic mollusks, brackish-water forms included (the assemblage of *Macrocallista kovatschensis, Melania snatolensis, Corbicula kamtschatica*, and others), are not very clear; and it is often difficult to determine their succession in the section. The upper group consists (from the base upsection) of the Getkilnin, Kamchik, and Tkapravayam horizons, or regional stages. They all have conformable contacts.

The Getkilnin Horizon is mostly represented by sandstones and siltstones (up to 1000 m thick). It is divided into three successive units bearing mollusks: (I) *Nuculana spheniopsis* Conr.–*Amanropsis fetteri* Marinc., (II) *Periploma eodiscus* Dev.–*Eocernina hespericosta* Zinsm. (Gabb.)–*Molopophorus acquicostatus* Yok., and (III) *Nuculana gabbi* (Conr.)–*Margarites semiornata* Zinsm.–*Dacridium penjicus* Sin. beds. The horizon is dated back to the Danian (late Danian?)–early Thanetian.

The Kamchik Horizon (up to 1000 m thick) is composed of marine sandstones with coal interbeds. It includes three units: (IV) *Thyasira baca* Dev.–*Nemocardium lintium* (Conr.), (V) *Ostrea ornata* Dev.–*Siphonalia bicarinata* Hend., and (VI) *Portlandella kilanskensis* Glad.–*Gilbertina popenoe* Zinsm. beds. The horizon is presumably of the Thanetian age.

The Tkapravayam Horizon of coastal-marine sandstones and lagoonal–continental deposits is over 1000 m thick. Two units are distinguished in its lower part: (VII) *Venericardia venturensis* Waring–*Eocernina hannibali* Zinsm. and (VIII) *Modiolus speciosus* Dev.–*Potamides penjica* Sin. The horizon spans the Thanetian and probably part of the Ypresian.

Molluscan assemblages. The mollusks under consideration are described, with their images (20 plates) and age substantiation, in a monograph published recently (Gladenkov *et al.*, 1997). A brief comparative analysis of the mentioned beds and horizons is given below.

The Early Paleogene fauna of West Kamchatka seems to be very representative. In total, nearly 190 molluscan species were identified as characterizing the

Table 1. Beds with mollusks of the Chemurnaut Group

Horizons and molluscan bed numbers	Getkilnin			Kamchik			Tkapravayam	
	I	II	III	IV	V	VI	VII	VIII
Total number of species	26	34	78	28	45	58	58	8
Newly appeared species	26	19	43	14	20	19	29	5
Extinct species	–	5	46	9	14	34	20	50
Endemics + new species	10	8	22	11	14	17	26	3
North American species	15	23	52	13	22	37	29	2
North Asian species	1	2	4	4	7	6	3	1
Paleocene species	10	17	42	7	11	27	19	–
Late Paleocene species	–	–	–	–	3	–	2	–
Paleocene–Eocene species	5	6	14	3	8	6	2	2
Eocene species	–	–	–	7	9	7	9	1
Age	Paleocene							Ypresian?

beds. The molluscan assemblages described below are variable in composition and diversity. Analysis of their historical (age) succession elucidates problems of this fauna's evolution and outlines the paleo-auto- and paleo-synecology, as well as the paleogeography and paleoclimate.

Distinctive features of the molluscan assemblages are summarized in Table 1. First of all, the beds yield different numbers (and percentage) early Paleocene, late Paleocene, and Eocene forms (it should be taken into consideration that these forms were found in coeval deposits of the neighboring areas, but their biozones have not been accurately recognized). Second, the beds differ from each other in the total abundance of identified species. The greatest number of individual species is recorded in beds III (78), VI (58); VII (58); this may suggest better living conditions for mollusks during the accumulation time of these beds. In general, the respective levels correspond to transgressive intervals of sedimentary cycles.

The next feature to be mentioned is the maximum abundance of newcomers in particular reference beds. These are beds III (43 new species) and VII (29 new forms). At the same time, some beds (III, VI, and VIII) are marked by peak abundance of extinct species (46, 34, and 50 forms, respectively).

The studied sections yielded a considerable number of endemics (or more exactly, "new" species, which have not been described so far in publications). In some beds, the endemic forms are rather abundant (22, 17, and 26 species in beds III, VI, and VII respectively), whereas, in other beds, we encountered only 10–15 forms of this kind. They usually represent up to 30%, and locally (beds I, IV, VII) up to 40–45%, of the molluscan assemblages.

Paleobiogeographic characteristics of the assemblages are also of interest. The assemblages include many species characteristic of Paleocene (partly of lower Eocene) deposits of the Pacific coasts of North America and Asia (beds I, II, IV, and V bear, on average, 20 species of this type; and 42, 27 and 21 forms occur in beds III, VI, and VII, respectively). These forms constitute 50–70% of the assemblages and are evidence in favor of broad biotic connections between the western and eastern North Pacific shelves during the Paleocene time. Some assemblages also include species (however, these are forms of open nomenclature) that have been reported from the Paleogene deposits of Japan (the Ishikari Formation).

The analysis shows that the beds may be grouped into three biohorizons corresponding to regional stages (Table 2).

The lower (Getkilnin) biohorizon contains 87 species, 52 of which (60%) are characteristic. They associate with 25 endemic forms (22 of them are newly described). The horizon spans the interval of molluscan beds I–III. The characteristic dominant species are *Nuculana (Costelloleda) powersi* (Dickerson), *N. (Sacella) alaeformis* (Gabb.), *N. (Sacella) devjatilovae* Sin., *Saulella undulifera* Zinsm., *Gyrodus robustus* Waring, *Hataiella getkilnensis* Titova, *Polinices (Polinices) hornii* (Gabb.), *Amauropsis fetteri* Marinc., *Molopophorus aequicostatus* Vokes, and *Gilbertina popenoe* Zinsm.

The middle (Kamchik) biohorizon spans the distribution range of 19 newcomers (about 22% of the molluscan assemblage). At this level, 27 species (30%) are endemics. The total assemblage of the horizon consists of 86 species, 30 of which (35%) are characteristic. The horizon unites beds IV–VI. The dominant molluscan species here are *Nemocardium linteum* (Conr.), *Acanthocardia (Schedocardia) breweri* (Gabb.), *Portlandella moriyai* (Marinc.), *P. kilanskensis* Glad., *Spisula merriami longifrons* Titova, *Callista (Costacallista) conradiana* (Gabb.), *Acrilla procerus* Zinsm., *Paraser-*

Table 2. Species distribution in molluscan assemblages of the Chemurnaut Group horizons

Molluscan species	Horizons		
	Getkilnin	Kamchik	Tkapravayam
Total amount	87	86	68
Characteristic	52(60%)	30(35%)	43(63%)
First appeared	87	19(22%)	43(63%)
Extinct	52	27	68
Transitional	35	5	25
Endemics and newly described forms	25(25%)	27(31%)	32(47%)
Total for all horizons	about 190		

aphs erraticus (Cooper), *Sassia bilineata* (Dickerson), and *Siphonalia bicarinata monospina* Hendon.

The upper (Tkapravayam) biohorizon corresponds to the distribution range of the renewed assemblage consisting of 68 species. In this assemblage, 43 (63%) species represent newcomers and 32 species (47%) are endemics. Abundance of characteristic species (43) is 63%. The horizon consists of two beds, VII and VIII. Their dominant species are *Venericardia (Venericor) venturensis* Waring, *Tivela penjinskensis* Dev., *Solena (Eosolen) stantoni* (Weaver), *Mytilus tener* Dev., *Modiolus speciosus* Dev., *Lucina (Lucina?) diaboli* Dickerson, *L. (lucina?) quadrata* (Dickerson), *Calyptraea calabasasensis* Nelson, *Callista (Macrocallista) stantoni* (Nelson), *Barbatia (Barbatia) landesi* (Weav. et Palm.), *Amauropsis meierensis* Zinsm., and *Melania kavranensis* Iljina. Upsection, the Tkapravayam assemblage is probably succeeded by the *Bathyarca–Variamussium* assemblage described from eastern Kamchatka, where it is correlated with the Ypresian planktonic zones (Volobueva *et al.*, 1994).

The comparative analysis of biohorizons shows that the characteristic forms represent 35–60% of their molluscan assemblage (30–50 species). Abundance of transient forms varies from 5 to 35, and 27–68 forms exemplify the extinct mollusks. The typical feature is a high content of endemics (and first described species) whose abundance rate is 25–47% (25 to 32 taxa). These data appear to be sufficient to subdivide the section into horizons. In addition, they reveal a general trend of abrupt changes in taxonomic composition of the assemblages (the appearance of numerous new forms parallel to the extinction of many "old" species). Differences between assemblages characterizing individual beds of one horizon may be related to the facies types of the beds.

Paleogeographic environment. Analysis of the marine fauna from the Chemurnaut Group revealed the migration of the Chemurnaut sea-basin shoreline with time. The greatest water depth in the basin was in the early Getkilnin time. The molluscan composition in the lower Getkilnin Formation is characteristic of the lower sublittoral–bathyal zone. The basin was shoaling from the early Getkilnin period to the Tkapravayam time. In addition to this general trend, the lower–middle sublittoral settings appeared during some transgressive phases (the Kamchik time). By the late Tkapravayam time, however, the continental regime became dominant in the study area. Assemblages of Paleocene mollusks from the Chemurnaut and Tigil areas suggest that the former was characterized by deeper water settings, in contrast to the continental and coastal-marine environment that prevailed in the latter. It cannot be excluded that the Chemurnaut basin was relatively small and semiclosed. Probably, it was connected with the Pacific Ocean through a strait located in northern Kamchatka.

As far as the Paleocene marine facies of the Tigil region are concerned, their formation may be explained by a short-term sea ingression from the north (from the Chemurnaut basin) or from the east (through the straits connecting the region with the East Kamchatka sea basin).

It is difficult to estimate the influence of eustatic sea level fluctuations and tectonic movements on the opening and closing of paleostraits and sea basins of the Chemurnaut time. However, from analysis of the Chemurnaut biota and lower Paleogene formations, one can infer that basin development was greatly affected by tectonic activity, although the Chemurnaut deposits may also reflect the global sea-level rise during the Selandian and Thanetian ages.

Paleobiogeographic connections. The Paleocene marine mollusks of the Chemurnaut Group characterize the type and extent of paleobiogeographic connections. They suggest a close connection between the Chemurnaut and North American basins, as in both of them a series of common coenoses developed in the relatively shallow shelf zones (down to the lower sublittoral–upper bathyal zone). Data on the coeval benthic foraminifers show that, in addition to the North Pacific region, the Chemurnaut sea was also connected with basins not only of the North Pacific region, but also of the Atlantic, Tethyan, and other regions. The suggestion is based on the great degree of affinity (abundance of common taxa) of Paleocene fauna in different basins.

Some Paleogene forms in common with the Chemurnaut and northeastern Kamchatka sections may indicate that it was the North Kamchatka, across which a past seaway connected the Chemurnaut basin with the Pacific Ocean in the Paleocene time. The fact that immigrants predominantly represented the relatively shallow-water benthic assemblages is evidence for the relatively shallow-water state of that seaway.

Climate. Analysis of the faunal and floral assemblages of the Chemurnaut Group shows that the Tkapravayam time marks the warmest climatic phase of the Paleogene, because the most thermophilic marine faunal and floral assemblages are confined to the respective stratigraphic levels. Probably, this stage in development of the paleobiota corresponded to the climatic optimum of the late Paleocene–early Eocene time. Some benthic foraminifers of this age were found in northeastern Kamchatka in association with subtropical planktonic assemblages (the Yuzhno-Il'pinskii Formation and lower beds of the Kylan Formation), which include the indicative *Morozovella* and other forms.

In general, climatic conditions on land and surface temperature in the Chemurnaut sea basin were rather stable during the Danian–Thanetian time. Some species of the studied assemblages were simultaneously typical of the Californian and Tethyan basins, and this may be evidence in favor of subtropical conditions in the studied region at that time.

CONCLUSION

For the first time, rich assemblages of Early Paleogene mollusks has been found in western Kamchatka, which is situated in the transitional zone from the Asian continent to the Pacific Ocean. The data presented help us to understand the evolution and distribution of the earliest Cenozoic mollusks, which were characteristic elements of the relatively shallow-water biota typical of shelf ecosystems in high latitudes of the North Pacific.

In particular, these data, which elucidate the development stages of Paleocene ecosystem and paleogeographic changes in the region under consideration, are of great scientific importance. In addition, these data can be used in practice, for example, by geological mapping and associated stratigraphic subdivision of Paleogene deposits on the basis of fossil assemblages.

Reviewer L.A. Nevesskaya

REFERENCES

Devyatilova, A.D. and Volobueva, V.I., *Atlas fauny i flory paleogena i neogena Severo-Vostoka SSSR* (Atlas of Paleogene and Neogene Fauna and Flora of the Northeastern USSR), Moscow: Nedra, 1981.

Gladenkov, Yu.B., Shantser, E.R., Chelebaeva, A.I., *et al.*, *Nizhnii paleogen Zapadnoi Kamchatki* (The Lower Paleogene of Western Kamchatka), Moscow: GEOS, 1997.

Krishtofovich, L.V., *Stratigrafiya i fauna Tigil'skoi tolshchi zapadnogo poberezh'ya Kamchatki* (Stratigraphy and Fauna of the Tigil' Deposits in the Western Coast of Kamchatka), Leningrad: Lengostopizdat, 1947.

Volobueva, V.I., Gladenkov, Yu.B., Benyamovskii, V.N., *et al.*, *Opornyi razrez morskogo paleogena Severa Dal'nego Vostoka* (The Reference Section of Marine Paleogene in the Northern Far East), Magadan: Severo-Vost. Kompl. Nauchno–Issled. Inst. Dal'nevost. Otd. Ross. Akad. Nauk, 1994.

Subscribe to the journals from the Russian Academy of Sciences

Translated and Published by MAIK "Nauka / Interperiodica"

(International Academic Publishing Company "Nauka / Interperiodica")

Distributed Worldwide by INTERPERIODICA

Copy this form to mail or fax your order today

	TITLE	Volume	ISSN	ISSUES	RATE IN US DOLLARS US/CAN	RATE IN US DOLLARS INTERNATIONAL	YOUR ORDER
❑	Biophysics	45	0006-3509	6	$2592	$2700	$ _____
❑	Computational Mathematics and Mathematical Physics	40	0965-5425	12	$2310	$2810	$ _____
❑	Doklady Earth Sciences	370-375A	1028-334X	9	$2905	$3340	$ _____
❑	Doklady Mathematics	61-62	1064-5624	6	$1395	$1600	$ _____
❑	Entomological Review	80	0013-8738	9 + 2 Suppl.	$2635	$3030	$ _____
❑	Environmental Geoscience	3	Pending	4	$610	$690	$ _____
❑	Eurasian Soil Science	33	1064-2293	12 + 2 Suppl.	$2390	$2750	$ _____
❑	Geochemistry International	38	0016-7029	12 + 3 Suppl.	$2890	$3320	$ _____
❑	Geology of Ore Deposits	42	1075-7015	6	$980	$1125	$ _____
❑	Geomagnetism and Aeronomy	39	0016-7932	6	$675	$775	$ _____
❑	Geomagnetism and Aeronomy	40	0016-7932	6	$745	$855	$ _____
❑	Geotectonics	34	0016-8521	6	$580	$630	$ _____
❑	Herald of the Russian Academy of Sciences	70	1019-3316	6	$1410	$1790	$ _____
❑	Izvestiya, Atmospheric and Oceanic Physics	36	0001-4338	6	$810	$870	$ _____
❑	Izvestiya, Physics of the Solid Earth	36	1069-3513	12	$850	$940	$ _____
❑	Journal of Communications Technology and Electronics	45	1064-2269	12 + 2 Suppl.	$3115	$3585	$ _____
❑	Journal of Computer and Systems Sciences International	39	1064-2307	6	$2100	$2420	$ _____
❑	Journal of Ichthyology	40	0032-9452	9 + 2 Suppl.	$2265	$2605	$ _____
❑	Laser Physics	10	1054-660X	6	$1130	$1365	$ _____
❑	Oceanology	40	0001-4370	6	$720	$775	$ _____
❑	Paleontological Journal	34	0031-0301	6 + 3 Suppl.	$2075	$2390	$ _____
❑	Pattern Recognition & Image Analysis	10	1054-6618	4	$700	$800	$ _____
❑	Petroleum Chemistry	40	0965-5441	6	$2840	$2950	$ _____
❑	Petrology	8	0869-5911	6	$980	$1125	$ _____
❑	The Physics of Metals and Metallography	89-90	0031-918X	12 + 2 Suppl.	$2770	$3190	$ _____
❑	Physics of Particles and Nuclei	31	1063-7796	6	$1965	$2085	$ _____
❑	Polymer Science. Series A	42	0965-545X	12	$2630	$3030	$ _____
❑	Polymer Science. Series B	42	1560-0904	6	$1000	$1150	$ _____
❑	Polymer Science. Series C	42	Pending	2	$350	$400	$ _____
	Series A + B + C discount 20%				$3180	$3680	$ _____
❑	Proceedings of the Steklov Institute of Mathematics	228-231	0081-5438	4 + 2 Suppl.	$1405	$1620	$ _____
❑	Russian Journal of Inorganic Chemistry	45	0036-0236	12 + 3 Suppl.	$3405	$3915	$ _____
❑	Russian Journal of Mathematical Physics	7	1061-9208	4	$570	$650	$ _____
❑	Russian Journal of Physical Chemistry	74	0036-0244	12 + 3 Suppl.	$3405	$3915	$ _____
❑	Stratigraphy and Geological Correlation	8	0869-5938	6	$980	$1125	$ _____
❑	Studies on Russian Economic Development	11	1075-7007	6	$715	$820	$ _____
❑	Thermal Engineering	47	0040-6015	12	$1530	$1760	$ _____
❑	Thermophysics and Aeromechanics (only distribution)	7	0869-8643	4	$650	$780	$ _____
						TOTAL	_____

❶ Name _____
Institution _____
Address _____
_____ State _____
City _____ Country _____
Zip/Postal Code _____
Telephone (_____)

Delivery is not made until payment is received

To order by phone call **1 800 633-4931**
or (205) 995-1567 outside the US and Canada

❷ ❑ My payment for $_____ is enclosed.
OR
❑ Bill me. My library's purchase order number is _____

❸ Send this order and payment to:
INTERPERIODICA
P.O. Box 1831
Birmingham, AL 35201-1831
Or fax this order form to (205) 995-1588

Order now for immediate delivery. All journals will be published in 2000!

MAIK "Nauka/Interperiodica" Publishing

is pleased to present to the international scientific community simultaneous Russian- and English-language publication of the journals of the Russian Academy of Sciences

International Academic Publishing Company "Nauka/Interperiodica" (MAIK "Nauka/Interperiodica"), in cooperation with the Russian Academy of Sciences, publishes the results of research in all fields of modern science performed by leading scientists and scientific institutions from Russia, the CIS, and other countries. Simultaneous English translation of the journals is provided by Interperiodica Publishing, the translation division of MAIK "Nauka/Interperiodica". Today, scientists around the world have direct access to the most significant Russian research at the time it is first published in Moscow – at the time it is most relevant to the worldwide scientific community. In addition to more timely publication, readers benefit from more precise translations of each journal, provided by a carefully chosen team of scientific translators with direct access to the authors and editors. English versions of the journals published by MAIK "Nauka/Interperiodica" are distributed worldwide by Interperiodica, Kluwer Academic/Plenum Publishers, and the American Institute of Physics.

MAIK "Nauka/Interperiodica" 2000 volumes include the following titles:

- *Biophysics*
- *Computational Mathematics and Mathematical Physics*
- *Doklady Earth Sciences*
- *Doklady Mathematics*
- *Entomological Review*
- *Environmental Geoscience*
- *Eurasian Soil Science*
- *Geochemistry International*
- *Geology of Ore Deposits*
- *Geomagnetism and Aeronomy*
- *Geotectonics*
- *Herald of the Russian Academy of Sciences*
- *Izvestiya, Atmospheric and Oceanic Physics*
- *Izvestiya, Physics of the Solid Earth*
- *Journal of Communications Technology and Electronics*
- *Journal of Computer and Systems Sciences International*
- *Journal of Ichthyology*
- *Journal of Journals*
- *Laser Physics*
- *Oceanology*
- *Paleontological Journal*
- *Pattern Recognition and Image Analysis*
- *Petroleum Chemistry*
- *Petrology*
- *Polymer Science, Series A*
- *Polymer Science, Series B*
- *Physics of Particles Nuclei*
- *Proceedings of the Steklov Institute of Mathematics*
- *Russian Journal of Inorganic Chemistry*
- *Russian Journal of Mathematical Physics*
- *Russian Journal of Physical Chemistry*
- *Stratigraphy and Geological Correlation*
- *Studies on Russian Economic Development*
- *The Physics of Metals and Metallography*
- *Thermal Engineering*
- *Thermophysics and Aeromechanics**

* *Thermophysics and Aeromechanics* is only distributed by MAIK "Nauka/Interperiodica" Publishing

Please direct all inquiries about the above journals to: **INTERPERIODICA**, P.O. Box 1831, Birmingham, AL 35201-1831.
For faster service call toll-free (800) 633-4931 or (205) 995-1567 (outside US and Canada). Fax: (205) 995-1588, E-mail: interperiodica@ebsco.com

- *Applied Biochemistry and Microbiology*
- *Automation and Remote Control*
- *Biochemistry (Moscow)*
- *Biology Bulletin*
- *Colloid Journal*
- *Cosmic Research*
- *Differential Equations*
- *Doklady Biochemistry*
- *Doklady Biological Sciences*
- *Doklady Biophysics*
- *Doklady Botanical Sciences*
- *Doklady Chemical Technology*
- *Doklady Chemistry*
- *Doklady Physical Chemistry*
- *Glass Physics and Chemistry*
- *High Energy Chemistry*
- *High Temperature*
- *Human Physiology*
- *Inorganic Materials*
- *Instruments and Experimental Techniques*
- *Journal of Analytical Chemistry*
- *Journal of Evolutionary Biochemistry and Physiology*
- *Kinetics and Catalysis*
- *Lithology and Mineral Resources*
- *Microbiology*
- *Molecular Biology*
- *Problems of Information Transmission*
- *Programming and Computer Software*
- *Protection of Metals*
- *Radiochemistry*
- *Russian Journal of Applied Chemistry*
- *Russian Journal of Bioorganic Chemistry*
- *Russian Journal of Coordination Chemistry*
- *Russian Journal of Developmental Biology*
- *Russian Journal of Ecology*
- *Russian Journal of Electrochemistry*
- *Russian Journal of General Chemistry*
- *Russian Journal of Genetics*
- *Russian Journal of Marine Biology*
- *Russian Journal of Nondestructive Testing*
- *Russian Journal of Organic Chemistry*
- *Russian Journal of Plant Physiology*
- *Russian Microelectronics*
- *Solar System Research*
- *Theoretical Foundations of Chemical Engineering*
- *Water Resources*

Please direct all inquiries about the above journals to: **Kluwer Academic/Plenum Publishers**, 233 Spring Street, New York, NY 10013. Phone: (212) 620-8467. Fax: (212) 807-1047, E-mail: journals@plenum.com

- *Acoustical Physics*
- *Astronomy Letters*
- *Astronomy Reports*
- *Crystallography Reports*
- *Doklady Physics*
- *JETP Letters*
- *Journal of Experimental and Theoretical Physics*
- *Optics and Spectroscopy**
- *Physics of Atomic Nuclei*
- *Physics of the Solid State*
- *Plasma Physics Reports*
- *Semiconductors*
- *Technical Physics*
- *Technical Physics Letters*

Please direct all inquiries about the above journals to: **American Institute of Physics**, Circulation and Fulfillment Services, 500 Sunnyside Boulevard, Woodbury, NY 11797-2999 USA. Tel. (516) 576-2270, (800) 344-6902. Fax: (516) 349-9704, E-mail: sub@aip.org

**Optics and Spectroscopy*: Optical Society of America, 2010 Massachusetts Ave., NW, Washington, DC 20036-1023, Attn.: Publications Department. Tel. (202) 223-8130, (800) 582-0416. Fax: (202) 223-1096.

International Academic Publishing Company "Nauka/Interperiodica" (MAIK "Nauka/Interperiodica")
Profsoyuznaya ul., 90, Moscow, 117864, Russia, Phone: 7 (095) 3361600; Fax: 7 (095) 336 0666,
E-mail:compmg@maik.rssi.ru, http://www.maik.rssi.ru